

**Geochemical Controls during the Biodegradation of Petroleum
Hydrocarbons in Soils**

Rosemary Nmavulem Orlu

Submitted in accordance with the requirements for the degree of
Doctor of Philosophy

The University of Leeds
School of Civil Engineering

August 2017

The candidate confirms that the work submitted is his/her own and that appropriate credit has been given where reference has been made to the work of others.

This copy has been supplied on the understanding that it is copyright material and that no quotation from this thesis may be published without proper acknowledgement.

The right of Rosemary Njavulem Orlu to be identified as Author of this work has been asserted by her in accordance with the Copyright, Design and Pattern Act 1988.

Acknowledgements

The completion of this project was made possible through the advice and guidance of my supervisors Professor Simon Bottrell from the School of Earth and Environment and Professor Douglas Stewart of the School of Civil Engineering here at the University of Leeds. I also owe a great deal of appreciation to my parents, siblings, and extended family for financial and moral support, guidance and prayers over the duration of the program of study. In addition I would like to acknowledge the professional guidance of the laboratory and technical staff at the Cohen Laboratory in the School of Earth and Environment and the iPHEE laboratory in the School of Civil Engineering for their professional guidance. My thanks also go to the Research Students and Post-Doctoral Researchers in the Schools of Civil Engineering and Earth and Environment who have in one way or another been a part of this journey. Finally I thank God for the grace to have seen this project through to the end.

Abstract

The microbial transformation of Fe (III) to Fe (II) can be coupled to the oxidation and reduction of organic contaminants in sub-oxic to anoxic environments. A multidisciplinary approach was adopted in this study to investigate the biogeochemical influences on the degradation of toluene (a representative of the class of aromatic hydrocarbons collectively known as BTEX) using experimental analogues of subsurface soil environments under predominantly iron-reducing conditions. The removal of toluene over the period of incubation indicated the soil-water mixture supported the degradation of toluene under predominantly iron-reducing conditions. Chemical sequential extractions showed the removal of toluene in the active mesocosms induced an increase in carbonate-bound iron fractions from 196.1 ± 11.4 mg/kg to $5,252.1 \pm 291.8$ mg/kg and a decrease in the reducible iron fraction from $2,504.4 \pm 1,445.9$ mg/kg to 375.6 ± 20.8 mg/kg. Analysis of the soil-water mixture showed slight shifts in the pH of the control and active mesocosms at the start of the experiments however these shifts occurred to a lesser degree over the remainder of the incubation period. Further experiments analysed the degree of influence of differing soil matrices and extraneous sources of iron (hematite, goethite, magnetite, ferrihydrite and lepidocrocite) on toluene removal. With the exception of the lepidocrocite-amended mesocosms, all of the iron-amended mesocosms were shown to have supported toluene removal. The presence of hematite, goethite and magnetite did not produce a significant change in the pH or total iron concentrations of the soil-water mixture. However the presence of ferrihydrite in the ferrihydrite-amended mesocosms induced a decrease in pH to slightly acid values ranging between pH 6.5 at the start of the experiments and 5.2 at the end of the experiments. The lepidocrocite-amended mesocosms induced a change to slightly alkaline values ranging between pH 8.4 and 8.8 during the period of incubation. All of the soil-amended mesocosms supported the removal of toluene in the soil-water mixture. The mesocosms containing soils with a greater percentage clay fraction removed higher amounts of toluene, possibly an indication that the bulk of this removal was sorption-induced and not microbially-mediated. An experimental approach based on the standard stable carbon isotope analytical method made it possible to determine the source of carbon in the incubated mesocosm material. The application of the mixed effects model approach to analyse the repeatedly measured experimental data demonstrated the possibility of producing predictive models for toluene removal in soil.

Keywords: bioremediation, BTEX, iron reduction, mixed effect models, sequential chemical extractions, soil microcosms, stable carbon isotope analysis, toluene.

Table of Contents

Acknowledgements	iii
Abstract	iv
Table of Contents	v
List of Tables	x
List of Figures	xiii
List of Abbreviations	xviii
Chapter 1 Introduction	1
1.1 Research background.....	1
1.2 Research aims and objectives	3
1.3 Research rationale.....	5
1.4 Thesis outline	5
Chapter 2 Literature review	7
2.1 Bioremediation	7
2.1.1 Anaerobic biodegradation.....	8
2.1.2 Anaerobic biodegradation of BTEX.....	10
2.2 Iron in soil environments	16
2.2.1 Iron (hydr)oxides.....	16
2.2.2 Biogeochemical cycling of iron.....	19
2.2.3 Microbial iron reduction.....	20
2.3 Chemical speciation	21
2.4 The isotope geochemistry of carbon cycling in soils	23
2.4.1 Stable carbon isotopes in soil environments	23
2.4.2 Reactions of carbonates in soils.....	25
2.5 Modelling repeated measures data.....	29
2.5.1 Repeated measures experiment designs	29
2.5.2 General linear models	30
2.5.3 Mixed effects models.....	31
Chapter 3 Materials and methods	34
3.1 Analytical method development.....	34
3.1.1 Analysis of aqueous phase toluene.....	34
3.1.2 Analysis of iron-bound soil carbonates.....	37
3.2 Toluene degradation studies	39

3.2.1 Soil mesocosms: design and considerations	40
3.2.2 Apparatus	45
3.2.3 Chemicals and analytical grade reagents.....	45
3.2.4 Analytical instrumentation: chemical and physical characterisation tests	46
3.2.5 Analytical instrumentation: degradation experiments	49
3.3 Statistical analysis.....	53
Chapter 4 Iron-mediated toluene degradation in batch mesocosms	64
Introduction	64
4.1 Results and discussions.....	64
4.1.1 Characterisation tests	64
4.1.2 Mesocosm experiments	65
4.1.3 Chemical sequential extractions	67
4.2 General discussion	73
4.3 Conclusion.....	78
Summary	78
Chapter 5 The influence of iron mineral (hydr)oxides on iron-mediated toluene degradation	79
Introduction	79
5.1 Results and discussions.....	79
5.1.1 Comparing degradation in the un-amended and hematite-amended mesocosms	79
5.1.2 Comparing degradation in the un-amended and goethite-amended mesocosms	81
5.1.3 Comparing degradation in the un-amended and magnetite-amended mesocosms	83
5.1.4 Comparing degradation in the un-amended and ferrihydrite-amended mesocosms	85
5.1.5 Comparing degradation in the un-amended and lepidocrocite-amended mesocosms	87
5.2 General discussion	89
5.3 Conclusion.....	93
Summary	95
Chapter 6 The influence of soil on iron-mediated toluene degradation	96
Introduction	96
6.1 Results and discussions.....	96
6.1.1 Comparing toluene degradation in the un-amended and amended mesocosms (Soil 1).....	96

6.1.2 Comparing toluene degradation in the un-amended and amended mesocosms (Soil 2).....	98
6.1.3 Comparing toluene degradation in the un-amended and amended mesocosms (Soil 3).....	101
6.2 General discussion	103
6.3 Conclusion.....	108
Summary	108
Chapter 7 Stable carbon (¹²C/¹³C) isotopes as a tool for identifying soil carbonates– a method development	110
Introduction	110
7.1 Results and discussions.....	110
7.1.1 Carbonate reactions in the un-amended live control mesocosms	111
7.1.2 Carbonate reactions in the un-amended active control mesocosms	113
7.1.3 Carbonate reactions in the hematite-amended mesocosms	114
7.1.4 Carbonate reactions in the goethite-amended mesocosms	115
7.1.5 Carbonate reactions in the magnetite-amended mesocosms.....	116
7.1.6 Carbonate reactions in the ferrihydrite-amended mesocosms	116
7.1.7 Carbonate reactions in the lepidocrocite-amended mesocosms	117
7.1.8 Carbonate reactions in the soil-amended mesocosms (Soil 1).....	118
7.1.9 Carbonate reactions in the soil-amended mesocosms (Soil 2).....	119
7.1.10 Carbonate reactions in the soil-amended mesocosms (Soil 3) ...	120
7.2 General discussion	120
7.3 Conclusion.....	124
Summary	124
Chapter 8 Predicting the natural attenuation of toluene with mixed effects models	126
Introduction	126
8.1 Results and discussions.....	126
8.1.1 Preliminary tests: Test for correlation	126
8.1.2 Preliminary tests: Test for normality	128
8.1.3 A predictive model for the natural attenuation of toluene in subsurface soil environments	130
8.2 General discussion	134
8.3 Conclusion.....	137
Summary	137
Chapter 9 Conclusion and recommendations	138
Conclusion.....	138

Recommendations for further studies	138
List of references	140
Glossary	176
Appendix A Presentations, publications and list of courses attended	180
A.1 Publications currently submitted for publication and in press.....	181
A.2 Conference and poster presentations.....	181
A.3 Conference platform presentations	181
A.4 Courses attended.....	181
Appendix B Laboratory apparatus.....	183
B.1 Degradation experiments	184
B.2 Sequential chemical extractions	185
B.3 Mineral synthesis	186
B.4 Analysis of total Fe and $\delta^{13}\text{C}$	187
Appendix C Supporting information	188
C.1 Experiment matrix of mesocosm experiments and variables measured.....	189
C.2 Soil sampling locations	190
C.3 Instrument calibration curves.....	191
C.4 Calculations and estimates	191
C.4.1 Toluene removal (in mg)	191
C.4.2 Relative sorption	191
C.5 Experimental procedures.....	192
C.5.1 Laboratory synthesis of lepidocrocite and 2-line ferrihydrite.....	192
C.5.2 Analysis of aqueous phase toluene (salting-out method).....	193
C.5.3 Analysis of total iron (Fe^{2+} and Fe^{3+}) in solution (ferrozine method) ..	194
C.5.4 Sequential chemical extractions for operationally-defined iron pools 195	
C.5.5 Stable carbon isotope analysis (cryogenic distillation).....	197
C.5.6 Predictive modelling with the mixed effects models approach.....	199
Procedure for modelling toluene removal without level 1 and 2 predictors ..	200
C.6 Analytical and experimental data	203
C.6.1 Characterisation tests: soil amendments.....	203
C.6.2 Characterisation tests: mineral amendments.....	204
C.6.3 Characterisation tests: moisture content analysis	204
C.6.4 Characterisation tests: particle size distribution analysis	204
C.6.5 Degradation experiments.....	206
C.6.6 Sequential chemical extractions	212

C.6.7 Stable carbon isotope analysis.....	212
C.6.8 Reaction kinetics - zeroth and first order rate fittings	213
C.6.9 BET surface areas of the starting and incubated soils	218
C.7 Summary of observations and findings	220
C.8 Combined concentration-time profiles	226
C.9 Statistical analysis.....	229
C.9.1 Descriptive statistics	229
C.9.2 Difference in means tests.....	248
C.9.3 Model parameters (Model 1).....	249
C.9.4 Model parameters (Model 2).....	252

List of Tables

Table 1.1 Distillate and carbon range of common petroleum products (Dragun, 1998; Atlas, R.M. , 1991; Atlas, M.T., 1981).....	2
Table 1.2 Toxicological effects of common petroleum hydrocarbons	2
Table 2.1 Electron acceptors in toluene degradation processes showing Gibbs free energy associated with each electron acceptor (Spence, M.J. et al., 2005)	9
Table 2.2 Chemical and physical properties of BTEX (Source:(Weelink, 2010; Kermanshahi pour et al., 2005)) ²	11
Table 2.3 Iron oxides, hydroxides and oxyhydroxides (Cornell, R.M. and Schwertmann, 2003).....	17
Table 3.1 Summary of sample preparation methods for volatile compounds (VOCs)	35
Table 3.2 Yield measurements for FeCO ₃ precipitate from Fe-reducing microcosm (experiment performed by S. Bottrell in December 2007)	39
Table 3.3 Experimental matrix showing the amounts of soil, toluene, river water and amendments used in each mesocosm set	40
Table 3.4 Summary of mesocosm test design applied in this study.....	43
Table 3.5 Properties analysed and instruments used in analyses	46
Table 3.4 Temperature setting of the gas chromatography instrument.....	50
Table 3.5 Summary of the sequential chemical extractions showing extractants and target phases (adapted from (Poulton and Canfield, 2005)	51
Table 8.1 Test for correlation ^a	127
Table 8.2 Tests for normality.....	129
Table 8.3 Parameter estimates for the level-2 mixed effects model of toluene removal without predictors.....	131
Table 8.4 Parameter estimates for the level-2 mixed effects model of toluene removal with predictors*.....	133
Table 8.5 Parameters for model selection.....	135
Table C.1 Experimental matrices and variables measured.....	189
Table B.5.2 Standards for ferrozine assay	194
Table C.6.1a Physico-chemical properties of the soil amendments. Soil 1, Soil 2, and Soil 3 represent the individual soil amendments used	203
Table C.6.1b BET surface area of iron mineral amendments	204
Table C.6.1c Gravimetric moisture content analysis for the starting soil material...	204
Table C.6.1d Particle size distribution (PSD) of starting soil material and soil amendments	204

Table C.6.3 Mean \pm standard error for pH and total iron concentrations in mesocosms with soil and water only (un-amended live controls).....	206
Table C.6.4 Mean \pm standard error for pH, total iron, and toluene concentrations in mesocosms with no amendment (un-amended active controls)	206
Table C.6.5 Mean \pm standard error for pH, total iron, and toluene concentrations in mesocosms with hematite amendment	207
Table C.6.6 Mean \pm standard error for pH, total iron, and toluene concentrations in mesocosms with goethite amendment	208
Table C.6.7 Mean \pm standard error for pH, total iron, and toluene concentrations in mesocosms with magnetite amendment	208
Table C.6.8 Mean \pm standard error for pH, total iron, and toluene concentrations in mesocosms with ferrihydrite amendment	209
Table C.6.9 Mean \pm standard error for pH, total iron, and toluene concentrations in mesocosms with lepidocrocite amendment.....	210
Table C.6.10 Mean \pm standard error for pH, total iron, and toluene concentrations in mesocosms with Soil 1 amendment.....	210
Table C.6.11 Mean \pm standard error for pH, total iron, and toluene concentrations in mesocosms with Soil 2 amendment.....	210
Table C.6.12 Mean \pm standard error for pH, total iron, and toluene concentrations in mesocosms with Soil 3 amendment.....	211
Table C.6.13 Mean \pm standard error of operationally-defined iron pools in the starting and incubated material in the un-amended live and active control mesocosms	212
Table C.6.14 Mean \pm standard error of $\delta^{13}\text{C}$ and carbonate carbon (mg per g of sample) of the starting and incubated soil material (starting soil material was not analysed in triplicate).....	212
Table C.6.15 Zeroth and first order rate fittings for mesocosms with no amendment (S_T)	213
Table C.6.16 Zeroth and first order rate fittings for mesocosms with hematite amendment.....	213
Table C.6.17 Zeroth and first order rate fittings for mesocosms with goethite amendment.....	214
Table C.6.18 Zeroth and first order rate fittings for mesocosms with magnetite amendment.....	214
Table C.6.19 Zeroth and first order rate fittings for mesocosms with ferrihydrite amendment.....	215
Table C.6.20 Zeroth and first order rate fittings for mesocosms with lepidocrocite amendment.....	215
Table C.6.21 Zeroth and first order rate fittings for mesocosms amended with Soil 1	216

Table C.6.22 Zeroth and first order rate fittings for mesocosms amended with Soil 2	216
Table C.6.23 Zeroth and first order rate fittings for mesocosms amended with Soil 3	216
Table C.6.24 Mean \pm standard error of zeroth and first order rate fittings.....	217
Table C.6.25 Toluene removal rates in the mesocosms (expressed per square metre of mesocosm soil and obtained as the average of three replicates)	217
Table C.7.1 Summary of findings - un-amended active mesocosms.....	220
Table C.7.2 Summary of findings - un-amended vs. hematite-amended mesocosms	221
Table C.7.3 Summary of findings - un-amended vs. goethite-amended mesocosms	221
Table C.7.4 Summary of findings - un-amended vs. magnetite-amended mesocosms	222
Table C.7.5 Summary of findings - un-amended vs. mesocosms with ferric citrate amendment	222
Table C.7.6 Summary of findings - un-amended vs. ferrihydrite-amended mesocosms	223
Table C.7.7 Summary of findings - un-amended vs. lepidocrocite-amended mesocosms	223
Table C.7.8 Summary of findings -un-amended vs. mesocosms amended with Soil 1	224
Table C.7.9 Summary of findings - un-amended vs. mesocosms with Soil 2	224
Table C.7.10 Summary of findings - un-amended vs. mesocosms with Soil 3.....	225
Table C.9.1 Descriptive statistics	229
Table C.9.2 Difference in means tests for mean toluene across mesocosm groups^a	248

List of Figures

Figure 1.1 Summary of thesis structure	6
Figure 2.1 Chemical structures of benzene, toluene, ethylbenzene, ortho-xylene, meta xylene and para-xylene (Weelink, 2010).....	13
Figure 2.2 Anaerobic toluene degradation route, according to (Kube et al., 2004) BssABC, benzylsuccinate synthase; BbsEF, succinyl-CoA:(R)-benzylsuccinate CoA-transferase; BbsG R)-benzylsuccinyl-CoA dehydrogenase; BbsH, phenylitaconyl-CoA hydratase; BbsCD, 2-[hydroxy(phenyl)methyl]-succinyl-CoA dehydrogenase; BbsAB, benzylsuccinyl-CoA thiolase (Weelink, 2010).....	14
Figure 2.3 Mechanism of toluene activation by BSS. BSS takes a proton from toluene and donates it to benzylsuccinyl radical formed from toluene and fumarate and generates a BSS radical (Boll et al., 2002; Washer, 2004).....	15
Figure 2.4 Overview of stable carbon isotopic composition of common organic and inorganic material showing relative positions on a $\delta^{13}\text{C}$ scale.....	24
Figure 3.1 Reaction rates of pure carbonate minerals with phosphoric acid showing changes in cumulative yields (expressed in percentage) with time at two temperatures - 25°C and 50°C (adapted from (Al-Aasm et al., 1990))	38
Figure 4.1 Concentration-time profiles showing toluene, total dissolved reactive iron and pH in the control and active mesocosms. Trend lines are separated according to time of addition of toluene spikes to the active mesocosms. Error bars represent the standard error of the mean of three replicates.	65
Figure 4.2 Toluene removal in the active mesocosms during the first spike period (0-15 days), second spike period (18-33 days), third spike period (36-51 days) and overall incubation period (0-51 days). Error bars represent the standard error of the mean of three replicates.....	67
Figure 4.3 Total extractable iron fractions in replicate samples of the starting soil material (S_S) and incubated material from the control mesocosms (S_O) and active experiments (S_T)	68
Figure 4.4 Total extractable and easily reducible iron fractions in replicate samples of the starting soil material (S_S) and incubated material from the control mesocosms (S_O) and active experiments (S_T)	69
Figure 4.5 Total extractable and carbonate-bound iron fractions in replicate samples of the starting soil material (S_S) and incubated material from the control mesocosms (S_O) and active experiments (S_T)	70
Figure 4.6 Total extractable and reducible iron fractions in replicate samples of the starting soil material (S_S) and incubated material from the control mesocosms (S_O) and active experiments (S_T).....	71
Figure 4.7 Total extractable and magnetite fractions in replicate samples of the starting soil material (S_S) and incubated material from the control mesocosms (S_O) and active experiments (S_T).....	72

Figure 4.8 Total extractable, easily reducible, carbonate-bound, reducible, and magnetite fractions in replicate samples of the starting soil material (S_S) and incubated material from the control mesocosms (S_O) and active experiments (S_T).....	73
Figure 5.1 Concentration-time profiles showing toluene, total dissolved reactive iron and pH in the un-amended and hematite-amended mesocosms. Error bars represent the standard error of the mean of three replicates.....	79
Figure 5.2 Toluene removal in the un-amended and hematite-amended mesocosms during the first spike period (0-15 days), second spike period (18-33 days), third spike period (36-51 days) and overall incubation period (0-51 days). Error bars represent the standard error of the mean of three replicates.	80
Figure 5.3 Concentration-time profiles showing toluene, total dissolved reactive iron and pH in the un-amended and goethite-amended mesocosms. Error bars represent the standard error of the mean of three replicates.....	81
Figure 5.4 Toluene removal in the un-amended and goethite-amended mesocosms during the first spike period (0-15 days), second spike period (18-33 days), third spike period (36-51 days) and overall incubation period (0-51 days). Error bars represent the standard error of the mean of three replicates.	82
Figure 5.5 Concentration-time profiles showing toluene, total dissolved reactive iron and pH in the un-amended and magnetite-amended mesocosms. Error bars represent the standard error of the mean of three replicates.	83
Figure 5.6 Toluene removal in the un-amended and magnetite-amended mesocosms during the first spike period (0-15 days), second spike period (18-33 days), third spike period (36-51 days) and overall incubation period (0-51 days). Error bars represent the standard error of the mean of three replicates.	84
Figure 5.7 Concentration-time profiles showing toluene, total dissolved reactive iron and pH in the un-amended and ferrihydrite-amended mesocosms. Error bars represent the standard error of the mean of three replicates.	86
Figure 5.8 Toluene removal in the un-amended and ferrihydrite-amended mesocosms during the first spike period (0-15 days), second spike period (18-33 days), third spike period (36-51 days) and overall incubation period (0-51 days). Error bars represent the standard error of the mean of three replicates.	87
Figure 5.9 Concentration-time profiles showing toluene, total dissolved reactive iron and pH in the un-amended and lepidocrocite-amended mesocosms. Error bars represent the standard error of the mean of three replicates.	88
Figure 5.10 Toluene removal in the un-amended and lepidocrocite-amended mesocosms during the first spike period (0-15 days), second spike period (18-33 days), third spike period (36-51 days) and overall incubation period (0-51 days). Error bars represent the standard error of the mean of three replicates.	89

Figure 6.1 Concentration-time profiles showing toluene, total dissolved reactive iron and pH in the un-amended mesocosms and soil-amended (S_1) mesocosms. Error bars represent the standard error of the mean of three replicates.	96
Figure 6.2 Toluene removal in the un-amended (S_T) mesocosms and soil-amended (S_1) mesocosms during the first spike period (0-15 days), second spike period (18-33 days), third spike period (36-51 days) and overall incubation period (0-51 days). Error bars represent the standard error of the mean of three replicates.	97
Figure 6.3 Concentration-time profiles showing toluene, total dissolved reactive iron and pH in the un-amended mesocosms and soil-amended (S_2) mesocosms. Error bars represent the standard error of the mean of three replicates.	99
Figure 6.4 Toluene removal in the soil-amended (S_2) mesocosms and un-amended (S_T) mesocosms during the first spike period (0-15 days), second spike period (18-33 days), third spike period (36-51 days) and overall incubation period (0-51 days). Error bars represent the standard error of the mean of three replicates.	100
Figure 6.5 Concentration-time profiles showing toluene, total dissolved reactive iron and pH in the un-amended mesocosms and soil-amended (S_3) mesocosms. Error bars represent the standard error of the mean of three replicates.	101
Figure 6.6 Toluene removal in the soil-amended (S_3) mesocosms and un-amended (S_T) mesocosms during the first spike period (0-15 days), second spike period (18-33 days), third spike period (36-51 days) and overall incubation period (0-51 days). Error bars represent the standard error of the mean of three replicates.	102
Figure 6.7 Relationship between sorption, toluene removal, surface area and clay content in the soil-amended material	106
Figure 7.1 Bivariate $\delta^{13}\text{C}$ / carbonate-carbon profile illustrating the effects of soil carbonate reactions on carbonate-carbon and $\delta^{13}\text{C}$ showing ‘a’ - the incubated material following carbonate dissolution and ‘b’ - the incubated material after addition of carbon from respiration of ^{13}C -depleted organic carbon	110
Figure 7.3 Bivariate $\delta^{13}\text{C}$ / carbonate-carbon profile showing the changes in $\delta^{13}\text{C}$ and mass of carbonate carbon following the degradation of toluene in the un-amended (S_T) mesocosms. The $\delta^{13}\text{C}$ signature of toluene is shown. ‘a’ and ‘b’ represent underlying reactions affecting the fast- and slow-reacting carbonate pools (dissolution and addition respectively). Error bars represent the standard error of the mean of three replicates.	113
Figure 7.4 Bivariate $\delta^{13}\text{C}$ / carbonate-carbon profile showing the changes in $\delta^{13}\text{C}$ and mass of carbonate carbon following the degradation of toluene in the hematite-amended (H_M) mesocosms. Error bars represent the standard error of the mean of three replicates.	114

Figure 7.5 Bivariate $\delta^{13}\text{C}$ / carbonate-carbon profile showing the changes in $\delta^{13}\text{C}$ and mass of carbonate carbon following the degradation of toluene in the goethite-amended (G_E) mesocosms. Error bars represent the standard error of the mean of three replicates.	115
Figure 7.6 Bivariate $\delta^{13}\text{C}$ / carbonate-carbon profile showing the changes in $\delta^{13}\text{C}$ and mass of carbonate carbon following the degradation of toluene in the magnetite-amended (M_T) mesocosms. Error bars represent the standard error of the mean of three replicates.	116
Figure 7.7 Bivariate $\delta^{13}\text{C}$ / carbonate-carbon profile showing the changes in $\delta^{13}\text{C}$ and mass of carbonate carbon following the degradation of toluene in the ferrihydrite-amended (F_H) mesocosms. Error bars represent the standard error of the mean of three replicates.	117
Figure 7.8 Bivariate $\delta^{13}\text{C}$ / carbonate-carbon profile showing the changes in $\delta^{13}\text{C}$ and mass of carbonate carbon following the degradation of toluene in the lepidocrocite-amended (L_P) mesocosms. Error bars represent the standard error of the mean of three replicates.	118
Figure 7.9 Bivariate $\delta^{13}\text{C}$ / carbonate-carbon profile showing the changes in $\delta^{13}\text{C}$ and mass of carbonate carbon following the degradation of toluene in the mesocosms amended with Soil 1. Error bars represent the standard error of the mean of three replicates.	119
Figure 7.10 Bivariate $\delta^{13}\text{C}$ / carbonate-carbon profile showing the changes in $\delta^{13}\text{C}$ and mass of carbonate carbon following the degradation of toluene in the mesocosms amended with Soil 2. Error bars represent the standard error of the mean of three replicates.	120
Figure 8.1 Changes in toluene with time for each mesocosm group over three periods A, B, and C, following the addition of toluene. The data is shown as the average of three replicates for each group	126
Figure C.2 Sampling locations of starting soil (SS) and soil amendments (Soil 1, Soil 2, Soil 3) (Image Source: GoogleImages).....	190
Figure C.3 Initial calibration curves for A - toluene analysis on GC instrument and B - ferrozine tests (calibration performed in triplicate) on UV-VIS.....	191
Figure C.5.1 Experimental set up for ferrihydrite and lepidocrocite synthesis	192
Figure C.5.4.1 Illustration of apparatus for pyrite extraction step showing reaction vessel for chromous chloride distillation	196
Figure C.5.4.2 Illustration of filtration apparatus for AVS and pyrite precipitate...	197
Figure C.6.1 Results of BET analysis for i) the starting soil material (S_S) ii) incubated material from the mesocosms with soil and water (S_O) and iii) incubated material from the mesocosms with no amendment (S_T)	218
Figure C.6.2 Results of BET analysis for i) the starting soil material (S_S) ii) incubated material from the mesocosms with soil and water (S_O) iii) incubated material from the mesocosms with no amendment (S_T) iv) incubated material from the mesocosms with hematite mineral amendment (H_M) v) hematite mineral amendment (h_m).....	218

Figure C.6.3 Results of BET analysis for i) the starting soil material (S_S) ii) incubated material from the mesocosms with soil and water (S_O) iii) incubated material from the mesocosms with no amendment (S_T) iv) incubated material from the mesocosms with goethite mineral amendment (G_E) v) goethite mineral amendment (g_e)	218
Figure C.6.4 Results of BET analysis for i) the starting soil material (S_S) ii) incubated material from the mesocosms with soil and water (S_O) iii) incubated material from the mesocosms with no amendment (S_T) iv) incubated material from the mesocosms with magnetite mineral amendment (M_T) v) magnetite mineral amendment (g_e).....	219
Figure C.6.6 Results of BET analysis for i) the starting soil material (S_S) ii) incubated material from the mesocosms with soil and water (S_O) iii) incubated material from the mesocosms with no amendment (S_T) iv) incubated material from the mesocosms with ferrihydrite mineral amendment (F_H) v) ferrihydrite amendment (f_h).....	219
Figure C.6.7 Results of BET analysis for i) the starting soil material (S_S) ii) incubated material from the mesocosms with soil and water (S_O) iii) incubated material from the mesocosms with no amendment (S_T) iv) incubated material from the mesocosms with lepidocrocite mineral amendment (L_P) v) lepidocrocite amendment (l_p).....	219
Figure C.6.8 Results of BET analysis for i) the starting soil material (S_S) ii) incubated material from the mesocosms with soil and water (S_O) iii) incubated material from the mesocosms with no amendment (S_T) iv) incubated material from the mesocosms amended with Soil 1 (S₁) v) soil 1 sample (s₁)	219
Figure C.6.9 Results of BET analysis for i) the starting soil material (S_S) ii) incubated material from the mesocosms with soil and water (S_O) iii) incubated material from the mesocosms with no amendment (S_T) iv) incubated material from the mesocosms amended with Soil 2 (S₂) v) soil 2 sample (s₂)	220
Figure C.6.10 Results of BET analysis for i) the starting soil material (S_S) ii) incubated material from the mesocosms with soil and water (S_O) iii) incubated material from the mesocosms with no amendment (S_T) iv) incubated material from the mesocosms amended with Soil 3(S₃) v) Soil 3 sample (s₃)	220
Figure C.8.1 Concentration-time profiles comparing toluene, total iron and pH in the un-amended mesocosms and mesocosms amended with the mesocosms amaended with natural iron minerals.....	226
Figure C.8.2 Concentration-time profiles comparing toluene, total iron and pH in the un-amended mesocosms and mesocosms amended with the synthesised iron minerals	227
Figure C.8.3 Concentration-time profiles comparing toluene, total iron and pH in the un-amended mesocosms and mesocosms amended with the soil-amended mesocosms	228

List of Abbreviations

AAS	Atomic Absorption Spectrophotometer
ANOVA	Analysis Of Variance
AVS	Acid Volatile Sulphates
BTEX	Benzene Toluene Ethylbenzene Xylene
BIC	Schwartz's Bayesian (Information) Criterion
GC	Gas Chromatograph
FID	Flame Ionisation Detector
GLM	General Linear Model
IRMS	Isotope Ratio Mass Spectrometer
MNA	Monitored Natural Attenuation
PDB	Pee Dee Belemnite
SCIA	Stable Carbon Isotope Analysis
TEA	Terminal Electron Acceptor
TDR Fe	Total Dissolved Reactive Iron
UV-VIS	Ultraviolet Visible Spectrophotometer
XRD	X-ray Diffraction Spectroscope
XRF	X-ray Fluorescence Spectroscope

Chapter 1

Introduction

1.1 Research background

Section 78 A (2) of the Environment Protection Act (1990) defines contaminated land as *'any land which appears to the local authority in whose area it is situated to be in such a condition, by reason of substances in or under the land, that significant harm is being caused or there is a significant possibility of such harm being caused; or pollution of controlled waters is being, or is likely to be caused'*. Chemical pollutants are a major cause of contamination in the environment and are of two main groups namely inorganic (including heavy metals, nutrients and organic pollutants) and organic (including pesticide, detergents, petrol, crude oil and polycyclic aromatic hydrocarbons Bamforth and Singleton (2005)). Organic chemical pollutants include pesticides, aliphatic hydrocarbons, alicyclic hydrocarbons, and aromatic hydrocarbons (Singh, 2016). Pesticides are compounds designed to protect plants products and wood from organisms that may cause them harm or to stop the growth of harmful organisms. Aliphatic hydrocarbons are chemicals with straight or branched chain structures that contain carbon and hydrogen atoms. Long chain aliphatics are usually waxy and of lower solubility in water. This property decreases the rate of biodegradation of these compounds. Aliphatic hydrocarbons are straight, branched or cyclic compounds that may be saturated or unsaturated. These compounds are generally subdivided into alkanes, alkenes and cycloalkanes. Heterocyclic hydrocarbons are also cyclic compounds but contain at least two different elements as members of its rings. These elements include nitrogen, sulphur, oxygen and metals Aromatic hydrocarbons are compounds which differ significantly from aliphatic hydrocarbons as a result of the presence of ring structures. Aromatic hydrocarbons are unsaturated due to the presence of two or more double bonds conjugated to form a ring-like structure. As they tend to be persistent in the environment, inducing increased toxicity in the process, they are the focus of many regulatory bodies.

Petroleum hydrocarbons are comprised of a mixture of hydrocarbons obtained from reservoirs of crude petroleum. These hydrocarbons vary from simple aliphatic and aromatic compounds to complex, polycyclic, aromatic and heterocyclic compounds. Light crude oil mostly contains a higher proportion of aromatic hydrocarbons with a high molecular weight. Petroleum hydrocarbons are large mixtures of chemicals found in crude oil, petroleum products, coal tar and natural gas. Petroleum

hydrocarbon products are made up of blends of distillate fractions obtained from crude oil. These products range from highly refined gasoline to heavy fuel oils and asphalt. The carbon and distillate range of some common petroleum hydrocarbons is given in Table 1.1 below:

Table 1.1 Distillate and carbon range of common petroleum products (Dragun, 1998; Atlas, R.M. , 1991; Atlas, M.T., 1981)

Petroleum products	Distillate range	Carbon range
Jet propulsion fuel (JP4 and JP5)	190°C-260°C	C ₃ -C ₅
BTEX		C ₄ -C ₇
Gasoline	60°C-170°C	C ₆ -C ₁₀
Kerosene	190°C-260°C	C ₁₀ -C ₂₀
Diesel fuel	260°C-360°C	C ₁₀ -C ₂₄

The pollution of soil and water environments by petroleum hydrocarbons is considered a global concern. The increased reliance on crude oil and its products as a result of industrialization as well as technological innovations has set world demand for crude oil and crude oil derivatives to rise from 81 million barrels per day (bpd) to 121 million bpd in 2025 ((USEIA, 2014)). The release of crude oil and derivatives of crude oil into the environment during the production and distribution is harmful to both micro and macro organisms as well as to humans. The impact of the release of these compounds is exacerbated when hydrocarbon compounds are volatile and thus mobile in the environment. Some major petroleum hydrocarbons and their effects on the environment are summarised in Table 1.2 below.

Table 1.2 Toxicological effects of common petroleum hydrocarbons

Components	Effects	References
Jet propulsion fuel (JP4 and JP5)	Damage to pulmonary epithelial cells in rats Chronic exposure may lead to renal damage	(Ritchie et al., 2003)
BTEX	Lymphocytic leukemia in children Liver cancer in adults Damage of blood-forming cells	(Enander, 1995)
Kerosene	Carcinogenicity in mice and rats Toxicity in soil fauna	(Heath et al., 1993)

Iron is ubiquitous in the environment, and being the 5th most abundant metal in the biosphere, it can be found in a combined/oxidised state in most soils environments (Cornell, R. and Schwertmann, 1996). At least 16 different ferric iron oxides, hydroxides, or oxidic hydroxides exist (Schwertmann, U., and Fitzpatrick, R.W., 1992). In many environments, Fe (III) is the most abundant terminal electron acceptor (TEA) for the oxidation of organic matter. Biotic reduction occurs in natural sediments in which the reduction of iron oxides serve as the terminal electron accepting process of organic matter degradation and is usually catalysed by iron-reducing microorganisms (Lovley, D.R., 1997a). The process is referred to as dissimilatory iron reduction and involves the transfer of electrons from microorganisms to external Fe (III), reducing it to Fe (II), thereby acting as an aid to the assimilation of iron into the biomass (Lovley, D.R., 2000). Iron reduction is an important means of mineralisation of organic matter (Kostka, J.E., et al, 2002). This is especially true for anoxic or oxygen-deficient environments where the amount of sulphates and nitrates are inadequate to support sulphate- and nitrogen- reducing conditions (Paul, 2007). Many subsurface organic contaminants which are persistent under oxic conditions may undergo reductive transformation under anaerobic conditions achieved as a result of the redox change between Fe (II) and Fe (III). The electron transfers occurring during iron reduction may support biodegradation of contaminants long after oxygen and nitrates have been exhausted.

1.2 Research aims and objectives

A substantial portion of serious contamination incidents in England and Wales are hydrocarbon-related. The group of hydrocarbons collectively referred to as BTEX (benzene, toluene, ethylbenzene, and xylene) are one of the more common volatile hydrocarbon contaminant groups found in hydrocarbon (gasoline) spill sites and are regarded as contaminants of concern by the UK Environment Agency (Foght, 2008). Benzene in particular is a known carcinogen. BTEX compounds are components of gasoline and aviation fuels and have similar chemical structures which consist of one parent benzene ring (Lueders, 2017; Johnson et al., 2003). The presence of BTEX in hydrocarbon spill sites may be problematic as these compounds are moderately soluble in water. Benzene has been shown to be highly mobile as a result of its higher solubility relative to the other BTEX compounds and is known to be the most recalcitrant of the BTEX group (Johnson et al., 2003). *{Policies on contaminated land in the United Kingdom can be found in Section 57 of the Environment Act (1995) (Pollard and Herbert, 1998). Guidelines for pollutant concentration limits can be found in the Interdepartmental Committee on Reclamation of Contaminated Land (ICRCL) of the Department of Environment*

(*DoE*}). The primary objective of this research was to investigate the mechanisms of intrinsic, iron-mediated degradation of volatile petroleum hydrocarbons in subsurface regions with toluene as a representative compound. Specific objectives of this study were:

1. To assemble experimental analogues of subsurface soils under predominantly iron-reducing conditions using mesocosms consisting of live soil and water.
2. To develop an analytical technique for measuring aqueous-phase toluene in water.
3. To investigate the effect of iron-mediated toluene degradation on pH and total dissolved iron in experimental analogues of subsurface soil environments.
4. To assess the effect of the presence of additional sources of Fe (III) on the rate and amount of toluene removal during the iron-mediated degradation of toluene.
5. To evaluate the impact of soil texture on the amount and rate of toluene removal.
6. To develop a method for determining the source of carbon during toluene removal using stable carbon isotope analysis.
7. To develop a predictive model for the natural attenuation of toluene in soil.

The following hypotheses were tested:

Hypothesis 1: Indigenous soil microorganisms in a previously-contaminated soil may be able to respire anaerobically and couple the reduction of Fe (III) to the oxidation of a hydrocarbon contaminant (toluene).

Hypothesis 2: The process of carbon cycling in soil may change as a result of addition of a hydrocarbon contaminant (toluene).

Hypothesis 3: The addition of extraneous iron sources as terminal electron acceptors can increase the extent / amount of contaminant removal as well as the rate of the reaction.

1.3 Research rationale

It was discovered in the early 1980s that microorganisms exist which are capable of conserving energy for growth from iron reduction (McCarty, 1994; Kuhn, E.P., Coldberg, P J, Schnoor, J L, Wanner, O, Zehnder, A J B & Schwarzenbach, R P, 1985). In more recent times, it has been realised that biological iron redox transformation, rather than abiotic reactions, greatly influence the geochemistry and quality of many aquifer and groundwater environments (Löffler, 2006). The redox transition between the Fe^{2+} and Fe^{3+} ionic species via dissimilatory iron reduction therefore plays an essential role in the biogeochemistry of the subsurface environment. For this reason there is a growing interest in the effect of iron (iii) reduction in the bioremediation of aquifer systems contaminated with metals or hydrocarbons (Kielhorn, 2000; Bouwer, 1983). An interesting feature of iron-reducing conditions is the ability to couple oxidation and reduction of organic contaminants, offering the possibility for the natural attenuation of various contaminant classes via different degradation pathways. Primary subsurface mechanisms (such as advection, volatilisation, dispersion, sorption and diffusion) which may influence the fate and transport of solutes in the vadose zone and groundwater, and ultimately contaminant concentrations in these regions, are not always accounted for during investigation of monitored natural attenuation on contaminated sites. The effect of these competing processes are difficult to isolate individually and may result in complications during bioavailability studies in the field. Laboratory-based mesocosm studies provide a means of avoiding these complications however most studies involve the use of laboratory-synthesised iron and/or incubations of isolated hydrocarbon-degrading microorganisms. This approach does not truly reflect the complex processes that occur in real soil environments. In this study iron-mediated toluene removal was investigated in mesocosms containing live sediment and water under anoxic conditions. The intent of this approach was for the mesocosms to serve as experimental analogues of subsurface environments.

1.4 Thesis outline

This thesis is made up of nine chapters, the content of which is summarised in Figure 1.1.

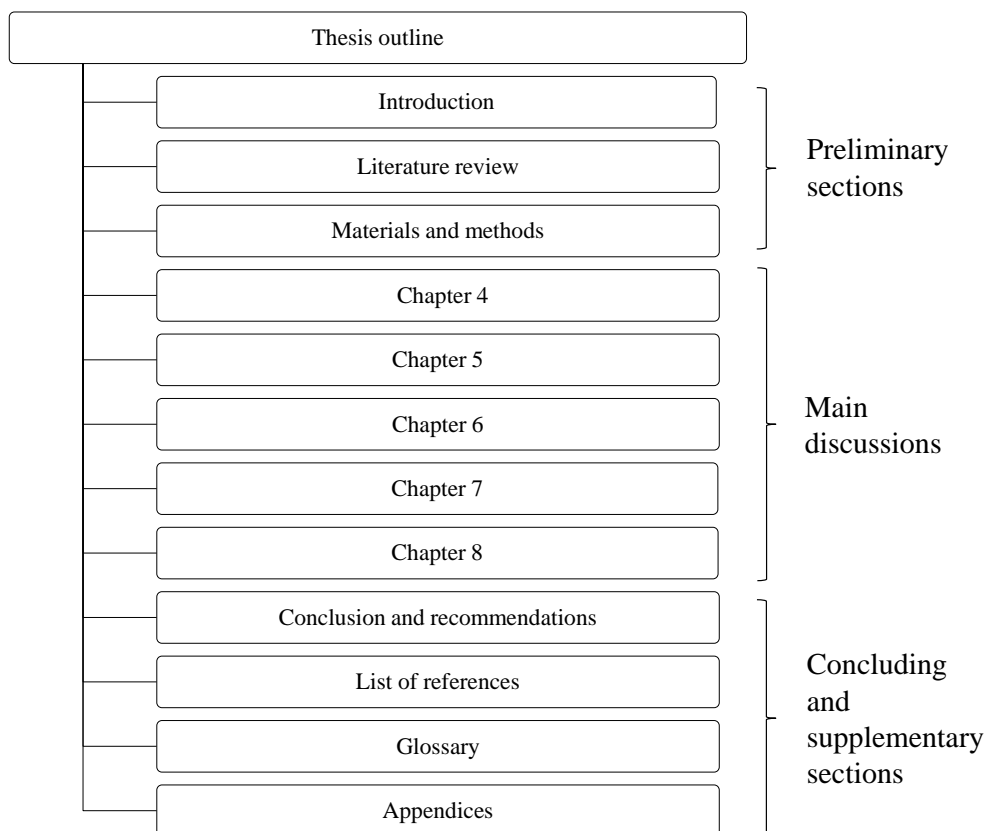


Figure 1.1 Summary of thesis structure

The main objective of this study was to investigate the mechanisms of iron-mediated intrinsic bioremediation therefore a review of current literature related to iron-mediated toluene degradation is provided in Chapter 2 and a documentation of experimental materials and methods used is provided in Chapter 3. The preceding chapters (Chapters 4, 5 and 6) contain a more detailed discussion of the results in the Preamble as well as results of supplementary experiments performed. The following chapters, Chapter 7 and 8 contain fairly novel experimental and analytical approaches relating to the main objectives of this study. In Chapter 7 an approach for analysing soil carbonates using stable carbon isotopes is presented and discussed. Chapter 8 contains a documentation of an analytical approach for creating predictive mathematical models using data obtained from experiments following a repeated measures design.

Chapter 2

Literature Review

2.1 Bioremediation

Many techniques exist for the removal of contaminants and may be classified as physical, chemical and biological methods. Physical methods such as land filling, excavation and incineration are more commonly used however these methods are expensive and cause harm to the environment in the long term. The cleanup of contaminants may be performed ex-situ (also referred to as pump and treat methods) or in-situ. Ex-situ remediation involves pumping of contaminated water or sediment to the surface using a series of extraction wells followed by treatment and re-use/re-injection into the soil. In-situ remediation, as the name implies, is the treatment of the pollutant in place. Remediation techniques currently in use are fully discussed in (Lu et al., 2011), (Megharaj et al., 2011), (Guimarães et al., 2010) and (Shukla et al., 2010). They include rhizoremediation, bioremediation, bioaugmentation through the use of biosurfactants or genetically modified microorganisms, composting, electro-bioremediation and microbe-assisted phytoremediation.

Bioremediation techniques may be intrinsic or engineered. Engineered or enhanced bioremediation applies to contaminated land in which soil conditions are designed to accelerate bioremediation of contaminants. Intrinsic bioremediation (also known as monitored natural attenuation) refers to microbial degradation of soil without any human interference. Monitored natural attenuation is widely adopted for the management of dissolved hydrocarbon plumes, in part, because of the tremendous costs associated with active remediation of thousands of releases from underground storage tanks (USTs). MNA is a passive remedial approach and depends on natural processes to degrade and distribute degraded contaminants in soil and groundwater; it may occur by physical, chemical and biological processes (Kao et al., 2010). Natural attenuation offers a potentially effective and economic clean-up technique through the partial or complete biodegradation of contaminants. Microorganisms have the ability to oxidise, bind, immobilise, volatilise or transform contaminants, therefore bioremediation offers an inexpensive, eco-friendly solution well suited to detoxify these contaminants in soil (George, 2010). For this reason bioremediation is generally preferred over other forms of remediation. However, although it is known that many hydrocarbon plumes biodegrade under ambient conditions without any active remediation, the current understanding of the processes controlling the

intrinsic bioremediation of dissolved hydrocarbon plumes in aquifer systems is limited.

Intrinsic bioremediation of both aromatic and saturated hydrocarbons under aerobic conditions has been well studied and documented for many years. However, the documentation of anaerobic conditions is relatively recent and is constantly generating new insights. There have, in fact, been fewer studies on anaerobic biodegradation of BTEX compounds and other aromatics, when compared to studies carried out under aerobic conditions (Gavrilescu, 2010). Hydrocarbon contaminants mostly migrate with the flow of groundwater forming contaminant plumes. In groundwater systems where organic pollutants accumulate, oxygen is depleted rapidly and the aquifers become anoxic, forming a redox gradient along the groundwater flow path (Christensen, H. et al., 1994; Lawrence, 2006). Intrinsic remediation of BTEX by anaerobic microbial degradation has been shown under sulphate-, nitrate-, and iron-reducing conditions (Kuhn, E.P. et al., 1985; Vogel and Grbic-Galic, 1986; Rabbus and Widdel, 1995; Ball et al., 1996; Hess et al., 1997; Meckenstock, R U, 1999; Rooney-Varga et al., 1999; Coates, J. et al., 2001). The studies showed that a major fraction of groundwater contaminants including BTEX can be degraded in the anoxic zone of plumes, implying anaerobic biodegradation plays an important role in intrinsic remediation of contaminated sites such as contaminated groundwater and deep soils and lake or marine sediments because anoxic conditions prevail in such sites (Christensen, H. et al., 1994; Rabbus and Widdel, 1995; Meckenstock, R U, 1999; Meckenstock, R U et al., 2004; Ramos et al., 2011; Farhadian et al., 2008; Margesin et al., 2003). Intrinsic bioremediation of contaminants is feasible in both field and laboratory studies under aerobic and anaerobic conditions. The experiments that make up the full body of this doctorate research encompass intrinsic bioremediation simulated under laboratory-controlled conditions.

2.1.1 Anaerobic biodegradation

The presence of an electron donor (the organic compound), electron acceptor and contaminant-degrading microorganisms are the main requirements for the bioremediation process. It is well known that microorganisms preferentially use electron acceptors that provide the maximum free energy during respiration. Geochemical evidence suggests that the primary terminal electron acceptors responsible for the decomposition of organic matter in anaerobic sediments are nitrate, Mn (IV), Fe (III), sulphate, and carbon dioxide (Reeburgh, 1983). It is frequently reported that there are distinct zones in sediments in which the metabolism of organic matter is coupled primarily to the reduction of one of these electron acceptors at any one time. The contribution of the electron acceptor is

dependent on the availability of the acceptor in the aquifer and how well the indigenous contaminant-degrading microorganisms are able to utilise it (Spence, M.J. et al., 2005). In these subsurface environments, oxygen is depleted rapidly and anoxic conditions set in quickly. When oxygen is diminished and nitrate is available, nitrate can be used as an electron acceptor by facultative denitrifiers to mineralise the hydrocarbons (Kao et al., 2010). When the available dissolved oxygen and nitrates are depleted, ferric iron-reducing bacteria becomes the next available electron acceptor, which is in turn replaced by sulphate-reducing bacteria when diminished (Nyer and Duffin, 1997). Therefore the redox cascade begins with aerobic conditions (see Table 2.1), followed by nitrate-reducing conditions, manganese-, iron- and sulphate-reducing conditions (Lovley, D.R., 1997b; Christensen, T.H. et al., 2000; Christensen, J.S. and Elton, 1996).

Table 2.1 Electron acceptors in toluene degradation processes showing Gibbs free energy associated with each electron acceptor (Spence, M.J. et al., 2005)

Microbial process	Electron acceptor	Reaction	Free energy change (ΔG_0) at pH 7 (kcal/equivalent)
Aerobic respiration	O ₂	$C_7H_8 + 9O_2 \rightarrow 7CO_2 + 4H_2O$	-29.9
Denitrification (nitrate reduction)	NO ₃ ⁻	$5C_7H_8 + 36NO_3^- + H^+ \rightarrow 35HCO_3^- + 3H_2O + 18N_2$	-28.4
Mn (IV) reduction	Mn (IV)	$C_7H_8 + 18MnO_2 + 29H^+ \rightarrow 7HCO_3^- + 18Mn^{2+} + 15H_2O$	-23.3
Fe (III) reduction	Fe (III)	$C_7H_8 + 36FeOOH + 65H^+ \rightarrow 7HCO_3^- + 36Fe^{2+} + 51H_2O$	-10.1
Sulphate reduction	SO ₄ ²⁻	$2C_7H_8 + 9SO_4^{2-} + 6H_2O \rightarrow 14HCO_3^- + 5H_2S + 4HS^-$	-5.9
Methanogenesis	CO ₂	$2C_7H_8 + 10H_2O \rightarrow 5CO_2 + 9CH_4$	-5.6

The solubility of many petroleum hydrocarbons causes them to spread rapidly and form a plume of contamination that displays a redox gradient (Christensen, H. et al., 1994; Lawrence, 2006). Although the idea of a system with defined biogeochemical zones is oversimplified as a result of the great deal of cross over in vertical stratification (Konhauser, K., 2007; Mortimer, R.J.G. et al., 2004), understanding of the biogeochemical redox processes in a contaminated system is crucial for

predicting the behaviour of contaminant fate and transportation in contaminated aquifer systems. This is because these regions of reduced sediment dominated by anaerobic processes may be difficult to remediate with aerobic bioremediation techniques as a result of the presence of the reduced products of anaerobic metabolism (Christensen, H. et al., 1994; Rabbus and Widdel, 1995; Meckenstock, R U, 1999; Meckenstock, R U et al., 2004; Ramos et al., 2011; Farhadian et al., 2008; Margesin et al., 2003). Contaminants can be eliminated by stimulating the anaerobic community and adding alternative soluble electron acceptors (Christensen, T.H. et al., 2000).

Anaerobic degradation of hydrocarbons in general was first described in (Kuhn, E.P. et al., 1985). Anaerobic bioremediation is slower in comparison to aerobic processes and is therefore most commonly used in the in-situ bioremediation of groundwater contamination, most frequently in monitored natural attenuation (MNA) or intrinsic bioremediation (Nyer and Duffin, 1997). Anaerobic degradation of petroleum hydrocarbons has long been established, including recalcitrant groups (Anderson, 1997; Weiner, J M et al., 1998). The understanding and use of this method has increased rapidly over the past two decades. Contaminated aquifers and subsurface environments are typically anaerobic, many MNA projects demonstrating anaerobic degradation forms a significant part of preliminary assessments, as in (Gieg et al., 2010). In highly anaerobic conditions, fermentation of organic contaminants to methane can occur.


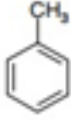
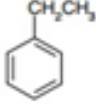
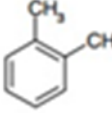
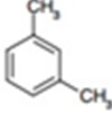
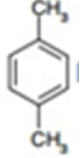
2.1.2 Anaerobic biodegradation of BTEX

Gasoline is a product of many refinery streams composed of a non-specific mixture of hydrocarbons with molecular weights ranging from C₄ to C₁₇ hydrocarbons (Spence, K.H., 2005). Gasoline may contain additives which may be added in relatively small amounts to enhance certain performance characteristics. Common additives include methyl-tert butyl ether (MTBE) and benzene, toluene, ethylbenzene and o-, m- and p-xylenes (collectively called BTEX¹ due to similarities in their chemical structures as well as their fate and transport properties). The proportion of BTEX compounds in gasoline varies quite significantly. The percent volume of benzene, toluene, ethyl benzene and mixed xylenes in gasoline are 1, 1.5, <1-1.5 and 8-10 respectively (An, 2004). (Vieira, 2007) state the percentage by weight ranges from about 10 to 59%. Gasoline spills from road accidents and

¹Benzene and ethylbenzene are IUPAC names. The IUPAC names of toluene and the xylenes are methylbenzene, 1,2 dimethylbenzene, 1,3 dimethylbenzene and 1,4 dimethylbenzene respectively LAWRENCE, S. J. 2006. Description, ²Properties, and Degradation of Selected Volatile Organic Compounds Detected in Ground Water - A Review of Selected Literature. US Department of the Interior

leaking underground storage tanks pose a threat to groundwater sources worldwide. BTEX compounds are of particular concern in the field of soil and groundwater contamination/remediation, as they are among the most abundant toxic organic pollutants in contaminated aquifers (USEPA, 1998; Van Hamme et al., 2003). BTEX compounds, due to their physical and chemical characteristics can be quite harmful when released in large amounts into the environment (see Table 2.2).

Table 2.2 Chemical and physical properties of BTEX (Source:(Weelink, 2010; Kermanshahi pour et al., 2005))²

Properties (unit)	Benzene	Toluene	m-Xylene	o-Xylene	p-Xylene	Ethylbenzene
Chemical structure						
Chemical Formula	C ₆ H ₆	C ₇ H ₈	C ₈ H ₁₀	C ₈ H ₁₀	C ₈ H ₁₀	C ₈ H ₁₀
Molecular Weight	78.11	92.14	106.17	106.17	106.17	106.17
Solubility in water (mg/L)	1785.5	532.6	161.5	171.5	181.6	161.5
Specific density (°C)	0.8765	0.8669	0.8642	0.8802	0.8611	0.8670

BTEX are mono-aromatic hydrocarbons and therefore possess higher solubilities than aliphatic, alicyclic and polycyclic hydrocarbons (Weelink, 2010). Furthermore, these compounds may comprise over 60% of the mass that goes into solution when gasoline is mixed with water (Kermanshahi pour et al., 2005). For this reason they are often the first breakthrough product seen when measuring petroleum contamination of water systems (Houghton and Hall, 2005).

BTEX compounds are mobile and present in water found in aquifer systems as they are not adsorbed by soil (Zytner, 1994; Langwaldt and Puhakka, 2000). They are

known to have acute and long term effects and are toxic to humans when ingested or adsorbed through skin or inhaled (De Burca et al., 2009; Morgan et al., 2009; Mos, 2010). The maximum level for monoaromatic compounds in potable water as stipulated by the USEPA are 0.05, 1, 0.7 and 10 mg/l for benzene, toluene, ethylbenzene and isomers of xylenes, respectively (USEPA, 2006). It is widely accepted that BTEX compounds are a major risk driver in contaminated sites. Benzene is the only known carcinogen in the group (Pohl et al., 2003; An, 2004; Reineke et al., 2006). (De Burca et al., 2009) state toluene has the ability to enhance carcinogenesis by other compounds. Thus BTEX compounds represent a significant environmental threat compared to other major hydrocarbon groups in petroleum-contaminated water (Anderson, 1997; Chakraborty, R. and Coates, 2004).

The ability of BTEX compounds to be degraded under anaerobic conditions and with the use of different electron acceptors has been shown by several studies including (Barbaro et al., 1992; Phelps and Young, 1999; Chakraborty, R et al., 2005). The order of degradation has consistently been observed as toluene < ethylbenzene < o-xylene < benzene. Toluene is considered the least recalcitrant and benzene the most recalcitrant of the BTEX group. Toluene can be degraded relatively quickly, allowing rapid growth of microorganisms under various electron-reducing conditions. This was first demonstrated in (Kuhn, E.P. et al., 1985) using nitrate as an electron acceptor. Anaerobic degradation of toluene has been studied in enriched microcosms and pure cultures using various electron acceptors (Lovley, D.R., Baedeker, M J, Lonergan, D J, Cozzarelli, M, Phillips E J P & Siegel, D, 1989; Evans, P.J. et al., 1991; Fries et al., 1994; Beller, H.R. et al., 1996; Lagenoff et al., 1996).

The three xylene isomers have also been studied under anaerobic conditions using various electron acceptors. (Kuhn, E.P. et al., 1985; Kuhn, E.P. et al., 1988; Haner et al., 1995) carried out studies of p- and m-xylene under nitrate-reducing conditions, (Jahn et al., 2005; Botton and Parsons, 2006) studied p- and o-xylene under iron-reducing conditions and (Edwards and Grbic-Galic, 1992; Morasch et al., 2004; Meckenstock, R U et al., 2004) studied all three isomers after a significant lag period under sulphate-reducing conditions. M-xylene has been found to be the most readily degraded xylene isomer in mixed cultures (Beller, H.R. et al., 1996) however its presence as a co substrate could inhibit p- and o-xylene degradation (Meckenstock, R U et al., 2004). Toluene has also been shown to inhibit o-xylene degradation in sulphidogenic sediment columns and pure cultures. (Meckenstock, R U et al., 2004; Rabbus and Widdel, 1995) report p-xylene as the most recalcitrant to degradation but (Haner et al., 1995) degraded the isomer in a mixture of denitrifying p-xylene selective culture and a sulphate-reducing enrichment culture.

Relatively little is known about ethylbenzene degradation. Its metabolism has been reported in situ and in enrichment cultures under sulphate-reducing (Elshahed et al., 2001) nitrate-reducing (Reinhard et al., 1997) and iron-reducing (Jahn et al., 2005).

Benzene is of major concern as it is highly stable, toxic, and highly soluble. There have been very few studies on enrichment cultures and far less on pure strains (Foght, 2008; Weelink, 2010). Initial studies on anaerobic benzene degradation made use of $^{14}\text{CO}_2$ -, $^{14}\text{CH}_4$ - and ^{18}O - labelled phenol-formation in methanogenic enrichment cultures that had been amended with ^{14}C -benzene and $^{18}\text{H}_2\text{O}$ (Vogel and Grbic-Galic, 1986; Grbic-Galic and Vogel, 1987). The mass balance showed that less than 6% of ^{14}C -labeled benzene was converted to $^{14}\text{CO}_2$. More recent studies (Mancini et al., 2003; Chakraborty, R et al., 2005; Kasai, Y et al., 2007; Kasai, YM et al., 2006) have made use of carbon and hydrogen stable isotope fractionation, 16S rRNA gene-targeted real time PCR, and DNA as well as RNA -based stable isotope probing approaches in petroleum-contaminated aquifers and enrichment cultures from aquatic sediments. There have been studies on anaerobic degradation of benzene in enrichment cultures under methanogenic (Kazumi et al., 1997; Weiner, J M and Lovley, 1998; Mancini et al., 2003) sulphate-reducing (Lovley, D R et al., 1995; Coates, J.D. et al., 1996; Oka et al., 2008; Musat and Widdel, 2008; Kleinstaubert et al., 2008) ferric iron-reducing (Caldwell et al., 1999; Kunapuli et al., 2007) and under nitrate-reducing conditions (Coates, J. et al., 2001; Mancini et al., 2003; Kasai, Y et al., 2007).

2.1.2.1 Pathways of anaerobic degradation: BTEX

The aromatic ring of BTEX hydrocarbons (see Figure 2.1) are a very stable chemical structure that poses significant biochemical demands on contaminant-degrading microorganisms. The degradation of all BTEX compounds follow similar reaction pathways. Studies on metabolic pathways indicate that these compounds are degraded via at least one pathway leading to a substituted catechol; benzene is degraded to catechol, toluene and ethylbenzene to 3-methylcatechol and 3-ethyl catechol respectively, and the xylenes to mono-methylated catechol (Weelink, 2010).

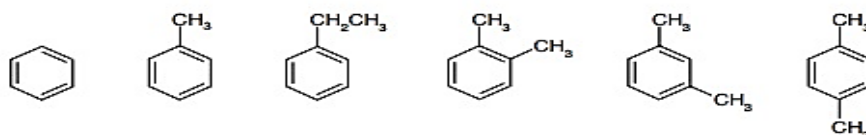


Figure 2.1 Chemical structures of benzene, toluene, ethylbenzene, ortho-xylene, meta xylene and para-xylene (Weelink, 2010)

The benzoyl-CoA pathway for aromatic hydrocarbons is the central pathway that appears to be common in microorganisms (Ramos et al., 2011). The benzylsuccinate synthase involves an enzyme radical reaction that has been reported in denitrifying, sulphate-reducing, anoxygenic phototrophic bacteria, and a methanogenic consortium. The pathway leads to the formation of benzoyl-CoA, the central metabolite of aromatic compounds degraded under anaerobic conditions. This metabolite is formed before ring saturation and cleavage takes place (Field, 2002).

The University of Minnesota Biocatalysis/Biodegradation Database and MetaPuter contains detailed information on the reaction pathways and products of biodegradation for specific hydrocarbons (Ellis, 1998; Pazos, 2004) and can be accessed on <http://umbbdd.ethz.ch/>

2.1.2.2 Pathways of anaerobic degradation: toluene

Toluene is a good model compound for anaerobic BTEX degradation because it is the most readily degraded of the group (Phelps and Young, 1999). Anaerobic biodegradation of toluene has been shown to occur in sub-surface environments where oxygen is a limiting factor. While aerobic degradation is well documented and proceeds at a faster rate, the complete pathway and organisms responsible for each of the steps in anaerobic biodegradation are yet to be fully understood.

Anaerobic bacteria make use of toluene as an energy source and activator for proliferation. Elevated levels of toluene-degrading bacteria at a contaminated site may represent environmental exposure to aromatic hydrocarbons as well as the presence of naturally occurring bioremediation pathways (Chakraborty, R. and Coates, 2004). Toluene is a monocyclic aromatic hydrocarbon made up of a six-carbon ring with a methyl group attachment. In anaerobic biodegradation, microorganisms make use of toluene as a source of energy in reactions where toluene acts as an electron donor and other compounds act as electron acceptors (Ulrich, 2004). The pathway of toluene degradation is illustrated in Figure 2.2.

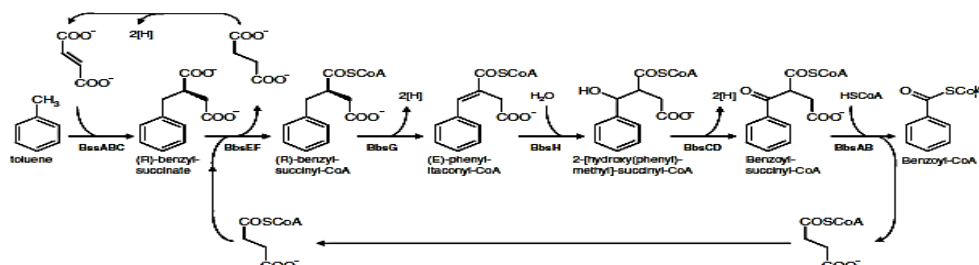


Figure 2.2 Anaerobic toluene degradation route, according to (Kube et al., 2004)
 BssABC, benzylsuccinate synthase; BbsEF, succinyl-CoA:(R)-benzylsuccinate CoA-transferase; BbsG R)-benzylsuccinyl-CoA dehydrogenase; BbsH, phenylitaconyl-CoA hydratase; BbsCD, 2-[hydroxy(phenyl)methyl]-succinyl-CoA dehydrogenase; BbsAB, benzoylsuccinyl-CoA thiolase (Weelink, 2010)

The anaerobic toluene degradation pathway is initiated by the enzyme benzylsuccinate synthase (BSS). The BSS enzyme acts as the catalyst for the addition reaction between methyl carbon and toluene. This reaction occurs across the double bond of a fumarate co-substrate and gives rise to the first intermediate, benzylsuccinate (Biegert et al., 1996; Beller, H. and Spormann, 1997; Leutwein and J. Heider, 2001). The benzylsuccinate intermediate is activated to CoA-thioester by a succinyl-CoA-dependent CoA-transferase (bbsEF) and benzylsuccinyl-CoA is converted to succinyl-CoA and benzoyl-CoA, a recognised central intermediate of many aromatic compounds (Weelink, 2010).

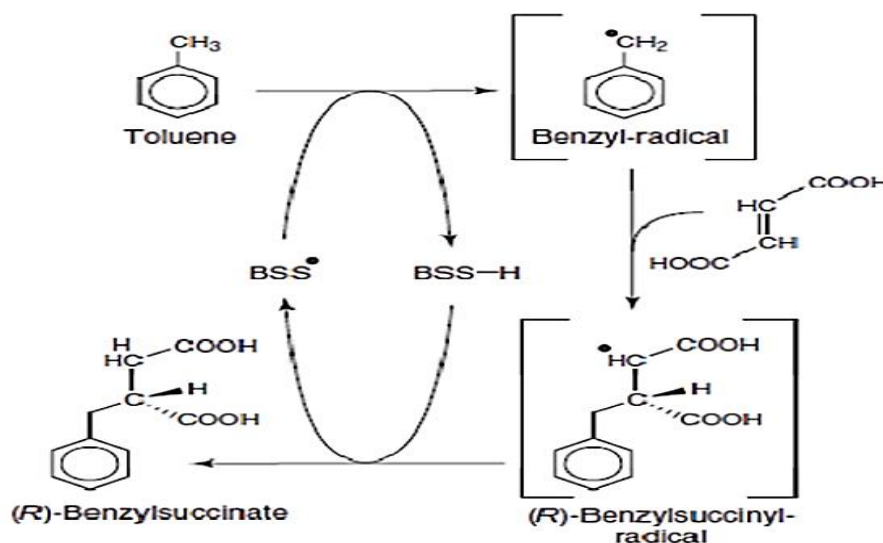


Figure 2.3 Mechanism of toluene activation by BSS. BSS takes a proton from toluene and donates it to benzylsuccinyl radical formed from toluene and fumarate and generates a BSS radical (Boll et al., 2002; Washer, 2004)

The degradation of benzoyl-CoA is initiated by Benzoyl-CoA reductase (bcrCABD) which is further oxidised via reductive ring cleavage to carbon dioxide (Harwood et al., 1999). The benzylsuccinate synthase enzyme (BSS) was first characterised in *Thauera aromatica*. BSS is an enzyme-bound radical that is believed to displace a hydrogen atom from toluene, which forms a benzyl radical intermediate, allowing the addition of the fumarate. The benzyl radical can then be converted to benzylsuccinate by transferring a hydrogen atom from the enzyme (see Figure 2.3). As BSS is used in the first step of toluene degradation, it may be useful for the identification of organisms involved in the initial breakdown of toluene. The presence of a significant amount of RNA encoding the BSS enzyme may indicate enrichment of this culture for one specific organism.

2.2 Iron in soil environments

2.2.1 Iron (hydr)oxides

Iron (hydr)oxides occur in abundance in many soils and sediments and play an important role in microbial redox processes as redox cycling of iron is coupled to many other biogeochemical reactions (Weber et al., 2006). Iron (hydr)oxides or minerals are composed of iron (Fe) together with oxygen (O) and hydroxyl (OH) ions. They are usually collectively referred to as oxides but are actually oxides, hydroxides or oxyhydroxides. Iron oxides are present in several mineral forms, in most soils, as well as in many sediments and weathered materials of various climatic regions (Schwertmann, U., Taylor, R.M., 1989). The iron oxide present in soil is dependent on the moisture content, pH and oxygen content of the soil. Wet, oxic soils generally would have iron existing in the ferrous state while wet anoxic soils would contain iron oxides in the ferric state. The concentration of Fe³⁺ oxides is related to pH and will increase from 10⁻⁸ to 10⁻²⁰ as pH increases from 4 to 8 (Romheld, 1986). At circum-neutral pH, Fe (III) minerals are characterised by low solubility and detectable concentration whereas at neutral or alkaline pH, Fe (II) is stable only in anoxic environments within which it is oxidised to Fe (III) minerals by molecular oxygen and are more soluble at neutral pH, with dissolved concentrations reaching the µM range (Cornell, R.M. and Schwertmann, 2003; Schwertmann, U., 1991). Processes that bring about the mobilisation and fixation of iron in soil will occur either under oxidising and alkaline conditions (to induce the precipitation of insoluble iron Fe³⁺ oxides) or under acidic and reducing conditions (to promote the Fe²⁺ compounds going into solution). The released iron may then precipitate as oxides and hydroxides, although it may also substitute for Mg and Al in other minerals or form complexes with organic ligands. Due to the general stability of the iron oxides, Fe (III) is found as solid phase Fe (III) in natural environments, and in the pH range 4 to 10. The concentration of Fe (III) in the absence of complexing agents is less than 10⁶M (Cornell, R.M. and Schwertmann, 2003).

Currently there are seventeen iron (hydr)oxides known to exist, these (hydr)oxides differ in composition, valence of Fe and crystal structure (Cornell, R.M. and Schwertmann, 2003; Schwertmann, U. and Cornell, 2000). The crystal order of the oxides is variable and dependent upon the conditions under which the oxides were formed. Most iron oxides are crystalline with the exception of ferrihydrite and schwertmannite which are poorly crystalline. The iron oxides are Fe (III)-minerals except FeO and Fe(O)₂ in which iron exists in its ferrous [Fe (II)] state. In terms of their occurrence in the environment, goethite and hematite are the most stable and frequently occurring Fe (III) oxides in soils while lepidocrocite, ferrihydrite and maghemite are common but occur less frequently. Akaganeite and feroxyhyte may

occur rarely or not at all (Schwertmann, U., 1991). Ferrihydrite is considered the most unstable form of Fe (III) while goethite and hematite are the most stable. Ferrihydrite has a high surface area and a structure that is thermodynamically metastable with respect to goethite and hematite. It has been speculated that the occurrence of the less of the stable forms of Fe (III) may be due to the slow formation kinetics of the more stable oxides (Schwertmann, U., 1991). In an oxidising environment, O₂ is the dominant terminal electron acceptor (TEA) and iron will form goethite as the stable mineral or some other hydroxyl phases in a metastable form. In highly reduced environments in which iron is the predominant TEA, high concentrations of sulphur (S₂) will yield pyrite (FeS₂). Low S₂ concentrations in highly CO₃ concentrated environments will yield siderite (FeCO₃) however Fe³⁺ will remain in solution if both S₂ and CO₂ are low (Cornell, R.M. and Schwertmann, 2003).

Table 2.3 Iron oxides, hydroxides and oxyhydroxides (Cornell, R.M. and Schwertmann, 2003)

Oxides (hydroxides and oxyhydroxides)	Oxides
Goethite α -FeOOH	Hematite α -Fe ₂ O ₃
Lepidocrocite γ -FeOOH	Magnetite Fe ₃ O ₄ (Fe ^{II} Fe ₂ ^{III} O ₄)
Akagenieite β -FeOOH	Maghemite - γ -Fe ₂ O ₃
Schwertmannite Fe ₁₆ O ₁₆ (OH) _y (SO ₄) _z .n H ₂ O	β -Fe ₂ O ₃
δ -FeOOH	ϵ -Fe ₂ O ₃
Feroxyhyte δ -FeOOH	Wustite FeO
High pressure FeOOH	
Ferrihydrite Fe ₅ H ₈ .4H ₂ O	
Bernatite Fe(OH) ₃	
Fe (OH) ₂	

Oxides (hydroxides and oxyhydroxides)	Oxides
Green rust $\text{Fe}_x^{\text{III}}\text{Fe}_y^{\text{II}}(\text{OH})_{3x+2y-z}(\text{A}^-)_z$; (A ⁻ = Cl ⁻ ; ½ SO ₄ ²⁻)	

In natural environments, iron oxides may be present as a mixture of several minerals; however ferrihydrite, lepidocrocite, goethite and hematite are considered the most common and may undergo phase transformations. (Zachara, J.M., Cowan, C.E., and Resch, C.T., 1991) showed the formation of lepidocrocite, goethite and hematite from ferrihydrite. The study demonstrated the formation of tiny particles of lepidocrocite and goethite in the presence of a lower electron donor to electron acceptor ratio. When the ratio of electron donors was higher, ferrihydrite was transformed to fine-grained magnetite. (Hansel et al., 2003) observed the transformation of ferrihydrite to the more crystalline hematite and goethite during Fe (III) reduction. The study demonstrated that ferrous iron species formed initially during abiotic oxidation of Fe (II) transform into colloids subsequently forming precipitates of ferrihydrite particles. It was mentioned that further transformations may occur in which ferrihydrite is converted to hematite and subsequently to goethite. Another study (Kappler, 2004) observed declining pH values during the transformation of ferrihydrite to goethite by Fe (II) oxidising bacteria. The observed phase transformations were attributed to structural rearrangement of iron and the transfer of electrons between iron and oxygen. Iron oxides possess the ability to undergo phase changes between different phases due to their thermodynamically unstable nature. It has been proposed that the presence of Fe²⁺ from Fe (III) reduction or some other source, may catalyse the transformation of ferrihydrite and lepidocrocite to the more crystalline-phase lepidocrocite and goethite (van Oosterhout, 1967; Schwertmann, U., and Taylor, R.M., 1973) or to the mixed valence Fe (II)-Fe (III) mineral magnetite (Sorensen and Thorling, 1991). The transformation of ferrihydrite and lepidocrocite to more crystalline phases or magnetite has been observed as far back as 1967 (van Oosterhout, 1967). The effect of this transformation could be that the Fe²⁺ initially produced during the reduction of ferrihydrite could cause a transformation of ferrihydrite and other iron oxides into less reactive phases. This transformation results in the decreased reactivity of the iron pool, decreasing or even terminating further bio reduction. Although Fe³⁺ is

generally known to be less soluble than Fe^{2+} at higher pH levels, it is possible for Fe (III) oxide to go into solution in the presence of a ligand. Fe^{2+} has been shown to catalyse the dissolution of Fe (III) oxides including ferrihydrite, and goethite (Hering, 1990; Ballesteros et al., 1998), hematite (Hering, 1990; Sulzberger, 1989) and magnetite (Hering, 1990). It was observed, in these studies, that the concentration of Fe^{2+} did not change however increases in the concentration of Fe^{3+} were observed. This is of great significance, especially in the field where the production of Fe^{2+} in an anaerobic environment may catalyse further dissolution and mobilisation of Fe.

Five iron minerals were used in this study namely hematite, goethite, ferrihydrite, lepidocrocite and magnetite. Hematite is blood red in colour and being one of the most thermodynamically stable iron minerals, is found widespread in rock and soil. Goethite is yellow in colour and also thermodynamically stable at ambient temperature. Ferrihydrite is reddish brown with a generally poorly ordered crystal structure and is commonly termed 'amorphous iron oxide' or 'hydrous ferric oxide'. Lepidocrocite is an orange-coloured mineral that is a common product of the oxidation of Fe^{2+} . Magnetite is a black coloured, ferromagnetic mineral oxide considered to be a mixed phase (Fe (II)/Fe (III)) iron mineral. These minerals are fully described in (Schwertmann, U. and Cornell, 2000) and (Cornell, R.M. and Schwertmann, 2003).

2.2.2 Biogeochemical cycling of iron

The pathways in which chemical elements move through biotic and abiotic components of the earth are demonstrated by biogeochemical cycles. These cycles consist of a system of inputs, outputs, sources and sinks in which elements are moved, used, transformed and reused between the biotic and abiotic components of the environment (Perez-Guzman et al., 2012). Common element cycles include the carbon, nitrogen, oxygen, phosphorous, sulphur, and the water cycle. However, the iron cycle is another important biogeochemical cycle. This is because iron as an element is critical for countless cellular processes and metabolic pathways in eukaryotic and prokaryotic organisms (Tobler, 2007). Furthermore iron, being a micronutrient is used by both macro and microorganisms in carrying out essential life processes such as respiration, photosynthesis, nitrogen-fixing and transportation of oxygen in the blood. Despite the important role iron can play in the natural environment, it may be in short supply for organisms because of the redox changes it undergoes that affect its availability. In soils the concentration of iron oxides ranges from less than 0.1% to over 50% and may be evenly distributed through the soil or occur as discrete concentrations. The crystal size of iron oxides range from very small (5 nm) to relatively large (150 nm). Iron may be released from Fe (III)

oxides as a result of three main reactions namely protonation, reduction and complexation (Schwertmann, U., 1991). Fe (III) oxides display low solubility, unlike under other oxidative regimes, reducing conditions lead to the dissolution of iron (Chuan et al., 1996; Tessier, A. et al., 1996). This results from the reduction of less mobile iron (iii) to mobile iron (ii) (Schwertmann, U., 1991; Schwertmann, U and Taylor, 1979). In reduced sediments or soils, iron (ii) is oxidised back to iron (iii), usually forming a solid precipitate due to its insolubility. Heavy metals that may have been liberated from other components will be co-precipitated with the metal oxides and become incorporated into the structure (Turner and Olsen, 2000; Calmano et al., 1993). Thus iron undergoes redox transformations as it is cycled in the environment (Stucki et al., 2007). In its pure state iron is a reactive metal that oxidizes readily in the presence of oxygen or water and thus elemental iron (Fe or Fe⁰) is not found in the natural environment. In its combined or oxidised state, it exists as reduced ferrous iron (Fe²⁺), or oxidized ferric iron, (Fe³⁺). These iron forms exist in nature as solids in the form of Fe (III) - and Fe (II)-bearing minerals or as ions (Fe³⁺ and Fe²⁺) dissolved in water. Iron is ubiquitous in sedimentary environments and can be found in a combined/oxidised state in clay minerals of most soils and sediments (Cornell, R.M.a.S., U., 1996). To a large extent, redox transformations of iron as well as dissolution and precipitation, mobilisation and redistribution are chemically-induced; however they may also be attributed to microbial processes. This would suggest that many of the Fe (II), Fe (III) and mixed Fe (II)-Fe (III) minerals found in nature occur as a result.

2.2.3 Microbial iron reduction

Microorganisms are able to reduce metals (Lovley, D. R., 1991), releasing electrons as a result of the oxidation of organic and inorganic compounds which are transferred to oxygen via an electron transport chain which generates energy in the form of adenosine-5'-triphosphate (ATP). Several microorganisms have the ability to conserve energy through the dissimilatory reduction of iron. This process involves the use of Fe (III) as either the dominant or exclusive terminal electron acceptor. The process occurs mostly under anaerobic conditions with ferric iron being reduced to ferrous iron. *Shewanella oneidensis* (formerly *Alteromonas putrefaciens*) (Lovley, D.R., Baedecker, M J, Lonergan, D J, Cozzarelli, M, Phillips E J P & Siegel, D, 1989) and *Geobacter metallireducens* (formerly strain GS-15) (Lonergan et al., 1996) were the earliest organisms identified to grow through iron reduction. Many strains have consequently been identified as iron reducers most of which belong to the *Geobacteraceae* family (this family includes the genera *Geobacter*, *Desulfuromonas*, and *Pelobacter*) and are able to oxidise a range of compounds coupled to the reduction of Fe (II) (Lloyd 2003). Iron reduction plays an important

role in the remediation of higher valence contaminants, including radionuclides, and may potentially be reduced via biogenically produced Fe (II) (Lloyd et al., 2000).

Dissimilatory Fe (III) reducing bacteria that gain energy by coupling the oxidation of hydrogen or organic compounds to the reduction of ferric iron oxides have been known for many years but their biogeochemical importance was only recently recognised. Dissimilatory iron reduction has been shown to occur in both fresh water (Lovley, D.R., 1997a) and marine environments (Poulton et al., 2004). Processes that bring about the mobilisation and fixation of iron in soil will occur either under oxidising and alkaline conditions (to induce the precipitation of insoluble iron Fe^{3+} oxides) or under acidic and reducing conditions (to promote the Fe^{2+} compounds going into solution). The released iron may then precipitate as oxides and hydroxides, although it may also substitute for Mg and Al in other minerals or form complexes with organic ligands (Kabata-Pendias, 1992).

In contaminated sites, the reduction of iron may influence the geochemistry of a site through the release of metals bound to Fe (III) minerals (Zachara, John M. et al., 2011; Zachara, J M et al., 2001). The potential for the biostimulation of microbial metal-reducing microorganisms in contaminated sites have been shown in several studies. Biostimulation was induced through the addition of different electron donors including acetate, glucose, yeast extract, lactate and H_2 (Stucki et al., 2007; Lovley, D.R., 1997a; Vrionis et al., 2005). Microbial iron reduction has been shown in a wide range of environments from natural high to low pH environments (Pollock et al., 2007; Zhilina et al., 2009).

2.3 Chemical speciation

Chemical speciation is defined as '*the distribution of an individual chemical element between different chemical species or groups of species*' (Tessier, A et al., 1994). Speciation may be defined functionally e.g. the plant-available fraction of a specific element extracted or quantified or operationally in which the extraction technique is used to extract an element associated with a particular element. Functional speciation is generally performed with a single extractant (Förstner, 1993) while operational speciation is performed with sequential extraction to provide an operational speciation scheme (Tessier, A. et al., 1979; Sahuquillo et al., 1999). The speciation of an element may be defined in terms of its i) physical attributes, ii) complex lability and size calculated indirectly from mass transport and iii) diffusion or free activity or potential concentration at equilibrium (Ure and Davidson, 2008). Speciation analysis is a multidisciplinary method which can be applied in studies of biogeochemical cycles of chemical compounds, quality control of food products, clinical analysis, and determination of toxicity of elements to mention a few (Kot

and Namiesnik, 2000). Speciation provides information that aids the understanding of processes such as mobilisation, transport and transformation of trace elements. The determination of the various mechanisms of binding provides insights into the mobility, availability or toxicity of the speciation of an element i.e. the distribution of its bound state in comparison with the total element content. Speciation of metals (including iron) in soils are controlled by several factors including pH, cationic exchange capacity (CEC), redox potential, and the presence of surfactants (Andersen and Engelstad, 1993; Lasat, 2002).

When the main objective is to quantify the elements in specific phases of a soil or sediment matrix, a series of single extractants may be used in combination in a sequence of extractions. Speciation will involve subjecting a solid sample to successive attacks using reagents of varying chemical properties, in order to partition the trace element content, with each reagent added being more 'vigorous' than the previous. The total or pseudo-total content of an element is not adequate to reliably predict the behaviour of elements in the environment however chemical extraction procedures can determine both bound and total content of element species (Tokalioglu, 2003). These procedures are important in speciation studies and are used in assessing availability of natural elements to plants, as well as in the study of contaminated soils and sediments. In contamination studies, heavy metals such as iron may act as both a sink and source particularly where there is heavy contamination or where environmental conditions undergo constant changes. In unpolluted soils or sediments iron and other trace metals can be found bound to silicates and minerals, forming immobile species. In polluted environments, iron may be more mobile and bound to other soil or sediment phases (Rauret, 1998). If soil is viewed as being comprised of pools of elements with different mobilities and solubilities that can be extracted by reagents with different strengths six pools may be distinguishable namely i) the water soluble fraction ii) the exchangeable and weakly adsorbed fraction iii) adsorbed, chelated or complexed ions exchangeable by other cations with high affinities for exchange sites (or extractable with strong chelating agents) iv) micronutrient cations in secondary clay minerals an insoluble metal oxides v) cations in primary minerals vi) the pools collectively held (i.e. the total amount of the element in the soil). Therefore the first target species are those in solution or in sediment pore water, or loosely attached at cation-exchange sites in soil water medium. This is followed by the carbonate phases, the mineral bound phases and phases bound to organic matter (Rao et al., 2008). Extractant reagents for single extractions may be classified as i) acid reagents of varying concentrations (HCl, HNO₃, aqua-regia, acetic acid, acid mixtures etc.) used singly or with chelating agents (EDTA (ethylene diamine tetra-acetic acid), DTPA (diethylene tri-amine penta-acetic acid) ii) buffered salt solutions) ii) weak neutral salt extractants

ii) aqueous solution iv) enzymes. Several sequential procedures exist, however the best known are the Tessier extraction procedure and the Community Bureau of Reference (BCR) scheme, a more recent methodology designed to create a sequential procedure that is universal to all scientific communities. Each scheme has its limitations and the choice of a reagent will depend largely on the type of soil and target element.

2.4 The isotope geochemistry of carbon cycling in soils

2.4.1 Stable carbon isotopes in soil environments

The major elements associated with organic compounds include carbon, hydrogen, nitrogen, oxygen and sulphur. Each of these elements have at least two stable isotopes that can be distinguished with the use of mass spectrometry. The chemical and physical properties of stable isotopes are nearly identical, however slight differences sometimes arise as a result of the quantum mechanical effect which is also dependent on the zero-point energies of the heavy and light isotopes. The higher zero-point energy of the lighter isotope suggests the chemical bond formed by a lighter isotope is weaker than that formed by a heavier isotope (Meckenstock, R U et al., 2004). A lighter isotope will react more rapidly than the heavy one, thus the product will be depleted in the heavier isotope. This is known as the kinetic isotope effect (KIE). So, a kinetic isotope effect occurs when an isotope reacts more rapidly than another in an irreversible system or a system in which the products are quickly used up before the reactant have the opportunity to reach equilibrium. Greater energy is required to break bonds containing a heavier isotope in an isotopic fractionating process, therefore molecules containing a lighter isotope will react at a slightly faster rate than those with a heavier isotope. In most cases, the heavier isotope will be concentrated in the component with the stronger bond with the element in question. Therefore equilibrium isotope effects reflect the relative differences in the bond strengths of isotopes in various components of a reversible system in equilibrium. In the event that the heavier isotope concentrates in the component of interest, that component is referred to as enriched or heavier. Biodegradation often causes a substantial kinetic isotope effect (Day et al., 2002). Light isotopes possess weaker bonds resulting in preferential enrichment of these isotopes in the product of a reaction. Heavy isotopes on the other hand accumulate in the non-reacted material. Thus degradation of contaminants may produce an increase in the proportion of heavier isotopes (Day et al., 2002). Isotopic fractionation therefore controls the isotopic compositions of different carbon reservoirs in environmental systems (Newton and Bottrell, 2007). Volatile organic compounds, including BTEX are strongly fractionated during degradation

(Hunkeler, D et al., 2001). These fractionation processes make it possible to obtain information on processes affecting the contaminant as well as the extent of this effect.

Isotopic fractionation of carbon makes it possible to distinguish between organic and inorganic carbon compounds. Using mass spectrometric analysis, these compounds can be differentiated by their isotope abundance relative to a standard. The isotope abundance of a compound may be indicated by an isotopically light (negative δ) or heavy (positive δ) signal. In stable isotope convention, a negative δ in an experimental observation is indicative of the sample being depleted in the less common isotope relative to the standard (usually Vienna Pee Dee Belemnite i.e. VPDB). A positive δ is indicative of a sample in which the less common isotope is in greater abundance compared to the standards (Schmidt et al., 2004). For example, crude oil possess a light isotope signature which, in stable isotope sign convention, is denoted by numerical values along the lower negative end of the $\delta^{13}\text{C}$ scale (see Figure 7.1). Marine carbonates on the other hand possess a heavier isotope signature in comparison denoted by numerical values closer to the positive end of the $\delta^{13}\text{C}$ scale.

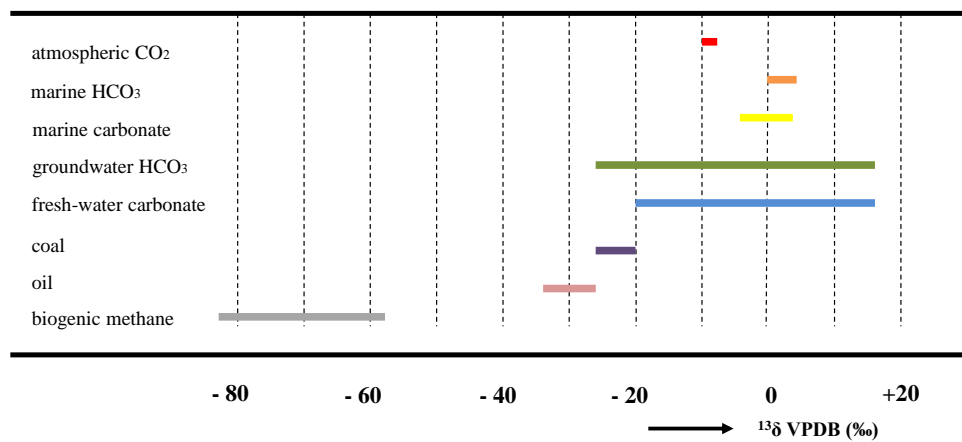


Figure 2.4 Overview of stable carbon isotopic composition of common organic and inorganic material showing relative positions on a $\delta^{13}\text{C}$ scale

Samples for stable isotope analysis come in the form of organically-bound carbon, carbonate (inorganic) carbon, or CO₂ gas. Organically-bound carbon is isotopically light i.e. it produces $\delta^{13}\text{C}$ values on the lower negative end of the $\delta^{13}\text{C}$ scale. Toluene for example has $\delta^{13}\text{C}$ values ranging between -25.8 and -29.0 ‰ (Dempster et al., 1997; Harrington et al., 1999). Inorganic carbon is isotopically heavier in comparison. Soil carbonates which have $\delta^{13}\text{C}$ values ranging between single-digit negative figures to 0 ‰ and above (Boutton, 1991). A study by (Cerling et al., 1989)

demonstrate modern soil carbonates differ systematically from coexisting soil organic matter by 14 to 16‰ in undisturbed soils from humid regions. Generally, soil CO₂ is approximately 5% more enriched in ¹³C than the associated vegetation and soil organic matter. This may be the result of differences in diffusion coefficients for ¹²CO₂ and ¹³CO₂ in air which allow more rapid diffusion of ¹²CO₂ from the soil than ¹³CO₂ (Quade et al., 1989). Soil CO₂ is derived from root respiration, decomposition of soil organic matter, and at least in the upper 30cm of the profile, diffusion of atmospheric CO₂ in the soil (Quade et al., 1989). In freshwater systems, dissolved carbonates show variable isotopic composition, mainly due to the variety of carbonate species present in freshwaters. These include biogenic sources such as CO₂ from bacterial oxidation of organic matter in soils or from freshwater plankton (Pawellek F, 1994; Cameron et al., 1995). In freshwater lakes and ponds the δ¹³C may vary depending on (i) the extent to which atmospheric CO₂ is in equilibrium with the water mass (ii) seasonal rates of photosynthesis and respiration (iii) the input of CO₂ from decomposition of ¹³C-depleted terrestrial detritus present in the lake (iv) the contribution from dissolution of ¹³C-enriched carbonate rock (Oana and Deevey, 1960). Freshwaters generally have lower total dissolved inorganic carbon in comparison to marine systems as a result of the presence of ¹³C-depleted CO₂ derived from decomposition of terrestrial organic matter. Freshwaters have been shown to have a δ¹³C range of -15 to 0‰ while rivers have a range of -15 to -5‰ (Fry, 1984). Stable carbon isotope ratios of dissolved inorganic carbon (CO₂, HCO₃⁻, CO₃⁼) in groundwater at the water table depend on the δ¹³C of soil CO₂ and the δ¹³C of dissolved carbonate originating from parent materials (e.g. limestone, which is relatively enriched in ¹³C at 0‰), meaning groundwaters could range from approximately -30 to 0‰ but are mostly found in the -25 to -10‰ range (Fritz et al., 1978). The range of values obtained from the soil and river water used in the mesocosms are representative of freshwater environments.

2.4.2 Reactions of carbonates in soils

Carbonates are often found as limestones on the Earth's surface (Ehrlich, 1998). Thus a significant portion of these carbonates are of biogenic origin. Carbonate minerals tend to be one of the most common groups of non-silicate minerals and can be found in several rock types. At least 277 carbonate-containing minerals occur in nature and are broadly classified as shown below (Railsback, 1999):

- Pure carbonate minerals
- Carbonate-containing minerals with chlorides, sulphates or fluorides
- Carbonate-containing minerals with phosphates or silicates
- Carbonate-containing minerals with two or more other anions

Dolomite, calcite and the iron carbonate siderite are the most common carbonate minerals found in soil. Dolomite is the most abundant of the over fifteen $R\bar{3}$ carbonates, five of which have the dolomite structure (Lackner, K.S. et al., 1995). Dolomite has a similar structure to that of calcite however with a lower degree of symmetry. The CO_3 group is the fundamental building block of carbonate minerals with a constant basic configuration. Several chemical elements form chemical bonds with this oxyanion group however calcium (Ca) and magnesium (Mg) are the two most commonly available chemical elements that form stable, poorly soluble carbonate minerals i.e. calcite, magnesite and dolomite (Lackner, K.S. et al., 1995). A list of carbonate-containing minerals is available in http://www.gly.uga.edu/railsback/CO3mins_intro.html as well as an appendix in the paper by L B Railsback titled 'Patterns in the Compositions, Properties, and Geochemistry of Carbonate minerals'. Extensive reviews of the two major carbonate minerals, calcite and dolomite can be found in (Goldsmith, 1990; Reeder, 1990; Wenk et al., 1990).

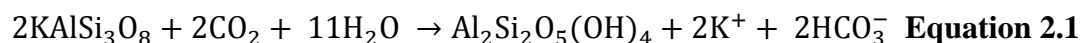
The total carbonate content in soil represents the organic and inorganic carbonate minerals consumed, produced and mobilised by biotic and abiotic processes. This carbonate fraction is mostly used in reference to the amount of carbonates in solid matter, however, a substantial proportion rapidly turned over through a soil solution ultimately becomes CO_2 in gaseous phase (Manning, 2008). Generally, organic carbon is differentiated into labile (rapid turnover) and recalcitrant (slow turnover) pools, with differing chemical reactivity and residence times. Inorganic carbon is composed of Ca- and to a lesser extent Fe- and Mg-carbonates (Schlesinger, 1982). In aquifers, the direct contact of CO_2 with groundwater lowers the pH of the environment. Carbon dioxide is a normal component of all natural waters, however it is typically introduced via absorption from the atmosphere. In the geologic sequestration of CO_2 , the naturally occurring carbonate minerals may provide a constant, inexhaustible source of alkalinity for converting CO_2 to bicarbonate salts.

Several microorganisms have the ability to deposit calcium carbonates (Verrecchia et al., 1990; Barua et al., 2012). Where carbonate precipitation is microbially-mediated, the process is referred to as bio-precipitation or bio-mineralisation. Bio-mineralisation is the removal of mobile contaminants from solution via the biological production of the precipitating chemical species. The process brings about the precipitation of a wide range of minerals including sulphates, phosphates, silicates and oxides (Barkay and Schaefer, 2001; Warren et al., 2001). Four groups of microorganisms have been observed to be involved in the process of bio-mineralisation (Hammes and Verstraete, 2002; Stocks-Fischer et al., 1999). These include (i) photosynthetic organisms, including cyanobacteria and algae, (ii)

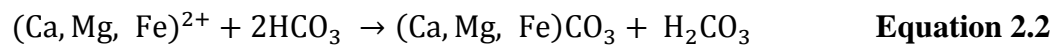
sulphate-reducing bacteria (iii) organisms utilising organic acids (iv) organisms involved in the nitrogen cycle Microorganisms including cyanobacteria and ureolytic bacteria are capable of enabling mineral formation (Ferris et al., 2003). Most cyanobacteria are able to precipitate carbonate minerals by photosynthesis. Microbial photosynthesis accelerates carbonate mineral precipitation by generating an alkaline aqueous environment. As described above this alkaline environment is as a result of hydroxyl (OH⁻) ions which increase the pH of the solution and allow for more dissolution of CO₂ in water, creating carbonate ions and increasing carbonate mineral saturation in the process. These carbonate minerals react with cations in solution to precipitate carbonate minerals.

The earth is composed of many elements however only eight (Si, O, Al, Ca, Mg, K, Na and Fe) compose a significant part (98%) of its crust (Reimens and de Caritat, 1998). During weathering processes of exposed silicate outcrops, the elemental components are released into the environment, transported or precipitated. Ca²⁺ and Mg²⁺ may be leached and transported in solution, with some of its content reacting with carbonate anions formed from CO₂ dissolution in soil pore waters or in the surface ocean.

Divalent cations including Mg²⁺ and Fe²⁺ are commonly found in phyllosilicates such as glauconite and clinichlore. Ca²⁺ is commonly found in the plagioclase solid solution series (i.e. albite to anorthite). Silicates and carbonates tend to have a much higher abundance in nature. Silicates will react with CO₂ by forming carbonates and bicarbonate salts in solution (Lackner, K S, 2002). Silicate minerals are more effective than carbonate minerals for the reduction of atmospheric carbon dioxide. The weathering of some common silicate minerals is shown in Equations 2.1 and 2.2 below:

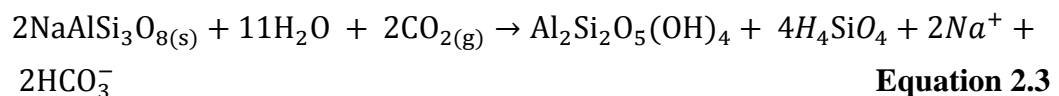


(feldspar)

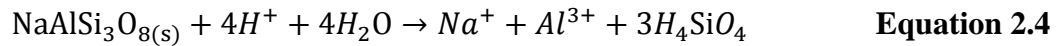


(calcite, magnesite, siderite)

The theoretical reaction for the mineralisation of albite follows the reaction in Equation 2.3 below:



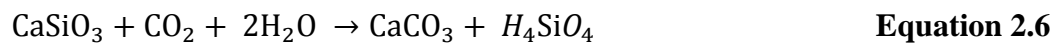
Gibbsite is the absolute end product of silicate mineral weathering. Equation 2.4 shows the dissolution of albite and 2.5 depicts the subsequent equilibrium equation for gibbsite (Appelo et al., 1996).



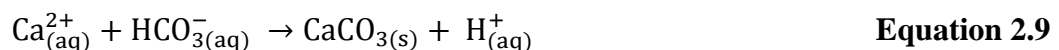
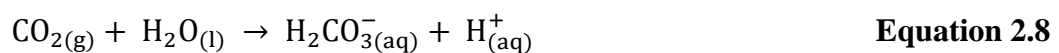
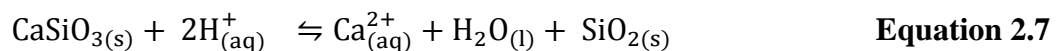
(gibbsite)

The dissolution rate depends strongly on pH and is least soluble at neutral pH (Appelo et al., 1996). Elevated PCO_2 in solution will lead to the dissolution of albite. A similar effect is observed for feldspars and other alumina-silicate minerals.

Solid carbonates such as calcite (CaCO_3), magnesite (MgCO_3), siderite (FeCO_3) and the sodium aluminium carbonate, dawsonite ($\text{NaAl}(\text{OH})_2\text{CO}_3$) are formed by slower precipitation processes that occur over long geological times. In geological formations, sediments and soil constitute an erosion-sedimentation-cycle composed of solid carbonate rock \rightarrow soil \rightarrow fluvial sediment \rightarrow estuarine sediment \rightarrow marine sediment \rightarrow salt marsh. Calcium and magnesium can be precipitated as carbonate minerals calcite (CaCO_3), aragonite (CaCO_3), magnesite (MgCO_3), or dolomite ($\text{CaMg}(\text{CO}_3)_2$). Carbonates formed in soils as a result of pedogenic processes occur as re-mobilised minerals from the bedrock (Goudie, 1996). These processes will lead to the precipitation of pedogenic and marine carbonates which aids the storage and capture of carbon (Berner et al., 1983). Equation 2.6 shows the precipitation of carbonates brought about by weathering of the silicate mineral wollastonite (CaSiO_3).



A breakdown of the reaction sequence is shown in Equations 2.7-2.9 below:



Carbon dioxide reacts with water to form carbonic acid which then reacts with the carbonate mineral (in this case calcite) generating calcium and bicarbonate ions. The extent to which these reactions will occur is dependent on the equilibrium pH. A plot of the equilibrium concentrations of CO_2 , carbonate and bicarbonate species (known as a Bjerrum plot) demonstrates the effect of pH on carbon-bearing chemical species. Under acidic conditions ($\text{pH} < 6$), $\text{CO}_2(\text{aq})$ is the more dominant species however under strongly alkaline conditions ($\text{pH} > 10.5$), carbonate and bicarbonate species are more dominant (Mitchell and Ferris, 2006). The reaction for the silicate mineral above (wollastonite CaSiO_3) induces an acidic environment as a result of the H^+ ions produced. This acidic environment favours each of the reactions. Weathering processes are slow, with timescales at natural conditions of thousand to millions of years. In weathering processes, eroded rock surfaces come

into contact with rainwater that has been saturated with dissolved atmospheric CO₂. The alkali and alkaline earth elements (Na, K, Ca and Mg) subsequently dissolve into the water and eventually form carbonate mineral (Huijgen, 2007). Weathering processes have been shown to be accelerated by biological processes. (Manning, 2008) state the mixing of calcium / magnesium-rich silicate minerals into the soil profile forms carbonate mineral precipitates where the carbon is dissolved CO₂ in equilibrium with soil pore gas from either organic matter degradation or diffusion from the atmosphere. The precipitation of carbonates is therefore influenced by pH, CO₂, partial pressure (PCO₂), alkalinity, temperature, carbonate, bicarbonate and metal ion concentrations (Chou and Garrels, 1989; Dromgoole and Walter, 1990; Pokrovsky and Golubev, 2009). Reviews on the chemistry / geochemistry of carbonate minerals can be found in (Railsback, 1999).

2.5 Modelling repeated measures data

2.5.1 Repeated measures experiment designs

The act of planning or designing experiments allows the experimenter to take into account the influence of different parameters that may influence the main observation in the experiment (Ryan, 2006; Leik, 1997). Experiment designs fall into two broad categories namely i) screening designs, and ii) optimisation designs (Krauth, 2000; Verma, 2015). The most common screening design is the factorial and Plackett-Burman design while the central composite design is considered the most common optimisation method. Full factorial designs are used in studies with a few number of variables and small number of experiments. The central composite design often finds application in response surface modelling and optimisation and is, in some cases, an extension of a previous factorial design for which response surfaces enable the optimum for value of each variable to be determined (Hinkelmann and Kempthorne, 2008).

Statistical testing through the use of experiment designs involves one or more tests in which changes are made to input variables of a process or system in order to make conclusions about the reasons for change in output or to identify the sources of variability in the process (Montgomery, 2006; Gliner et al., 2009). Statistical tests may be performed on simple comparative designs, single-factor experiments, or factorial design experiments (Ryan, 2006; Quinn and Keough, 2002). Simple comparative experiments compare two treatments or conditions to make inferences about the difference in means of two populations. This comparison is achieved using either a two sample t-test or a paired t-test (Blaikie, 2003; Marsh and Elliott, 2008). Single-factor experiments compare the effect of two treatments using two levels of the same factor or more than two levels in some cases. Factorial designs are used in

the study of the effects of two or more factors and are considered the most effective for situations as they take account all possible interactions between factors. Two-factor and 2^k factorial designs are common factorial designs.

Data obtained from experimental or observational studies in which data is collected over several points in time are referred to as repeated measures data (Taris, 2000; Verma, 2015; Nemec and Branch, 1996). Repeated measures data are of three main types namely i) Time series data which involve many observations (large t) on as few as one unit (small n), ii) Pooled cross sections which consist of two or more independent samples of many units (large n) drawn from the same population at different time periods, and iii) Panel data which consists of two or more independent samples of many units (large n) drawn from the same population at different time periods. (Verma, 2015; Crowder and Hand, 1990; Islam and Chowdhury, 2017). In statistics and econometrics, the term panel data (or longitudinal data) refers to multi-dimensional data frequently involving measurements over time (Diggle, 2002; Singer and Willett, 2003). An alternative description of these three types of repeated measures data may be made in terms of the number of observations, individuals and time points over which observations are made. In this context, time series data may be regarded as a collection of observations (behaviors) for a single subject (entity) at different time intervals (generally equally spaced). Cross sectional data can be seen as a collection of observations (behaviour) for multiple subjects (entities) at a single point in time while panel data can be taken to be a combination of the above mentioned types i.e. collection of observations for multiple subjects at multiple instances .

2.5.2 General linear models

Classical general linear models (including regression analysis, analysis of variance or ANOVA, and analysis of covariance or ANCOVA) or GLMs are used as statistical tools for experiments with continuous variables and are naturally studied in the framework of the multivariate normal distribution. Correlated data arise frequently in statistical analysis. Correlation is a form of standardized covariance i.e. if the covariance is divided by the product of the two standard deviations (i.e. the square root of the variances), the correlation coefficient is obtained (Myers et al., 2013). Correlation may arise due to grouping of subjects or repeated measures on each subject over time or space (as is the case in the repeated measures experiment design of the degradation experiments in this study) or due to multiple related outcome measures at one point in time. Classical methods capture some part of the estimated coefficient however the correlation in error terms are not adequately explored (Judd et al., 2011; Howitt and Cramer, 2003).

2.5.3 Mixed effects models

Linear model estimation for panel data is based on the classical general linear model (West et al., 2014). Parameter estimation for these models are determined over two main steps that involve i) the estimation of parameters using ordinary least squares and ii) estimation of parameters using generalized least squares. Estimation of parameters using mixed models is performed over two or more steps which include modeling i) independently pooled panels, ii) fixed effects (first difference models), and iii) random effects. A mixed effect model incorporates the fixed effects assumption (i.e. that the individual specific effects are correlated with the individual variables) as well as the random effects assumption (i.e. that the individual specific effects are uncorrelated with the independent variables). With independently pooled panels it is assumed that there are no unique attributes of subjects within the measurement set and no universal effects across time (Myers et al., 2013). The fixed effect model assumes there are unique attributes of subjects that do not vary across time, these attributes may or may not be correlated with the individual dependent variables. The random effects model assumes the subjects have unique, time constant attributes which are not correlated with individual regressors. The term mixed model refers to the use of both fixed and random effects in the same analysis (Wu, 2009; Song and Song, 2007). In both experimental and observational studies, subject effects are mostly random while treatment levels are fixed effects. In repeated measures designs the mixed effects model is a more appropriate method for analysing repeatedly measured continuous data as it is based on less restrictive assumptions and so provides a generally more flexible approach by allowing a wide variety of correlation patterns (or variance-covariance structures) to be explicitly modeled (Bagiella et al., 2000; Wu, 2009). The correlation between observations is one assumption that may be relaxed with mixed models. In mixed models, the covariance structure of the data can adequately model data in which observations are not independent (Song and Song, 2007). This makes the mixed effects model approach particularly suitable for modeling repeatedly measured data. Mixed models are generally favored over classical GLMs as they i) can be extended to non-normal outcomes, ii) are often more interpretable than classical repeated measures, iii) handle uneven spacing of repeated measurements, and iv) handle missing measurements/data where other repeated measures approaches will discard results on subjects with missing measurements/data, v) can flexibly model time effects, and vi) allows the use of realistic variance and correlation patterns, which results in a more accurate treatment effect and standard error estimates and helps control Type I error (Gueorguieva and Krystal, 2004; Verbeke, 1997; Zeger et al., 1988).

Linear mixed effects models model fixed and random effects as having a linear form (see Equation 2.10). To obtain a two-level multilevel model where observations are nested within groups, (Woltman et al., 2012; Hershberger and Moskowitz, 2013; Tango, 2017; Huitema, 2011) recommend a two-step procedure beginning with a null model (without predictors) followed by a model in which the predictor variables are explicitly specified. The first model (Equation 2.10) reflects the relationship between lower-level units. The second model (Equation 2.11) demonstrates how the relationship within lower-level units varies between units.

$$Y_{ij} = \beta_{0j} + \beta_{1j}X_{ij} + r_{ij} \quad \text{Equation 2.10}$$

$$Y_{ij} = \gamma_{00} + \gamma_{10} X_{ij} + \gamma_{01}G_j + \gamma_{11}G_jX_{ij} + U_{ij}X_{ij} + U_{0j} + r_{ij} \quad \text{Equation 2.11}$$

In Equation 2.10,

Y_{ij} = dependent variable measured for the i^{th} level-1 unit nested within the j^{th} level-2 unit

X_{ij} = value on the level-1 predictor

β_{0j} = intercept for the j^{th} level-2 unit

β_{1j} = regression coefficient associated with X_{ij} for the j^{th} level-2 unit, and

r_{ij} = random error associated with the i^{th} level-1 unit nested within the j^{th} level-2 unit

In Equation 2.11 β_{0j} and β_{1j} are re-written as $\beta_{0j} = \gamma_{00} + \gamma_{01}G_j + U_{0j}$ and $\beta_{1j} = \gamma_{10} + \gamma_{11}G_j + U_{1j}$

where

β_{0j} = intercept for the j^{th} level-2 unit

β_{1j} = slope for the j^{th} level-2 unit

G_j = value for the level-2 predictor

γ_{00} = overall mean intercept adjusted for G

γ_{10} = overall mean slope adjusted for G

γ_{01} = regression coefficient associated with G relative to level-1 intercept

γ_{11} = regression coefficient associated with G relative to level-1 slope

U_{0j} = random effects of the j^{th} level-2 unit adjusted for G on the intercept

U_{1j} = random effects on the j^{th} level-2 unit adjusted for G on the slope

The two terms U_{0j} and U_{1j} demonstrate that there is dependency between level-1 units nested within each level-2 unit. This two-level model estimates three types of parameters namely a) fixed effects (γ_{00} , γ_{10} , γ_{01} , γ_{11}); b) random level-1

coefficients, and c) variance-covariance components which include i) covariance between level-2 error terms (cov (U_{0j}) or cov (U_{1j})); ii) variance in level-1 error terms (ie. The variance of r_{ij} denoted by σ^2); iii) variance in level-2 error terms (i.e. the variance of the U_{0j} and U_{1j} or β_{0j} and β_{1j}).

Chapter 3

Materials and Methods

3.1 Analytical method development

3.1.1 Analysis of aqueous phase toluene

3.1.1.1 Rationale

One of the main objectives of this study was to design a method for analysing toluene concentrations in the mesocosms. Gas chromatography (GC), high performance liquid chromatography (HPLC) and gas chromatography combined with mass spectrometry (GC-MS) are commonly used analytical methods for the quantification of petroleum hydrocarbons in soil (Wang, Z. et al., 1998). A full review of other methods and their limitations can be found in (Parr et al., 1996; Whittaker et al., 1995). The most common detectors fitted to gas chromatography instruments include flame ionization detectors (FID), flame photometry detectors (FPD), electron capture detectors (ECD) and thermal conductivity detectors (TCD). The sensitivity of the detector is what translates electron signals to its mass from which concentrations are determined. The lower the concentration of a compound, the more difficult it is to determine its mass (Whittaker et al., 1995). GC-FID has been developed for the determination of gasoline and diesel range organics in petroleum and was used in all toluene analyses conducted in this study.

The choice of an analytical method for a volatile organic compound such as toluene also calls for a compatible sampling method. Toluene is a volatile, aromatic hydrocarbon therefore, in sealed microcosms, sampling of the vapour phase is more advantageous than its aqueous phase. When working with volatile compounds, errors in experimentation may arise as a result of sorption to plastic surfaces such as the lids of containing vessels, volatilisation to air as a result of improper sealing of vessels, or sorption to solid media such as sediment. The key to obtaining consistent results during analysis of such compounds lies in the sample preparation. A review of sample preparation techniques for volatile organic compounds can be found in (Pawliszyn, 1995) and (Demeestere et al., 2007). A summary of conventional sample preparation methods for volatile compounds is given in Table 3.1.

Table 3.1 Summary of sample preparation methods for volatile compounds (VOCs)

Sample preparation method	Principle of technique
Grab sampling	The (gaseous) sample is pulled or pumped into an evacuated vessel (e.g. metal bulb, syringe, or plastic bag). Mainly suitable for sampling organic compounds in air.
Solid-phase trapping (SPE)	The sample is passed through an adsorbent (silica gel or activated carbon), trapped analytes are eluted with a strong solvent. Mainly suitable for semi-volatile organic compounds.
Liquid trapping (Impinging)	The sample is bubbled through a solution / solvent for which analytes of interest have a high affinity.
Headspace sampling	<p>The sample is placed in a closed gas vial until it reaches a state of equilibrium i.e. where the analytes of interest partition between their gas phase and solid / liquid phase. The gas phase is then sampled and injected into a GC. The method is mainly for determining trace concentrations of VOCs in samples difficult to handle by conventional GC.</p> <p><u>Note:</u> A shift in the equilibrium of the analytes in the sample matrix can be achieved by salting out, adjustment of the system pH or by increasing the temperature of the system.</p>
Purge & trap (dynamic headspace)	The sample, in its solid or liquid phase, is placed in a closed container and the VOCs are purged by an inert gas and subsequently trapped by a sorbent followed by thermal desorption into GC. The method is mainly used for quantifying trace concentrations of VOCs in samples and also for analytes with unfavourable partition coefficient in static headspace sampling

Sample preparation method	Principle of technique
Thermal desorption	Mainly used as an accompaniment with purge and trap and solid microphase extraction procedures to obtain a concentrated of the VOCs. The sorbent (e.g. Tanex TA, glass beads) is rapidly heated and the analytes of interest transferred to a GC. Used with purge & trap and SPME to concentrate VOCs; sorbent is rapidly heated and analytes are transferred to a GC
Pyrolysis	Mainly for non-volatile samples with large molecules e.g. polymers and plant fibres. Such samples usually have defined degradation mechanisms and predictable breakdown mechanisms which make it possible to identify the starting compound by its structural information and by fingerprinting methods.

The choice of a sampling technique is dependent on the physical state of the sample in question i.e. whether it exists in solid, liquid, or gas phase. Solid phase micro-extraction and headspace analysis of gaseous phase are two of the most commonly used methods for the measurement of toluene and other volatile, mono-aromatic hydrocarbons in water matrices (Hewitt, 1998). The headspace method was adopted in this study because i) it is known to be a suitable method for qualitative and quantitative analysis of volatile species in samples which can be efficiently partitioned into the headspace gas volume from either a solid or liquid matrix ii) it is suitable for 'dirty' samples e.g. a soil-water mixture containing either a single hydrocarbon or a mixture of hydrocarbons, iii) it is a suitable method for cases where the analyte of interest is present in trace levels.

3.1.1.2 Method

Headspace gas chromatography involves the use of an indirect measure to estimate the amount of the analyte of interest (toluene in this case) in the liquid phase. When the content of the headspace in a closed system attains equilibrium, the amount of analyte in the headspace can be equated to the amount in the liquid phase. The 'translation' between the headspace or gaseous phase and the liquid phase is referred to as the partition ratio, K (Kolb and Ettre, 2006). A high partition ratio implies it is more difficult for the analyte in question to elute or go into the gas phase. Similarly, compounds with low K values tend to partition more readily into the gas phase.

Partitioning of organic chemicals between water and other phases such as air, organic matter, and polymers is influenced by the salt content in the aqueous phase. Salts such as NaCl consist of small ions that enhance the structuring of aqueous phases due to their strong interactions with the dipoles of water molecules, giving the name 'structure-making salts' (Bowen and Yousef, 2003). This structural increase can induce a shift of the partition equilibrium of neutral organic solutes toward non-aqueous phases. This effect is called the salting-out effect and is deliberately used to maximize the extraction efficiency in analytical procedures by adding salt to water samples (Jochman et al., 2007). The salting-out effect was adopted in this study for the analysis of toluene in the mesocosms. 10mL aliquots from the mesocosms were added to 25 mL Whatman™ vials containing 7.5 g of NaCl salt and subsequently sealed gastight with crimped Teflon-coated butyl rubber stoppers. Analysis of gas phase toluene released into the headspace was achieved by means of a syringe into which toluene was sampled and transferred to the GC. Where it was not possible for samples to be analysed immediately the sealed salted vials containing the samples were stored in an upturned position at 20°C and analysed within 7-10 days.

3.1.1.3 Instrument calibration

Two sets of standards were prepared to calibrate the GC. The first set consisted of toluene stock solutions of equal concentrations but varying volumes (15 mL, 16 mL, 17 mL, 18 mL, 19 mL, 20 mL) and the second set contained stock solutions of equal volumes but varying concentrations (25 mg/L, 50 mg/L, 75 mg/L, 100 mg/L, 150 mg/L, 200 mg/L). The latter set was adopted for subsequent calibrations. A five-point calibration curve was produced from the heights and areas of the peaks obtained (see section C.3 of Appendix C). This initial calibration curve was linear up to a concentration of 100mg/L, therefore the mesocosm experiments were designed such that the end concentrations of toluene in the vessels did not exceed this value. A spiking concentration of 200 mg/L permitted from a freshly prepared toluene stock solution met this requirement and also did not exceed the solubility range of toluene in water (i.e. 520 mg/L at room temperature).

3.1.2 Analysis of iron-bound soil carbonates

3.1.2.1 Rationale

Field and laboratory studies such as (Mortimer, R.J. et al., 2011) and (Driese et al., 2010) have reported the occurrence of carbonate build-up during biodegradation of hydrocarbon contaminants. It was therefore part of the research objectives of this study to propose a method to assess the effect of toluene degradation on iron-bound

carbonates in soil using a novel method that differentiates this carbonate pool from other carbonate pools that may be found in a typical soil system.

3.1.2.2 Method

The method proposed for identifying and distinguishing iron-bound carbonates from other carbonate pools was selected based on the reactivities of calcite, dolomite, siderite and magnesite in phosphoric acid published in (Al-Aasm et al., 1990). The study involved the use of a selective acid extraction procedure and revealed distinct differences in the reaction times of the minerals. Calcites, particularly the finer-grained fractions, reacted faster than the other carbonate minerals. The results of the study showed approximately 60% of calcite reacted with the acid during the first 45 minutes. The initial step in the protocol for the stable isotope procedure is the acidification of the sample with a strong acid, usually phosphoric acid. The results of the study therefore suggest an acidified soil sample would be stripped of its major calcite content after the first 45 minutes of reacting with the acid extractant. The reaction rates of calcite, dolomite, siderite and magnesite are shown in Figure 3.1 below, with the open circles indicating the fine-sized fraction and the closed circles indicating the more coarse fractions.

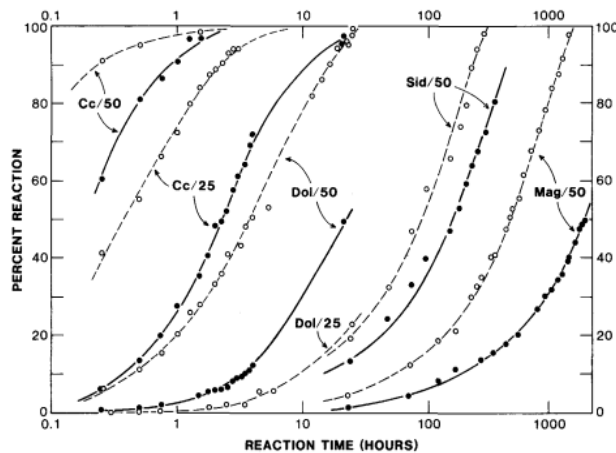


Figure 3.1 Reaction rates of pure carbonate minerals with phosphoric acid showing changes in cumulative yields (expressed in percentage) with time at two temperatures - 25°C and 50°C (adapted from (Al-Aasm et al., 1990))

Another study conducted in the Cohen Laboratories at the School of Earth and Environment, University of Leeds showed iron carbonates underwent complete reaction after an acidification period of approximately 24 hours. The experiments revealed the formation of precipitates in experimental microcosms (Mortimer, R.J. et al., 2011). Analysis of the precipitate indicated it to be iron carbonates (FeCO_3) likely a product of iron reduction occurring in the mesocosms. This precipitate was further analysed by initially freeze-drying and subsequently reacting the solid with

‘wet’ phosphoric acid over an extended period of time. The reaction resulted in the evolution of CO₂ gas, the yields of which are shown in Table 3.2. It can be seen from the table that the maximum yield of FeCO₃ occurred within the first 24 hours.

Table 3.2 Yield measurements for FeCO₃ precipitate from Fe-reducing microcosm (experiment performed by S. Bottrell in December 2007)

Time (hours)	2.5	5.0	7.5	10.0	12.5	24.0	26.0
Yield (linear units)	0.046	0.121	0.194	0.266	0.320	0.411	0.409

The results of these two studies served as a basis for establishing time frames within which common soil carbonates may be expected to undergo complete reaction with phosphoric acid. On the basis of these time frames as well as the stable carbon isotope procedure used in this study, two operationally-defined soil carbonate pools are proposed namely the fast-reacting soil carbonate pool and slow-reacting carbonate pool. The fast-reacting pool will mainly comprise calcite and other similar calcium carbonates. This pool is expected to completely react with phosphoric acid over a 45-minute period. The soil carbonates of interest in this study (i.e. iron carbonates) will fall under the slower-reacting pool. This pool would be expected to completely react with phosphoric acid over a 24-hour period.

3.2 Toluene degradation studies

A series of soil mesocosm experiments were designed to address the key objectives of this study i.e. to investigate the degradation of toluene under predominantly iron-reducing conditions. Mesocosm (or microcosm) experiments were chosen as the primary method for studying biodegradation because the experiments allow for i) the analysis of a contaminant and its ability to undergo degradation under ambient conditions ii) the evaluation of the effect of environmental variables on the rate and extent of biodegradation (Borden et al., 1997).

3.2.1 Soil mesocosms: design and considerations

The experimental matrices for the soil mesocosms are presented in Table 3.3 below.

Table 3.3 Experimental matrix showing the amounts of soil, toluene, river water and amendments used in each mesocosm set

Mesocosm sets [†]	Soil (g)	Soil/Mineral amendment (g)	Groundwater (mL)	Toluene (mL)	Liquid amendment (mL)
S _o	80	-	500	-	-
S _t	80	-	500	300	-
H _m	80	2	500	300	-
G _e	80	2	500	300	-
M _t	80	2	500	300	-
F _c	80	-	500	150	150
F _h	80	2	500	300	-
L _p	80	2	500	300	-
S _{pc}	50	30	500	300	-
S _s	50	30	500	300	-
S _l	50	30	500	300	-

[†]So – Mesocosms with soil and water only

St - Mesocosms with no amendment

Hm – Mesocosms with hematite amendment

Ge – Mesocosms with goethite amendment

Mt – Mesocosms with magnetite amendment

Fc – Mesocosms with ferric citrate amendment

Fh - Mesocosms with ferrihydrite amendment

Lp – Mesocosms with lepidocrocite amendment

Spc – Mesocosms with previously contaminated soil amendment

Ss – Mesocosms with sandy soil amendment

Sl – Mesocosms with loamy soil amendment

Although the experiments conducted simulate anaerobic conditions, the mesocosms were designed in close accordance with the British Standards 7755 Subsection 4.1.1., '*Guidance on the selection and conduct of tests for determining the biodegradation of organic chemicals in soil under aerobic conditions*', now replaced by ISO 11266:1994. As there is presently no generally agreed upon standard methodology, this international standard provides general guidance for soil mesocosm (or microcosm) studies on aerobic biodegradation. Reference was also made to the following studies, (Chaineau et al., 1995), (Huesemann, M.H., 1995), and (Hatzinger and Alexander, 1995), which made use of microcosms in their experimental methodology. A further consideration in the study design was the use of serially-sampled mesocosms as opposed to the smaller sacrificially-sampled microcosms, reason being that i) the soil-water medium in these types of mesocosms tend to be more stable over time in the sacrificially- sampled mesocosms and ii) the larger vessel size allows for more flexibility with sample volumes while maintaining the chemical equilibrium and iii) they tend to be less complicated than the larger batch-reactor type systems.

Due to the toxic nature of toluene, safety precautions were required including the acquisition of material safety data sheets and the use of a chemical fume-hood during the spiking procedure. Blank mesocosms containing no toluene were prepared to assess the contribution of soil natural organic matter. Total dissolved iron concentrations and pH in the mesocosms were chosen as geochemical indicators of microbial degradation to be monitored along with toluene concentrations.

3.2.1.1 Soil specifications

The primary purpose of the mesocosm experiments was to demonstrate removal of toluene in a controlled anaerobic soil-water environment with iron as the predominant terminal electron acceptor. (Jin et al., 1994), in a study on the transport and degradation of toluene in an unsaturated soil, demonstrated the relationship between the rate of toluene degradation and the history of the contamination of the soil. Pre-exposed soil showed higher rates of toluene biodegradation in comparison to fresh soils. The river water and soil samples used in our study were obtained from an area of Leeds that receives run-off from a location in which a hydrocarbon (diesel) spill occurred. A full documentation of this incident can be found in (Reporter, 1999). The soil and water samples were therefore expected to contain a microbial population adapted to a hydrocarbon contaminant and as such support toluene degradation in the mesocosms. Furthermore, the chosen sampling location provided adequate access to required quantities of soil and water samples for the pilot (Chapter 4) and subsequent degradation studies (Chapters 5, 6 and 7).

3.2.1.2 Field collection

Stainless-steel tools and plastic bags and buckets were used where possible to avoid contamination during sampling. A composite sample (ca. 10kg) of soil was collected using a spade at the subsurface horizon (about 0.6-0.9 m below surface) from the sampling point in Leeds. The soil samples were transported to the laboratory in plastic bags placed in sealed, sterile plastic containers. After collection the water samples were sealed in sterilised plastic bottles and placed in storage at 16°C.

3.2.1.3 Soil preparation and preservation

After being transported to the laboratory the soil sample was disaggregated and cleared of foreign material such as pebbles, metal objects, sticks, small stones and other unidentified objects. Pre-treatment procedures such as autoclaving were not conducted as it was intended for the soil to be as representative of its natural state as possible. After preparation, the sample was placed in a sealed inert (plastic) container with minimal headspace. The container was stored at 4°C temperature prior to its use in the mesocosm experiments. Subsamples (10 g) were taken for characterisation tests (see section 3.2.4). Water samples were stored under similar conditions after a 300mL subsample was taken for characterisation.

3.2.1.4 Mesocosm preparation

The mesocosms used in this study were constructed in acid-washed and autoclaved 1,000mL Schott Bottles filled with the starting soil, iron and soil amendments and river water samples in a self-fabricated glove bag' supplied with nitrogen (see section B.1 of Appendix B). The solid amendments (iron minerals and soil samples) were added along with the soil and the liquid amendments (ferric citrate) with the water sample. The sealed environment required to establish anaerobic conditions was achieved with the use of VICI™ opti-cap assemblies with PEEK™ plug and fittings (VICI-Jour) attached to the 1,000mL-Schott™ bottle. The PEEK system consisted of twin valves with female luer fittings and Teflon tubing fitted with a nut and ferrule. The tubings attached to each valve were of differing lengths. The mid-length and short-length design allowed for the sampling of air and liquid samples respectively. The opti-cap set up was particularly chosen as it meets the requirements in the ASTM Standard, 'Guide for monitoring the fate of chemicals in site-specific sediment/water microcosms' (ASTM:E1624-94, 2008).

After the mesocosms were filled, the O-rings on the screw cap and lip of the bottle were wiped clean with ethanol before sealing to eliminate residual soil and ensure a proper seal. With a nitrogen-filled ballast volume attached to the valve of the shorter

tube, toluene from a freshly prepared stock solution was added to the sealed vessels with the aid of a syringe (see section B.1 of Appendix B). This method was adopted to minimise errors that may have been caused by air entering the mesocosms during sampling and toluene addition (spiking). The soil-water mixture was homogenised by shaking and left to stand for half an hour to allow a clear partition between the soil and water. 10mL subsamples were obtained similarly (i.e. with the use of the syringe and ballast volume) and centrifuged at 2,000 rpm for 10 minutes prior to performing analysis for toluene, total aqueous iron concentrations and pH. A total of 33 individual mesocosms were prepared for the degradation studies, 6 for the pilot study (Batch A), 18 for the studies on the effects of iron amendments (Batch B) and 9 for the studies on the effects of soil amendments (Batch C) as shown in Table 3.4 below.

Table 3.4 Summary of mesocosm test design applied in this study

Batch	Treatment	Amendments	Mesocosm set up
A	Control (No toluene)	None	3 replicates containing 80g (wet soil), 500mL river water, 300mL toluene stock solution and 300mL headspace in 1000mL Schott vial, VICI opti-cap assembly sealed
A	Active (Toluene added)	None	
B	Active with iron amendment	Hematite, Goethite, Magnetite, Ferric citrate, Ferrihydrite, Lepidocrocite	-

To ensure samples for toluene analysis did not exceed the linear range of the GC (see section 3.1.3), an initial toluene stock solution was prepared by adding 150 μ L of aqueous toluene to 1000mL of deionised water. This was judged to be low enough to avoid inhibition of soil microbial activity and high enough to allow changes to toluene concentrations to be clearly discerned through chemical analysis. After the removal of aqueous phase toluene in the liquid, the mesocosms were drained to the 500mL mark to accommodate the re-addition of 300mL of toluene from a freshly prepared toluene stock solution. The actual amount of toluene degraded (in mg) was therefore estimated as the product of the fraction of toluene removed and the amount of toluene (in mg/L) in the stock solution from which toluene was added to the mesocosms (see section B-4 of Appendix B).

3.2.1.5 Mesocosm sampling

A serial sampling method was employed in this study. Removal of liquid samples and addition of toluene stock solutions were both achieved with the aid of a 300mL FORTUNA® glass syringe with a luer tip style. The choice of a glass syringe as opposed to plastic was to minimise sorption or adhesion of toluene to the surface of the syringe during sampling and toluene addition. Mesocosms were shaken by hand to ensure proper mixing of toluene, soil and water and re-suspend any precipitates present in the soil-water mixture. In both instances of removal of liquid samples and addition of toluene stock, a nitrogen-filled ballast volume was always attached to the second valve to ensure anaerobic conditions within the vessel and minimise the introduction of oxygen while sampling and spiking. As previously mentioned, samples were taken over 3-day intervals. The sampling frequency was, in part, determined from the results of the pilot study (Batch A). The total incubation period for each mesocosm set was dependent on the point at which suppressed removal of toluene was observed. The proposed experiment design was that evidence of iron-mediated toluene degradation was to be inferred by changes in pH and total dissolved iron corresponding to toluene degradation. Therefore analysis of pH and total dissolved iron was performed along with the analysis of toluene concentrations. Analysis of toluene concentrations was achieved by gas chromatography. Inorganic anions were analysed at the beginning and end of the experiments and showed no competing terminal electron acceptors (particularly nitrates and sulphates) were present in appreciable levels. A summary of the mesocosms and analyses performed can be found in Appendix B.

3.2.2 Apparatus

At the start of each mesocosm set up, all glassware were properly washed and rinsed with deionised water and left to dry in oven. After use, glassware were left to soak overnight in an acid bath before re-use.

3.2.3 Chemicals and analytical grade reagents

Laboratory-grade toluene obtained from Fluka™ was used in the preparation of toluene stock solutions for spiking and re-spiking procedures. The reagents for sequential extractions (purchased from Sigma Aldrich™) include nitric acid, hydrofluoric acid, perchloric acid, boric acid, ferrocene, HEPES, hydrochloric acid, chromium (ii) chloride, silver nitrate, ammonium oxalate monohydrate and sodium dithionite. Liquid nitrogen and solid carbon dioxide (dry ice) for stable isotope analysis were obtained from the University storage supply. Laboratory-grade phosphoric acid for stable carbon isotope analysis was obtained from Sigma Aldrich™ as well as reagents for ferrozine analysis which included ammonium acetate, hydroxylamine hydrochloride, and hydrochloric acid.

Additional reagents and chemicals for the laboratory-prepared iron amendments include laboratory grade, ferric chloride tetrahydrate, $\text{FeCl}_2 \cdot 4\text{H}_2\text{O}$, and ferrous nitrate nonahydrate, $\text{Fe}(\text{NO}_3)_3 \cdot 9\text{H}_2\text{O}$. These were purchased from Sigma Aldrich™. Ferric chloride tetrahydrate, $\text{FeCl}_2 \cdot 4\text{H}_2\text{O}$, and ferrous nitrate nonahydrate, $\text{Fe}(\text{NO}_3)_3 \cdot 9\text{H}_2\text{O}$ were used in the synthesis of lepidocrocite and ferrihydrite respectively. 2-line ferrihydrite was synthesized using $\text{Fe}(\text{NO}_3)_3 \cdot 9\text{H}_2\text{O}$ solutions titrated with 1N NaOH following the method in (Parkman, R.H. et al., 1999) and lepidocrocite in fresh, unoxidised $\text{FeCl}_2 \cdot 4\text{H}_2\text{O}$ filtered and adjusted to pH 6.7 with freshly prepared 1M NaOH solution as described in (Yu, J.Y. et al., 2002). The mineralogical composition of the synthesized ferrihydrite and lepidocrocite samples were confirmed by x-ray powder diffraction. Laboratory-grade ammonium hydroxide and sodium hydroxide, used to adjust the pH during the mineral synthesis experiments, were obtained from Fluka™. The natural minerals, namely hematite, goethite and magnetite, were obtained as rock samples. Preparation of these samples followed a two-step procedure beginning with cutting with the aid a rotating saw followed by crushing to fine-sized particles in an automated pestle and mortar.

3.2.4 Analytical instrumentation: chemical and physical characterisation tests

Subsamples (10 g) were taken and analysed for pH, initial moisture content, particle size distribution, surface area, total elemental concentration, mineralogical content, and dissolved ion concentrations (see summary in Table 3.5). Reference was made to methods described in (Page et al., 1982) and (Carter, 1993).

Table 3.5 Properties analysed and instruments used in analyses

Characteristic	Method
Colour	Physical inspection
Moisture content	Gravimetric
pH	Potentiometric
Texture	Laser diffraction particle size analysis
Surface area	Brauner-Emmett-Teller (BET) analysis
Total elemental concentration	X-ray fluorescence (XRF) spectroscopy
Mineralogy	X-ray diffraction (XRD)

3.2.4.1 pH measurement

Before each reading was made, the pH electrode was calibrated over the appropriate range using standard buffers. The method for soil pH determination was based on (Henning, 2004) which involves the use of 5 g of crushed dried soil placed in a vial and thoroughly mixed with 5 mL of deionised water. Following mixing with deionised water, the solution was left to stand for 1-2 h with occasional stirring. A pH probe was then inserted for 5 minutes measurements were made in triplicate.

3.2.4.2 Determination of soil moisture content

Soil moisture content was determined gravimetrically by the change in weight after drying at 105°C for 24 h (Braddock et al., 1997; Gogoi et al., 2003; ISO, 1993). Triplicate subsamples (10 g) were weighed on watch glasses and left overnight in an oven at 105°C. The weight after drying was taken and the weight of the soil in both cases adjusted by subtracting the weight of the watch glass. Gravimetric moisture content, M was then calculated from the equation below and the weight of soil (see Equation 3.1)

$$\text{Gravimetric moisture content, } M = \frac{m_w}{m_{od}} \dots\dots\dots \text{Equation 3.1}$$

where

m_w = weight of moist or air-dried soil

and m_{od} = weight of oven dried-soil

(All masses were measured in grammes)

The gravimetric moisture content was expressed as a percentage of the total weight of sample dry solids.

3.2.4.3 Texture

Particle size analysis was performed on a Mastersizer 2000™ laser diffraction instrument fitted with a pump system. Analysis was carried out at a laser obscuration range of between 7.5 and 15% and mid-range obscuration of 9-11% to minimise errors that could arise due to the formation of floccs from sample particles within the pump system. The data on the size distribution of the samples was generated using the Tabsmastersizer software and exported in excel spreadsheet format.

3.2.4.4 Brunauer emmet teller (BET) surface area

BET analysis works by the principle of adsorption of nitrogen gas on a solid surface to determine the surface area of the sample, with the BET surface area is determined by the extent of nitrogen adsorption to an outgassed sample. To begin the experiments, sub-samples weighing 10 g were measured into tube holders to which a nitrogen line was inserted. The tubes were capped and the degasser switched on and left overnight. BET analysis was performed on a micron II™ Brauner Emmett Teller (BET) instrument. Data acquisition was with the aid of Gemini VII 2390™ software.

3.2.4.5 Total elemental concentration

X-ray Fluorescence spectroscopy (XRF) was performed on a portable PANalytical Axios Advanced X-ray Fluorescence (XRF) spectrometer. The analysis involved grinding and sieving to 2mm, freeze dried soil samples. Samples were inserted into the instrument in a loose powder mount covered with Mylar film (Evans, J.R. et al., 2003; Shefsky, 1997). A palladium x-ray source was used as the primary radiation with helium gas. The instrument was pre-calibrated with two settings - mining plus and soil plus modes; soil plus mode did not cover % levels and did not include Mg, Al or Si. The analysis was conducted for 2h and the total elemental concentration of the soil samples determined. This analysis was also performed in the School of Earth and Environment by Lesley Neve.

3.2.4.6 Mineralogical analysis

The freeze-dried soil sample was crushed in a mortar and pestle and a small amount placed on the centre of a silicon holder. X-ray diffraction analysis of the samples on the side was carried out on a Bruker D8™. For data acquisition, a Cu anode was supplied with 40 kV and a current of 40 mA to generate Cu-K α radiation ($\lambda = 1.54180 \text{ \AA}$) or Cu-K α_1 ($\lambda = 1.54060 \text{ \AA}$). The data was collected over a range of 2-90°2 θ with a nominal step size of 0.009°2 θ and nominal time per step of 1.00 seconds. Fixed anti-scatter and divergence slits of 1/4° were used together with a beam mask of 10mm. All scans were carried out in 'continuous' mode using the X'Celerator RTMS detector. Data interpretation was achieved using the X'Pert accompanying software program High Score Plus® in conjunction with the ICDD Powder Diffraction File 2 database (1999) and the Crystallography Open Database (October 2010; www.crystallography.net).

Quantitative or Rietveld analysis was performed on the Philips PW1015™ configured to use Cu K alpha radiation with the power set to 50 kV and 40 mA. The scan parameters were 3-70 °2 θ scan range at a speed of 0.6° per minute and a step size of 0.01°. The samples were prepared by spray-drying with the addition of a 20 % corundum spike giving spherical particles which are randomly oriented in the XRD. Data interpretation was initiated using a method called RIR (relative intensity ratio) on the whole pattern. The analysis was performed in the School of Earth and Environment by Lesley Neve.

3.2.4.7 Dissolved anion and cation concentrations

The analysis of inorganic anions (sulphate – SO_4^{2-} , nitrate - NO_3^- and chloride - Cl^-) in the water sample was performed on a Metrohm™ 850 Professional ion chromatograph (IC), consisting of an auto-sampler equipped with a conductivity detector. The instrument consisted of a Dionex DX-600 with AS50 auto-sampler using a 2mm AS11 analytical column, designed for gradient elution to 15mM potassium hydroxide. Samples for analysis were further diluted to a 1 in 1000 dilution by taking 0.1mL of supernatant and making up to 9.9 mL with DI H_2O and then transferred into falcon tubes and loaded onto the Dionex auto-sampler for analysis at a sample injection volume of 10 μL . In-between loading samples, the column was flushed with deionised water for 1.5minutes. Individual runs were made over a 25-minute period with detection times at 6.2 minutes for chlorides, 9.6 minutes for nitrates, 14.9 minutes for sulphates and 13.3 minutes for phosphates.

3.2.5 Analytical instrumentation: degradation experiments

3.2.5.1 Toluene concentrations

Analysis by gas chromatography was performed on an Agilent™ J & W DB-5 column (30m length, 0.25 line and 0.25 μm film) coupled to a flame ionisation detector (FID) (hydrogen flow 30 mL/min and air flow 400 mL/min) with an injector (temperature 270°C, split ratio of 100:1). The DB5 column is commonly used for analysis of petroleum hydrocarbons (Gough and Rowland, 1990) and is the low temperature equivalent of the aluminium-clad diphenyl:disiloxane carborane (5 % : 95 %) column (SGE HT5) with a 0.53 mm i.d. and 0.15 micron film thickness. 2 μL aliquots were injected in splitless mode. A linear temperature gradient was employed. The GC oven temperature was 190°C isothermal for 3minutes then 7°C/minute to 150°C and 20°C per minute to 220°C (see Table 3.4). A nitrogen carrier gas was used at a flow rate of 2.5 ml/min. gas samples from salting out vials (see Appendix C) were injected into the instrument. Identification of toluene peaks was achieved by comparing peak characteristics of analysed samples with calibrated standards. During each run, toluene was detected at approximately 6.2 minutes. This analysis was to determine toluene concentrations in the mesocosms and was performed by David Elliott in the School of Civil Engineering.

Table 3.4 Temperature setting of the gas chromatography instrument

	Target Temperature	Rate	Hold Time
Initial	40°C	N/A	3mins
Ramp 1	150°C	7°C/min	N/A
Ramp 2	220°C	20°C/min	N/A

3.2.5.2 Total (aqueous) iron

Total dissolved aqueous iron concentrations were analysed using the ferrozine assay following the protocol in Viollier 2000. The test makes use of three reagents namely ferrozine solution, a reducing agent (1.4M hydroxylamine hydrochloride) and a buffer solution (5 M ammonium acetate). The ferrozine solution consisted of 0.01 M ferrozine in a 0.1M-ammonium acetate ($\text{CH}_3\text{COONH}_4$) solution prepared by dissolving 0.5077 g of ferrozine and 0.7708g of ammonium acetate in DI water. The solution was stored away from light in a refrigerator at 14°C and was used within a month of preparation, as it oxidises over the time. The 1.4 M hydroxylamine hydrochloride solution ($\text{H}_2\text{NOH.HCl}$) reducing agent acts to reduce aqueous Fe (III) to Fe (II) and was prepared by dissolving 9.728g of hydroxylamine hydrochloride in 50 mL of DI water, followed by 17 mL of concentrated HCl made up to 100 mL with DI water. Hydroxylamine hydrochloride is hygroscopic, and was prepared immediately before use and stored in a closed container. The 5 M ammonium acetate buffer solution was prepared by dissolving 38.54 g of ammonium acetate ($\text{CH}_3\text{COONH}_4$) in DI water followed by the addition of 28-30 % ammonium hydroxide (NH_4OH) to adjust the pH to 9.5.

1000 μL of standards, centrifuged samples and blank solution (deionised water) were pipetted into each cuvette followed by 100 μL of ferrozine reagent and 200 μL of hydroxylamine hydrochloride. The content of the cuvettes was homogenised by shaking and left to stand for 10minutes to allow for complete reduction of Fe (III) to Fe (II). 50 μL of ammonium hydroxide buffer solution was added to complete the reaction and the solution re-homogenised by shaking. The blank was first measured to zero the instrument, followed by the standards and samples.

3.2.5.3 Operationally-defined extractable iron phases

The most commonly used techniques for the determination of trace metals in soil are based on atomic spectroscopy. Two common techniques include atomic absorption spectroscopy (AAS) and atomic emission spectroscopy (AES). In this study, soil samples (10 g) were subjected to sequential extraction by isolating operationally-defined iron-bound fractions in soil as put forward by (Poulton and Canfield, 2005). The chemical extractions targeted the following iron fractions:

- (a) **Carbonate Fe** (including siderite and ankerites) extracted with Na acetate adjusted to pH 4.5 for 24 h;
- (b) **Easily reducible oxides** (including ferrihydrite and lepidocrocite) with Hydroxylamine-HCl for 48h;
- (c) **Reducible oxides** (including goethite, hematite and akaganeite) with Dithionite for 2h;
- (d) **Magnetite** with Oxalate for 6h;
- (e) **Pyrite Fe** with Boiling 12N HCl;
- (f) **Unreactive silicate** with Chromous chloride distillation and
- (g) **Total Fe (II) and Fe (III) fractions** with Perchloric, HF and boric acid treatment.

A summary of the extractions sequence is given in Table 3.5, the experimental protocol is documented in section C.6.6 of Appendix B.

Table 3.5 Summary of the sequential chemical extractions showing extractants and target phases (adapted from (Poulton and Canfield, 2005))

Extraction	Target iron phase	Terminology
<u>Sequential Fe extractions</u>		
Na acetate pH 4.5, 24 h	Carbonate Fe, including siderite and ankerite	Fe carb
Hydroxylamine-HCl, 48h	Easily reducible oxides (including ferrihydrite and lepidocrocite)	Fe ox1
Dithionite, 2h	Reducible oxides (including goethite, hematite and akaganeite)	Fe ox2
Oxalate, 6h	Magnetite	Fe _{mag}

Extraction	Target iron phase	Terminology
<u>Sulphate extractions</u>		
Boiling 12N HCl	Pyrite Fe	Fe _{py}
Chromous chloride distillation	Unreactive silicate	Fe _U
<u>Total Fe extractions</u>		
Perchloric, HF and boric acid treatment	Total Fe (II) and Fe (III) fractions	Fe _T
<u>Bioavailable fraction</u>		
Fe = (Total Fe-(sum of first 5 stages + pyrite Fe))		

After each fraction was extracted, the supernatant was separated via centrifugation and vacuum filtration, made up to a 2 % HNO₃ solution and stored at 10°C for radiochemical analysis. This analysis was performed by Romain Guildbald in the School of Earth and Environment on a ContrAA 600™ automated absorption spectrophotometer (AAS) instrument. Further dilution and re-analysis was performed for samples with excessively high concentrations (over the range of the calibration curve i.e. 10 ppm). Concentrations were converted to weight percentages using the formula below:

$$(\text{ppm concentration}) * (\text{original factor}) * (\text{further dilution factor (if required)}) / (1000 \text{ (1L)}) * \frac{0.01\text{mL}}{\text{original sample weight}} * (100)$$

where

ppm concentration is the concentration of Fe in ppm, and
original sample weight is the weight of the soil sample in mg

3.2.5.4 δ¹³C signatures

Isotope ratios are expressed in terms of δ¹³C values, which are reported in per mil and calculated relative to the standard Pee Dee belemnite (PDB), according to the relationship.

$$\delta^{13}\text{C} (\text{‰}) = \frac{R_{\text{sample}} - R_{\text{standard}}}{R_{\text{standard}}} \times 10^3 \quad \text{Equation 3.2}$$

GC-IRMS is generally adopted for stable isotope analysis as it allows for the measurement of small but significant variations in stable isotope ratios with high precision (Boutton, 1991). The protocol for the stable isotope analyses in this study was a two-step procedure of acidification followed by cryogenic distillation of evolved gas as documented in (McCrea, 1950). Combustion tubes containing the samples and CuO were sealed under vacuum by a standard glass-blowing torch.

Sample CO₂ isolation and purification was accomplished on a vacuum system by vacuum line manipulation and cryogenic distillation. 10g of the freeze-dried soil sample was placed in the sample holder and reacted with 'wet' phosphoric acid (H₃PO₄) acid slowly released from an acid dispenser. Gas volumes were monitored with the use of the capacitance manometer to which a gauge displaying readings was attached. After passing through the silica CuO combustion chamber, individual compounds were detected on a dedicated SIRA II Triple Collector isotope ratio mass spectrometer. Sample isotope ratios are, by standard procedure, evaluated initially relative to a reference CO₂ stream calibrated relative to the standard PDB carbonate formation. Final sample $\delta^{13}\text{C}$ were reported relative to the standard PDB with corrections made for ¹⁷O contributions. The instrument was calibrated with an internal strontium carbonate standard (APB-2) and the change in the ratio of ¹³C to ¹²C ($\delta^{13}\text{C}$) was obtained from raw data derived from measurements of m/e ion beams 44, 45, 46 as described in (Craig, 1957).

As described in section 3.1.2, we propose a study for distinguishing between iron-bound soil carbonates using stable carbon measurements on the basis of their reaction times with phosphoric acid. Therefore the first gas fraction released within the first 45 minutes of acidification and the second gas fraction released after a 24-hour period were taken to be representative of the fast (e.g. calcium carbonates) and slow reacting soil carbonates respectively (e.g. iron carbonates). Both fractions were analysed separately on the GC-IRMS instrument.

3.3 Statistical analysis

IBM SPSS Statistics® 23 was used for statistical hypothesis testing. Except otherwise stated all statistical tests were performed on a .05 alpha level.

Preamble

Results of degradation experiments

P-1 Mesocosms with soil and water only (S₀)

The mesocosms containing soil and water only served as live control experiments. Analysis of the liquid fraction of the soil-water mixture showed no traces of toluene in the mixture. The total iron in this mesocosm group was consistent among replicates (see Figure P-1). There was however a gradual decline in total iron concentrations at the start of the experiments during the first three days of the incubation period. Between the third and twelfth day, the total iron concentrations did not vary appreciably however a gradual rise in total iron occurred after the twelfth day and continued over the period of incubation.

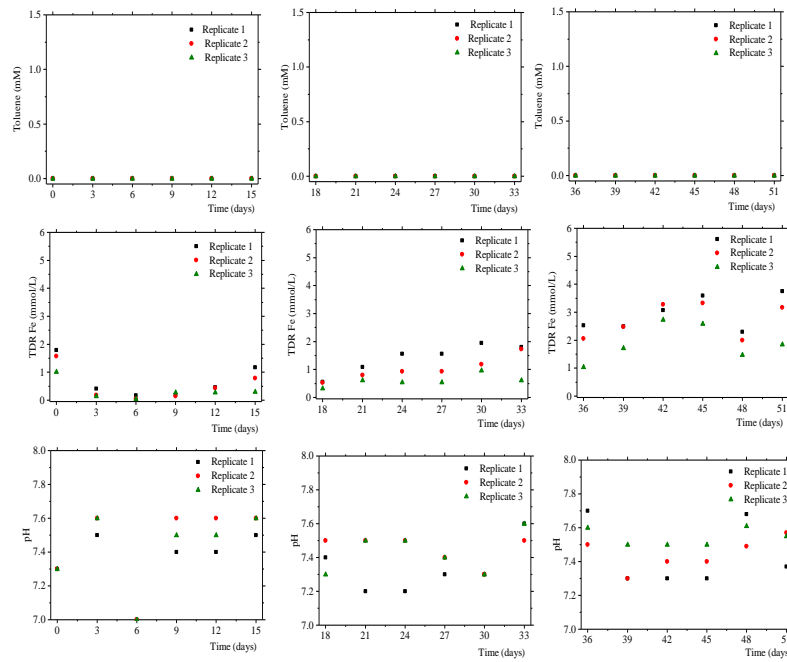


Figure P-1 Concentration-time courses for total dissolved reactive (TDR) iron and pH in mesocosms with soil and water

P-2 Mesocosms with soil, water, and toluene (S_T)

The mesocosms containing soil, water and toluene were set up as active control experiments and contained the same soil-water matrix successively spiked with toluene. The plot of toluene concentrations with time show toluene removal occurred with each successive spike made to the soil-water mixture (see Figure P-2). These concentrations did not show much variation among replicates during the period following the addition of the initial toluene spike (0-15 days). Toluene concentrations however varied more significantly among the replicates during the period following the addition of the second spike (18-33 days). Each toluene spike was made from stock solutions of similar concentrations however the data obtained shows slightly higher concentrations for the points at which each spike was added. These differences in concentrations were either due to errors during GC analysis or residual toluene present in the soil-water at the time at the time of spiking. Toluene removal was less pronounced from day 45 onwards. Suppressed removal of toluene was observed from this point onwards i.e. no further toluene removal was observed. Toluene removal did not have a noticeable effect on total iron concentration in the soil-water mixture as total iron concentrations did not vary significantly during the period of incubation. The total iron in the system remained in a 0.2-0.4 mM range over the period of incubation. The pH of the soil-water environment increased gradually during the period after the addition of the second spike and remained in a 7.2-7.6 range over the incubation period.

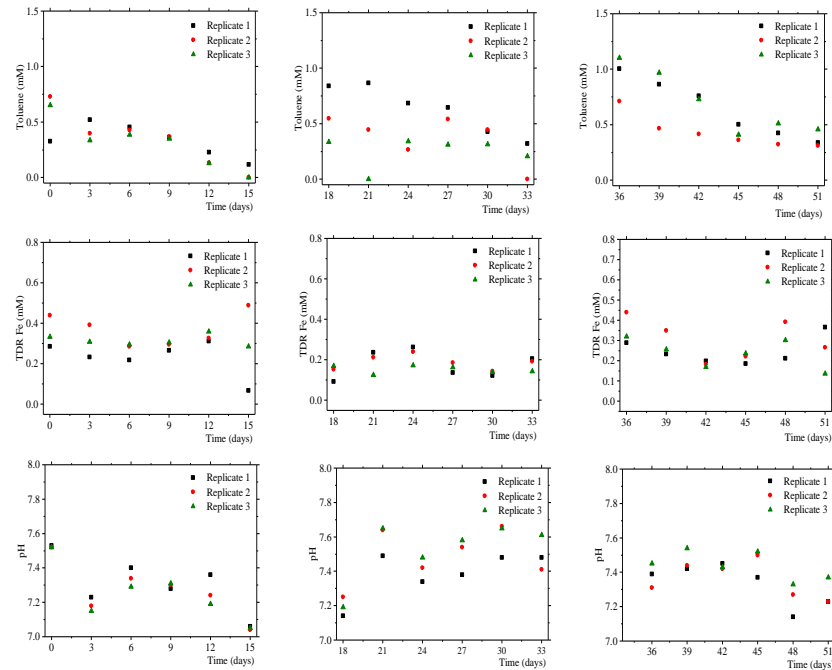


Figure P-2 Concentration-time courses for total dissolved reactive iron and pH in mesocosms with soil and toluene

P-3 Mesocosms with hematite amendment (H_M)

The mesocosms hematite amendment contained the same water and soil mixture amended with hematite and successively spiked with toluene. The experimental results show these mesocosms supported the removal of toluene with each successive spike (see Figure P-3). The point at which suppressed toluene removal was induced in the soil-water mixture occurred during the period after the third spike, around the day 48 time point. The total iron concentrations in the mesocosms varied between 0.1-0.5 mM during the period of incubation. A slight decline in pH was observed after the initial spike and remained between 7.1-7.7 over the course of the experiments.

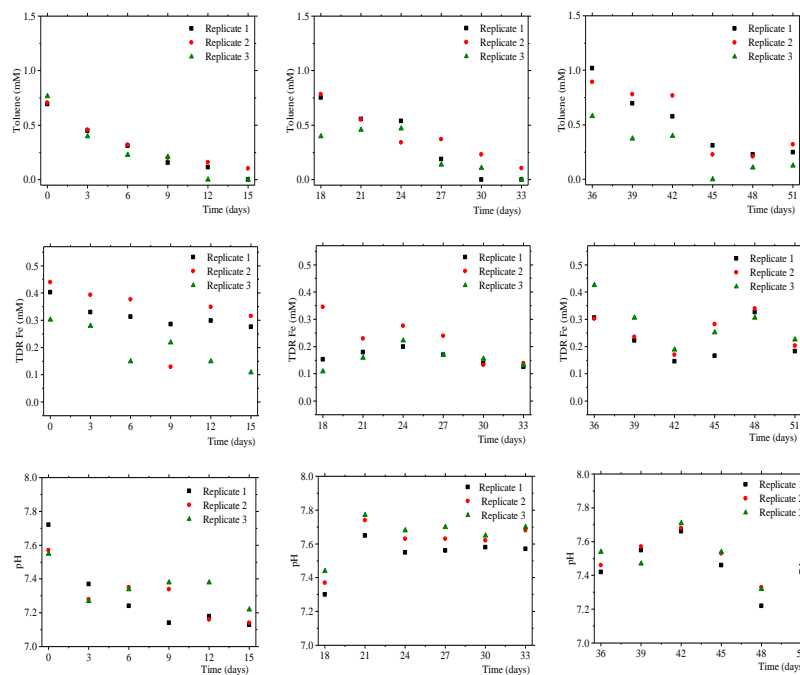


Figure P-3 Concentration-time courses for toluene, total dissolved reactive iron and pH in the mesocosms amended with the hematite

P-4 Mesocosms with goethite amendment (G_E)

The goethite-amended mesocosms also supported toluene removal with each successive spike. The addition of each new spike resulted in higher toluene concentrations at the start of each period after spiking (see Figure P-4). Suppressed removal of toluene was induced in the period after the addition of the third toluene spike. The total iron concentrations in the soil-water mixture indicate the presence of goethite increased this content. After the initial spike a decrease of about 0.4 units in pH was observed however the pH in all replicates remained in the 7.2-7.7 range during the period of incubation.

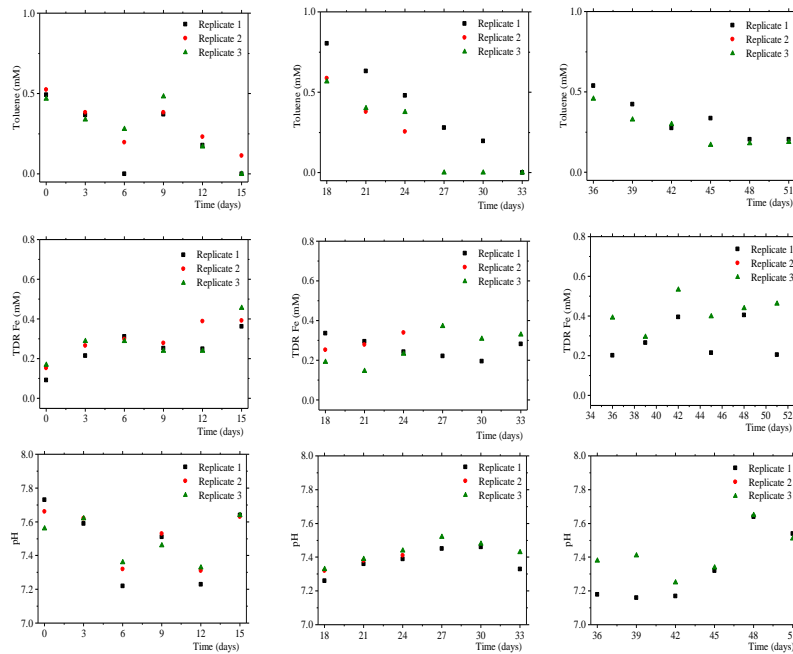


Figure P-4 Concentration-time courses for toluene, total dissolved reactive iron and pH in the mesocosms with the goethite amendment

P-5 Mesocosms with magnetite amendment (M_T)

The soil-water mixture amended with magnetite supported toluene removal with the addition of each successive spike (see Figure P-5). After the initial spike, toluene removal was observed by the sixth day in two replicates. A similar trend was observed during the period after the second spike. Suppressed removal of toluene was observed after the addition of the third toluene spike. The total iron in the soil-water mixture was in the 0.1-0.7 mM range over the period of incubation.. A slight decline in pH was observed after the initial toluene spike however no appreciable changes in pH occurred during the periods after the second and third spikes. The mesocosm pH ranged between 7.2 and 7.8 over the period of incubation.

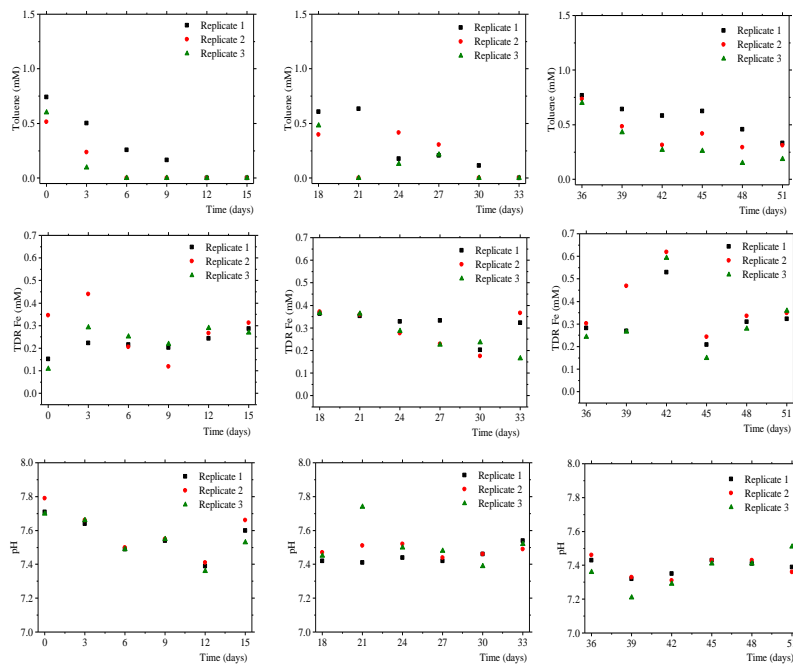


Figure P-5 Concentration-time courses for toluene, total dissolved reactive iron and pH in the mesocosms with the magnetite amendment

P-6 Mesocosms with ferrihydrite amendment (F_H)

The ferrihydrite-amended mesocosms supported toluene removal with a significant portion of toluene removed shortly after the initial spike (see Figure P-7). Complete toluene removal occurred by the sixth day in all replicates. Suppressed removal of toluene was observed at a time point during the period after the second spike was made. In two replicates the total iron remained in the 0.2-0.4 mM range over the period of incubation. A decline in pH was observed from 6.5 at the start of the experiments to 5.2 at the end of the period of incubation.

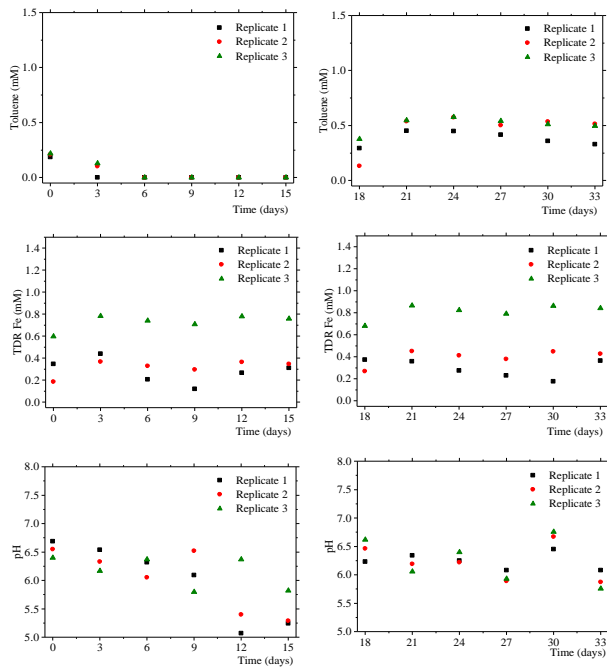


Figure P-6 Concentration-time courses for toluene, total dissolved reactive iron and pH in the mesocosms with the ferric citrate amendment

P-7 Mesocosms with lepidocrocite amendment (L_P)

The soil-water mixture amended with lepidocrocite did not support toluene removal, as toluene concentrations in the mesocosms did not vary significantly (see Figure P-7). These concentrations remained between 0.4 mM and 0.6 mM throughout the fifteen-day period after the introduction of the initial toluene spike. No further analysis was made due to time constraints. Total iron concentrations were found in the 0.2-0.6 mM range in all replicates. The pH readings obtained suggest the presence of lepidocrocite in the mesocosms induced alkaline conditions as the pH remained between 8.4 and 8.8 during the period of incubation.

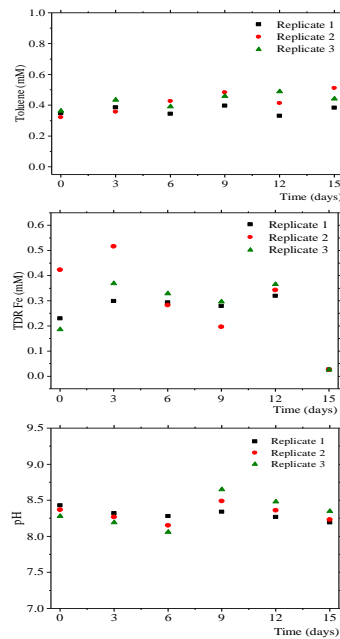


Figure P-7 Concentration-time courses for toluene, total dissolved reactive iron and pH in the mesocosms with the lepidocrocite amendment

P-8 Mesocosms with soil 1 amendment (S₁)

The mesocosms with the soil 1 amendment were the first of the soil-amended mesocosms which contained the starting soil material mixed with a soil sample identified as ‘Soil 1’. Toluene removal was supported by the mixture of the starting soil and Soil 1 amendment (see Figure P-8). Complete toluene removal was observed in all replicates on the fifteenth day after the addition of the initial toluene spike. The replicates showed suppressed removal during the period after the second spike. The analysis of toluene concentrations show appreciably lower concentrations at the start of the period following the addition of the first spike when compared to the concentrations at the start of the period after the second spike. An increase in total iron was observed after the first spike, continuing till the ninth day at which point a gradual decline occurred as the experiments progressed. It is likely the presence of the soil amendment induced this increase. The soil-water pH remained between 7.0 and 7.5 all through the period of incubation.

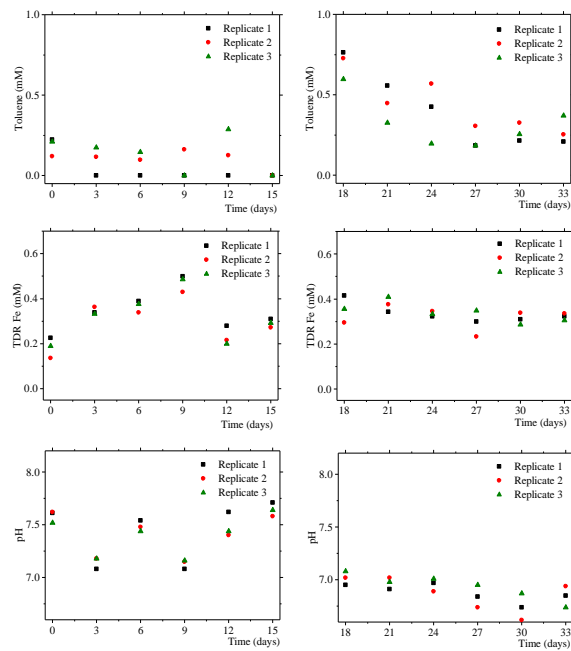


Figure P-8 Concentration-time courses for toluene, total dissolved reactive iron and pH in the mesocosms with the contaminated soil amendment

P-9 Mesocosms with soil 2 amendment (S₂)

The mesocosms with the soil 2 amendment supported the removal of toluene (see Figure P-9). Suppressed removal was observed during the period after the second spike. An increase in total iron concentrations in the mesocosms was observed during the period after the first spike and continued to the ninth day after which these concentrations remained unchanged. A decline in mesocosm pH from 7.4 to 6.9 was observed between the first and last day of the incubation period.

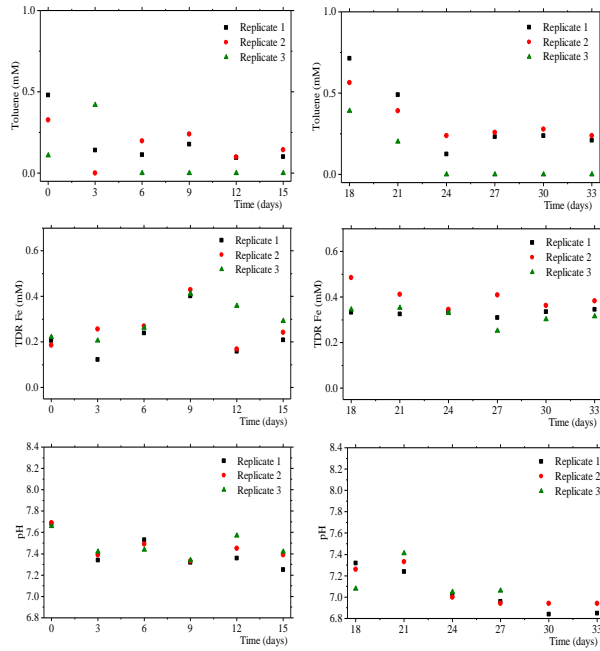


Figure P-9 Concentration-time courses for toluene, total dissolved reactive iron and pH in the mesocosms with the sandy soil amendment

P-10 Mesocosms with soil 3 amendment (S₃)

The last group of the soil-amended mesocosms contained the sample identified as ‘Soil 3’ and was seen to have also supported toluene removal after spiking (see Figure P-10). Similar initial toluene concentrations were observed after the addition of the first and second spikes. Suppressed removal of toluene occurred during the period after the second spike. Total iron concentrations did not show appreciable variations over the period of incubation however the pH was found to have increased slightly during the period after each spike. Lower initial pH readings were observed after the addition of the second spike.

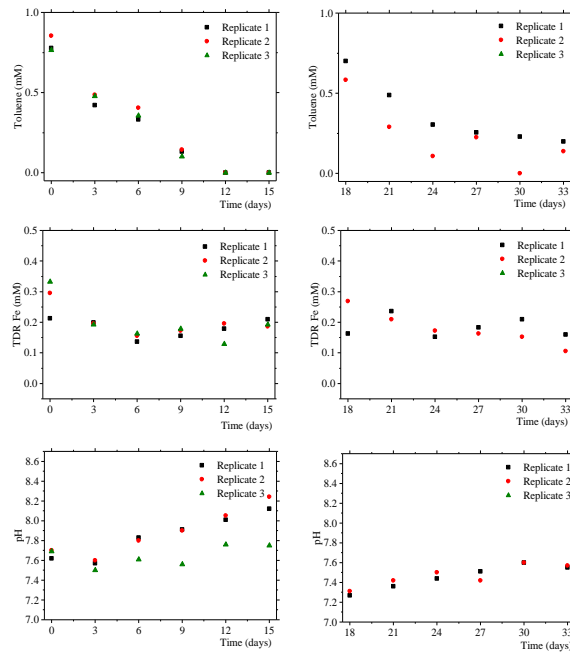


Figure P-10 Concentration-time courses for toluene, total dissolved reactive iron and pH in the mesocosms with the loam soil amendment

Chapter 4

Iron-Mediated Toluene Degradation in Batch Mesocosms

Introduction

The main objective of the mesocosm experiments was to demonstrate the removal of toluene under predominantly iron-reducing conditions. Replicate 1,000mL vessels containing 80g of uncontaminated soil and 500mL of river water sealed under oxygen-free conditions served as experimental analogues of subsurface soils constructed for the purpose of assessing toluene removal under predominantly iron-reducing conditions. In this chapter the initial study for the active and control mesocosms is reported.

4.1 Results and discussions

4.1.1 Characterisation tests

Characterisation tests were performed on the river water sample specifically to assess its pH and dissolved anion composition. Analysis of the ion concentrations of the river water sample detected nitrates at 56 mg/L, sulphides at 137 mg/L and chlorides at 69 mg/L. Fluorides, bromides, nitrites, and phosphates were not detected in the water sample. The sample pH was found to be near-neutral at pH 7.5. Similarly the tests conducted on the soil sample were to assess specific physicochemical properties namely pH, particle size distribution, moisture content, elemental composition and mineralogy. The soil pH was near neutral at pH 7.5. Soil particle size analysis indicated a clay content (particles < 0.002 microns) of 0.5 %, a silt content (particles 0.002 – 0.063 microns) of 50.4% and a total sand content (particles 0.063 microns to 2.000 mm) of 49.2% w/w. Soil moisture content was determined by the difference in weights before and after drying the soil (at 105°C for 24hours) and was found to have a value of 31.7% (see section B-5 of Appendix B). Determination of the BET (Braun-Emmett-Teller) surface area by nitrogen gas adsorption produced a value of 14.9m²/g. The major elements identified in the starting soil material were sodium, magnesium, aluminium, potassium, iron and silicon. X-ray fluorescence spectroscopy (XRF) indicated high levels of elemental concentrations of silicon (Si) at 24%, aluminium (Al) at 6% and iron (Fe) at 3% with magnesium, sulphur and potassium at concentrations approximately 0.1%. Other trace elements such as Cr, Ni, Ba, Nb, Zr, Y, Sr, Rb, and Co were identified in more minute amounts (0.01% or less). Analysis of mineral composition by x-ray

diffraction (XRD) revealed the dominant minerals present were silicate and phyllosilicate minerals. The analysis revealed the predominant minerals as quartz – SiO₂ with some percentage of kaolinite (orthoclase), illite and smectite (feldspar). Quartz was identified by Rietveld analysis at 61.5% and feldspars (or aluminosilicates) were detected in smaller amounts and include kaolinite (7%), albite (5.8%), and microcline (4.8%). The clay mineral illite was found at 2%. Other common soil minerals such as dolomite, siderite and pyrite were not detected in the sample. The soil pH was found to be near-neutral at 7.5.

4.1.2 Mesocosm experiments

The concentration-time profiles for toluene, total iron and pH in the active and control mesocosms is shown in Figure 4.1.

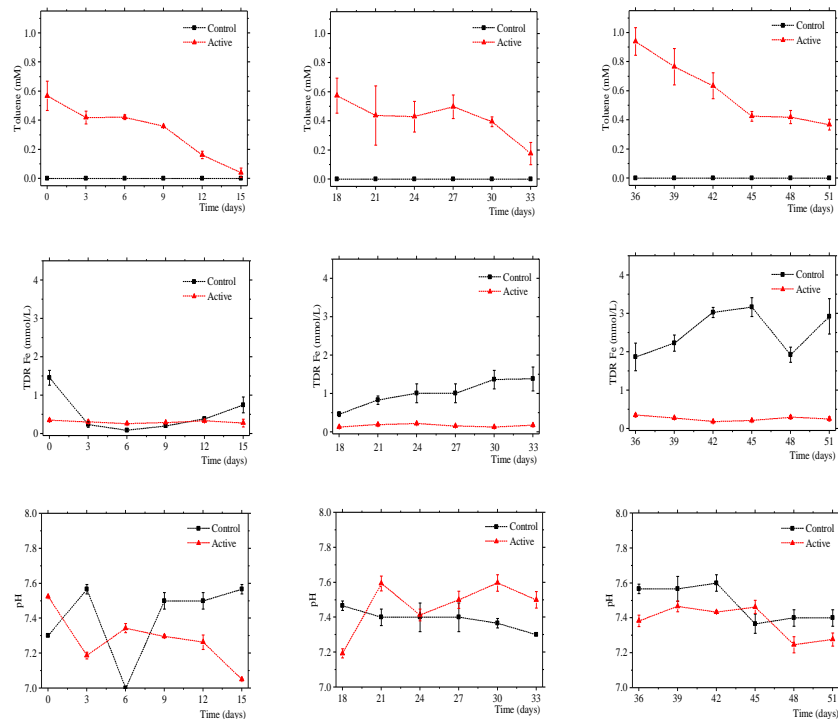


Figure 4.1 Concentration-time profiles showing toluene, total dissolved reactive iron and pH in the control and active mesocosms. Trend lines are separated according to time of addition of toluene spikes to the active mesocosms. Error bars represent the standard error of the mean of three replicates.

A comparison of the total dissolved iron concentration and pH in the active and control mesocosms show similarities in the pH of the soil-water mixture of both mesocosm sets however the total iron concentrations were not similar. There was a gradual increase in total iron concentrations in the control mesocosms as described in the Preamble (section P-1). The control mesocosms (i.e. the mesocosms containing soil and water only) contained 1.5 ± 0.19 mM of total dissolved iron at

the start of the experiments, however a decline in this concentration was observed as it was found to be at 0.2 ± 0.07 mM on the third day. Although the total dissolved concentrations did not vary significantly over the following 9-day period, a gradual rise in total dissolved iron concentrations was observed by day 12, and continued over the period of incubation. Under neutral conditions of pH, Fe^{2+} is more soluble than Fe^{3+} therefore the total dissolved iron concentrations in the active and control mesocosms were likely to be more representative of the amount of Fe^{2+} in solution. The gradual increase in total dissolved iron concentrations in the control mesocosm from day 21 onwards suggests the mesocosms may have, at that point, been under the influence of an on-going process that contributed to the overall total dissolved iron concentrations in the liquid. The total dissolved concentrations in the active mesocosms were found to be at 0.4 ± 0.04 mM after the addition of the first toluene spike and remained within this range after the addition of the second and third toluene spikes (see Figure 4.1). The amount of dissolved iron concentrations in the active mesocosms remained unchanged during the three periods following the addition of toluene. The characterisation tests did not reveal significant amounts of competing terminal electron acceptors (i.e. nitrates and sulphates). Therefore, under the assumption that toluene degradation occurred under predominantly iron-reducing conditions, the electron transfer process between toluene (the electron donor) and Fe^{3+} (the terminal electron acceptor) occurred with iron in the micro- and nanomolar range as opposed to the processes occurring in the control mesocosms which induced a build-up in dissolved iron concentrations in the millimolar range. The pH in the control mesocosms were initially at 7.3 ± 0.01 and remained within a 7.3-7.6 range all through the period of incubation. Similarly the initial pH in the active mesocosms, initially at 7.5 ± 0.01 , remained within the range of 7.1-7.6. The concentration-time profile suggests the activities occurring in the control and active mesocosms produced no significant effects on the pH in these mesocosms.

A concentration of 0.6 ± 0.10 mM was observed in the mesocosms after the first toluene spike (see Figure 4.1). The starting concentrations mesocosms after the addition of the second and third spike were 0.6 ± 0.12 mM and 0.9 ± 0.10 mM respectively. The concentration-time profile indicates a gradual suppressing of toluene removal was observed during the period following the addition of the third spike. Analysis of the time series experimental data showed 96.7 ± 10.4 mg of toluene was degraded in the active mesocosms at the end of the first spike period (see Figure 4.2). Slightly lower amounts of removal occurred at the end of the period following the addition of the second and third spikes (71.7 ± 15.8 mg and 69.1 ± 2.8 mg respectively).

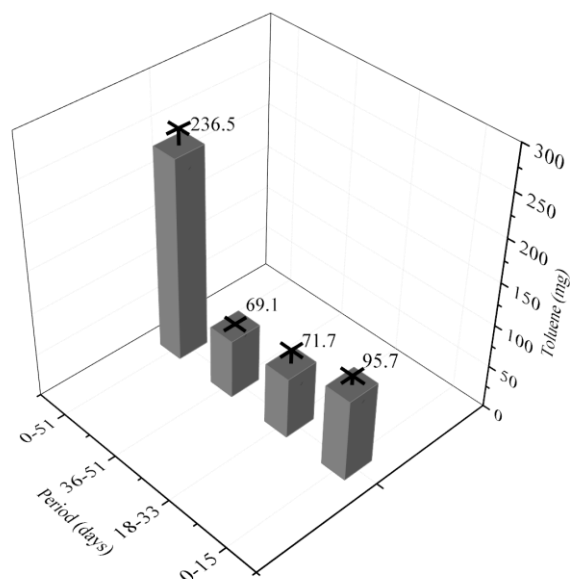


Figure 4.2 Toluene removal in the active mesocosms during the first spike period (0-15 days), second spike period (18-33 days), third spike period (36-51 days) and overall incubation period (0-51 days). Error bars represent the standard error of the mean of three replicates.

When fitted to zeroth order rate kinetics, the rates of toluene degradation were $3.05 \pm 0.5 \text{ mg}^{-1}\text{I}^{-1}\text{day}^{-1}$, $1.95 \pm 0.76 \text{ mg}^{-1}\text{I}^{-1}\text{day}^{-1}$, and $3.60 \pm 0.57 \text{ mg}^{-1}\text{I}^{-1}\text{day}^{-1}$ for the first, second and third periods after spiking. When fitted to first order rate kinetics the degradation rates were $0.09 \pm 0.02 \text{ day}^{-1}$, $0.06 \pm 0.02 \text{ day}^{-1}$, and $0.06 \pm 0.01 \text{ day}^{-1}$ for the respective time periods (see section B-6 of Appendix B). The rate fittings show the rate of toluene removal did not vary significantly during each spike period.

4.1.3 Chemical sequential extractions

Each mesocosm was drained to the 500 mL mark at the end of the spiking period to accommodate the subsequent 300 mL re-spiking from a prepared toluene stock solution. The process of draining the liquid may have removed a portion of the solid and dissolved constituents in the soil-water matrix. It is therefore likely that the total dissolved aqueous concentrations in the active mesocosms during the second and third spike periods were not a true representation of the total dissolved iron fraction in the system. For a more accurate estimation of iron content, a sequential extraction method was applied. This method was used to analyse iron in the solid phase according to operationally-defined fractions or pools (see section 3.3.4 of the methods chapter) and was performed on material from the starting soil, control mesocosms and active mesocosms. The results of the single-step extraction for the total extractable iron content showed the total extractable iron content was $10,181.7 \pm 370.5 \text{ mg/kg}$ in the starting soil material (S_S), $9,023.6 \pm 1,454.2 \text{ mg/kg}$ in the

incubated material from the control (S_0) mesocosms, and $10,702.8 \pm 918.0$ mg/kg, in the active (S_T) mesocosms respectively (see Figure 4.3). From Figure 4.3 it can be seen that the a smaller total iron pool was present in the incubated material from the control mesocosms when compared to the starting soil material as well as the incubated material from the active mesocosms.

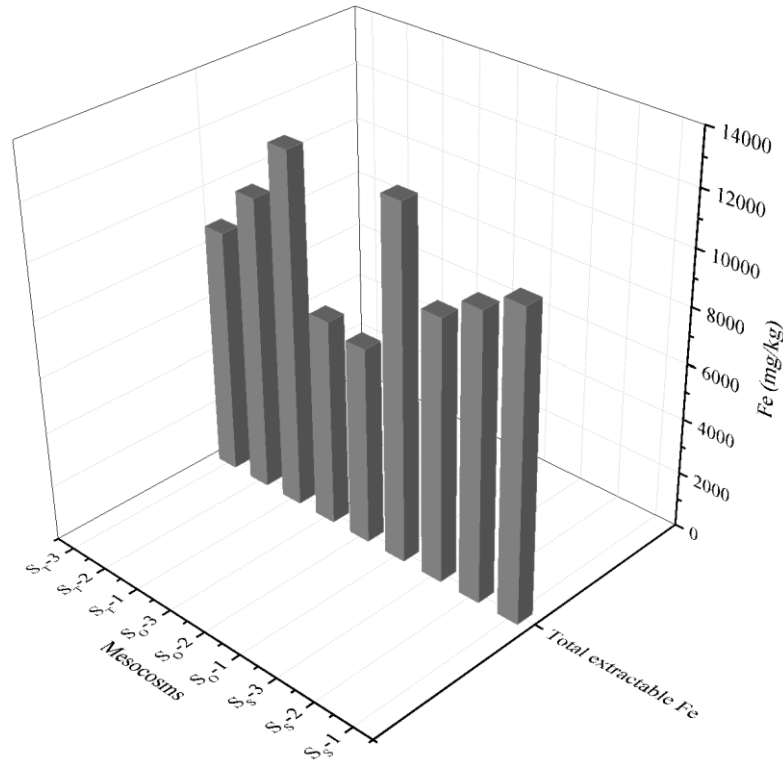


Figure 4.3 Total extractable iron fractions in replicate samples of the starting soil material (S_S) and incubated material from the control mesocosms (S_0) and active experiments (S_T)

The results for the amount of the easily reducible pool in the starting soil material and incubated material from the control and active mesocosms were $6,736 \pm 270.7$ mg/kg, $4,711.6 \pm 579.7$ mg/kg, and $4,387.7 \pm 557.5$ mg/kg respectively. A comparison of the total extractable iron pool with the easily reducible iron pool indicates the easily reducible pool made up approximately 75% of the total extractable pool in the starting material as well as the incubated material from the control and active mesocosms (see Figure 4.4). The results suggest the period of incubation in both control and active mesocosms induced a decline in the amount of the easily reducible iron pool present in the soil material.

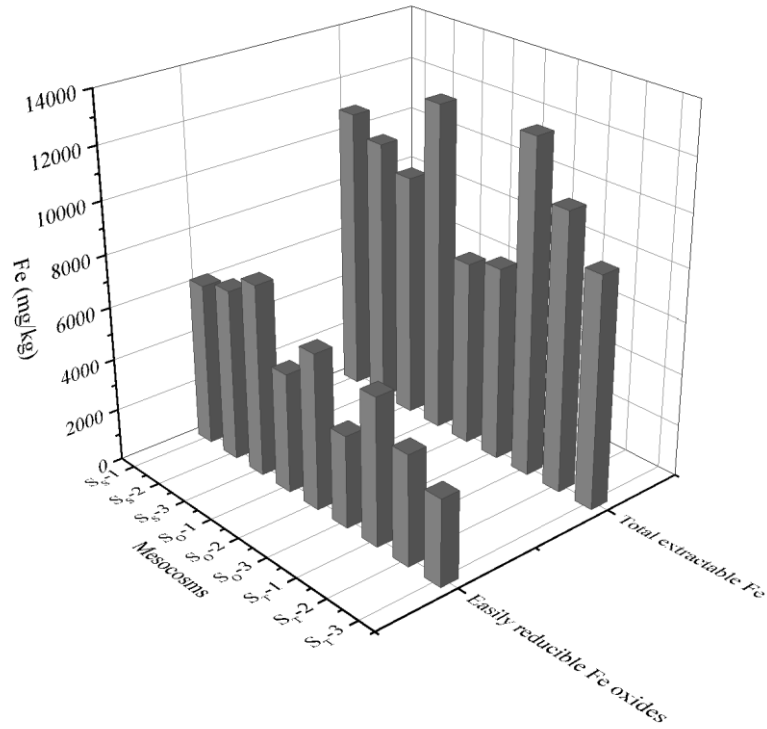


Figure 4.4 Total extractable and easily reducible iron fractions in replicate samples of the starting soil material (S_S) and incubated material from the control mesocosms (S_O) and active experiments (S_T)

The extractions for the carbonate-bound iron showed the starting material, control mesocosm material and active mesocosm material contained 196.1 ± 11.4 mg/kg, 196.1 ± 11.4 mg/kg, and $5,252.1 \pm 291.8$ mg/kg of this fraction respectively. The comparatively higher content of the carbonate pool found in the material from the active mesocosms suggests the degradation of toluene in this material may have led to an increase in this carbonate pool in the soil. A comparison of the carbonate-bound iron pool and the total extractable iron pool show the carbonate-bound pool comprised about 34% of the total extractable iron in the soil material (see Figure 4.5).

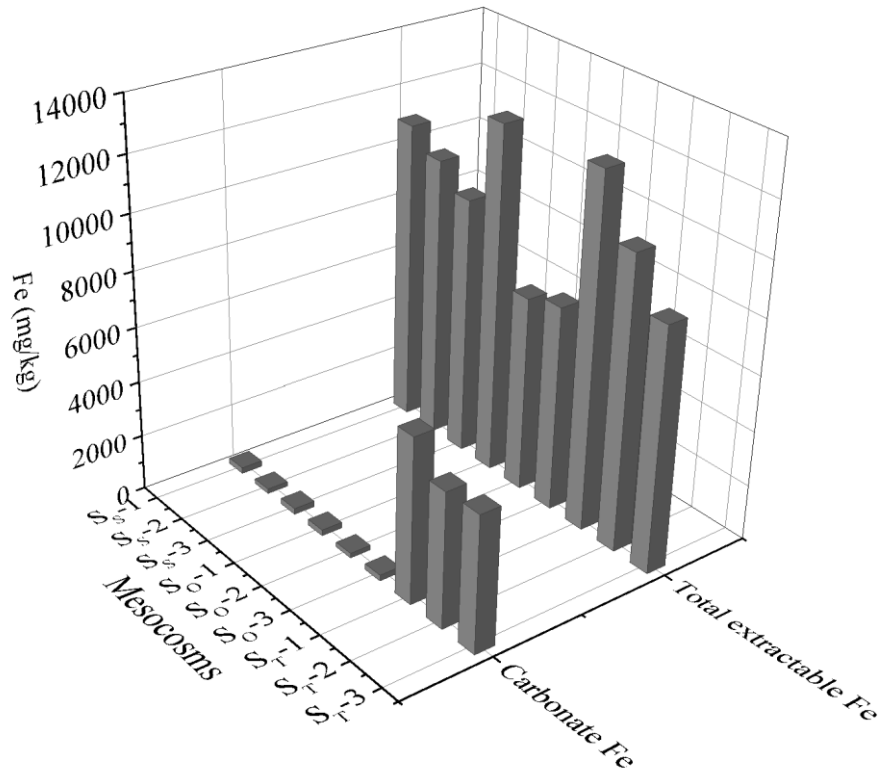


Figure 4.5 Total extractable and carbonate-bound iron fractions in replicate samples of the starting soil material (S_S) and incubated material from the control mesocosms (S_O) and active experiments (S_T)

The results showed the reducible iron fraction in the starting soil material, material from the control mesocosms and the material from the active mesocosms in quantities $2,504.4 \pm 1,445.9$ mg/kg, $2,308.1 \pm 343.3$ mg/kg, and 375.6 ± 20.8 mg/kg in respectively. The results obtained may be an indication that iron-mediated toluene degradation occurred in the active mesocosms with the reducible pool acting as a source of Fe³⁺ for iron-mediated toluene degradation or a source of Fe²⁺ for a different mechanism. A comparison of the reducible iron fraction and the total extractable iron fraction shows this pool consisted approximately 7% of the total extractable iron in the starting material.

The amount of the magnetite fraction in the starting starting soil material, incubated material from the control mesocosms and the incubated material from the active mesocosms was 275.7 ± 24.4 mg/kg, 238.9 ± 45.0 mg/kg, and 253.2 ± 32.3 mg/kg respectively (see Figure 4.6).

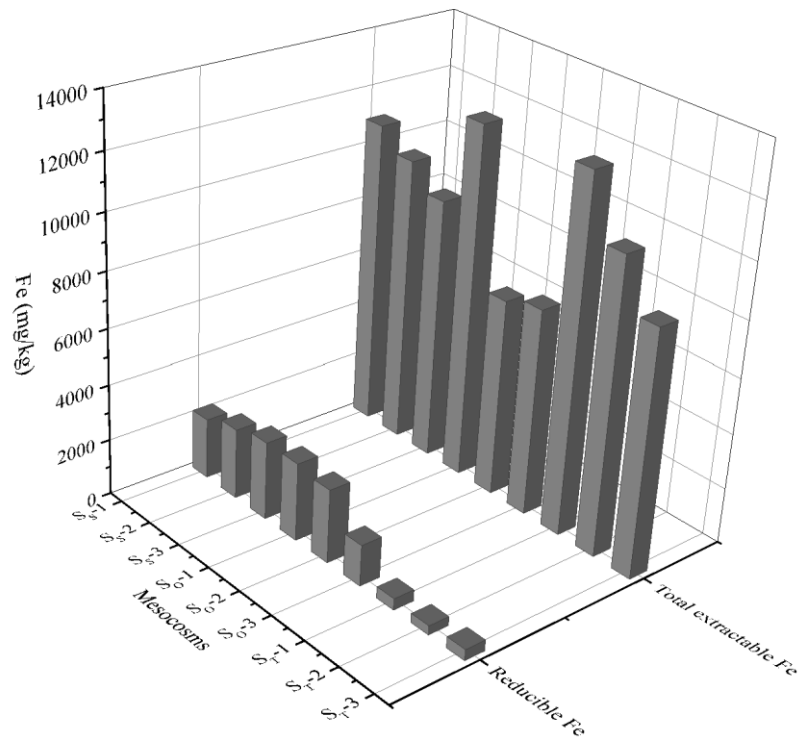


Figure 4.6 Total extractable and reducible iron fractions in replicate samples of the starting soil material (S₅) and incubated material from the control mesocosms (S₀) and active experiments (S_T)

The results indicate the magnetite pool made up about 1% of the total extractable iron. The results also show this pool was not affected by toluene degradation in the active mesocosms. It can also be seen that the magnetite pool was largely similar in the replicate samples for the starting soil material and material from the control and active mesocosms. This may be attributed to the low reactivity of magnetite as an iron mineral and its relatively low abundance in typical soil systems.

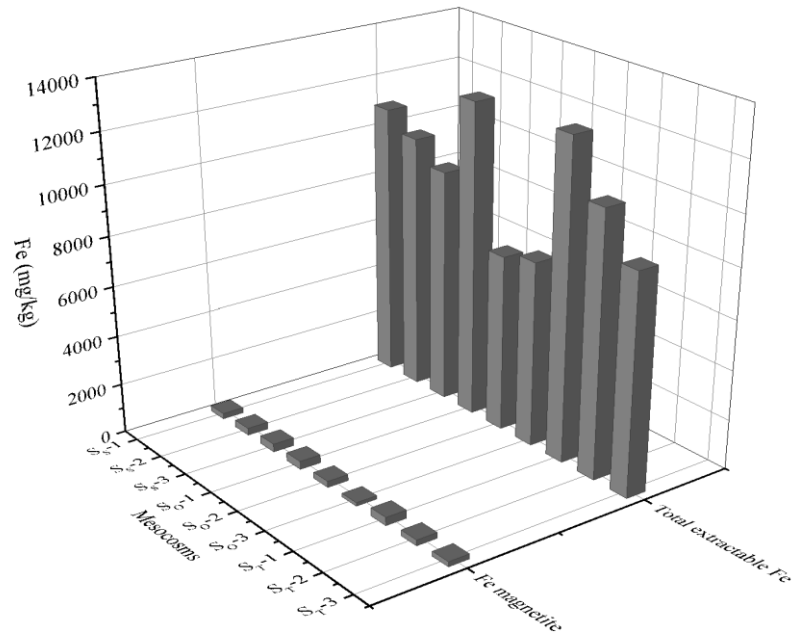


Figure 4.7 Total extractable and magnetite fractions in replicate samples of the starting soil material (S_S) and incubated material from the control mesocosms (S_O) and active experiments (S_T)

The results of the extraction experiments indicate the degradation of toluene induced a build-up in carbonate content and a decrease in the more crystalline reducible oxide pool. These may have occurred concomitantly with toluene degradation or via separate mechanisms influenced by the presence of toluene degradation. The protocol for the sequential extraction includes iron minerals such as goethite, hematite, and akageneite as part of the reducible oxide pool (refer to table 3.5). Crystalline phases which possess less stable structures that are more accessible to these organisms and are, as a result, more readily degraded than poorly crystalline or amorphous phases. Therefore it is possible that the lower concentrations of the reducible oxide pool in the material from the active mesocosm may have been due to a separate mechanism occurring in the active mesocosms. The combined results of the extraction can be seen in Figure 4.8 below.

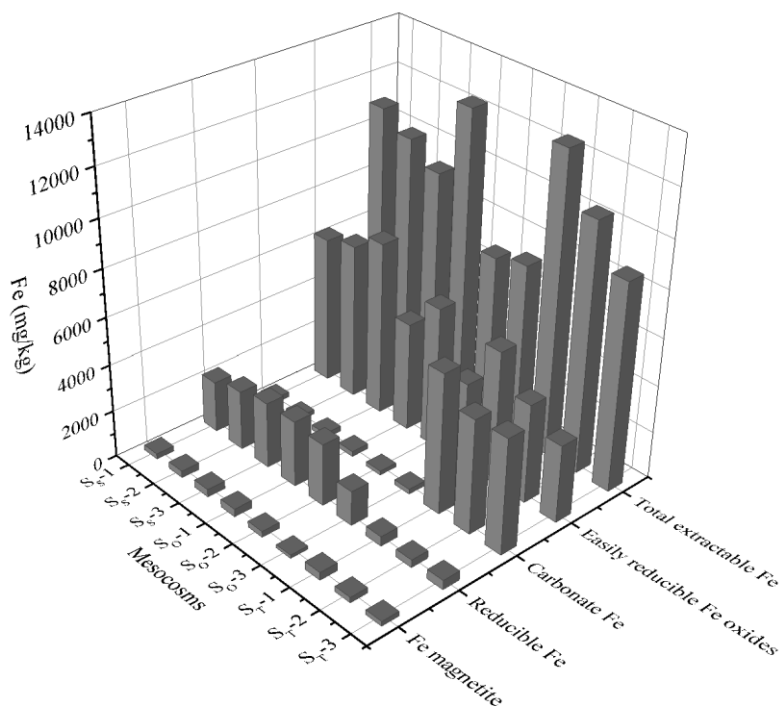


Figure 4.8 Total extractable, easily reducible, carbonate-bound, reducible, and magnetite fractions in replicate samples of the starting soil material (S_S) and incubated material from the control mesocosms (S_O) and active experiments (S_T)

The two-step extraction procedure for sulphate-bound iron gave no indication of the presence of pyrites or acid volatile sulphates in the analysed samples.

4.2 General discussion

Soil is generally composed of a mixture of carbonates, clay minerals, hydrous oxides of Fe, Mn, and Al, sand, silt, and organic matter. Soil type plays an important role in the fate of hydrocarbon contaminants (Semple, K.T. et al., 2003). The breakdown of hydrocarbons is influenced by the soil environment and its physical, chemical and microbiological components (Scherr et al., 2007). A typical mineral soil is comprised of approximately 45% mineral material (i.e. sand, silt and clay in varying proportions), 25% air and 25% water (i.e. 50% pore space, commonly half saturated with water) and 5% organic matter (variable). The ratio of sand to clay and silt in the starting material indicate the sample to be a suitable environment for microbial activity as soils of a high clay content tend to restrict the flow of oxygen and limit biotransformation (Sims, 1990; BSI, 1995). XRF analysis revealed the major elements were silicon (Si) at 24.4 %, aluminium (Al) at 5.5%, and iron (Fe) at 2.7% and was in agreement with the findings of the XRD analysis which showed the soil material was predominantly composed of quartz and phyllosilicate minerals. The

results of the characterisation tests demonstrated the suitability of the chosen soil sample for the biodegradation experiments in this study.

Soil water is a catalyst for many microbial reactions, however an excess of water can limit oxygen availability and reduce microbial activity (Sims, 1990). The analysis showed the soil moisture content determined by gravimetric analysis was 31.7% (at 0.05 bar). This moisture content is in a range known to be suitable for soil microbial activities. The soil had a pH of 7.5, a range also suitable for microbial activities as the most common heterotrophic bacteria are active at soil pH near neutral (Leahy and Colwell, 1990). During the course of the experiments, this pH was monitored to ensure it remained in a range suitable for soil microorganisms. Soil microorganisms (bacteria, fungi) are known to play an important role in the biodegradation of contaminants (Bastiaens et al., 2000; Johnsen et al., 2002; Ho et al., 2000). They are however more tolerant to neutral or basic pH, therefore the bacterial population in the soil in the mesocosms may be expected to be greater at neutral and basic pH. The results showed the active and control mesocosm environment to be predominantly circum-neutral (i.e. between pH 6.5 and 7.5) during the period of incubation.

Although the active mesocosms supported toluene removal, the results suggest the total iron concentrations in the soil-water mixture was not significantly affected during the period of incubation. In contrast, a build-up of total iron was observed in the control mesocosms and was possibly indicative of iron cycling processes occurring as a result of soil microbial processes. This build up was not observed at the start of the experiments. It may be speculated that this was due to the soil microbes being in their adaptation or lag phase over that period.

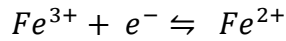
The main objective of the degradation experiments reported in this chapter was to investigate toluene degradation in subsurface soil systems having iron reduction as the dominant electron accepting process. It is widely accepted that under anaerobic conditions, nitrate-reduction is the most energetically-favourable terminal electron accepting process, followed by manganese reduction, iron reduction, sulphate reduction and methanogenesis (Lovley, D.R., 1997b; Lawrence, 2006). Analysis of the dissolved ion content in the starting soil material and river water samples in the mesocosms (see section 4.1) revealed both samples contained trace amounts of nitrates and sulphates (from IC analysis) as well as trace amounts of manganese (from XRF and XRD analysis). The absence and / or low concentration of these competing electron acceptors confirmed the dominant terminal electron-accepting process in the mesocosms was iron reduction. Furthermore, no sulphide was detected in the mesocosms, indicating significant sulphate reduction did not occur.

The results of the time-series experiments indicated initial toluene concentrations in the mesocosms at the time of spiking were in the 0.3–0.7 mM range (the equivalent of 28–64 mg/L). It is possible for losses in the concentration of the volatile contaminant to occur as a result of sorption to solids such as soil particles and volatilisation in air (Reid et al., 2000). The mesocosms contained 500 mL of river water and 300 mL of toluene at the end of each spike (i.e. the end toluene concentration in the mesocosm was 0.8 mM or 75 mg/L). Therefore it is possible that losses due to sorption to soil may have taken place after the initial toluene spike was made. Vaporisation losses may also have occurred. The soil-water mixture was shown to have supported toluene removal over the period of incubation. Suppressed toluene removal was observed during the period after the addition of the third toluene spike. Studies have shown and it is well documented that organic contaminants may be accumulated within the soil, the soil biota, or retained within the soil's mineral organic matter fractions during biodegradation. The decline in toluene removal during the period after the addition of the third spike may have been brought about by any one of these processes. It is also possible this decline in toluene removal was induced by the toxic inhibition of bacterial cells or toluene-degrading microorganism in the sealed soil-water environment of the mesocosms during the period after the addition of the third spike. The effect of toxic inhibition of microbial cells has been demonstrated by several studies. A study by (Lovley, D.R. and Lonergan, 1990) investigated the degradation of toluene, phenol, and p-cresol under anaerobic conditions with Fe (III) as the sole electron acceptor using the bacterial strain GS-15, isolated from soil. During the growth on toluene (92 mg/L, dark, 100 mM iron oxide), GS-15 had mineralised 55% of toluene after 60 weeks of incubation however toluene degradation was inhibited at concentrations higher than 920mg/L. In (Sikkema et al., 1995) prolonged interaction of hydrocarbons with microbes (including iron-metabolising microorganisms) was shown to produce a resultant decrease in microbial activity due to the toxic effect on microbial membranes. Although increased toxicity brought about by degradation is disadvantageous to soil biota, it is an indication of the success of bioremediation as the production of metabolites which are more toxic than the parent compound may serve as an index for toluene degradation occurring in a system (Watson et al., 1999).

Zeroth and first order rate fittings obtained from the toluene time-series data provide an indication of the rate at which toluene removal occurred during the periods after the addition of the first, second and third spikes to the soil-water mixture. A zero order biodegradation implies the contaminant concentration is high relative to available contaminant-degrading microbes. A first order biodegradation, on the other hand, implies the concentration is not high enough to saturate the ability of the

contaminant-degrading microbes. Therefore, first order kinetics apply where contaminant concentration is low relative to soil biological activity, meaning at any given time the rate of contaminant degradation is proportional to its concentration. Under certain conditions, increasing contaminant concentrations may induce a change in the relationship between concentration and degradation from being proportional to being independent of one another. Michaelis-Menten kinetics may apply under such conditions (Riser-Roberts, 1998). An average initial toluene concentration of 0.57 mM was observed in the active mesocosms after the first and second spike. Toluene removal during both periods occurred at 0.09 d^{-1} . In the period following the third toluene spike an initial concentration of 0.94 mM was observed on average and removed at a rate of 0.06 d^{-1} over the period. Similar findings are reported in (Søvik et al., 2002) in which first order degradation coefficients for toluene were obtained in the range of $0.19 - 0.21 \text{ d}^{-1}$. The results obtained show toluene removal did not increase after the re-addition of toluene. These results may be attributed to the complexities that may arise as a result of conducting experiments using live soil as opposed to microbial cultures grown under laboratory conditions. A study by (Mathura and Majumder, 2010) reported an increase in specific degradation rates of BTEX degradation at initial concentrations within the range of 10 to 400 mg L^{-1} (0.11- 4.34 mM) in the presence of a pure microbial culture. Similarly (Lee et al., 2002) report increased rates in degradation at initial concentrations within the range of 23 to 70 μM (0.023-0.07 mM). It may be concluded that the degradation experiments in this study demonstrate toluene removal in laboratory-constructed soil systems and suggest the rate of removal did not change significantly with the re-introduction of toluene into the mesocosms.

The results of the chemical sequential extractions provided an indication of the amount of the solid iron content in the starting soil material and incubated mesocosm material from the active and control mesocosms. In anoxic freshwater habitats, ferric iron is usually the dominant electron acceptor for the mineralisation of carbon (Thamdrup, 2000). The results showed toluene degradation affected two iron fractions namely the carbonate-bound iron fraction and the reducible iron fraction. The two fractions were seen to vary between the starting and incubated material however the total iron fraction in the control and active mesocosms were the same. This was likely an indication of the mass balance effect of iron cycling in which Fe (II) and Fe (III) remain in equilibrium. The carbonate-bound iron fractions targeted by the extraction procedure include ankerites and siderite, while the reducible iron fractions include goethite, hematite and akaganeite. The carbonate-bound iron fraction is therefore representative of iron in the Fe^{2+} oxidation state while the reducible fraction includes iron in the Fe^{3+} oxidation state. The underlying reaction for iron cycling is given by the equilibrium reaction (Equation 4.1) below:



Equation 4.1

As Fe^{2+} and Fe^{3+} remain in constant equilibrium, the effect of the incubation period on both fractions may be taken to be a reflection of this mass balance effect in which the build-up of Fe (II) minerals induces the removal of Fe (III) minerals. The reducible iron fraction is composed of the more crystalline iron hydr (oxides) in contrast to the easily reducible fraction which contain less crystalline and amorphous iron (hydr) oxides. Crystalline iron phases are known to be harder to degrade due to their stable structures (Dollhopf et al., 2000; Luu and Ramsay, 2003). Therefore the observed decrease in the reducible phase in preference to the easily reducible phase is a deviation from the wider literature. The increase in carbonate fractions was likely due to carbonate precipitation which may have occurred during the period of incubation. Soil environments are made up of a vast array of macro and micro living organisms. The mesocosms used in this study may be regarded as experimental analogues of subsurface soil environment. At subsurface levels, bacteria, protozoa and phytoplankton are the dominant microorganisms in soil environments. Bacteria are one of the smallest living organisms but possess the largest surface area to volume ratio and therefore are able to sorb metal cations forming more concentrated solutions in comparison to the surrounding environments. These organisms are therefore able to precipitate metals in quantities equal to or exceeding their own weight and are thought to be responsible for mineral transformations in soils induced by iron cycling processes (Schultze-Lam et al., 1996). Several studies have reported the formation of dissolved Fe^{2+} (or its precipitation as goethite, green rust, vivianite or siderite) during microbial Fe (III) reduction. The formation of these compounds was dependent on Fe (III) reduction rates and on geochemical conditions such as the presence of anions, mineral nucleation sites and humic substances. An extensive review of Fe (II) formation induced by Fe (III) reduction can be found in (Konhauser, K.O., 1998) and (Fortin and Langley, 2005). Field and laboratory studies citing instances of siderite precipitation during iron cycling and contaminant degradation can be found in (Driese et al., 2010; Langmuir, 1997; Renard et al., 2017). The sequential extractions provided information on the solid iron content in the sample soil material. In anoxic freshwater habitats, ferric iron is usually the dominant electron acceptor for the mineralisation of carbon (Thamdrup, 2000). The concentration of Fe (II) from Fe (III) reduction / Fe cycling in natural environments is controlled by the adsorption or precipitation of Fe (II). Dissolved Fe (II) may adsorb to soil particles, cell surfaces or to the surface of iron oxides (Liu, C. et al., 2001). The experimental results in this study suggest solid Fe (II) may play a more significant role than Fe (II) in the dissolved phase.

4.3 Conclusion

The experiments conducted demonstrate toluene removal in sealed, anaerobic mesocosm environments. Changes in selected geochemical factors affected by iron-mediated toluene degradation were observed over the period of incubation. These were rate and amount of toluene removal, solid and dissolved iron concentrations, pH and surface area. The starting soil and water sample in the mesocosms were pH neutral. No significant changes in pH or total iron was observed however changes in operationally-defined iron fractions in the soil gave evidence for the occurrence of iron carbonate precipitation. It may be concluded from the experiments that the input of hydrocarbons into soils had a direct influence on microbial Fe (III) reduction and indirectly (via Fe (II) formation) on microbial Fe (II) oxidation. BSI Guidelines suggest the presence of an active microbial population in soil may be determined through the use of a biodegradable reference mixture. In this study, the use of control systems with no toluene may be considered to be a satisfactory means of confirming biological activity of the soil. In addition, the focus of this study was the geochemical changes of toluene in soil, therefore a full speciation of the soil's microbial consortia was considered unnecessary.

Summary

In this chapter, toluene degradation was assessed in analogues of subsurface soil environments. The removal of toluene over the period of incubation indicated the soil-water mixture supported toluene degradation under predominantly iron-reducing conditions. Chemical sequential extractions performed on the mesocosm soil material suggested the degradation of toluene in the active mesocosms induced an increase in carbonate-bound iron from 196.1 ± 11.4 mg/kg to $5,252.1 \pm 291.8$ mg/kg and a decrease in the reducible iron fraction from $2,504.4 \pm 1,445.9$ mg/kg to 375.6 ± 20.8 mg/kg. Shifts in pH were observed in the control and active mesocosms at the start of the experiments however the pH of both mesocosms showed little variation during the incubation period(see section C.7 of Appendix C).

Chapter 5

The Influence of Iron Mineral (Hydr)Oxides On Iron-Mediated Toluene Degradation

Introduction

The results of the previous chapter showed the active and control mesocosms supported anaerobic toluene degradation. The effect of iron amendments on toluene removal was investigated with the use of additional, serially-sampled batch mesocosms. The results of these experiments are discussed in this chapter.

5.1 Results and discussions

5.1.1 Comparing degradation in the un-amended and hematite-amended mesocosms

A comparison of the experimental results for the un-amended and hematite-amended mesocosms show both groups had similar total dissolved iron concentrations at the time of spiking (see Figure 5.1).

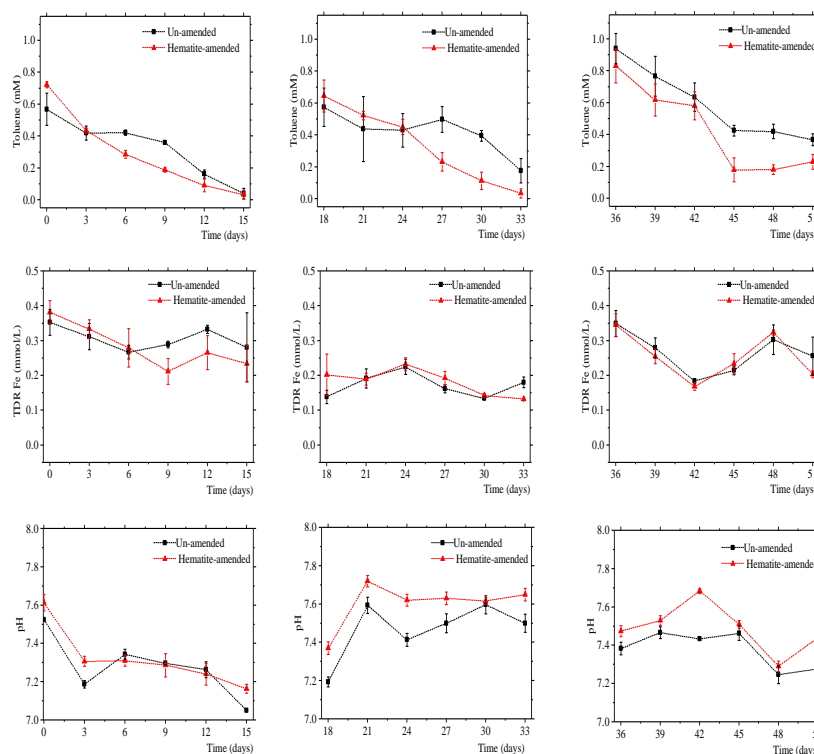


Figure 5.1 Concentration-time profiles showing toluene, total dissolved reactive iron and pH in the un-amended and hematite-amended mesocosms. Error bars represent the standard error of the mean of three replicates.

The values for total iron concentrations at the start of the experiments were 0.4 ± 0.03 mM in the hematite-amended mesocosms and 0.4 ± 0.04 mM in the un-amended mesocosms. Similarly, both mesocosm groups did not show significant variation in initial pH as initial mesocosm pH was measured at 7.6 ± 0.04 in both groups. The similarity in the concentration-time profile for pH and total iron concentrations in the un-amended and hematite-amended mesocosms suggest the presence of hematite did not significantly affect the pH and total dissolved iron concentrations of the soil-water mixture.

A comparison of toluene concentrations also showed similarities in toluene concentrations at the start of the experiments (0.7 ± 0.02 mM in the hematite-amended and 0.6 ± 0.10 mM in the un-amended mesocosms respectively). The experimental results show toluene was removed in both the amended and un-amended mesocosms over similar periods however the amount of toluene removed over the incubation period was appreciably higher in the hematite-amended mesocosms compared to the un-amended mesocosms (see Figure 5.2). A difference in means test (see section C.9.3 of Appendix C) showed the difference in mean toluene concentrations in the un-amended and amended mesocosms were not statistically significant ($p=0.021$). This suggests the comparatively larger amount of toluene removal observed in the hematite-amended mesocosms may not have been due to the presence of hematite.

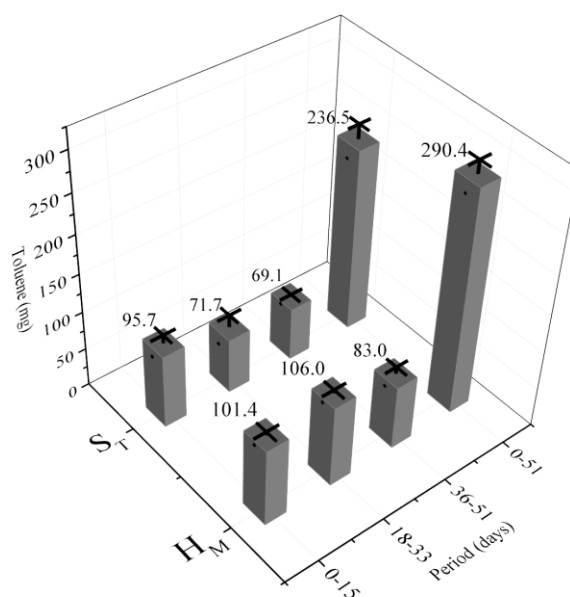


Figure 5.2 Toluene removal in the un-amended and hematite-amended mesocosms during the first spike period (0-15 days), second spike period (18-33 days), third spike period (36-51 days) and overall incubation period (0-51 days). Error bars represent the standard error of the mean of three replicates.

The zeroth order rate fittings for toluene in the hematite-amended mesocosm were $4.98 \pm 0.19 \text{ mg}^{-1}\text{L}^{-1}\text{day}^{-1}$, $3.94 \pm 0.50 \text{ mg}^{-1}\text{L}^{-1}\text{day}^{-1}$ and $4.13 \pm 0.45 \text{ mg}^{-1}\text{L}^{-1}\text{day}^{-1}$ during the periods after the first, second and third toluene spikes respectively. These rate fittings were similar to those obtained for the un-amended mesocosms ($3.05 \pm 0.54 \text{ mg}^{-1}\text{L}^{-1}\text{day}^{-1}$, $1.95 \pm 0.76 \text{ mg}^{-1}\text{L}^{-1}\text{day}^{-1}$, and $3.60 \pm 0.57 \text{ mg}^{-1}\text{L}^{-1}\text{day}^{-1}$ for the respective periods). The first order rate fittings for the hematite-amended mesocosms were $3.20 \pm 0.05 \text{ day}^{-1}$, $0.18 \pm 0.06 \text{ day}^{-1}$, and $0.17 \pm 0.03 \text{ day}^{-1}$ for the three respective periods. Both zeroth and first order rate fittings suggest the rate of toluene removal was not significantly affected by the presence of hematite.

5.1.2 Comparing degradation in the un-amended and goethite-amended mesocosms

A comparison of the concentration-time profiles of the goethite-amended mesocosms and un-amended mesocosms showed similarities in the trend for toluene removal, total dissolved iron concentrations and pH in both groups (see Figure 5.3).

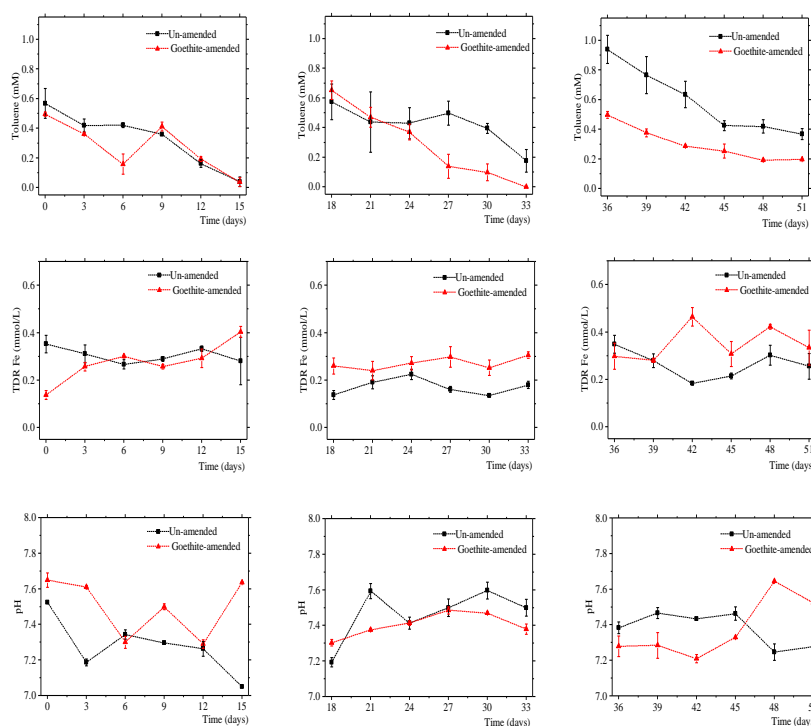


Figure 5.3 Concentration-time profiles showing toluene, total dissolved reactive iron and pH in the un-amended and goethite-amended mesocosms. Error bars represent the standard error of the mean of three replicates.

A slight decline in total iron concentrations was observed as toluene removal occurred following the addition of the first toluene spike. The results show the pH in the amended and un-amended mesocosms remained in the 7.2-7.4 range over the period of incubation. These results suggest the presence of magnetite in the soil-

water mixture did not significantly affect its pH and total dissolved iron concentration.

The goethite-amended mesocosms had initial toluene concentrations of 0.5 ± 0.01 mM, 0.7 ± 0.06 mM, and 0.5 ± 0.02 mM after the addition of the first, second and third spikes respectively. These concentrations were mostly similar to what was observed in the un-amended mesocosms (0.6 ± 0.10 mM, 0.6 ± 0.12 mM, and 0.9 ± 0.10 mM). The removal of toluene ceased gradually on day 45 and suppressed toluene removal can be observed to have occurred from that time point onwards. A total of 108.5 ± 0.01 mg, 109.5 ± 0.01 mg, and 60.4 ± 1.0 mg of toluene was removed in the goethite-amended mesocosms at the end of the first, second and third period after spiking (see Figure 5.4).

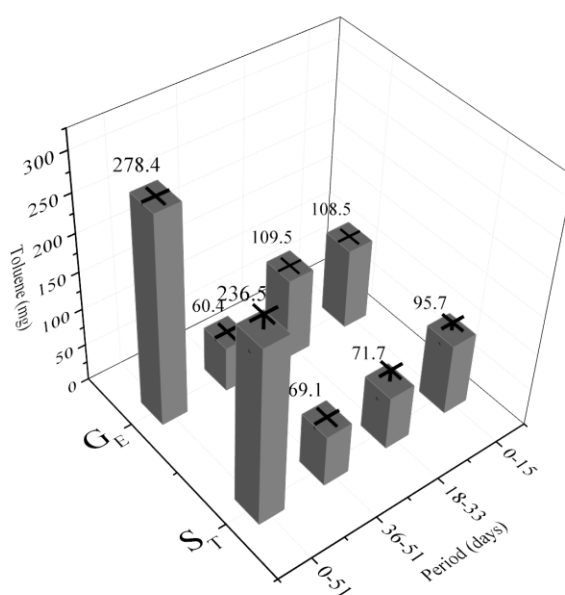


Figure 5.4 Toluene removal in the un-amended and goethite-amended mesocosms during the first spike period (0-15 days), second spike period (18-33 days), third spike period (36-51 days) and overall incubation period (0-51 days). Error bars represent the standard error of the mean of three replicates.

It can be seen from Figure 5.4 that toluene removal was notably higher in the amended mesocosms than in the un-amended mesocosms which removed 95.7 ± 10.4 mg, 71.7 ± 15.8 mg, 69.1 ± 2.8 mg over the respective periods. Pairwise comparisons (see section C.9.3 of Appendix C) showed the differences in toluene concentrations in the amended and un-amended mesocosms were not statistically significant ($p = .001$). This suggests the differences in the amount of toluene removed may not have been entirely due to the presence of the goethite amendment. The zeroth order rate fittings for the goethite-amended mesocosms were 2.33 ± 0.003 $\text{mg}^{-1}\text{L}^{-1}\text{day}^{-1}$, 4.37 ± 0.280 $\text{mg}^{-1}\text{L}^{-1}\text{day}^{-1}$, and 1.84 ± 0.089 $\text{mg}^{-1}\text{L}^{-1}\text{day}^{-1}$ for the

first, second and third periods after spiking. A comparison of this data to the zeroth order rate data for the un-amended mesocosms ($3.05 \pm 0.5 \text{ mg}^{-1}\text{L}^{-1}\text{day}^{-1}$, $1.95 \pm 0.76 \text{ mg}^{-1}\text{L}^{-1}\text{day}^{-1}$, and $3.60 \pm 0.57 \text{ mg}^{-1}\text{L}^{-1}\text{day}^{-1}$) show it was likely the presence of goethite did not significantly alter the rate of toluene removal in the goethite-amended mesocosms. Similarly, the first order rate fittings for the goethite-amended mesocosms ($0.07 \pm 0.003 \text{ day}^{-1}$, $0.25 \pm 0.0075 \text{ day}^{-1}$, and $0.08 \pm 0.003 \text{ day}^{-1}$) did not differ significantly from the un-amended mesocosms ($0.09 \pm 0.02 \text{ day}^{-1}$, $0.06 \pm 0.02 \text{ day}^{-1}$ and $0.06 \pm 0.01 \text{ day}^{-1}$). This may also be taken to be an indication that the presence of goethite did not significantly alter the rate at which toluene was degraded in the soil-water mixture.

5.1.3 Comparing degradation in the un-amended and magnetite-amended mesocosms

A comparison of the experimental results for the un-amended and magnetite-amended mesocosms show both mesocosm groups contained similar total iron concentrations ($0.1 \pm 0.02 \text{ mM}$ and $0.4 \pm 0.01 \text{ mM}$ respectively) at the time of spiking (see Figure 5.5).

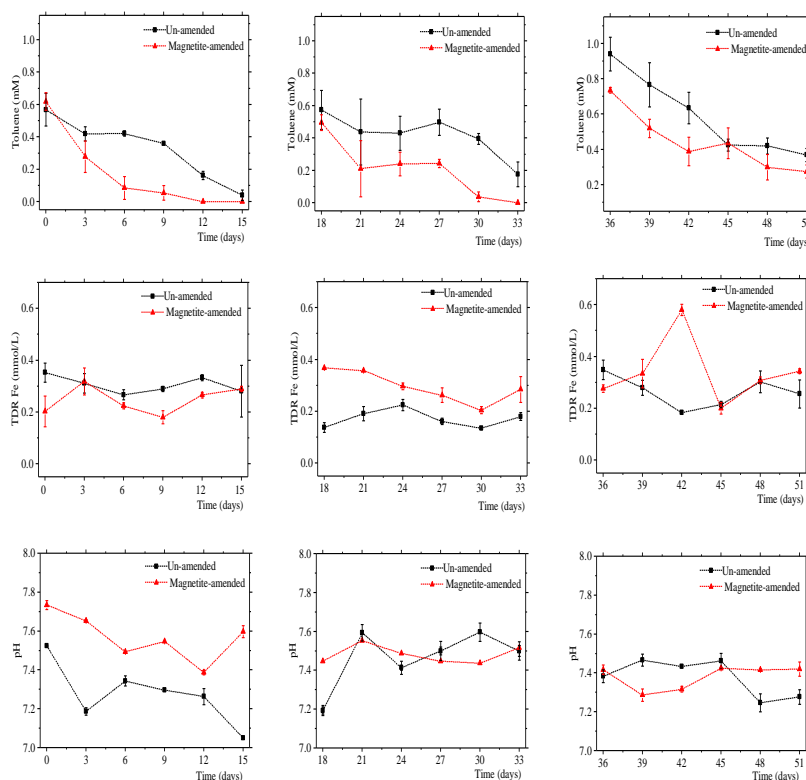


Figure 5.5 Concentration-time profiles showing toluene, total dissolved reactive iron and pH in the un-amended and magnetite-amended mesocosms. Error bars represent the standard error of the mean of three replicates.

No discernible change in pH was observed as a result of the presence of the magnetite amendment as both mesocosm groups had similar profiles for pH. The initial pH in the magnetite-amended mesocosms was 7.7 ± 0.02 on average. This was similar to the un-amended mesocosms in which the initial pH was found to be at 7.5 ± 0.01 . These results suggest the presence of magnetite did not significantly affect the mesocosm pH or total dissolved iron concentrations.

The magnetite-amended mesocosms also had similar initial toluene concentrations of 0.6 ± 0.05 mM and 0.6 ± 0.10 mM respectively. The initial toluene concentrations after the second and third toluene spikes were also similar. The initial toluene concentrations after the second and third toluene spikes were 0.6 ± 0.12 mM and 0.9 ± 0.10 mM respectively in the un-amended mesocosms and 0.5 ± 0.05 mM, and 0.7 ± 0.02 mM respectively in the magnetite-amended mesocosms. Suppressed toluene removal was also observed over the same period in both groups. A comparison of the amount (in mg) of toluene degraded by both groups after each addition of toluene shows the magnetite-amended mesocosms removed more toluene (at 100.0 ± 0.01 mg) after the first toluene spike when compared to the un-amended mesocosms in which 96.7 ± 10.4 mg of toluene was degraded over the same period (see Figure 5.6).

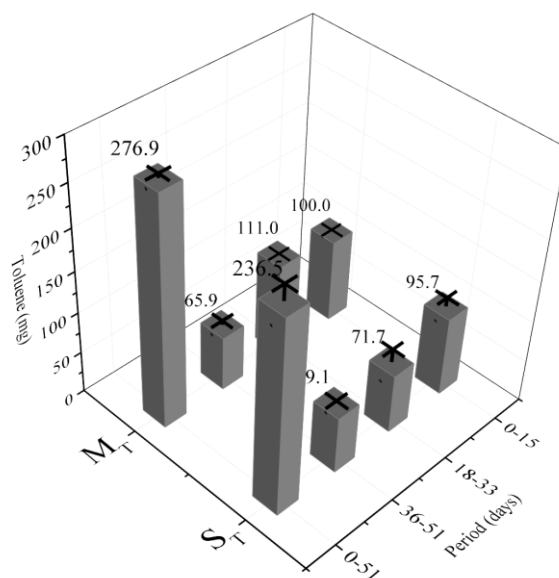


Figure 5.6 Toluene removal in the un-amended and magnetite-amended mesocosms during the first spike period (0-15 days), second spike period (18-33 days), third spike period (36-51 days) and overall incubation period (0-51 days). Error bars represent the standard error of the mean of three replicates.

Similarly the magnetite-amended mesocosms also degraded a greater amount of toluene in the period after the second toluene spike (111.0 ± 0.01 mg) in comparison to the un-amended mesocosms (71.7 ± 15.8 mg). The results for the third spike

period however show the un-amended and amended mesocosms degraded similar amounts of toluene (65.9 ± 4.6 mg and 69.1 ± 2.8 mg respectively). The difference in means test (see section C.9.3 of Appendix C) indicate toluene concentrations for the magnetite-amended and un-amended mesocosms were statistically significant ($p = .0001$). This may be indicate the comparatively larger amount of removal in the amended mesocosms was likely to have been due to the presence of magnetite.

The rate of toluene degradation in the magnetite-amended mesocosms when fitted to zeroth order rate kinetics was 3.48 ± 0.48 $\text{mg}^{-1}\text{L}^{-1}\text{day}^{-1}$, 2.63 ± 0.56 $\text{mg}^{-1}\text{L}^{-1}\text{day}^{-1}$ and 2.56 ± 0.19 $\text{mg}^{-1}\text{L}^{-1}\text{day}^{-1}$ for the period after the first, second and third spikes respectively. As the rates in the un-amended mesocosms were similar at 3.05 ± 0.5 $\text{mg}^{-1}\text{L}^{-1}\text{day}^{-1}$, and 1.95 ± 0.76 $\text{mg}^{-1}\text{L}^{-1}\text{day}^{-1}$, and 3.60 ± 0.57 $\text{mg}^{-1}\text{L}^{-1}\text{day}^{-1}$, it may be concluded that the magnetite amendment did not greatly affect the rate of toluene removal in the magnetite-amended mesocosms. A comparison of the first order rate fitting for the three spike periods in the magnetite-amended mesocosms (0.14 ± 0.01 day^{-1} , 0.14 ± 0.01 d day^{-1} and 0.08 day^{-1}) and un-amended mesocosms (0.09 ± 0.02 day^{-1} , 0.06 ± 0.02 day^{-1} 0.07 ± 0.01 day^{-1}) also leads to this conclusion.

5.1.4 Comparing degradation in the un-amended and ferrihydrite-amended mesocosms

A comparison of the concentration-time profile for toluene, total dissolved iron and pH in the ferrihydrite-amended and un-amended mesocosms indicate the presence of ferrihydrite in the soil-water mixture induced changes in the system pH and also in toluene usage (see Figure 5.7).

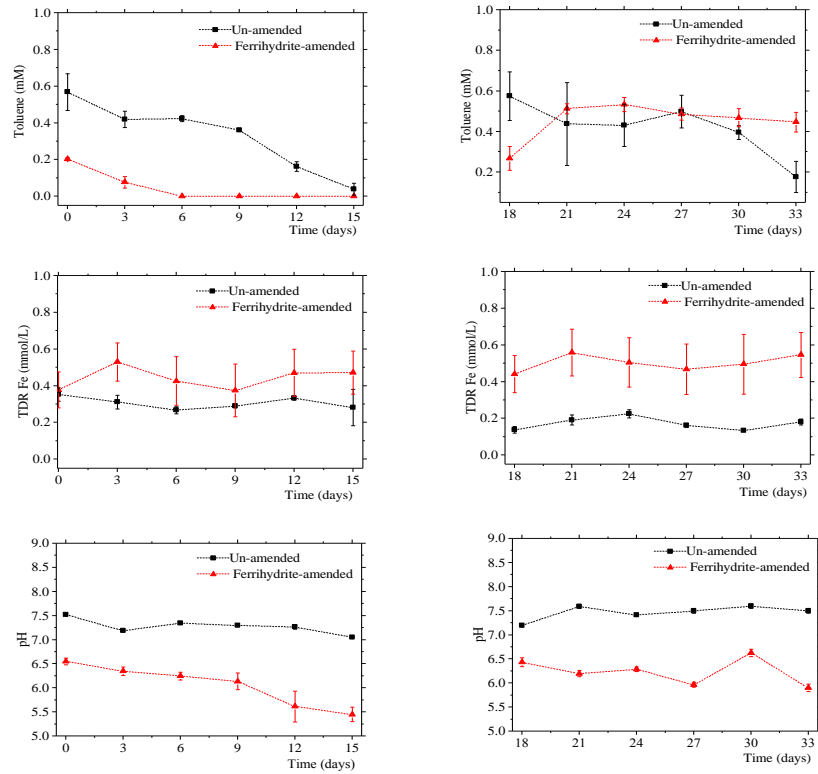


Figure 5.7 Concentration-time profiles showing toluene, total dissolved reactive iron and pH in the un-amended and ferrihydrite-amended mesocosms. Error bars represent the standard error of the mean of three replicates.

In the early stages after spiking, the pH was found to be at 6.5 ± 0.07 in the amended mesocosms 1-unit lower than the pH in the un-amended mesocosms (7.5 ± 0.01). The total iron concentrations were slightly lower (0.3 ± 0.06 mM) in comparison to the un-amended mesocosms (0.6 ± 0.10 mM). The results suggest the presence of the ferrihydrite amendment may have induced an increase in total iron concentration to 0.6 ± 0.12 mM after the addition of the second toluene spike. The pH was however not affected by the re-addition of toluene as shown by the similar concentration-time profiles of both groups.

The gradual decrease in toluene removal (or suppressed removal) observed in previous mesocosms was also observed in the ferrihydrite-amended mesocosms on day 27 in contrast to the un-amended mesocosms in which suppressed removal was observed from day 45 onwards. The soil-amended mesocosms removed a comparatively larger amount of toluene (at 112.0 ± 0.01 mg after the initial toluene spike) in comparison to the un-amended mesocosms in which 96.7 ± 10.4 mg of toluene was degraded over the same period (see Figure 5.8). The difference in means test (section C.9.3 of Appendix C) indicate mean toluene concentrations in

the un-amended in comparison to the amended mesocosms were statistically significant ($p = .0001$).

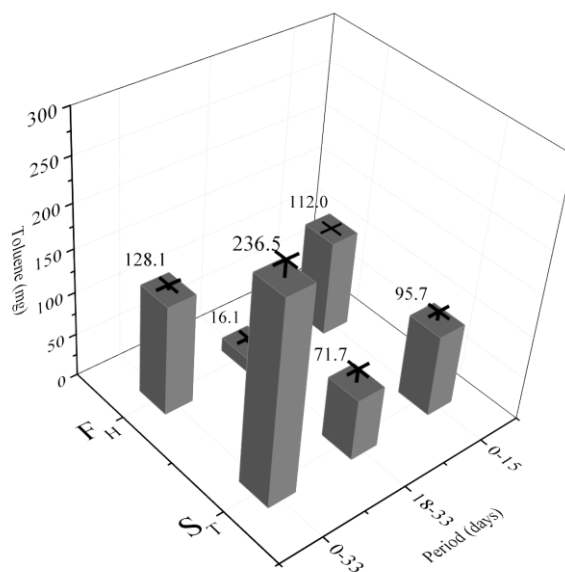


Figure 5.8 Toluene removal in the un-amended and ferrihydrite-amended mesocosms during the first spike period (0-15 days), second spike period (18-33 days), third spike period (36-51 days) and overall incubation period (0-51 days). Error bars represent the standard error of the mean of three replicates.

During the period after the second toluene spike both mesocosm groups degraded similar amounts of toluene (16.1 ± 5.5 mg in the ferrihydrite-amended and 71.7 ± 15.8 mg in the un-amended mesocosms). The lower amounts observed for the period after the second spike may have been due to the suppression of toluene removal observed from day 27 onwards. Zeroth order rate fittings for the period after the first and second spike were 1.1 ± 0.12 $\text{mg}^{-1}\text{L}^{-1}\text{day}^{-1}$ and 0.70 ± 0.37 $\text{mg}^{-1}\text{L}^{-1}\text{day}^{-1}$ respectively for the ferrihydrite-amended mesocosms. The first order fitting rate fittings were 0.25 ± 0.02 day^{-1} and 0.04 ± 0.02 day^{-1} for the periods after the first and second toluene spikes. These results differ from those obtained for the un-amended mesocosms and show the presence of ferrihydrite affected the rate of toluene removal in the mesocosms.

5.1.5 Comparing degradation in the un-amended and lepidocrocite-amended mesocosms

A comparison of the concentration-time profiles of the lepidocrocite-amended mesocosms and the un-amended mesocosms show the the initial total dissolved iron concentrations in the lepidocrocite-amended mesocosms (0.3 ± 0.06 mM) did not differ significantly from that in the un-amended mesocosms (0.4 ± 0.04 mM) (see Figure 5.9).

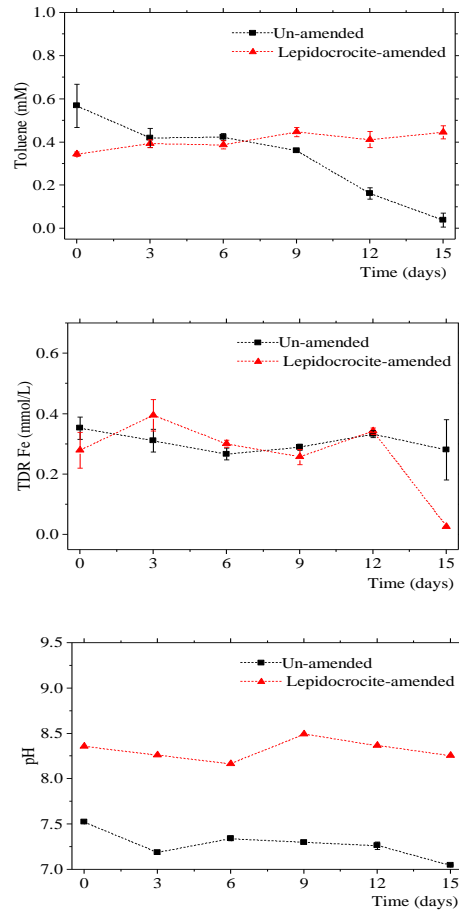


Figure 5.9 Concentration-time profiles showing toluene, total dissolved reactive iron and pH in the un-amended and lepidocrocite-amended mesocosms. Error bars represent the standard error of the mean of three replicates.

The results suggest the presence of lepidocrocite in the amended mesocosms may have induced alkaline conditions as the mesocosm pH after the initial toluene spike was appreciably higher at 8.4 ± 0.04 in comparison to the un-amended mesocosms which had a pH of 7.5 ± 0.01 .

In contrast to the un-amended mesocosms in which complete degradation occurred by the fifteenth day, no significant changes in toluene concentrations were observed in the lepidocrocite-amended mesocosms during the period after the introduction of the initial spike (Figure 5.9)

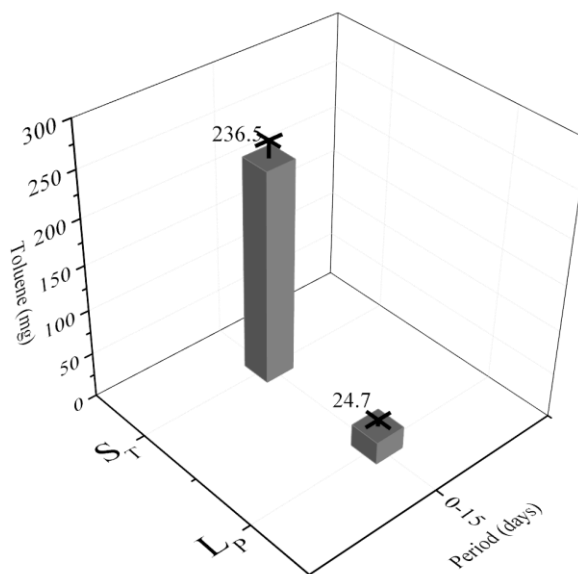


Figure 5.10 Toluene removal in the un-amended and lepidocrocite-amended mesocosms during the first spike period (0-15 days), second spike period (18-33 days), third spike period (36-51 days) and overall incubation period (0-51 days). Error bars represent the standard error of the mean of three replicates.

The un-amended mesocosms removed a total of 96.7 ± 10.4 mg of toluene over the same period (see Figure 6.2). The difference in means test for the amended and un-amended mesocosms (see section C.9.3 of Appendix C) show the mean toluene in the amended and un-amended mesocosms were not statistically significant ($p = .445$) and suggest the 24.7 ± 7.2 mg of toluene removed in the lepidocrocite-amended mesocosms was not due to the presence of lepidocrocite. Lepidocrocite is not known to be a readily available iron source to iron reducers in soil, due to its highly crystalline structure hence the lower amount of removal in the amended mesocosms over the sampling period. Time constraints did not allow for continued sampling of the amended mesocosms after the initial fifteen-day period. The toluene time series data could only be fit to zeroth order kinetics and show toluene removal over the period proceeded at a rate of 0.55 ± 0.22 $\text{mg}^{-1}\text{L}^{-1}\text{day}^{-1}$. This rate is considerably lower than the observed rate in the un-amended mesocosms (3.05 ± 0.5 $\text{mg}^{-1}\text{L}^{-1}\text{day}^{-1}$) and further supports the proposition that the presence of the lepidocrocite amendment did not support toluene removal in the soil-water mixture.

5.2 General discussion

The mesocosm experiments presented in this chapter were conducted to assess the effect of iron amendments on toluene degradation under predominantly iron-reducing conditions. The results of the degradation experiments indicate a total of 290 ± 16.1 mg, 278.4 ± 1.0 mg, and 276.9 ± 4.6 mg of toluene was removed in the

hematite-, goethite- and magnetite-amended mesocosms respectively over the incubation period. The un-amended mesocosms were shown to have removed a total of 236.5 ± 18.0 mg over the same period. Toluene removal was not observed in the lepidocrocite-amended mesocosms over the period of incubation. The results therefore indicate the removal of toluene in the presence of these three minerals (hematite, goethite, and magnetite) was of the order $H_M > G_E > M_T$. A comparison of the rate of toluene removal in the iron-amended and un-amended mesocosms indicated the ferrihydrite-amended mesocosms removed toluene more quickly in comparison to the other iron-amended mesocosms. Conversely the magnetite-amended mesocosms removed toluene at slower rates. Ferrihydrite is known to be one of the most widespread and most active iron hydroxides in soils with a distinctive colour thought to be responsible for pigments observed in certain soils (Schwertmann, U. and Fitzpatrick, 1992). Ferrihydrite rarely occurs as a chemically-pure compound but as admixtures of oxyanions SiO_4^{4-} , PO_4^{3-} as well as cations Al^{3+} (Vodyanitskii, Yu N. and Shoba, 2016). Ferrihydrite has a large specific area and high proportion of reactive sites, therefore a small amount present may contribute largely to the overall properties of a soil and may be responsible for its involvement in organic transformations (Childs, 1992). Ferrihydrite has been shown to interact strongly with organic molecules in soils and may contribute to the stability of aggregates and to soil structure (Schwertmann, U. and Taylor, 1989). A study by (Thamdrup, 2000) showed ferrihydrite remained the primary source of microbial Fe (III) oxide reduction even when it constituted less than 20% of the Fe (III)-pool in the sediment. (Larsen and Postma, 2001) investigated the kinetics of dissolution of 2-line ferrihydrite, 6-line ferrihydrite, lepidocrocite and goethite and report 2-line ferrihydrite as the fastest dissolving iron (III) (hydr)oxide. The findings in this chapter are therefore in agreement with the general literature on the reactivity of ferrihydrite.

The first order rate fittings show the rate of toluene removal per square meter of mesocosms soil per day (see section C.6 of Appendix C) proceeded following the order $F_H > G_E > M_T \geq H_M$ for the period after first spike, $F_H > G_E > M_T \geq H_M$ for the period after second spike, and $H_M > M_T \geq G_E$ for the period after third spike (where F_H , G_E , M_T , H_M represent the mesocosms amended with ferrihydrite, goethite, magnetite and hematite respectively). Hematite therefore had the least influence on the rate of toluene removal and ferrihydrite the highest. These results are in agreement with a similar study (Larsen and Postma, 2001) in which lepidocrocite was found to be less reactive in comparison to other common iron oxides. The zeroth and first order rate fittings suggest the magnetite amendment induced the least effect on toluene removal rates in the soil-water system. In (Sweeton and Baes, 1970) magnetite dissolution was observed to occur faster in comparison to the other

pure ferric oxides studied. The rate of chemical and microbial transformations of iron minerals has been shown to be influenced by the number of available reactive surface sites e.g. –OH functional groups in ferric hydroxides (Roden, 2003). Mineral grains of natural and experimentally-altered soils provide a means of demonstrating the dependence of dissolution processes on soil surface area because distinct proportions of mineral surfaces dissolved with different kinetics. The crystal size of ferric iron oxide is inversely proportional to its surface area. Iron minerals (as well as samples of the same iron mineral) which differ in crystal size will vary significantly in surface area and therefore stability and reactivity as well as dissolution kinetics, transformation reactions and adsorption of organic and inorganic compounds. Surface areas determined by the BET as extent of N₂-adsorption to an outgassed sample of the respective mineral span from a few m²/g (e.g. 8-16m²/g for highly crystalline goethite) to a few hundred m²/g (e.g. 100-400 m²/g for poorly crystalline ferrihydrite) (Cornell, R.M. and Schwertmann, 2003). Characterisation tests performed on the mineral samples suggest the lepidocrocite and hematite mineral samples had the smallest surface area (see Table C.6.1b of Appendix C) while the ferrihydrite amendment had the largest surface area. The comparatively larger surface area of the ferrihydrite sample used in this study likely contributed to the faster rate of toluene removal observed in the ferrihydrite-amended mesocosms. Likewise, the smaller surface area of the magnetite amendment may have contributed to the smaller effect on toluene removal rates observed. The dissolution rate of a mineral is not only dependent on the availability of surface but also on the nature of surface area. This is because the availability of reactive surface area is arguably more important than the amount of available surface area. The mineral surface areas actively involved in dissolution reactions have been termed effective surface area (Helgeson et al., 1984) or reactive surface area (Hochella and Banfield, 1995). The reactive surface area has been said to be made up of high-energy surface sites however experiments have shown this to be a somewhat ambiguous term (Casey et al., 1988; Oelkers, 2002; Murphy, 1989). Magnetite has been shown to serve as an electron acceptor for Fe (III)-reducing microorganisms (Kostka, J.E. and Nealson, 1995; Brown et al., 1997). Natural and synthesised magnetite crystals are not porous and have metallic lustre with an opaque, jet black colour (Cornell, R. and Schwertmann, 1996). The typical surface area of magnetite is 6 m²/g however its effective surface area is believed to vary depending on its texture i.e. whether its particles are coarse or fine (Mannweiler, 1966). The magnetite sample used in this study was jet black in colour, of fine-grained texture and with a surface area of 9 m²/g (see Table C.6.1b of Appendix C). The magnetite-amended mesocosms supported toluene removal however removal occurred at lower rates in comparison to the un-amended mesocosms as well as the

other four groups of iron-amended mesocosms. It may be speculated that the low removal rates in the magnetite-amended mesocosms may have been due to the limited availability of surface sites as well as a lack of reactive surface sites.

The presence of the iron amendments induced no significant changes in the total iron concentrations in the magnetite-, ferrihydrite- and lepidocrocite-amended mesocosms. Total iron concentrations in the hematite-amended mesocosms decreased gradually over the period of toluene removal following the introduction of the initial toluene spike. In the goethite-amended mesocosms, increasingly higher concentrations were observed after the initial spike. With the exception of the ferrihydrite- and lepidocrocite-amended mesocosms, toluene removal in the presence of the iron amendments occurred at circum-neutral pH. Several studies (Madden, A.S. and Hochella, 2005; Madden, A.S. et al., 2006; Yan, 2008) have shown the high crystallinity and low solubility of iron hydroxides at circum-neutral pH account for the low reactivity of macro-particulate iron hydroxides. Hematite, goethite and magnetite minerals are highly crystalline in comparison to ferrihydrite and lepidocrocite. Thus the differences in the behaviour of the amended mesocosms may be attributed to the crystallinity of these minerals.

A comparison of the pH in the un-amended and amended mesocosms indicated the presence of the mineral amendments hematite, goethite, and magnetite did not induce a significant change in pH over the experimental period. The presence of ferrihydrite imposed slightly acidic conditions in the soil-water mixture. Conversely, the presence of lepidocrocite induced slightly alkaline conditions. Goethite, ferrihydrite, and lepidocrocite are Fe (III) minerals. Hematite is an Fe (II) mineral and magnetite an Fe(II) / Fe(III) mineral known as a spinel. Fe (III) mineral oxides are barely soluble at circum-neutral pH and exist in hardly detectable concentrations in the range of 10^{-9} M of Fe (III) in solution (Cornell, R.M. and Schwertmann, 2003; Kraemer, 2004). Fe (III) mineral oxides display amphoteric characteristics which make them soluble at strongly alkaline or strongly acidic pH. In contrast, Fe (II) mineral oxides (such as siderite or ferrous mono-sulphides) are considerably more soluble at neutral pH and may, as a result, exist in solution at concentrations in the micromolar range, even in the presence of bicarbonate or sulphide. The study documented in this chapter was conducted with the use of laboratory-synthesised ferrihydrite and lepidocrocite. Although the presence of ferrihydrite in the soil-water mixture induced slightly higher total iron concentrations in the soil-water mixture (see Figure 5.7) the presence of lepidocrocite did not affect the total iron concentrations (see Figure 5.8). It is possible the slightly acidic environment induced by ferrihydrite improved its solubility and accessibility to iron reducers during the incubation period and may have aided the quicker removal rates observed

in the ferrihydrite-amended soils as well as the comparatively larger amount of toluene removed in these mesocosms during the period following the first spike.

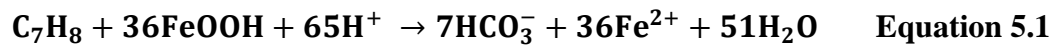
The results of the experiments conducted show all of the iron-amended mesocosms supported anaerobic toluene degradation with the exception of lepidocrocite. Suppressed toluene removal was observed in the un-amended mesocosms after the introduction of the third toluene spike. Suppressed toluene removal also occurred in the hematite-, goethite- and magnetite-amended mesocosms after the addition of the third spike. In the ferrihydrite-amended mesocosms however suppressed toluene removal was observed after the second spike was introduced into the soil-water mixture. Anaerobic degradation is a complex process that usually requires more than one species of anaerobes for complete mineralization to occur (Alexander, 1999). A number of microorganisms have a high affinity for metal cations, as their cell walls have a net negative charge at physiological pH values (Beveridge, 1989). Metal ions in solution undergo hydrolysis with increases in pH. A metal will change from the divalent to monovalent hydroxylated cation depending on the pH range (this is referred to as charge reversal). A 1-unit increase in pH will precipitate iron hydroxides (as well as hydroxides of Cu, Ni, Zn) at lower pH values while hydroxides of calcium (as well as Mg, Hg and Pb) precipitate at pH 9 or above (Collins and Stotzky, 1992). The amount of metal adsorbed by the microorganism increases from almost 0 to 100%. The process of hydrolysis of a metal ion followed by precipitation of a metal hydroxide onto the negative surface of microbial cells reverses its electro-kinetic potential. Depending on the amounts of metal cations present, the reversal in charge might affect physiological functions of the cell or its interactions with other cells and inanimate particulates in soil. Thus the toxic inhibition of iron-reducing microorganisms was also likely to be the reason for suppressed levels of toluene removal observed in the iron-amended mesocosms after the third spike as in the un-amended (S_T) mesocosms. The slightly acidic conditions induced by the presence of ferrihydrite during toluene removal may have contributed to the ferrihydrite-amended mesocosms showing suppressed removal at a point earlier than observed in the other iron-amended mesocosms. This may either have been as a result of die-off of iron reducers induced by the change in pH or by the process described above.

5.3 Conclusion

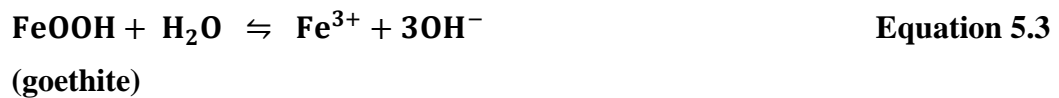
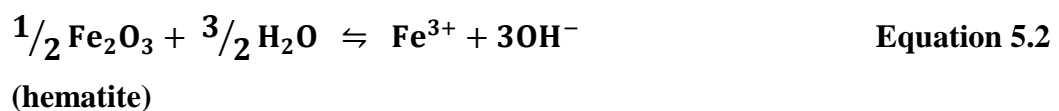
The experiments reported in this chapter were conducted to assess the effect of five selected ferric oxides (hematite, α - Fe_2O_3 and magnetite, α - Fe_3O_4 , goethite, α - $FeOOH$, lepidocrocite, γ - $FeOOH$ and ferrihydrite) on toluene removal. The presence of the amendments in the soil-water mixture supported the removal of toluene and

also enhanced the rates and amounts of toluene removal. All of the iron minerals used were ferric (hydr) oxides with the exception of magnetite, an Fe²⁺/Fe³⁺ oxide. Hematite, goethite, and magnetite are crystalline minerals and were obtained as natural, hard rock minerals. Ferrihydrite and lepidocrocite are poorly crystalline and were laboratory-synthesised. The experimental results demonstrate anaerobic toluene removal in the presence of these crystalline and amorphous iron minerals. From the results, the rate and extent of toluene removal in the presence of these minerals (hydr) oxides is a function of their surface area and crystallinity. The results obtained may provide information for further studies on the behaviour of iron (hydr) oxides in soils.

The iron-mediated degradation of toluene is given by Equation 5.1 below:



In the iron-amended mesocosms, FeOOH is replaced by the iron amendments hematite (Fe₂O₃), goethite (FeOOH), magnetite (Fe₃O₄), ferrihydrite and lepidocrocite. The chemical formula of ferrihydrite has remained uncertain as its chemical composition depends on the size of the domains in its chemical structure which consists of anions on the surface represented by OH-groups bound to H₂O molecules which change the O: OH: H₂O ratio depending on the volume of the particles. As a result there is a disagreement in the literature on the actual chemical formula of the mineral (Vodyanitskii, Y.N., 2008). The half reactions for the dissolution of the iron amendments in the soil-water mixture of the mesocosms are given below (ferrihydrite and lepidocrocite are taken to be the chemical equivalent of amorphous iron (Fe (OH)₃):



Summary

With the exception of the lepidocrocite-amended mesocosms, all of the iron-amended mesocosms were shown to have supported toluene removal. The presence of hematite, goethite and magnetite did not produce a significant change in the pH or total iron concentrations of the soil-water mixture. However the presence of ferrihydrite in the ferrihydrite-amended mesocosms induced a decrease in pH to slightly acid values ranging between pH 6.5 at the start of the experiments and 5.2 at the end of the experiments. The lepidocrocite-amended mesocosms induced a change to slightly alkaline values ranging between pH 8.4 and 8.8 during the period of incubation. A summary of these findings is presented in section C.7 of Appendix C.

Chapter 6

The Influence of Soil on Iron-Mediated Toluene Degradation

Introduction

A discussion of the results of biodegradation experiments conducted with the soil-amended mesocosms is presented in this chapter. The main aim of these experiments was to assess the effect of particle size distribution and surface area of soils on the rate and amount of toluene degradation. Details of the sampling location and sampling depths from which the soils were obtained can be found in section C.2 of Appendix C.

6.1 Results and discussions

6.1.1 Comparing toluene degradation in the un-amended and amended mesocosms (Soil 1)

A comparison of the concentration-time profiles of the amended and un-amended mesocosms groups shows the presence of the soil amendment may have affected the total initial iron concentration of the soil-water mixture (see Figure 6.1).

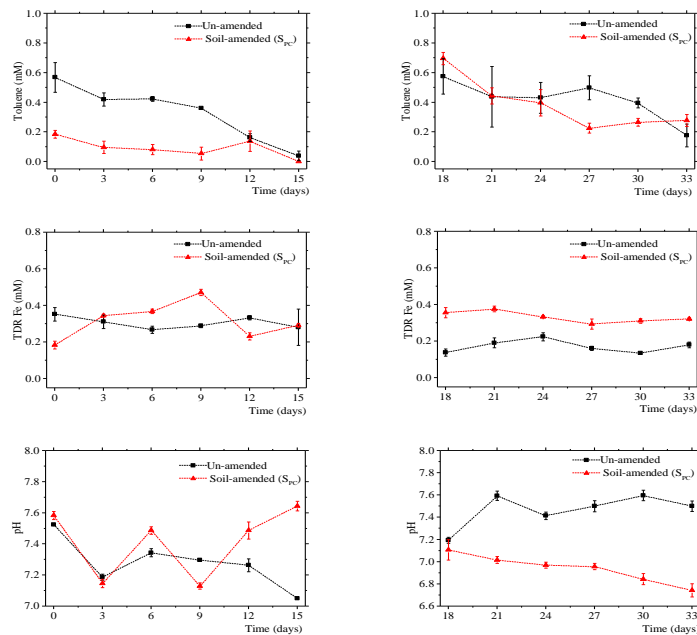


Figure 6.1 Concentration-time profiles showing toluene, total dissolved reactive iron and pH in the un-amended mesocosms and soil-amended (S_1) mesocosms. Error bars represent the standard error of the mean of three replicates.

At the start of the experiments the soil-amended mesocosms total dissolved iron concentrations detected in the soil-amended mesocosms were slightly lower (at 0.2 ± 0.02 mM) when compared to the results for the un-amended mesocosms (0.4 ± 0.04 mM). Initial pH values in both mesocosm groups show the soil amendment may have induced a change in mesocosm pH as the soil-amended mesocosms were found to be at a pH of 6.7 ± 0.06 after the initial toluene spike and the un-amended mesocosms at 7.1 ± 0.09 .

A comparison of the initial concentration of toluene in the amended and un-amended mesocosms show the un-amended mesocosms contained significantly higher toluene concentrations (0.6 ± 0.10 mM) on the day of spiking in comparison to the soil-amended mesocosms (0.2 ± 0.03 mM) (see Figure 6.1). The difference in initial concentrations suggests the presence of the soil amendment induced lower toluene concentrations possibly as a result of toluene sorbing to the added amendment. Suppressed removal of toluene was observed in the soil-amended mesocosms during the period following the addition of the second toluene spike. In contrast to the un-amended mesocosm which showed suppressed removal occurring during the period after the third spike. A comparison of the amounts degraded show the soil-amended mesocosms degraded 113.5 ± 0.01 mg of toluene at the end of the period after the initial toluene spike. This was a significantly higher amount in comparison with the un-amended mesocosms which degraded 96.7 ± 10.4 mg (see Figure 6.2).

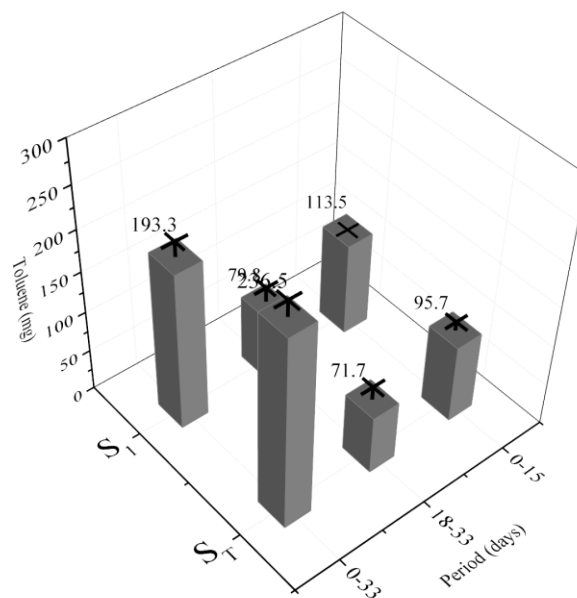


Figure 6.2 Toluene removal in the un-amended (S_T) mesocosms and soil-amended (S₁) mesocosms during the first spike period (0-15 days), second spike period (18-33 days), third spike period (36-51 days) and overall incubation period (0-51 days). Error bars represent the standard error of the mean of three replicates.

Similarly, in the period after the second spike, the soil-amended mesocosms removed a comparatively larger amount of toluene (79.8 ± 17.3 mg) compared to the amended mesocosms (71.7 ± 15.8 mg). These differences were statistically significant ($p = .0001$) and suggest the higher removal observed was due to the presence of the soil amendment (see section C.9.3 of Appendix C).

The rate of toluene degradation in the soil-amended mesocosms when fitted to zeroth order rate kinetics showed the rate of removal for the period after the first spike was 0.72 ± 0.135 $\text{mg}^{-1}\text{L}^{-1}\text{day}^{-1}$ and 2.13 ± 0.815 $\text{mg}^{-1}\text{L}^{-1}\text{day}^{-1}$ for the second spike. The data suggests toluene degradation was faster during the period after the second spike was made. The first order fitting showed toluene removal occurred at 2.13 ± 0.81 day^{-1} after the first spike and 0.09 ± 0.01 day^{-1} after the second spike (see section B-10 and B-11 of Appendix B). The first order fitting therefore suggests toluene was degraded at a comparatively slower rate after the second spike was made. The un-amended mesocosms were shown to remove toluene at a zeroth order rate of 3.05 ± 0.5 $\text{mg}^{-1}\text{L}^{-1}\text{day}^{-1}$, and 1.95 ± 0.76 $\text{mg}^{-1}\text{L}^{-1}\text{day}^{-1}$, for both respective periods and a first order rate of 0.09 ± 0.02 day^{-1} and 0.06 ± 0.02 day^{-1} for both respective periods. From both sets of rate data it may be concluded that the presence of the soil amendment resulted in slower rates of toluene removal in the soil-water mixture.

6.1.2 Comparing toluene degradation in the un-amended and amended mesocosms (Soil 2)

A comparison of the experimental results of the un-amended and amended mesocosms is presented in Figure 6.3. The results show the amended and un-amended mesocosms had similar concentration-time profiles for pH and total dissolved iron concentrations. The initial dissolved iron concentrations after the addition of the first and second toluene spike were 0.4 ± 0.04 mM and 0.1 ± 0.02 mM in the un-amended mesocosms and 0.2 ± 0.01 mM and 0.4 ± 0.04 mM in the soil-amended mesocosms (see Figure 6.3). The pH and total iron concentrations in the amended mesocosms did not vary significantly over the incubation period.

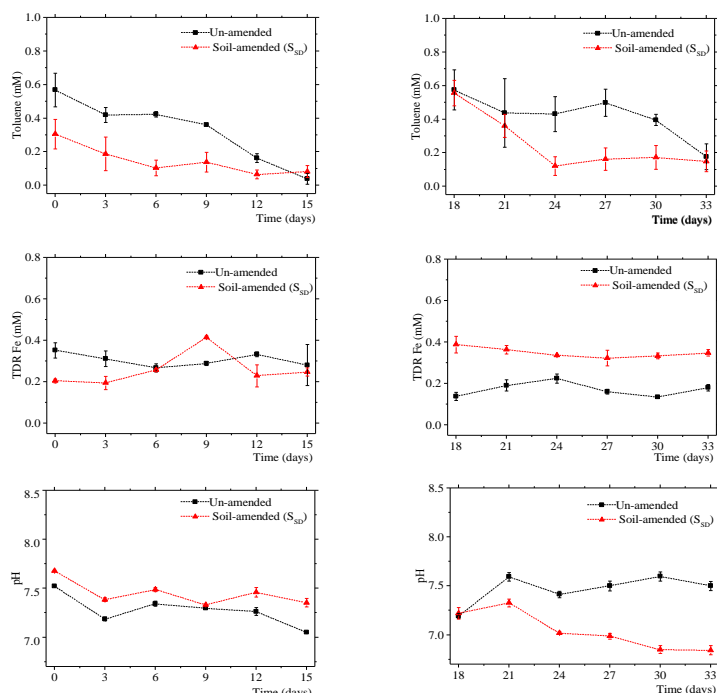


Figure 6.3 Concentration-time profiles showing toluene, total dissolved reactive iron and pH in the un-amended mesocosms and soil-amended (S₂) mesocosms. Error bars represent the standard error of the mean of three replicates.

The results show within the first few hours after the addition of the first toluene spike, toluene concentrations were 0.3 ± 0.09 mM in the soil-amended mesocosms and 0.6 ± 0.10 mM in the un-amended mesocosms. The toluene concentrations in the amended and un-amended mesocosms (see Figure 6.3) suggest losses in toluene may have occurred at the time of spiking, possibly by sorption. The results show the removal of toluene stalled gradually during the period after the addition of the second spike. The gradual slowing down of toluene observed after day 27 may have been due to the increase in the toxicity induced by the degradation of toluene. It is likely the presence of the soil played a contributing role as this trend was not observed in the un-amended mesocosms. A comparison of the amount of toluene removal (Figure 6.4) that occurred during the period after the first and second spikes show the soil-amended mesocosms degraded a larger amount of toluene (at 92.7 ± 12.3 mg and 70.4 ± 5.0 mg in the first and the second spike periods).

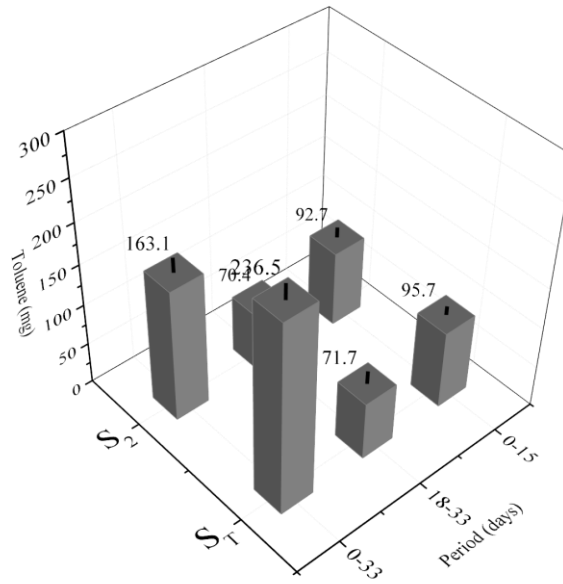


Figure 6.4 Toluene removal in the soil-amended (S₂) mesocosms and un-amended (S_T) mesocosms during the first spike period (0-15 days), second spike period (18-33 days), third spike period (36-51 days) and overall incubation period (0-51 days). Error bars represent the standard error of the mean of three replicates.

The difference in means test performed on the time series data suggest the differences in toluene concentrations in the un-amended and amended mesocosm were statistically significant ($p = .0001$). Therefore it is likely the presence of the soil amendment induced higher toluene removal in the amended mesocosms.

Zeroth order rate fittings showed toluene was degraded at a rate of $3.05 \pm 0.5 \text{ mg}^{-1}\text{L}^{-1}\text{day}^{-1}$ and $1.95 \pm 0.76 \text{ mg}^{-1}\text{L}^{-1}\text{day}^{-1}$ after the first and second spikes respectively in the un-amended mesocosms. In the soil-amended mesocosms however the zeroth order rate fittings were $1.27 \pm 0.31 \text{ mg}^{-1}\text{L}^{-1}\text{day}^{-1}$ and $2.25 \pm 0.25 \text{ mg}^{-1}\text{L}^{-1}\text{day}^{-1}$ for the respective periods. The differences in the zeroth order rate fittings for both groups suggest the presence of the soil amendment induced slower removal rates. The first order rate fitting showed toluene degradation after the first and second spikes proceeded at a rate of $0.13 \pm 0.06 \text{ day}^{-1}$ and $0.17 \pm 0.07 \text{ day}^{-1}$ respectively. These rates were significantly lower than observed in the un-amended mesocosms ($3.98 \pm 0.19 \text{ day}^{-1}$ and $3.94 \pm 0.50 \text{ day}^{-1}$ for the periods after the first and second toluene spikes respectively). The first order rate fittings therefore also suggest the presence of the soil amendment induced slower rates of toluene removal.

6.1.3 Comparing toluene degradation in the un-amended and amended mesocosms (Soil 3)

A comparison of the time-series data for the un-amended and amended mesocosms show the presence of the soil amendment did not increase the total dissolved iron concentrations in the soil-water mixture (see Figure 6.5).

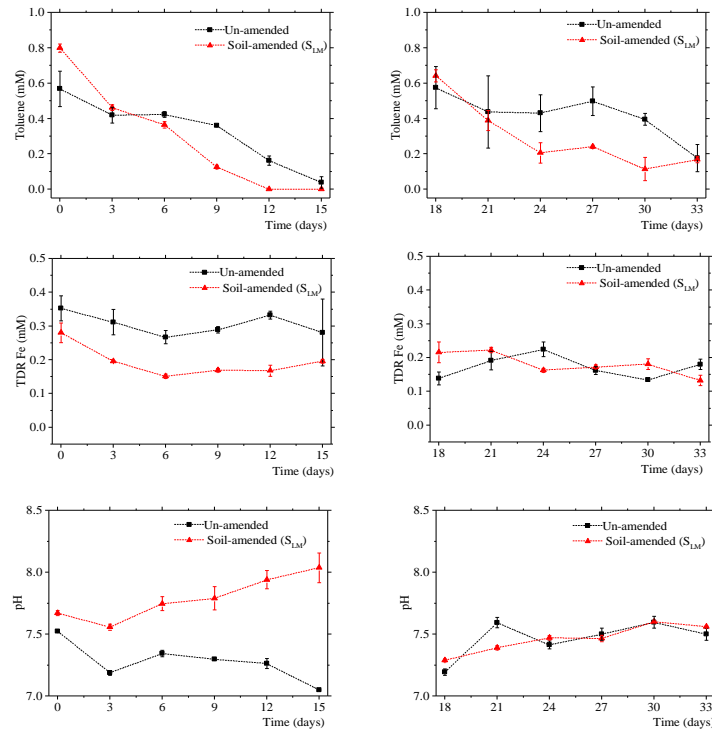


Figure 6.5 Concentration-time profiles showing toluene, total dissolved reactive iron and pH in the un-amended mesocosms and soil-amended (S₃) mesocosms. Error bars represent the standard error of the mean of three replicates.

The total dissolved iron concentrations in the un-amended and soil-amended mesocosm groups at the time of spiking were 0.3 ± 0.03 mM and 0.4 ± 0.04 mM respectively. The total iron concentrations after the addition of second toluene spike were also similar (0.6 ± 0.03 mM and 0.6 ± 0.12 mM for the soil-amended and un-amended mesocosms respectively). A comparison of the pH in the mesocosms show there was an increase in mesocosm pH as a result of the presence of the soil amendment. The profile shows a progressive increase in pH from the beginning to the end of the period after the first spike. A decline in pH was observed after the re-addition of toluene and increased over a comparatively lower range of pH values.

The amended and un-amended mesocosms had similar initial toluene concentrations at the time of adding the first and second toluene spikes. However the soil-amended mesocosms contained a slightly higher initial concentration of 0.8 ± 0.02 mM in comparison to the un-amended mesocosms which contained initial concentrations of

0.6 ± 0.10 mM (see Figure 6.5). Suppressed removal was observed during the period following the addition of the second toluene spike. The presence of the soil amendments induced the removal of 93.0 ± 0.1 mg of toluene during the first spike period and 78.1 ± 1.5 mg during the second spike period). The un-amended mesocosms removed a higher 95.7 ± 10.4 mg during the period after the addition of the first toluene spike and a lower 71.7 ± 15.8 mg during the period after the addition of the second spike (see Figure 6.6).

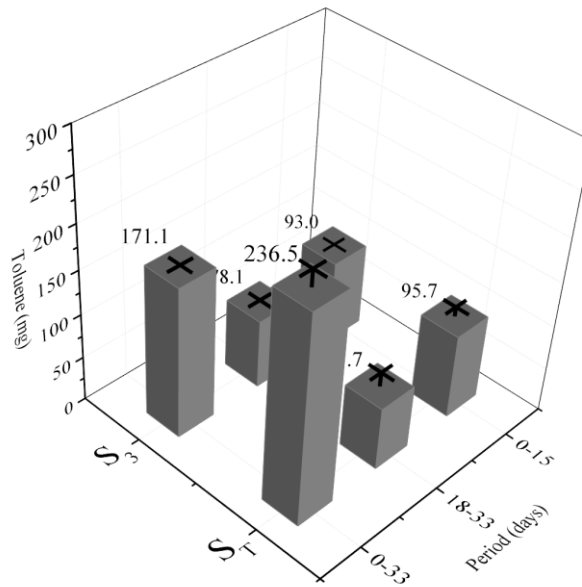


Figure 6.6 Toluene removal in the soil-amended (S₃) mesocosms and un-amended (S_T) mesocosms during the first spike period (0-15 days), second spike period (18-33 days), third spike period (36-51 days) and overall incubation period (0-51 days). Error bars represent the standard error of the mean of three replicates.

The test for differences in means (see section C.9.3 of Appendix C) indicate the differences in mean toluene concentrations were statistically significant ($p = .0001$) and suggest the higher amount of removal observed in the soil-amended mesocosms was due to the presence of the soil. The rate of toluene degradation in the soil-amended mesocosms when fitted to zeroth order rate kinetics showed the rate of removal for the period after the first spike was 1.27 ± 0.31 $\text{mg}^{-1}\text{L}^{-1}\text{day}^{-1}$ and 1.78 ± 1.16 $\text{mg}^{-1}\text{L}^{-1}\text{day}^{-1}$ for the second spike. The zeroth order kinetics indicate toluene removal in the amended mesocosms was slower in comparison to the un-amended mesocosms as the un-amended mesocosms were shown to remove toluene at a zeroth order rate of 3.05 ± 0.5 $\text{mg}^{-1}\text{L}^{-1}\text{day}^{-1}$, and 1.95 ± 0.76 $\text{mg}^{-1}\text{L}^{-1}\text{day}^{-1}$, for both respective periods. The first order fittings showed toluene removal in the soil-amended mesocosms occurred at 0.33 ± 0.01 day^{-1} after the first spike and $0.83 \pm$

0.06 day⁻¹ after the second spike. The first order rates in the un-amended mesocosms were 0.09 ± 0.02 day⁻¹ and 0.06 ± 0.02 day⁻¹ for both respective periods.

6.2 General discussion

All of the experimental soil-amended mesocosms in this study supported the removal of toluene in the soil-water mixture. At the start of the experiments, lower initial concentrations were observed in the mesocosms containing Soils 1 and 2 when compared with the un-amended mesocosms. This may have been due to the sorption of toluene to soil amendments in these mesocosms. It is well known that in addition to losses due to biodegradation, leaching or volatilisation, sorption of organic contaminants to soil may also inhibit the complete bioremediation of these contaminants in soil. In contaminated soil environments, organic contaminants tend to accumulate in the pores between soil particles, which results in reduced oxygen and water permeability through the soil. Furthermore the low solubility of hydrophobic organic compounds in water results in residual organic phases of these compounds being a source of long-term contamination in soil and groundwater. This is as a result of the tendency of organic contaminants to bind tightly to soil particles. Therefore organic chemicals which have been in contact with the soil matrix for prolonged periods may be unavailable however the length of time over which the residual fraction exists. As a result, many contaminants that have been weathered and sequestered in soil are not necessarily available for biodegradation although freshly added compounds are biodegradable (Alexander, 1995).

The results of the degradation experiments showed toluene removal in the soil-amended mesocosms lessened during the period following the addition of the second spike. This pattern of toluene removal was not observed in the un-amended (S_T) mesocosms as suppressed levels of toluene concentrations were observed during the period following the addition of the third spike. These dissimilarities may be attributed to the presence of the soil amendments. The results also showed the soil-amended mesocosms degraded a larger amount of toluene at the end of each period of spiking in comparison to the un-amended mesocosms. The amount of toluene removed in the soil-amended mesocosms was of the order $S_1 > S_3 > S_2$ for the period after the first and second toluene spikes (where S₁, S₃ and S₂ represent the mesocosms amended with Soil 1, Soil 3, and Soil 2 respectively). Soil is generally composed of a mixture of carbonates, clay minerals, hydrous oxides of iron, manganese, and aluminium, sand, silt, and organic matter. A typical mineral soil is comprised of approximately 45% mineral material (i.e. sand, silt and clay in varying proportions), 25% air and 25% water (i.e. 50% pore space, commonly half saturated with water) and 5% organic matter (variable). Characterisation tests assessed four

soil properties namely particle size distribution, surface area, moisture content and pH. The results of these tests can be found in Table C.6.1a of Appendix C. Soil particle size analysis indicated Soil 1 had a clay content (particles < 0.002 microns) of 0.5 %, a silt content (particles 0.002 – 0.063 microns) of 50.4% and a total sand content (particles 0.063 microns to 2.000 mm) of 49.2% w/w. Soil 2 had a 19.7% clay content, 77.8% silt content and 2.5% sand content and Soil 3 was composed of 83.1% clay, 16.3% silt and 0.6% sand. Determination of the BET (Braun-Emmett-Teller) surface area by nitrogen gas adsorption produced values 8 m²/g, 4 m²/g and 21 m²/g for Soil 1, Soil 2 and Soil 3 respectively. The measurement of soil pH showed Soil 1 was of pH 7.6, Soil 2 pH 7.7, and Soil 3 pH 7.7. The analysis of particle size distribution indicates Soil 2 had the least percentage clay fraction and Soil 3 the highest while Soil 1 had an equal ratio of the silt and clay fractions (see section C.6.1 of Appendix C). The three soils (Soils 1, 2 and 3) may therefore be described as clayey, silty and mixed. Clayey soils are generally more plastic and sticky and prone to swelling and shrinkage. This is because clayey soils have smaller pore sizes and therefore retain more water (Hammel et al., 1981). The presence of petroleum products in clay soils makes them stickier and increases binding and clogging. The clay fractions in soils bind molecules more strongly than silt or sand, therefore the bioavailability of contaminants is lower in soils with higher clay content. The order of toluene removal in the amended mesocosms suggests Soils 1 and 3 induced higher removal of toluene in comparison to Soil 2. It is possible this removal was not microbially-induced but may have been due to sorption of toluene to the soil amendments. (Schwarzenbach and Westall, 1981) define sorption as ‘*the process in which chemicals become associated with solid phases (either adsorption onto a two-dimensional surface or absorption onto a three-dimensional matrix)*’. The solid-water distribution (sorption) coefficient K_d (Equations 6.1-6.5) may be used as an index for measuring sorption.

$$K_d = \frac{c_s}{c_w} \quad \text{Equation 6.1}$$

$$c_s = \frac{m_s}{s_m} \quad \text{Equation 6.2}$$

$$c_w = \frac{m_w}{v_w} \quad \text{Equation 6.3}$$

$$m_s = m_t = m_a + m_w \quad \text{Equation 6.4}$$

$$m_a = c + v_a; m_w = \frac{c}{H} + v_w \quad \text{Equation 6.5}$$

where c_w and c_s denote the constituent concentration in the soil-water and solid respectively

s_m = total soil mas (kg)

m_s = constituent mass in soil (g)

v_a and v_w denote the total system air and water volume respectively

C = measured constituent concentration in the headspace of the batches (g/L)

H = Henry's law constant (dimensionless)

The parameters above were not measured during the experiments therefore sorption of toluene in the mesocosms was determined by simple proportion (see Equation 6.5). From this equation sorption indices for the materials amended with Soils 1, 2 and 3 were obtained as 0.333, 0.500 and 1.333 respectively.

$$\text{Sorption index} = \frac{\text{Starting concentration in amended mesocosms (mM)}}{\text{Starting concentration in un-amended mesocosms (mM)}}$$

Equation 6.5

$$S_1: \quad \frac{0.2}{0.6} = 0.333$$

$$S_2: \quad \frac{0.3}{0.6} = 0.500$$

$$S_3: \quad \frac{0.8}{0.6} = 1.333$$

where S_1 , S_2 and S_3 represent mesocosms amended with Soil 1, Soil 2 and Soil 3 respectively

The K_d of toluene in the soil-amended, incubated material will be inversely proportional to the estimate of sorption index shown above. The soil-amended material with a smaller sorption coefficient will have a comparatively higher relative sorption index i.e. it will sorb toluene more strongly. The relative sorption of toluene in the amended material was of the order $S_3 > S_2 > S_1$ therefore $K_{d \text{ soil 1}}$ and $K_{d \text{ soil 2}} > K_{d \text{ un-amended}} > K_{d \text{ soil 3}}$. Thus it may be concluded that the lower initial concentrations observed in the mesocosms amended with Soils 1 and 2 were due to sorptive processes and not enhanced microbial degradation brought about by the presence of the two soils. Similarly, the higher amount of removal induced by Soil 3 was biologically induced and not as a result of physical processes including sorption. The sorption index of a soil will depend on its surface area and percentage clay fraction. These properties will in turn influence the degree to which it can degrade a contaminant. The relationship between the surface area, percentage clay fraction, sorption index and toluene removal observed in the incubated, soil-amended mesocosm material is illustrated in Figure 6.7.

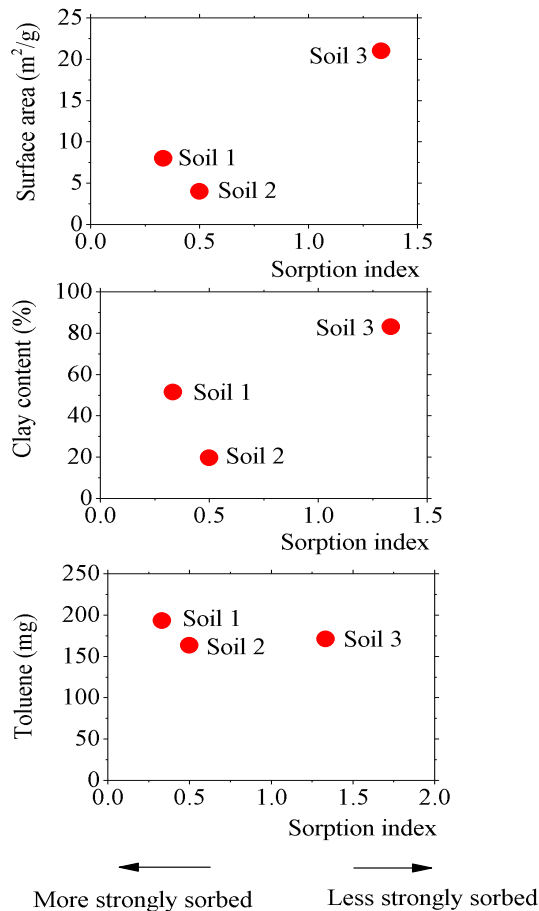


Figure 6.7 Relationship between sorption, toluene removal, surface area and clay content in the soil-amended material

It can be seen from the figure that the sorption of toluene in the amended material relative to the un-amended material was not influenced by the surface area or percentage clay fraction of the soil amendments. A sorbed compound may exist in a soil environment in four states namely i) bioavailable, rapidly reversible and temporarily constrained, ii) bioavailable, slowly reversible and temporarily constrained, iii) bioaccessible and physically constrained and iv) non-bioaccessible or occluded (Semple, K. T. et al., 2004). The experimental results suggest i) all sorption was dominantly on to bio-accessible sites, and ii) stronger sorption was not to inaccessible sites.

The sorption and/or sequestration of organic contaminants can be influenced by pH, organic matter content, temperature and nature of the contaminant in question. The bioavailability of electron acceptors also influences microbial activity. Soil pH determines the type of microorganism involved in degradation processes. Most studies investigating the influence of pH on degradation report increasing degradation of a hydrocarbon contaminant with increasing pH, with optimum

degradation occurring under slightly alkaline conditions (Atlas, R.M., 1981). Slightly alkaline conditions are generally more conducive for biodegradation compared to acidic conditions (Bossert and Barther, 1984). The pH in all mesocosm sets remained in the circum-neutral range during the period of toluene removal after each spike however the pH in the mesocosms containing Soils 1 and 2 could be seen to have declined gradually towards the end of the period following the addition of the second toluene spike. (Bauder et al., 2005) report an increase in pH in crude oil-contaminated soil. Chemical reactions between petroleum hydrocarbons and soil elements may induce changes in soil pH (Sun and Zhou, 2007). A decrease in pH was observed in the mesocosms containing Soils 1 and 2 towards the end of the incubation period. It is likely the gradual change in pH contributed to the gradual decrease in toluene removal during the period after the addition of the second toluene spike.

The breakdown of hydrocarbons in soils is influenced by the soil environment and soil properties including surface area as surface area is known to affect the rate of chemical reactions in soil (Scherr et al., 2007). The range of particle sizes for clay, silt and sand fractions are < 0.002 microns, $0.002 - 0.063$ microns, and 0.063 microns – 2.000 mm respectively. Biodegradation rates are known to be affected by the fraction of fines (0.75mm) in soil. The increased sorptive surface area of soil with larger fines may affect the bioavailability of hydrocarbons. Therefore soils with a greater percentage fines are believed to support greater contaminant degradation due to the larger surface area provided for degradation reactions. For example (Lee et al., 2002) showed sandy soils were able to recover larger amounts of toluene (73%) when tested in batch experiments. Although this is generally true, reaction rates are thought to be enhanced by the availability of reactive surface areas, not necessarily the availability of large surface areas. The analysis of BET surface area showed Soil 3 had the largest surface area. This may be attributed to its larger percentage clay fraction. Similarly, the lower surface area of Soil 2 may be a reflection of its predominantly silty composition. Using the first order rate fittings derived from the toluene time series data, the rate of toluene removal expressed per square metre per day is given in Table C.6.26 (see section C.6 of Appendix C). From the table, the rate of toluene removal per square metre of soil mesocosm was of the order $S_2 > S_3 > S_1$ for both the period after first spike and after second spike (where S_2 , S_3 and S_1 represent the mesocosms amended with Soil 2, Soil 3, and Soil 1 respectively). Soil 2 therefore induced the highest rate of toluene removal in the soil-water mixture. Soil texture plays an important role in biodegradation rates of hydrocarbon contaminants in soil. Although clay soils provide a large surface area for degradation reactions, clay soils contain more micro pores and are therefore more susceptible to water logging which adversely affects microbial activity.

Therefore a water logged or clayey soil will show low degradation rates and activity. In (Huesemann, M. et al., 2004) soils with low percentages of fine silt and clay degraded hydrocarbons at higher rates. The higher rates observed were attributed to the aeration porosity of the soils. The Soil 2 amendment induced toluene removal at faster rates in comparison to the Soil 1 and 3 amendments. It is likely this was due to the predominantly silty texture of Soil 2 which provided an adequate amount of surface area as well as adequate pore size for the activities of toluene-degrading and iron-reducing microorganisms in the soil-amended material.

6.3 Conclusion

Petroleum hydrocarbons generally display hydrophobic and lipophilic characteristics and may be retained within soil and persist for long periods. Soils therefore present a major sink for organic contaminants in the environment. The three soils used in this experimental study were representative of three different environmental matrices with varying physicochemical properties and demonstrate toluene removal in these soil environments. Characterisation tests showed the three soils differed on the basis of texture, pH, and mineralogy. Soil physical properties such as texture and structure affect microbial activities and consequently the degree of remediation potential of the soil. The aim of the experiments reported in this chapter was to assess the effect of specific physicochemical properties on the amount and rate of toluene removal. The experimental results of the experiments reported suggest toluene removal was higher in the soils with a greater percentage clay fraction. The bulk of this removal was however due to sorption and not microbial degradation. The rate of removal was found to have been enhanced by soils with a lower clay fraction. The results therefore demonstrate the effect of contaminant sorption on the rate and amount of toluene removal. While studies have investigated the impact of soil type on biodegradation under both aerobic and anaerobic conditions, there is no data that expresses degradation rates as a function of surface area. This data has been provided in this chapter.

Summary

In this chapter the findings of a laboratory investigation of toluene removal in controlled batch mesocosm experiments under predominantly iron-reducing conditions are reported. All of the soil-amended mesocosms supported the removal of toluene in the soil-water mixture. The total dissolved iron concentrations were unaffected by the presence of the soil amendments although there was a slight increase in the total iron concentrations of the mesocosms containing Soils 1 and 2

during the period following the addition of the first toluene spike. The mesocosms containing Soil 3 did not show this trend. A decline in total iron concentrations in these mesocosms was observed during the first three days after the initial toluene spike. The mesocosm pH although initially unaffected after the addition of the first toluene spike, decreased gradually in the mesocosms containing Soils 1 and 2 during the period after the addition of the second toluene spike. The results indicated a large fraction of toluene was degraded after the first toluene spike in the mesocosms containing Soil 1 and Soil 2 samples. In the mesocosms amended with Soil 3 a significant amount of toluene was removed at the end of the incubation period. Toluene removal was higher in the soils with a greater percentage clay fraction therefore the bulk of this removal was attributed to sorption and not microbial degradation of toluene. The rate of toluene removal was higher in the soils with lower percentage clay fractions. These findings are presented in section C.7 of Appendix C.

Chapter 7

Stable Carbon ($^{12}\text{C}/^{13}\text{C}$) Isotopes as a Tool for Identifying Soil Carbonates— A Method Development

Introduction

The sequential chemical extractions showed there was an increase in the carbonate-bound iron pool of the incubated material which supported toluene degradation (see section 4.1.3). The results of further experimental analysis of this material with stable carbon isotope analysis are discussed in this chapter.

7.1 Results and discussions

The build-up in carbonate-bound iron phases in the active mesocosms (see section 4.1.3) suggests the period of incubation in the mesocosms induced changes in the overall carbonate composition of the incubated material. A method was proposed to determine the source of carbon i.e. whether it was as a result of addition or dissolution of carbonates. The effects of carbonate dissolution and addition are illustrated in the bivariate $\delta^{13}\text{C}$ / carbonate-carbon profile below.

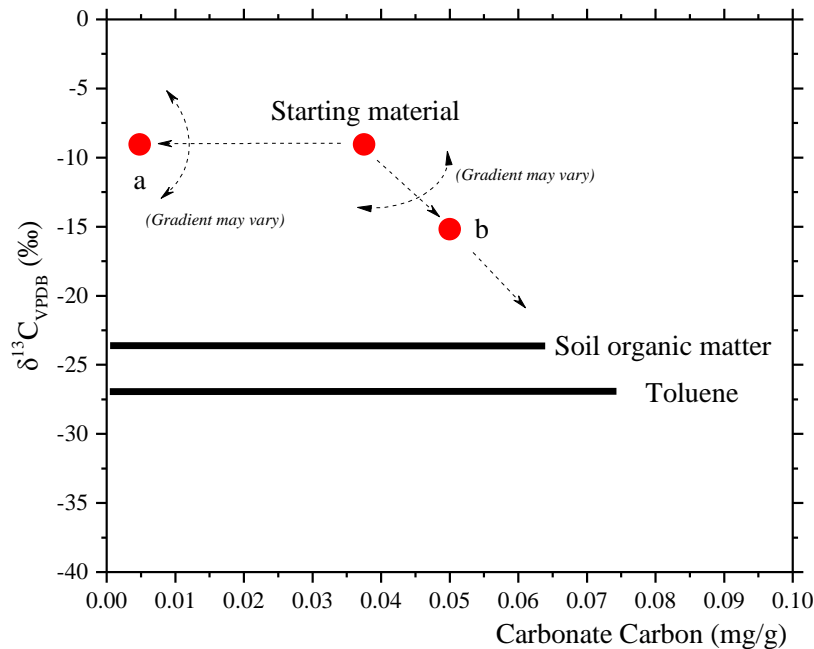


Figure 7.1 Bivariate $\delta^{13}\text{C}$ / carbonate-carbon profile illustrating the effects of soil carbonate reactions on carbonate-carbon and $\delta^{13}\text{C}$ showing 'a' - the incubated material following carbonate dissolution and 'b' - the incubated material after addition of carbon from respiration of ^{13}C -depleted organic carbon

The stable isotope procedure used in this study provides the $\delta^{13}\text{C}$ signature and mass of carbonate carbon in analysed samples. From Figure 7.1, carbonate dissolution will result in decreasing carbonate concentration with little change in $\delta^{13}\text{C}$ between the starting and residual carbonate while addition will lead to increased carbonate concentrations. Addition of carbonates results in a change in $\delta^{13}\text{C}$ of the carbonate pool towards the source of carbon. If the source of carbonates added is from the respiration of organic carbon either from indigenous soil organic matter or toluene, negative values will be derived (see Figure 7.1). The methodology proposed in this study identifies two groups of soil carbonates that may have been involved in the removal of toluene in the mesocosms. These operationally-defined pools are the fast-reacting carbonates and the slow-reacting carbonate pools. The fast-reacting pool is composed mainly of calcium carbonates (e.g. calcite, aragonite and vaterite). The slow-reacting pool is composed mainly of slower-reacting dolomite and iron-bound carbonates such as siderite and ankerite (see section 3.1.2).

7.1.1 Carbonate reactions in the un-amended live control mesocosms

The results for the un-amended live controls (see Figure 7.3) show there was an increase in the mass of carbonate carbon (0.005 mg/g in the starting soil material and 0.03 ± 0.002 mg/g in the incubated material).

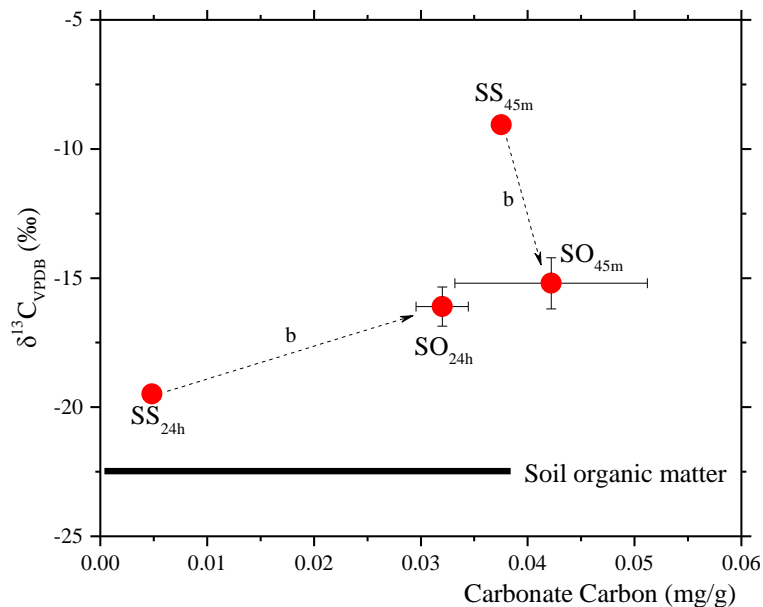
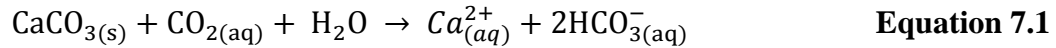


Figure 7.2 Bivariate $\delta^{13}\text{C}$ / carbonate-carbon profile showing the changes in $\delta^{13}\text{C}$ and mass of carbonate carbon following the degradation of toluene in the mesocosms with soil and water only. The $\delta^{13}\text{C}$ signature of soil organic matter is shown. ‘b’ represents the underlying carbonate reaction carbonate addition in the fast-reacting carbonate pool (subscript -45m and slow-reacting pool (subscript -24h). Error bars represent the standard error of the mean of three replicates.

With respect to Figure 7.1, the bivariate $\delta^{13}\text{C}$ / carbonate-carbon profile suggests the period of incubation induced the addition of carbonates to both the fast-reacting (subscript 45m) and slow-reacting (subscript 24h) pools. The isotope signatures indicate this added carbonate to be isotopically-light carbon, possibly the by-product of soil microbial respiration. The reaction for the dissolution of calcium carbonates (calcite) in the fast-reacting carbonate pool is given in Equation 7.1.



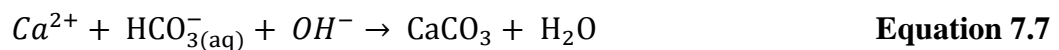
A breakdown of Equation 7.1 is shown in Equations 7.2-7.5.



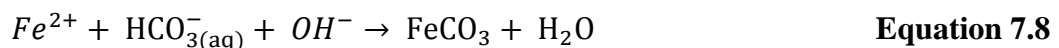
The dissolution of CO_2 into water forms carbonic acid (Equation 7.3 and 7.4). Carbonic acid dissociates to form HCO_3^- and CO_3^- ions (Equation 7.5). The dissolution of calcite induces the release of an equivalent amount of calcium ions as well as bicarbonate as shown in Equation 7.6.



Bicarbonate ($\text{HCO}_{3(aq)}^-$) released in solution increases the alkalinity of the solution which results in an increase in hardness (Sawyer et al., 1994) and the precipitation of new carbonates. Therefore the dissolution of carbonates will be followed by the re-addition of newly-formed carbonates. The precipitation of solid carbon (carbonate addition) therefore requires alkalinity and a cation source. In the presence of a hydroxyl ion bicarbonate will form calcite (Equation 7.7). This is an example of carbonate addition to the fast-reacting carbonate pool. Similarly Equation 7.8 illustrates carbonate addition to the slow-reacting carbonate pool.



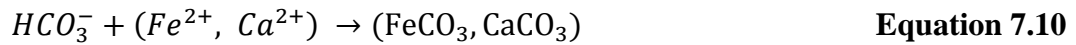
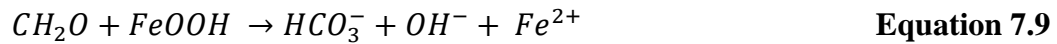
(**calcite**)



(**siderite**)

The isotope signatures of the starting material (Figure 7.2) suggest isotopically light carbon was added to the fast-reacting pool and that isotopically heavy carbon was added to the slow-reacting pool. The similar isotope signatures of both materials suggest the carbon added to the slow pool originated from the fast pool. It may be speculated that the period of incubation induced a transfer of carbonates from the

fast pool to the slow pool as a result of the addition of solid carbonates occurring during the period. The mesocosms were not spiked with toluene, therefore iron reduction occurred with soil organic matter as a substrate (Equation 7.9).



This solid carbonate added from the new, isotopically light HCO_3^- (Equation 7.9), resulted in the addition of new carbonate to the fast and slow-reacting pools (Equation 7.10).

7.1.2 Carbonate reactions in the un-amended active control mesocosms

The results obtained for the un-amended live control show the period of incubation and toluene degradation did not affect the mass of carbonate carbon in the fast-reacting pool (see Figure 7.3).

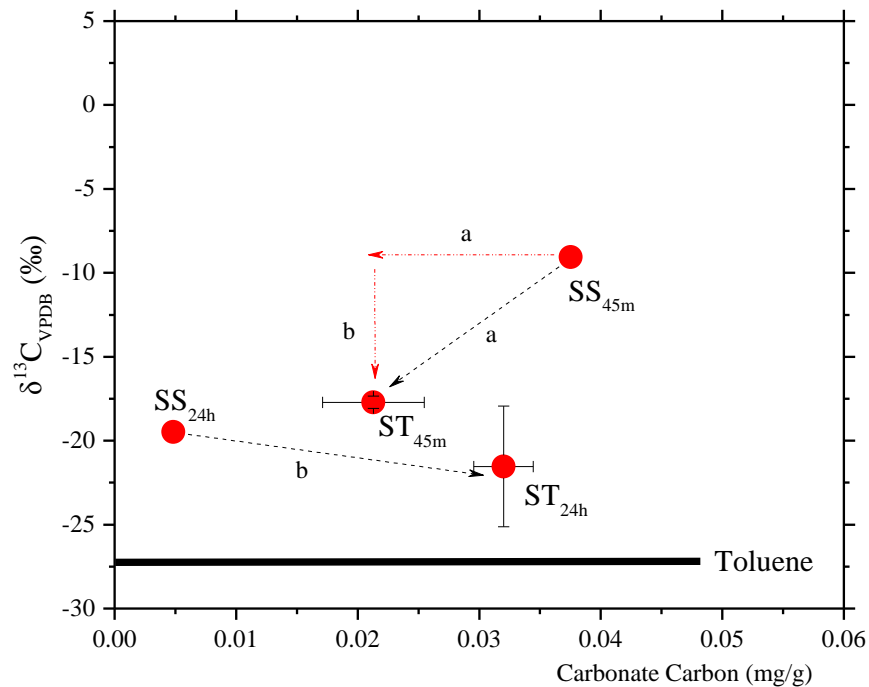
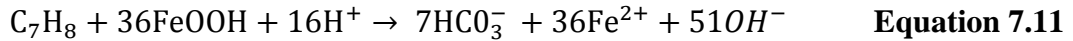


Figure 7.3 Bivariate $\delta^{13}C$ / carbonate-carbon profile showing the changes in $\delta^{13}C$ and mass of carbonate carbon following the degradation of toluene in the un-amended (S_T) mesocosms. The $\delta^{13}C$ signature of toluene is shown. ‘a’ and ‘b’ represent underlying reactions affecting the fast- and slow-reacting carbonate pools (dissolution and addition respectively). Error bars represent the standard error of the mean of three replicates.

In the slow pool however the mass of carbonate carbon was observed to have increased as the experimental results yielded values 0.005 mg/g to $0.03 \pm 0.002 \text{ mg/g}$. The results of the sequential extractions suggest carbonate-bound iron was

precipitated during the period of toluene removal in the mesocosms. The reaction of iron-mediated toluene removal is given by Equation 7.11 below.



From this equation, toluene removal under iron-reducing conditions will produce HCO_3^- and OH^- . The addition of solid carbon requires alkalinity and a cation source (Equations 7.1-7.6), therefore on-going toluene removal induces on-going precipitation or addition of solid carbonate. With respect to Figure 7.2 dissolution and addition were the underlying reactions affecting the fast- and slow-reacting pools respectively. The values obtained show large similarities in the results for the fast and slow pools in the incubated material (see Figure 7.3). It is therefore likely that the carbonates added to the slow pool were derived from the newly formed carbonates produced by carbonate dissolution in the fast pool.

7.1.3 Carbonate reactions in the hematite-amended mesocosms

The bivariate $\delta^{13}C$ / carbonate-carbon profile suggests the period of incubation in the hematite-amended material induced carbonate addition to both the fast-reacting carbonate pool and slow-reacting carbonate pool (see Figure 7.4).

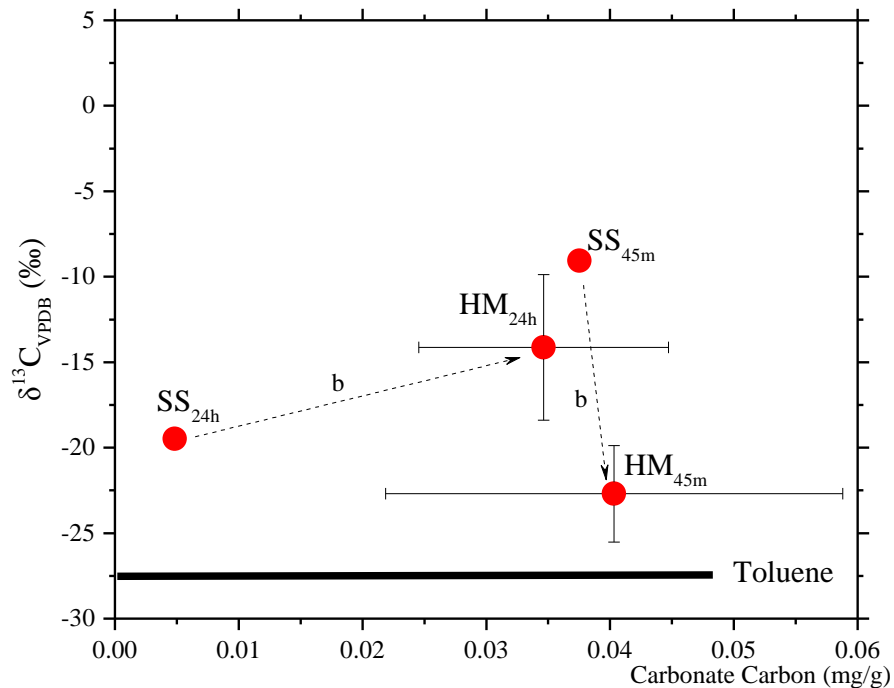


Figure 7.4 Bivariate $\delta^{13}C$ / carbonate-carbon profile showing the changes in $\delta^{13}C$ and mass of carbonate carbon following the degradation of toluene in the hematite-amended (H_M) mesocosms. Error bars represent the standard error of the mean of three replicates.

The results suggest toluene removal in the presence of hematite induced the addition of isotopically light carbon to the fast pool and isotopically heavy carbon to the slow pool. The similarity in the values obtained for the $\delta^{13}\text{C}$ and the mass of carbonate-carbon for the fast and slow pools in the incubated material suggest the carbon added to the slow pool originated from the fast pool (see Table C.6.14 of Appendix C). The differences in isotope signatures of the starting and incubated material suggest isotopically light carbon was added to the fast pool after dissolution and isotopically heavy carbon was added to the slow pool. These changes were likely to have been induced by toluene removal.

7.1.4 Carbonate reactions in the goethite-amended mesocosms

Carbonate addition to the fast- and slow-reacting carbonate pool occurred over the period of incubation in the goethite-amended mesocosms as shown in Figure 7.5.

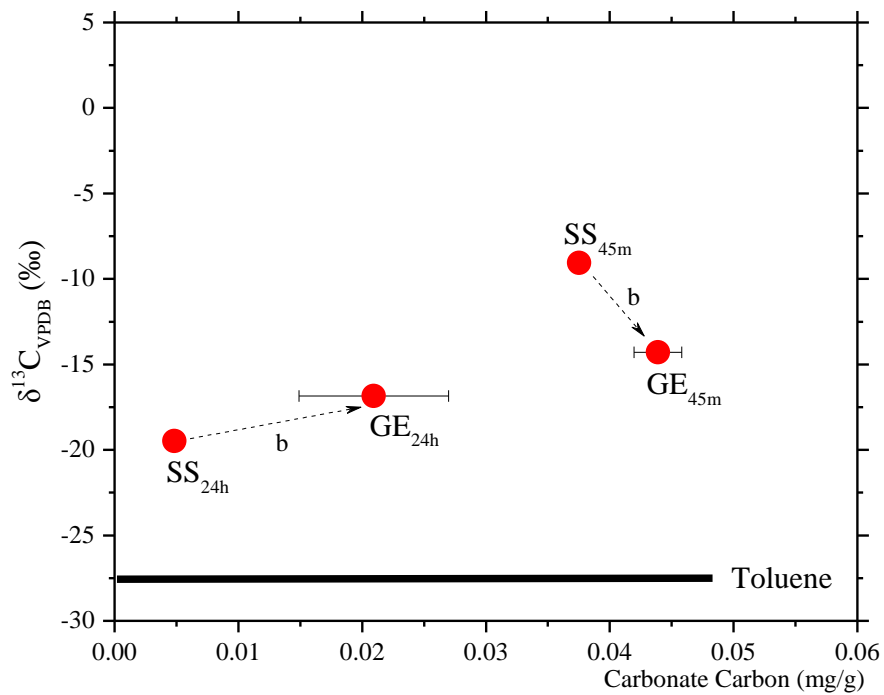


Figure 7.5 Bivariate $\delta^{13}\text{C}$ / carbonate-carbon profile showing the changes in $\delta^{13}\text{C}$ and mass of carbonate carbon following the degradation of toluene in the goethite-amended (G_E) mesocosms. Error bars represent the standard error of the mean of three replicates.

The experimental results suggest the period of incubation induced the addition of isotopically light carbon to the fast-reacting carbonate pool and heavy carbon to the slow-reacting carbonate pool. The similarities of the isotope data for the starting material and goethite-amended material suggest this addition did not occur to a great extent as observed in previous mesocosms.

7.1.5 Carbonate reactions in the magnetite-amended mesocosms

In the magnetite-amended mesocosms (shown in Figure 7.6), carbonate addition to the fast- and slow-reacting carbonate pool occurred during the period of incubation.

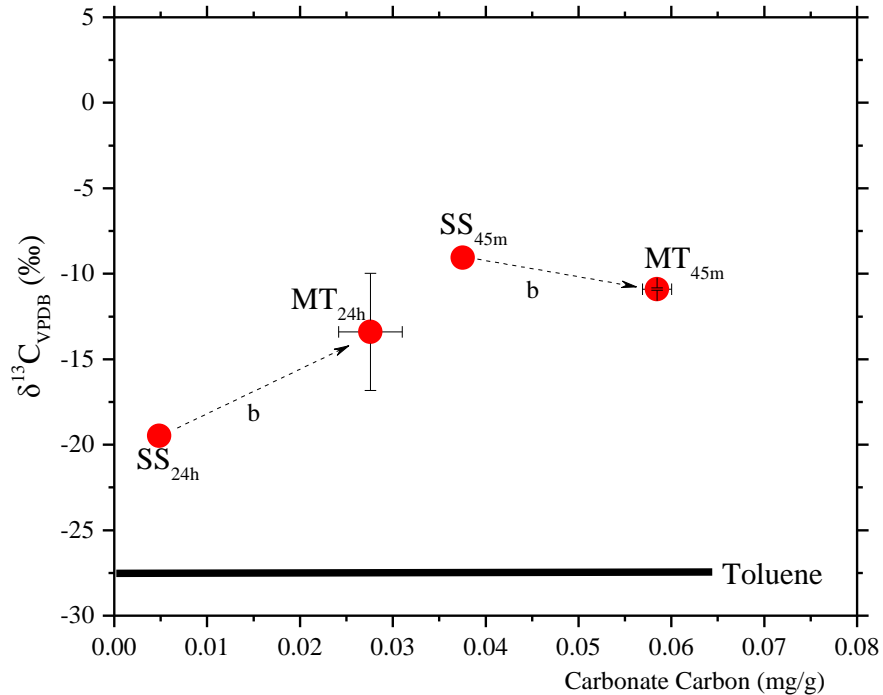


Figure 7.6 Bivariate $\delta^{13}C$ / carbonate-carbon profile showing the changes in $\delta^{13}C$ and mass of carbonate carbon following the degradation of toluene in the magnetite-amended (M_T) mesocosms. Error bars represent the standard error of the mean of three replicates.

The results indicate the incubation period induced the addition of light carbon to the fast-reacting pool and heavy carbon to the slow-reacting pool. The bivariate $\delta^{13}C$ / carbonate-carbon profile suggests the goethite- and magnetite-amended material behaved similarly during the period of incubation. This is in agreement with the results of the degradation experiments which showed similarities in concentration time profiles as well as amounts of removal that occurred in these mesocosms (see section 5.1).

7.1.6 Carbonate reactions in the ferrihydrite-amended mesocosms

The profile for the incubated material in the ferrihydrite-amended material indicates the period of incubation induced carbonate addition to both the fast- and slow-pools (see Figure 7.7).

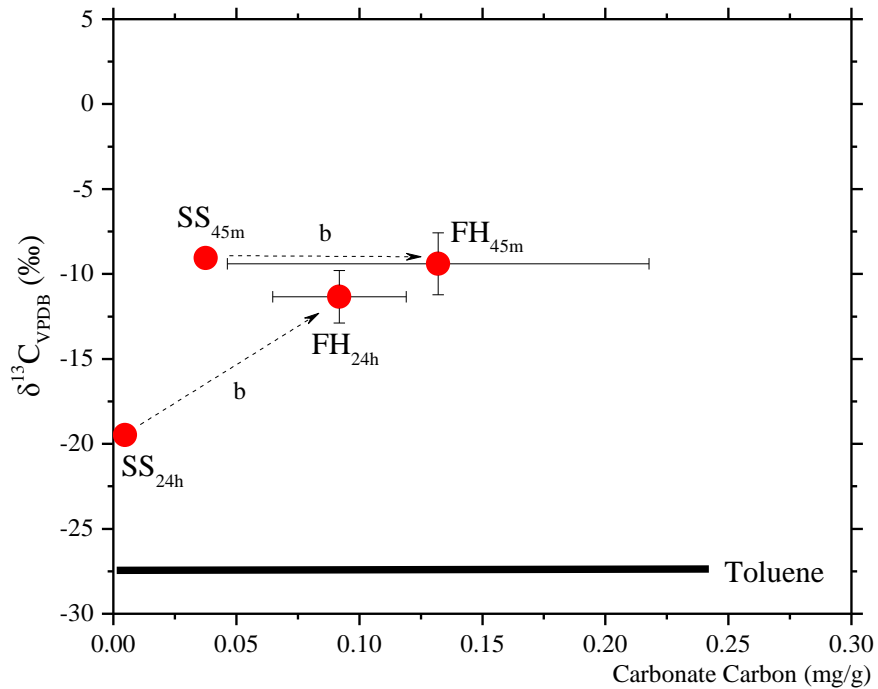


Figure 7.7 Bivariate $\delta^{13}\text{C}$ / carbonate-carbon profile showing the changes in $\delta^{13}\text{C}$ and mass of carbonate carbon following the degradation of toluene in the ferrihydrite-amended (F_H) mesocosms. Error bars represent the standard error of the mean of three replicates.

The experimental results show there was carbonate addition to the fast- and slow-reacting carbonate pools over the period of incubation. Isotopically heavier carbon was added to the slow-reacting pool. This is consistent with the previous amendments.

7.1.7 Carbonate reactions in the lepidocrocite-amended mesocosms

The profile for the lepidocrocite-amended mesocosms show there was carbonate addition to the slow-reacting pool (see Figure 7.8).

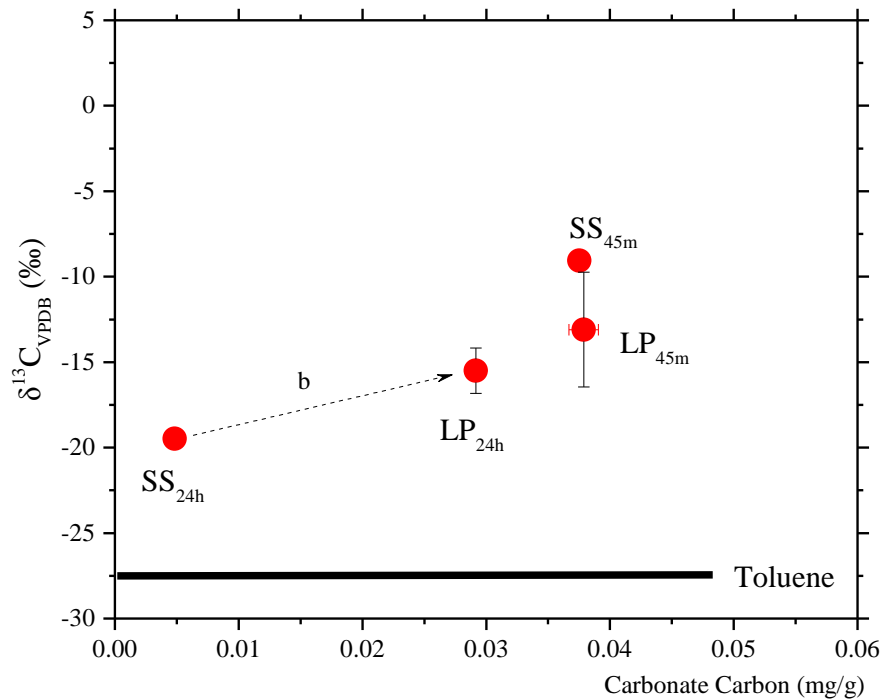


Figure 7.8 Bivariate $\delta^{13}\text{C}$ / carbonate-carbon profile showing the changes in $\delta^{13}\text{C}$ and mass of carbonate carbon following the degradation of toluene in the lepidocrocite-amended (L_P) mesocosms. Error bars represent the standard error of the mean of three replicates.

The results showed the starting and amended material contained a similar mass of carbonate carbon and suggest isotopically light carbon was added to the fast-reacting pool during the period of incubation. Isotopically heavy carbon was added to the slow-reacting pool of the incubated material.

7.1.8 Carbonate reactions in the soil-amended mesocosms (Soil 1)

The results for the mesocosms containing the Soil 1 amendment suggest there was carbonate dissolution to the fast-reacting pool and addition to the slow-reacting pool (see Figure 7.9).

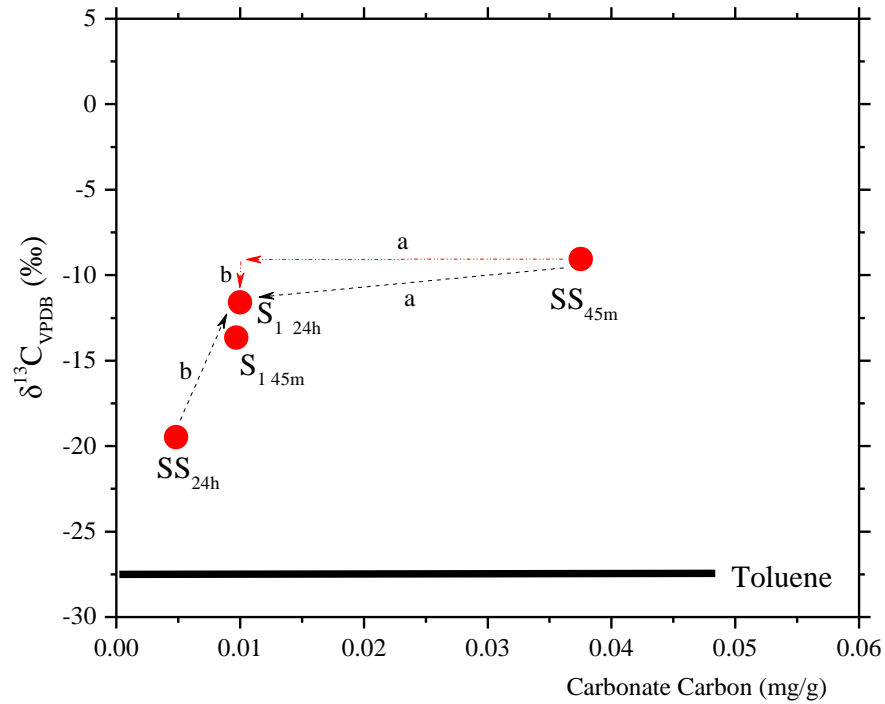


Figure 7.9 Bivariate $\delta^{13}\text{C}$ / carbonate-carbon profile showing the changes in $\delta^{13}\text{C}$ and mass of carbonate carbon following the degradation of toluene in the mesocosms amended with Soil 1. Error bars represent the standard error of the mean of three replicates.

With respect to Figure 7.2 the results for the incubated material amended with Soil 1 showed there was carbonate dissolution and re-addition of isotopically light carbon to the fast-reacting pool. Isotopically heavy carbon was added to the slow-reacting pool. The results show the behaviour of the mesocosms amended with Soil 1 was similar to the un-amended (S_T) mesocosms.

7.1.9 Carbonate reactions in the soil-amended mesocosms (Soil 2)

The experimental results for the incubated (S_2) material suggest the period of incubation induced carbonate addition to both the fast- and slow-reacting carbonate pool.

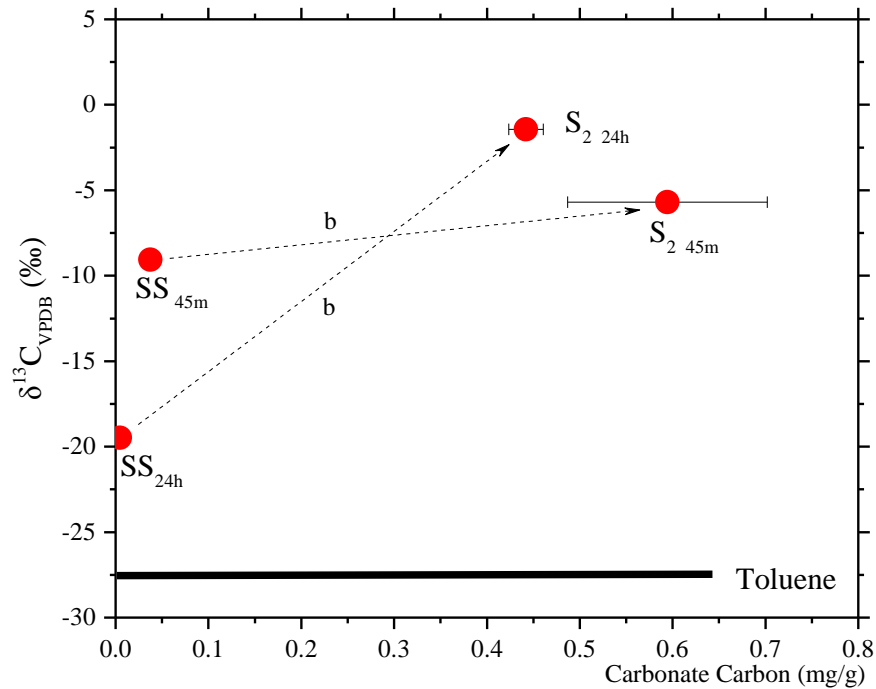


Figure 7.10 Bivariate $\delta^{13}\text{C}$ / carbonate-carbon profile showing the changes in $\delta^{13}\text{C}$ and mass of carbonate carbon following the degradation of toluene in the mesocosms amended with Soil 2. Error bars represent the standard error of the mean of three replicates.

Isotopically heavy carbon was added to the slow-reacting pool and may have been derived from the fast pool similar to the un-amended (S_T) mesocosms (see Figure 7.4). The results showed the soil-amended material contained a comparatively larger mass of carbonate carbon. The isotope procedure was not performed on the soil amendment, however the comparatively large values may be an indication the organic content of the soil 3 amendment was higher in comparison.

7.1.10 Carbonate reactions in the soil-amended mesocosms (Soil 3)

The incubated material from the mesocosms containing Soil 3 affected the normal functioning of the GC-IRMS during analysis. Further analysis was discontinued as a result and there is no available stable carbon isotope data for this mesocosm set.

7.2 General discussion

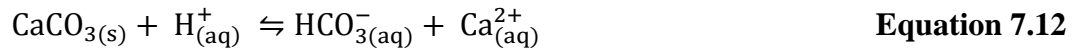
The experiments in this chapter were performed to further investigate the build-up of carbonate-bound iron observed in the un-amended mesocosms (see section 4.4). Several natural soil minerals have carbon and iron as part of their chemical structure,

a common example of which is siderite. Siderite is an iron carbonate mineral which occurs in several geological environments and may dissolve, releasing iron that becomes oxidised and precipitated in the form of iron oxides and oxy-hydroxides with a high affinity for pollutants. Siderite commonly occurs in sedimentary rocks along with calcite and dolomite (Appelo et al., 1996). Siderite is formed under reducing conditions and often occurs as a solid with substitutions of the Fe ion by Mg^{2+} , Mn^{2+} , Zn^{2+} and Ca^{2+} (Renard et al., 2017). Although time constraints did not allow for sequential extractions to be performed on the amended material, it is well known that the precipitation of siderite may be induced by iron reduction processes. Several studies have shown that siderite precipitates under shallow and deep soil conditions (Romanov et al., 2015). In sub-oxic to highly-reduced anoxic aqueous environments, Fe (II) is known to combine with CO_2 species and will form a siderite precipitate (Langmuir, 1997). Potential sources of Fe (II) in aquifer systems may also include Fe (II)-bearing minerals such as magnetite, biotite and smectite. Siderite in natural environments can be found in highly concentrated Fe^{2+} environments. (Romanov et al., 2015) show siderite is a key component in a range of mineral reactions that occur during reactive transport in groundwater. Siderite precipitation in aqueous systems occurs in typically highly alkaline environments rich in dissolved Fe (II) (Bruno et al., 1992).

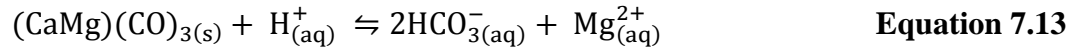
In this study a methodology was proposed to differentiate between carbonate-bound iron and carbonates bound to other elements found in soil on the basis of their reaction time with 'wet' phosphoric acid (section 3.1.2). With this approach it was possible to determine the source of carbon in the mesocosms during the period of incubation i.e. whether there was carbonate addition or dissolution. The results for the un-amended, active (S_T) mesocosms and the mesocosms amended with Soil 1 suggest toluene degradation in the mesocosms induced the dissolution of carbonates associated with the fast-reacting pool. This dissolution was followed by the re-addition of newly-formed carbonates to the slow-reacting pool. The results for the other soil-amended and iron-amended mesocosms gave evidence for (only) carbonate addition to the fast- and slow-reacting pools.

Carbonate minerals tend to be the most reactive minerals in subsurface environments. Their occurrence in geological formations is influenced by dissolution and precipitation (or addition) reactions. Calcite, dolomite and siderite are the most common carbonate minerals, with calcite being the most reactive and dolomite least reactive of the three minerals. Carbonate dissolution may occur in three steps, the first of these is leaching followed by dissolution of CO_2 and subsequent conversion of (bi) carbonate species. Addition may occur in the form of nucleation and growth of the new carbonate species. The dissolution reactions of

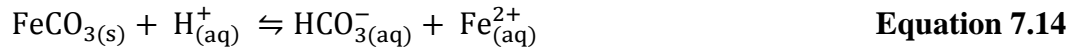
these three carbonate minerals are shown in Equations 7.12-14 below (André et al., 2007):



(calcite)



(dolomite)



(siderite)

Precipitation reactions are influenced by the alkalinity of the water medium and the reactions of divalent cations. A solution that has become saturated with a cation will have further cation contribution exceeding the rate at which it is removed from solution. When this happens the solution will no longer support the formation of carbonates. As the mesocosms were anaerobically sealed, the dissolution of carbonates will lead to the re-addition of newly formed carbonates. Carbonate dissolution and re-addition may be likened to precipitation reactions. The precipitation of carbonates is influenced by pH, CO₂, partial pressure (PCO₂), alkalinity, temperature, carbonate, bicarbonate and metal ion concentrations (see section 2.4.2).

The pH of the mesocosms amended with Soil 1 declined during the period after the addition of the second toluene spike. A decline in pH may enhance the dissolution of fast-reacting calcium carbonates. This is because a decline in pH increases the concentration of H⁺ ions by forming carbonic acid and other complex acid species (see section 2.4.2). The formation of carbonic acid from the dissolution of calcite induces the formation of calcium bicarbonate Ca (HCO₃)₂ and will increase the solubility of CaCO₃. Bicarbonate formation promotes the precipitation of carbonates. Increased precipitation may create supersaturated conditions in the soil-water environment. The pH in the amended and un-amended mesocosms fluctuated over a circum-neutral range during the period of incubation (see sections 4.1, 5.1 and 6.1) with the exception of the ferrihydrite- and lepidocrocite-amended mesocosms in which the mesocosm pH varied over acidic and alkaline ranges respectively. The precipitation of carbonates is increased by bicarbonate formation however to promote on-going precipitation, this reaction must be buffered by a weak acid solution. Therefore variations in pH / buffering activity can be expected to have a complex effect on soil carbonates.

The presence of the soil and iron amendments may have been responsible for carbonate addition being the only process observed in these mesocosms. The

reactions of divalent cations affect the precipitation of carbonates (or carbonate addition). Iron (Fe) is one of a few chemical elements that forms stable, poorly soluble carbonate minerals. Divalent iron reacts to form siderite, a poorly soluble carbonate. Dissolved divalent metals can react with dissolved CO₂ to precipitate carbonate minerals (see section 2.4.2). Trivalent iron, the most abundant form of iron in nature cannot form carbonate however minerals with suitable amounts of MgO, CaO, and FeO in the presence of CO₂ may experience carbonation reactions depending on external conditions in the system under consideration. Iron (hydr)oxides are known to dissolve faster under sub-oxic conditions as oxic conditions induce coating of mineral surfaces with FeOOH layers. Complexes formed as a result of bi-carbonate induced dissolution are responsible for the enhanced solubility of iron minerals. For example hematite has been shown to dissolve faster in bi-carbonate rich environment (Bruno et al., 1992). Iron (iii) reduction to iron (ii) promotes further dissolution of iron-bearing minerals by lowering the Fe³⁺ saturation levels. The subsequent utilisation of Fe²⁺ to form siderite will help drive the dissolution of iron minerals. The (iron-mediated) degradation of toluene in the presence of the iron amendments (hematite, goethite, magnetite, ferrihydrite and lepidocrocite) will induce a change in the amount of divalent cations in the mesocosms therefore the predominance of carbonate addition was likely to be a reflection of increased siderite precipitation induced by the presence of the iron amendments in the soil-water mixture.

Biodegradation is a uni-directional reaction and is often accompanied by significant kinetic isotope effects (Vieth and Wilkes, 2010). The decomposition of organic matter in sediments consumes oxygen, releasing isotopically-light CO₂ to the pore water in the process. Carbonate addition to the slower-reacting carbonate pool in the mesocosm with soil and water only (S_O) was found to have produced isotopically light carbon. Furthermore the isotope signatures obtained for mesocosms with soil and water only (S_O) and mesocosms with soil and toluene (S_T) correlate with the isotope signatures of soil organic matter and toluene respiration respectively. The results are therefore in agreement with the literature. The experimental results show that regardless of the soil and mineral amendment used, the δ¹³C changed over a limited range over the incubation period. ¹³C and ¹²C in the degradation process is determined by several factors including the type and amount of substrate degraded, species of bacteria as well as whether the environment is aerobic or anaerobic (Hunkeler, Daniel and Aravena, 2000; Morasch et al., 2004; Meckenstock, Rainer U. et al., 2002). Stable carbon isotopes have been used widely in the study of the mechanisms of carbonate dissolution and precipitation (Nordt et al., 1996; Mermut et al., 2000). Information so obtained is useful in soil management as well as in the elucidation of processes associated with the carbon cycle. The results of the stable

carbon isotope experiments illustrate the inter-relationship of soil carbonates and hydrocarbon contaminants and may be applicable to iron-mediated contaminant degradation in sub-oxic to anoxic environments.

7.3 Conclusion

In this work, method development results indicate that GC-IRMS can be used to assess the distribution of soil carbonate pools. Stable carbon isotope analysis of toluene in the samples during the period of incubation demonstrated the validity of GC-IRMS in the analysis of toluene in soil samples and provided bench-mark isotopic fingerprints in the un-amended and amended incubated material obtained from the mesocosms. The large error bars in the experimental results were due to variations in the data obtained from replicates as well as the number of replicate samples. These errors may also have been a reflection of the heterogeneity of the analysed samples as the method used is originally designed for pure carbon samples, and not soil samples. The results indicate the period of incubation induced carbonate addition to the slow-reacting carbonate pool of the soil in the un-amended and amended mesocosms. This pool was made up of less reactive carbonates including iron-bound carbonates such as siderite. The addition of heavy carbonates provides supporting evidence that siderite precipitation in the un-amended (ST) mesocosms (section 4.1.3) was as a result of iron-mediated toluene degradation. The differences in the amount of carbonate carbon in the starting material and incubated mesocosm material provide evidence of the overall carbonate composition of the soil being affected by toluene degradation. Most carbonate reactions are thought to occur over relatively larger time scales, however the results of the isotope experiments show the indigenous carbonate pool in the soil material used is reactive on a 10-day time scale.

Summary

Identifying two groups of soil carbonates (broadly classified as the faster-reacting carbonate pool e.g. calcium carbonates and the slower-reacting carbonate pool e.g. dolomite and siderite) on the basis of their reaction times with 'wet' phosphoric acid made it possible to determine the source of carbon during toluene removal in the incubated mesocosm material (i.e. whether there was carbonate addition or dissolution during the period of incubation). The results of the experiments gave evidence for carbonate dissolution in the fast-reacting carbonate pool of the un-amended active mesocosms and the active mesocosms amended with the soil sample Soil 2. The experimental results from the un-amended control mesocosms and

mesocosms amended with Soil 3 indicated there was carbonate addition to the fast- and slow-reacting pools in the incubated, mesocosm material. Similarly, there was carbonate addition to the fast- and slow-reacting carbonate pools of the hematite-, goethite-, magnetite-, and ferrihydrite--amended mesocosms. The results obtained for the fast-reacting pool in the lepidocrocite-amended mesocosms gave no evidence for carbonate dissolution or addition. This may have been due to the alkaline environment in these mesocosms during the incubation period affecting the chemical reactivity of the calcium carbonate pool in the lepidocrocite-amended, incubated material. Overall the experimental results provide evidence for changes in the carbonate content of the incubated material induced by the period of incubation and toluene removal in all of the experimental mesocosms with the exception of the lepidocrocite-amended mesocosms.

Chapter 8

Predicting the Natural Attenuation of Toluene with Mixed Effects Models

Introduction

The previous chapters focus on the analysis of the results obtained from the degradation experiments. The time-series data generated from these experiments are further analysed in this chapter with the use of inferential statistical tools. A mathematical model for toluene removal is proposed using the mixed effects model approach.

8.1 Results and discussions

The combined concentration-time profiles of the un-amended (S_T), soil-amended and iron-amended mesocosms are presented in Figure 8.1.

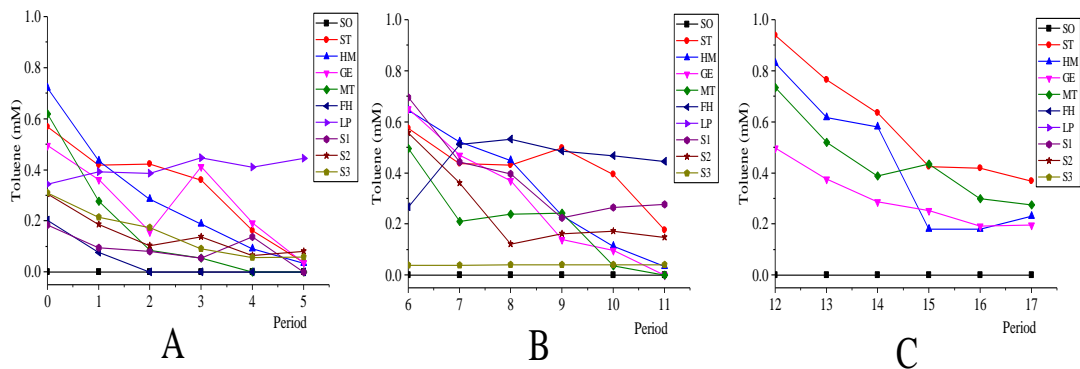


Figure 8.1 Changes in toluene with time for each mesocosm group over three periods A, B, and C, following the addition of toluene. The data is shown as the average of three replicates for each group

The mixed effects model procedure was run separately for the data for each period after spiking (i.e. Periods A, B and C). This approach made the data more representative of longitudinal (panel_ data (see section 2.5.3), making it more suitable for the mixed model approach.

8.1.1 Preliminary tests - test for correlation

Panel data consist of observations of multiple phenomena obtained over multiple periods for the same subjects/entities (see section 2.5.3). As data collection involves carrying out repeated measures on single or multiple subjects over time, a

correlation coefficient is obtainable. A test for correlation was performed on the data using the Pearson test of correlation (see Table 8.1).

Table 8.1 Test for correlation ^a

(Period A)

			Toluene	Fe	pH
Toluene	Period A	Pearson Correlation (r)	1	-.158*	.407**
		p-value		.035	.000
		Interpretation*		r indicates weak correlation	r indicates moderate correlation
	Period B	Pearson Correlation (r)	1	.330**	-.287**
		p-value		.000	.000
		Interpretation*		r indicates moderate correlation	r indicates moderate correlation
	Period C	Pearson Correlation (r)	1	-.036	.153
		p-value		.748	.168
		Interpretation*		p > .05, no correlation	p > .05, no correlation
Fe	Period A	Pearson Correlation (r)	-.158*	1	-.370**
		p-value	.035		.000
		Interpretation*	r indicates weak correlation		r indicates moderate correlation
	Period B	Pearson Correlation (r)	.330**	1	-.628**
		p-value	.000		.000
		Interpretation*	r indicates moderate correlation		r indicates strong correlation
	Period C	Pearson Correlation (r)	-.036	1	-.233*

			Toluene	Fe	pH
p-value			.748		.034
Interpretation*			p > .05, no correlation		r indicates moderate correlation
pH	Period A	Pearson Correlation (r)	.407**	-.370**	1
		p-value	.000	.000	
		Interpretation*	r indicates moderate correlation	r indicates moderate correlation	
Period B		Pearson Correlation (r)	-.287**	-.628**	1
		p-value	.000	.000	
		Interpretation*	r indicates moderate correlation	r indicates strong correlation	
Period C		Pearson Correlation (r)	.153	-.233*	1
		p-value	.168	.034	
		Interpretation*	r indicates weak correlation	r indicates moderate correlation	

*. Correlation is significant at the 0.05 level (2-tailed).

**. Correlation is significant at the 0.01 level (2-tailed).

- 0<r<0.2 = weak correlation, 0.2<r<0.5 = moderate correlation, 0.5<r<1.0 = strong correlation

Longitudinal data naturally show correlation among observations in repeated measures. The results above show there is a moderate to strong correlation between the three variables over the three periods. The mesocosms amended with synthesised iron amendments and the soil amendments were not sampled beyond the second spike period (Period B). The results for this period showed there was either no correlation or a weak correlation between the variables. This may therefore be attributed to the comparatively large number of missing observations in the data for this period.

8.1.2 Preliminary tests - test for normality

The correlation among observations in repeated measures data occur as a result of shared, unobserved variables and can be represented by an appropriate probability distribution. There are several tests of normality broadly categorized as graphical and traditional tests (Argyrous, 2011; Howitt and Cramer, 2003). It is often

recommended that both graphical and traditional tests be performed when assessing the normality of a data set. Kolmogorov-Smirnov and Shapiro-Wilk tests are the most common traditional tests of normality. The results of both tests (Table 8.2) show the data for Periods A and B are normally distributed ($p < .05$). The test results however show the data set for Period C is not normally distributed ($p > .05$), possibly as a result of the large number of missing values in the data set.

Table 8.2 Tests for normality

	Period	Kolmogorov-Smirnov ^a		Shapiro-Wilk	
		Statistic	p-value	Statistic	p-value
Toluene	Period A	.184	.0001	.859	.0001
	Period B	.164	.0001	.913	.0001
	Period C	.119	.006	.929	.0001
Fe	Period A	.169	.0001	.895	.0001
	Period B	.172	.0001	.796	.0001
	Period C	.095	.060	.939	.001
pH	Period A	.187	.0001	.863	.0001
	Period B	.200	.0001	.829	.0001
	Period C	.088	.167	.981	.255

a. Lilliefors Significance Correction

Q-Q plots (Figures 8.2 – 8.4) were used as graphical tests for normality. The spread of the data for toluene removal, total iron concentrations and pH over the three periods indicate the data follows a normal distribution.

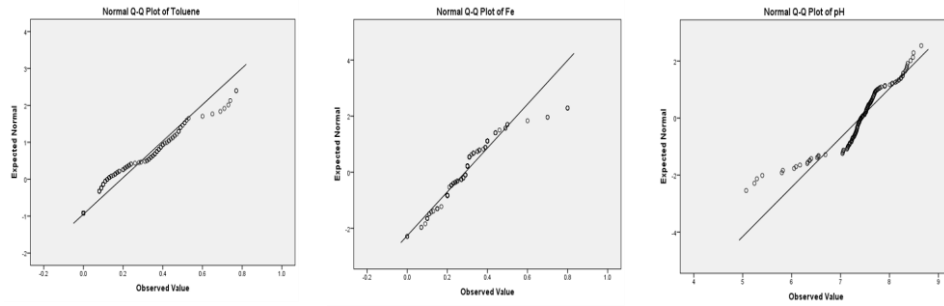


Figure 8.2 Normal Q-Q plots for toluene, Fe and pH across the un-amended and soil-amended mesocosm groups (Period A)

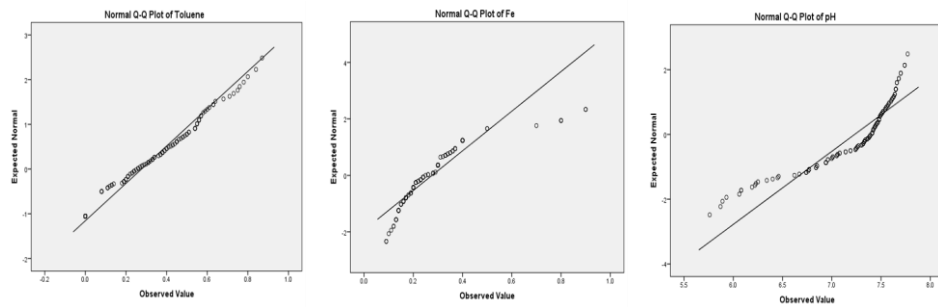


Figure 8.3 Normal Q-Q plots for toluene, Fe and pH in the un-amended and soil-amended mesocosm groups (Period B)

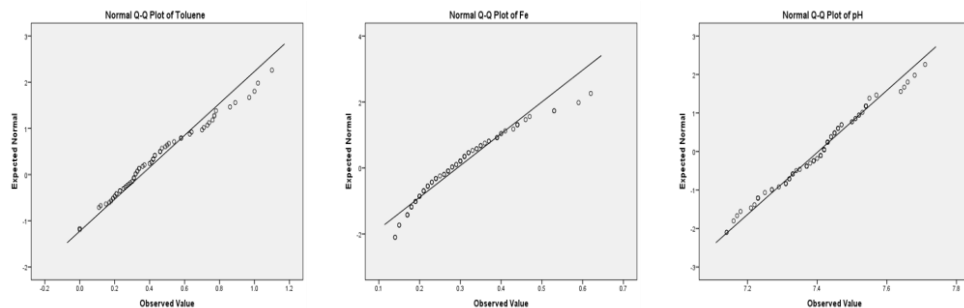


Figure 8.4 Normal Q-Q plots for toluene, Fe and pH across the un-amended and soil-amended mesocosm groups (Period C)

8.1.3 A predictive model for the natural attenuation of toluene in subsurface soil environments

The main objective of the analysis in this chapter is to determine if toluene removal can be predicted by total iron concentration and pH with a two-level multilevel model. Modelling of hierarchical data is achieved as a two-stage process with the use of two models (see section 2.5.3). The two-level model estimates three sets of parameters namely i) fixed effects (Υ_{00} , Υ_{01} , and Υ_{10}), ii) random level-1 coefficients (β_{0j} and β_{1j}), and iii) variance-covariance components expressed as

covariance between level-2 error terms (cov (U_{0j}) or cov (U_{1j}) which demonstrate the dependency between level-1 units nested within each level-2 unit), variance in level-1 error terms (ie. the variance of r_{ij} denoted by σ^2) and variance in level-2 error terms (i.e. the variance of the U_{0j} and U_{1j} or β_{0j} and β_{1j}).

In this analysis, the first equation (Equation 8.1) models toluene removal without predictors.

$$Toluene_{ij} = \beta_{0j} + \beta_{1j}Period_{ij} + r_{ij} \quad \text{Equation 8.1}$$

In Equation 8.1,

$Toluene_{ij}$ = toluene concentration for a sampling occasion i in a sampling period j (in mM)

$Period_{ij}$ = value of toluene concentration on a sampling occasion i in a sampling period j (in days)

B_{0j} = intercept for a sampling period j

B_{1j} = regression coefficient associated with a sampling occasion i during a sampling period j

r_{ij} = random error associated with a sampling occasion i in sampling period j

The model parameters to be determined are B_{0j} , B_{1j} , and r_{ij} . An unstructured covariance structure was specified during the analysis with sampling occasions (coded ‘Time’) as random effects. The estimates of these parameters can be found in SPSS output data showing the estimates of fixed effects and the estimates of covariance parameters in section C.9 of Appendix C. These parameters are estimated using the z and t test statistic (Lomax and Hahs-Vaughn, 2013). The values of the parameters of interest are given in Table 8.3 below.

Table 8.3 Parameter estimates for the level-2 mixed effects model of toluene removal without predictors

Parameter	Period	Estimate	Value of test statistic	p-value
Intercept (B_{0j})	Period A	.329	t = 8.096	p = .0001
	Period B	.796	t = 6.875	p = .0001
	Period C	1.48	t = 5.515	p = .0001
Time (B_{1j})	Period A	-.055	t = 5.467	p = .0001
	Period B	-.062	t = 5.186	p = .0001
	Period C	-.078	t = 5.326	p = .0001
Residual (r_{ij})	Period A	.009	z = 7.746	p = .0001
	Period B	.012	z = 7.122	p = .0001
	Period C	.008	z = 5.263	p = .0001

- All tests were performed at the .05 alpha level

From these parameters, the model for toluene removal without predictors may be re-written as Equations 8.1a, 8.1b and 8.1c for the Period A, B and C data respectively:

$$Toluene_{ij} = 0.329 - 5.467Period A_{ij} + 0.009 \quad \text{Equation 8.1a}$$

$$Toluene_{ij} = 0.796 - 5.186Period B_{ij} + 0.012 \quad \text{Equation 8.1b}$$

$$Toluene_{ij} = 1.48 - 5.326Period C_{ij} + 0.008 \quad \text{Equation 8.1c}$$

The concentration-time profiles for Fe and pH showed Fe concentrations remained constant regardless of the amendment used however the pH in the mesocosms varied over a wide range in the amended and un-amended groups of mesocosms (see sections 4.1, 5.1 and 6.1). In addition, the tests of correlation showed the correlation between toluene and pH was comparatively stronger than the correlation between toluene and Fe. In this model Fe is regarded as a level 1 (i^{th} level) predictor and pH a level 2 (j^{th} level) predictor. In this model, the level-1 regression coefficients (B_{0j} and B_{1j}) are used as outcome variables and are related to each of the level-2 predictors. The fixed effect parameters become $\beta_{0j} = \gamma_{00} + \gamma_{01}(Fe, pH)_j + U_{0j}$ and $\beta_{1j} = \gamma_{10} + \gamma_{11}(Fe, pH) + U_{1j}$ (where β_{0j} = intercept for the j^{th} sampling period and β_{1j} = slope for the j^{th} sampling period). A combined model for toluene removal with Fe as a predictor at the sampling period level and pH as a predictor at the sampling occasion level will therefore be given by Equation 8.2:

$$Toluene_{ij} = \gamma_{00} + \gamma_{10} pH_{ij} + \gamma_{01} Fe_j + \gamma_{11} Fe_j pH_{ij} + U_{ij} pH_{ij} + U_{0j} + r_{ij} \quad \text{Equation 8.2}$$

where

$Toluene_{ij}$ = toluene concentration for a sampling occasion i in a sampling period j (in mM)

Fe_j = total iron concentrations in sampling period j (in mM)

γ_{00} = overall mean intercept adjusted for pH

γ_{10} = overall mean slope adjusted for pH

γ_{01} = regression coefficient associated with pH relative to level-2 intercept

γ_{11} = regression coefficient associated with pH relative to level-2 slope

U_{0j} = random effects of the j^{th} level-2 unit adjusted for pH on the intercept

U_{1j} = random effects on the j^{th} level-2 unit adjusted for pH on the slope

r_{ij} = random error associated with a sampling occasion i in sampling period j

In this model, $Toluene_{ij}$ may be regarded as an effect size parameter dependent on the value of the level-2 predictor. The results of the parameter estimates are presented in Table 8.4.

Table 8.4 Parameter estimates for the level-2 mixed effects model of toluene removal with predictors*

Parameter	Period	Estimate	Value of test statistic	p-value
FIXED EFFECTS PARAMETERS				
γ_{00}	Period A	1.610	t = -3.305	p = .001
	Period B	1.773	t = -1.028	<u>p = .283</u>
	Period C	15.2	t = -1.696	<u>p = .096</u>
γ_{10}	Period A	.261	t = 4.132	p = .0001
	Period B	.309	t = 1.415	<u>p = .160</u>
	Period C	2.23	t = 1.854	<u>p = .069</u>
γ_{01}	Period A	.259	t = 2.140	p = .035
	Period B	.332	t = 1.865	<u>p = .065</u>
	Period C	.985	t = 1.691	<u>p = .097</u>
γ_{11}	Period A	.041	t = -2.615	p = .010
	Period B	.048	t = -2.141	p = .035
	Period C	.413	t = -1.810	<u>p = .076</u>
VARIANCE-COVARIANCE PARAMETERS				
U_{0j}	Period A	.047	z = 3.368	p = .001
	Period B	.294	z = 2.904	p = .004
	Period C	.853	z = 2.269	p = .023
U_{1j}	Period A	.294	z = 2.904	p = .004
	Period B	.003	z = 2.640	p = .008
	Period C	.002	z = 2.093	p = .036
r_{ij}	Period A	.008	z = 7.612	p = .0001
	Period B	.012	z = 7.000	p = .0001
	Period C	.008	z = 5.049	p = .0001

*All tests were performed at the .05 alpha level

An unstructured covariance was also specified for this model (see model dimensions in section C.9 of Appendix C). The results show a large number of p-values for the fixed effect parameters were not statistically significant at the 0.05 alpha level (see underlined and italicised values in Table 8.4) however the Wald Z statistic were significant at the 0.05 alpha level. This was mainly for the Period B and C data and may be an indication that Fe and pH are not suitable predictors of toluene removal during these periods. It was stated in chapter 4 that the draining of the mesocosms may have resulted in loss of soil material and as such the measured total iron concentrations in the mesocosms after the first spike period may not have been true representations of the actual concentrations (see section 4.1.3). The results for the parameter estimates for the Period A and B data may be a reflection of this misrepresentation.

8.2 General discussion

In field observations, the fate of petroleum hydrocarbons in the unsaturated zone is best assessed through a complete natural attenuation monitoring process. Sorption, diffusion, evaporation and biodegradation are the main processes affecting the presence of VOC contaminants (Atlas, R. M. and Philip, 2005). Repeated measures experiments are a common design in experiments assessing the biodegradation of hydrocarbon contaminants. The analysis refers to multiple measurements made on the same experimental unit observed over either time or space. The usual practice in these designs is to apply treatments to experimental units in a completely randomized design and make measurements sequentially over time. The repeated measures design incorporates two fixed effects (treatment and time) and two sources of random variation (between and within replicates of treated and untreated experiments (Wang, L.A. and Goonewardene, 2004). The degradation experiments in this study provided repeated measurements of toluene, total iron concentrations and pH on replicates of soil mesocosms randomly allocated to fixed treatment effects. A model for toluene removal in anoxic soil environments was therefore proposed using the mixed effects model approach by analysing the time series experimental data as a 2-level hierarchical data set. As measurements were made on the same soil-water mixture, the measurements are more likely to be correlated than two measurements taken on different soil and / or water mixtures. In addition measurements taken closer to time are likely to be more correlated than those taken further apart in time. The analysis of repeated measures data therefore accounts for correlations between the observations made on the same subject, making them more suitable for repeated measures than other classical methods (Wang, L.A. and Goonewardene, 2004).

Mixed effects modelling and hierarchical modelling are viewed in the same context and sometimes used interchangeably (Bell and Jones, 2015; Woltman et al., 2012). The use of mixed effects in the same model can be thought of hierarchically as a close relationship exists between mixed models and the class of models referred to as hierarchical linear models (Huitema, 2011). In this hierarchy one level may be regarded as being for subjects and another level as being for measurements within subjects. A factor is fixed when it has levels that are of primary interest and would be used again were the experiment to be repeated. A random factor will have levels that are not of primary interest but rather are thought of as being a random selection from a much larger set of levels. In this study toluene removal was modeled with the use of the mixed effects approach. The approach for two-level multilevel mixed effects models is to first produce a model without predictors. This model determines the appropriate starting values for modeling toluene removal (see section 2.5.3). The

fixed effect and covariance parameters in the first model were statistically significant. Equations modeling toluene removal over these three periods were obtained with these parameters. Recall that the mixed effects model approach avoids violations caused by missing observations (see section 2.5.3). Therefore although the number of observations in the three periods differ (see data set in section C.6.5 of Appendix C), a choice can be made between these three models to obtain the model that best represents toluene removal in the mesocosms. Penalised methods estimate the likelihood of the observed data using a particular method. Although SPSS provides five options for the estimates of penalised likelihood, the three commonly used parameters are the 2-Restricted Log Likelihood, Akaike's Information Criteria and Schwarz's Bayesian Criterion (BIC) the values of which are given in Table 8.5.

Table 8.5 Parameters for model selection

Period	-2 Restricted Log Likelihood	Akaike's Information Criterion (AIC)	Schwarz's Bayesian Criterion (BIC)
Period A	-205.257	-197.257	-184.530
Period B	-128.319	-120.319	-108.249
Period C	-100.663	-92.663	-83.085

The most basic idea concerning model development is to find the model that uses the least number of parameters (freeing up the largest number of data items or degrees of freedom) along with the best fit (Liu, H., 1995; Judd et al., 2011). Defining parameters as fixed effect parameters means only a single value is estimated (a point estimate), the degree of dependency between any two repeated measures pairs mean is not defined. This results in the estimate of a fixed parameter (i.e. covariance / correlation) value for each pair using up a large number of degrees of freedom. Thus, the model with a lower BIC value gives a better balance between complexity and good fit and is most likely to be closest to the true model of the data under study (Doncaster and Davey, 2007; Raykov and Marcoulides, 2012). The approach for model selection is therefore to use the 'smaller is better' rule of thumb of which the BIC provides the smallest value as it penalises the likelihood based on both the total number of parameters in a model and the number of subjects studied.

From Table 8.2, the Period C data gives the smallest BIC value therefore the mathematical model for the monitored attenuation of toluene, based on the mesocosm data, is given by Equation 8.3.

$$Toluene_{ij} = 1.48 - 5.326Period_{ij} + 0.008 \qquad \text{Equation 8.3}$$

where

$Toluene_{ij}$ = toluene concentration for a sampling occasion i in a sampling period j (in mM)

$Period_{ij}$ = value of toluene concentration on a sampling occasion i in a sampling period j (In days)

B_{0j} = intercept for a sampling period j

B_{1j} = regression coefficient associated with a sampling occasion i during a sampling period j

r_{ij} = random error associated with a sampling occasion i in sampling period j

The equation modelling toluene removal with the use of level-2 predictors did not yield statistically significant values for the parameter estimates of the Period B and C data. The addition of interactions Fe*Time and pH*Time (see section C.9.3 of Appendix C) demonstrate how the mixed effects model allow for cross-level interactions between higher-level (level 2) and lower-level (level 1) variables in hierarchical data. These interactions give an indication of whether the time-varying predictor varies by time-invariant predictors (Fe) and vice versa. The interaction effects show the changes in pH with time occur to a larger extent in comparison to the changes between Fe and time (see section C.9.3 of Appendix C). These relationships are of interest when analysing treatment effects over time. In repeated measures data, measurement occasions are nested within entities. In this study measurements of toluene, Fe and pH per sampling occasions in individual replicates of amended and un-amended mesocosms are nested within the sampling periods representing each period after spiking. The results show mixed effects models are a good exploratory tool for the analysis of repeated measures data from biodegradation experiments. Using the parameters for Period A, the model for toluene removal with Fe and pH as predictors is given by Equation 8.4:

$$Toluene_{ij} = 1.610 + 0.261pH_{ij} + 0.259Fe_j - 0.041Fe_jpH_{ij} + .294_{ij}pH_{ij} + 0.047 + .008$$

Equation 8.4

where

$Toluene_{ij}$ = toluene concentration for a sampling occasion i in a sampling period j

Fe_j = total iron concentrations in sampling period j

The equation above serves as a model for toluene removal with Fe as a level 1 (i^{th} level) predictor and pH a level 2 (j^{th} level) predictor based on the time series data for toluene removal after the addition of the first toluene spike.

8.3 Conclusion

Mixed effects models are a rapidly growing application of basic multilevel modelling of longitudinal data. Mixed effects models avoid violations due to missing data and unequal spacing. It is therefore recommended that the mixed model be used for the analysis of repeated measures in biodegradation studies.

Summary

The experimental data for the toluene degradation experiments showed toluene concentrations, total dissolved iron and pH differed across the amended and un-amended mesocosms therefore the use of statistical inferential tools were employed to estimate the effect sizes for the various treatments by using a difference in means test (see C.9.1 of Appendix C) reported in the discussion of results in chapters 5 and 6. With the mixed effects model, the main objective was to produce an equation for modelling toluene removal over time on the basis of the time series data obtained from the un-amended and amended mesocosm groups. This equation was to incorporate the three variables Toluene, Fe and pH. Specifying Fe and pH as predictors made it possible to test the suitability of these variables as predictors of toluene removal in toluene-contaminated subsurface soil environments. This model was achieved by a simple regression analysis using the mixed effects modelling approach. Therefore the equation modelling toluene removal is a regression line fitted across the data obtained from the un-amended mesocosms as well as the iron- and soil-amended mesocosms. The choice of the mixed effects model approach lay in its main features which make it more suitable for the analysis of repeated measures data, particularly those with missing observations. The p-values indicated that the differences in the test parameters were statistically significant at $p = .0001$. The inclusion of Fe and pH as additional fixed effects gave p-values which were only statistically significant ($p < 0.05$) for the Period A data.

Chapter 9

Conclusion and Recommendations

Conclusion

The primary objective of this research was to investigate the mechanisms of intrinsic, iron-mediated degradation of volatile petroleum hydrocarbons in subsurface regions with toluene as a representative compound. This thesis has explored several disciplines and analytical approaches that may offer additional insight to aid the understanding of geochemical influences affecting the biodegradation of petroleum hydrocarbons in subsurface soil environments. The experiments conducted tested three main hypotheses namely i) indigenous soil microorganisms in a previously-contaminated soil may be able to respire anaerobically and couple the reduction of Fe (III) to the oxidation of a hydrocarbon contaminant (toluene), ii) the process of carbon cycling in a soil environment may change as a result of addition of a hydrocarbon contaminant (toluene), iii) the addition of extraneous iron sources as a terminal electron acceptor can increase the extent / amount of contaminant removal as well as the rate of the reaction. The main conclusions from the experimental findings are:

- Indigenous microbial soil organisms will degrade toluene in soil environments prepared under laboratory conditions.
- Indigenous microorganisms in soil will degrade toluene in the presence of hematite, goethite, magnetite and ferrihydrite under laboratory conditions. The rate and amount of removal will be a function of the crystallinity of these iron mineral (hydr) oxides.
- The texture of soils will affect the rate and amount of toluene removal in subsurface environmental conditions. Microbially-mediated removal will be a function of the percentage clay fraction and surface area of these soils.
- Stable carbon isotope analysis can be used to differentiate between common carbonates found in soil on the basis of the reactivities of these carbonates in soil.
- Given the right experimental variables, mixed effects models may offer a means of predicting toluene removal by natural attenuation in subsurface soil environments.

Recommendations for further studies

1. The analysis of operationally-defined iron pools in the iron- and soil-amended mesocosm material was not performed due to time constraints. If this analysis was performed it would have enabled comparisons to be made

between the amended and incubated material to assess the effect of the amendments on the operationally-defined iron pools. The results of such analysis may allow for inferences to be made about carbonate precipitation during iron-mediated toluene removal.

2. The influence of soil on toluene removal may be further explored with the use of soils ranging from highly organic (e.g. peat) to highly inorganic (e.g. chalk or limestone aquifer material) to provide additional information on the influence of the percentage clay fraction and surface area on toluene removal. These experiments may be designed with control mesocosms consisting of successively-spiked mesocosms containing water and the soil amendments only (i.e. mesocosms without starting soil material) to further investigate the influence of soil processes such as sorption and diffusion as well as to monitor the effect and extent of losses due to volatilisation using the parameters in Equations 6.1 to 6.5.
3. Further experimentation with the use of batch mesocosms may generate time series data that may serve as more suitable predictors of toluene removal and produce predictive models of greater complexity incorporating three or more factor levels. Suitable predictors may include factors known to affect biodegradation rates such as temperature, pH, amount (in mg) of amendments, volume of toluene stock for spiking.

List of References

- Al-Aasm, I., Taylor, B.E. and South, B. 1990. Stable isotope analysis of multiple carbonate samples using selective acid extraction. *Chemical Geology (Isotope Geoscience Section)*. **80**, pp.119-125.
- Alexander, M. 1999. *Bioremediation and Bioremediation*. [Online]. 2nd ed. San Diego: Academic Press.
- An, Y.J. 2004. Toxicity of benzene, toluene, ethylbenzene and xylene (
- Andersen, S. and Engelstad, F. 1993. Application of Factorial Designs: Estimating The Pollution Potential Inferred From Changes in Soil Water Chemistry. In: *Selected Proceedings of the First European Conference on Integrated Research for Soil and Sediment Protection and Remediation (EUROSOL)*. 30 April 1993, pp.227-2230.
- Anderson, R., and Lovley, D. 1997. Ecology and biochemistry of insitu groundwater bioremediation. *Adv Microb Ecol*. **15**, pp.289-350.
- André, L., Audigane, P., Azaroual, M. and Menjoz, A. 2007. Numerical modeling of fluid-rock chemical interactions at the supercritical CO₂-liquid interface during CO₂ injection into a carbonate reservoir, the Dogger aquifer (Paris Basin, France). *Energy Conversion and Management*. **48**(6), pp.1782-1797.
- Appelo, C.A.J., Postman, D. and Balkema, A.A. 1996. *Geochemistry, groundwater and pollution*. Rotterdam, Netherlands.
- Argyrous, G. 2011. *Statistics for Research: With a Guide to SPSS*. SAGE Publications.
- ASTM:E1624-94. 2008. *Standard Guide for Chemical Fate in Site-Specific Sediment/Water Microcosms*. West Conshohocken, PA: ASTM International.

Atlas, M.T. 1981. Microbial degradation of petroleum hydrocarbons: an environmental perspective. *Microbiological Review*. **45**, pp.180 - 209.

Atlas, R.M. 1991. Bioremediation of fossil fuel contaminated soils. In: Hincsee, R.E. and Olfenbuttel, R.F. eds. *In situ Bioreclamation. Applications and Investigations for Hydrocarbon and Contaminated Site Remediation*. [Online]. MA: Butterworth – Heinemann, Stoneham, pp.14-33.

Atlas, R.M. 1981. Microbial degradation of petroleum hydrocarbons: an environmental perspective. . *Microbiological Review* **45**, pp.180-209.

Atlas, R.M. and Philip, J. 2005. *Bioremediation: Applied Microbial Solutions for Real world Environmental Cleanup*. Washington, DC, : American society for Microbiology (ASM) Press.

Bagiella, E., Sloan, R.P. and Heitjan, D.F. 2000. Mixed-effects models in psychophysiology. *Psychophysiology*. **37**(1), pp.13-20.

Ball, H.A., Johnson, H.A., Reinhard, M. and Spormann, A.M. 1996. Initial reactions in anaerobic ethylbenzene oxidation by a denitrifying bacterium, strain EB1. *J.Bacteriol*. **178**, pp.5755-5761.

Ballesteros, M.C., Rueda, E.H. and Blesa, M.A. 1998. The influence of iron (II) and (III) on the kinetics of goethite dissolution by EDTA. *Journal of Colloidal and Interface Science*. **201**, pp.13-19.

Bamforth, S.M. and Singleton, I. 2005. Bioremediation of polycyclic aromatic hydrocarbons: current knowledge and future directions. *Journal of Chemical Technology & Biotechnology*. **80**(7), pp.723-736.

Barbaro, J.R., Barker, J.F., Lemon, L.A. and I, M.C. 1992. Biotransformation of BTEX under anaerobic denitrifying conditions: field and laboratory observations *J Cont Hydrol*. **11**, pp.245-272.

Barkay, T. and Schaefer, J. 2001. Metal and radionuclide bioremediation: Issues, considerations and potentials. *Current Opinion in Biotechnology*. **4**(3), pp.318-323.

Barua, B.S., Suzuki, A., Pham, H.N. and Inatomi, S. 2012. Sdaptation of ammoniafungi to urea enrichment environment. *Journal of Agricultural Science and Technology*. **8**, pp.173-189.

Bastiaens, L., Springael, D., Wattiau, P., Harms, H., deWacher, R., Verachtert, H. and Diels, L. 2000. Isolation of adherent polycyclic aromatic hydrocarbons (PAH)-degrading bacteria using PAH-sorbing carriers. *Applied Environmental Microbiology*. **66**, pp.1834-1843.

Bauder, T., Barbarick, K., Ippolito, J., Shanahan, J. and Ayers, P. 2005. Soil properties affecting wheat yields following drilling-fluid application. *J Environ Qual* **34**, pp.1687–1696.

Bell, A. and Jones, K. 2015. Explaining fixed effects: Random effects modeling of time-series cross-sectional and panel data. *Political Science Research and Methods*. **3**(1), pp.133-153.

Beller, H. and Spormann, A. 1997. Anaerobic activation of toluene and o-xylene by addition to fumarate in denitrifying strain T. *J. Bacteriol.* **179**, pp.670-676.

Beller, H.R., Spormann, A.M., Sharma, P.K., Cole, J.R. and M, R. 1996. Isolation and characterisation of a novel toluene-degrading, sulphate-reducing bacteium. *Appl Environ Microbiol.* **62**, pp.1188-1196.

Berner, R.A., Lasaga, A.C. and Garrels, R.M. 1983. The carbonate-silicate geochemical cycle and its effect on atmospheric carbon dioxide over the past 100 million years. *Am J Sci* **283**, pp.641-683.

Beveridge, T.J. 1989. Role of cellular design in bacterial metal accumulation and mineralisation. *Ann. Rev. Microbiol.* **43**, pp.147-171.

Biegert, T., Fuchs, G. and Heider, J. 1996. Evidence That Anaerobic Oxidation of Toluene in the Denitrifying Bacterium *Thauera aromatica* is Initiated by Formation of Benzylsuccinate from Toluene and Fumarate. *European Journal of Biochemistry*. **238**, pp.661-668.

Blaikie, N. 2003. *Analyzing Quantitative Data: From Description to Explanation*. SAGE Publications.

Boll, M., Fuchs, G. and Heider, J. 2002. Anaerobic oxidation of aromatic compounds and hydrocarbons. *Current Opinion in Chemical Biology*. **6**, pp.604-611.

Borden, R.C., Hunt, M.J., Schafer, M.B. and Barlaz, M.A. 1997. *Anaerobic biodegradation of BTEX in aquifer material*. Ada, OK: Research and Development, National Risk Management Research Laboratory.

Bossert, I. and Barther, R. 1984. The Fate Of Petroleum in Soil Ecosystem in Petroleum

Botton, S. and Parsons, J. 2006. Degradation of BTEX compounds under iron-reducig conditions in contaminated aquifer microcosms. *Environ Toxicol Chem*. **25**, pp.2630-2638.

Boutton, T.W. 1991. 11 - Stable Carbon Isotope Ratios of Natural Materials: II. Atmospheric, Terrestrial, Marine, and Freshwater Environments. In: Coleman, D.C., Fry, B. ed. *Carbon Isotope Techniques*. Academic Press, pp.173-185.

Bouwer, E.J., McCarthy, P.L. 1983. Transformations of 1- and 2- carbon halogenated aliphatic organic compounds under methanogenic conditions
Applied and Environmental Microbiology. **45**, pp.1286-1294.

Bowen, W.R. and Yousef, H.N.S. 2003. Effect of salts on water viscosity in narrow membrane pores. *J.Colloid Interface Sci*. **264**(2), pp.452-457.

Braddock, J.F., Ruth, M.L., Catterall, P.H., Walworth, J.L. and McCarthy, K.A. 1997. Enhancement and inhibition of microbial activity in hydrocarbon-

contaminated arctic soils: implications for nutrient-amended bioremediation. *Environmental Science Technology* **31**, pp.2078-2084.

Brown, D.A., Sherriff, B.L. and Sawicki, J.A. 1997. Microbial transformation of magnetite to hematite. *Geochim. Cosmochim. Acta.* **61**, pp.3341-3348.

Bruno, J., Stumm, W., Wersin, P. and Brandberg, F. 1992. On the influence of carbonate in mineral dissolution: I. The thermodynamics and kinetics of hematite dissolution in bicarbonate solutions at T=25oC. *Geochimica et Cosmochimica Acta.* **55**, pp.1129-1147.

BSI. 1995. *Guidance on laboratory testing for biodegradation of organic chemicals in soil under aerobic conditions. BS 7755 Part 4, Subsection 4.1.1*

Caldwell, M.E., S, T.R. and M, S.J. 1999. Microbial metabolism of benzene and the oxidation of ferrous iron under anaerobic conditions: Implications for bioremediation. *Anaerobe.* **5**, pp.595-693.

Calmano, W., Hong, J. and Förstner, U. 1993. Binging and mobilization of heavy metals in contaminated sediments affected by pH and redox potential. *Wat. Sci. Tech.* **28**(8-9), pp.223-235.

Cameron, E.M., Hall, G., Veizer, J. and Krouse, H. 1995. Isotopic elemental hydrogeochemistry of a major river system: Fraser River, British Columbia, Canada. *Chem Geol* **122**, pp.149-169

Carter, M.R. 1993. *Soil sampling and methods of analysis.* Boca Raton, FL. USA: Lewis Publishers.

Casey, W.H., Carr, M.J. and Graham, R.A. 1988. Crystal defects and the dissolution kinetics of rutile. *Geochim. Cosmochim. Acta* **52**, pp.1545-1556.

Cerling, T.E., Quade, J., Wang, Y. and Bowman, J.R. 1989. Carbon isotopes in soils and palaeosols as ecology and palaeoecology indicators. *Nature* **341**, pp.138-139.

Chaineau, C.H., Morel, J.L. and Oudot, J. 1995. Microbial degradation in soil microcosms of fuel oil hydrocarbons from drilling cuttings. . *Environ. Sci. Technol.* **29**, pp.1615-1621

Chakraborty, R. and Coates, J.D. 2004. Anaerobic degradation of monoaromatic hydrocarbons. *Appl Microbiol Biotechnol.* **64**, pp.437-446.

Chakraborty, R., O'Connor, S.M., Chan, E. and Coates, J.D. 2005. Anaerobic degradation of benzene, toluene, ethylbenzene and xylene compounds by Dechloromonas strain RCB. *Appl Environ Microbiol.* **71**, pp.8649-8655.

Childs, C.W. 1992. Ferrihydrite: A review of structure, properties and occurrence in relation to soils. *Zeitschrift für Pflanzenernährung und Bodenkunde.* **155**(5), pp.441-448.

Chou, L. and Garrels, R.M. 1989. Comparative Study of the Kinetics and Mechanisms of Dissolution of Carbonate Minerals. *Chemical Geology* **78**, pp.269-282.

Christensen, H., Kjeldsen, P., H, A., G, H., P, N., P, B. and P, H. 1994. Attenuation of landfill leachate pollutants in aquifers. *Crit Rev Environ Sci Technol.* **24**, pp.119-202.

Christensen, J.S. and Elton, J. 1996. Soil and Groundwater Pollution from BTEX. *Groundwater Pollution Primer.* [Online]. Available from: <http://www.webapps.cee.vt.edu/ewr/environmental/teach/gwprimer/btex/btex.html>

Christensen, T.H., Bjerg, P.L., Banwart, S.A., Jakobsen, R., Heron, G. and Albrechtsen, H.-J. 2000. Characterization of redox conditions in groundwater contaminant plumes. *Journal of Contaminant Hydrology.* **45**(3–4), pp.165-241.

Chuan, M., Shu, G. and Liu, J. 1996. Solubility of heavy metals in a contaminated soil: Effects of redox potential and pH. *Water Air Soil Pollution.* **90**, pp.543 - 556.

Coates, J., Chakraborty, R., Lack, J., O'Connor, S., Cole, K.A., Bender, K.S. and Achenbach, L.A. 2001. Anaerobic benzene oxidation coupled to nitrate reduction in pure culture by two strains of *Dechloromonas*. *Nature*. **411**, pp.1039-1043.

Coates, J.D., Anderson, R.T. and Lovley, D.R. 1996. Oxidation of polycyclic aromatic hydrocarbons under sulphate-reducing conditions. *Appl Environ Microbiol*. **62**, pp.1099-1101.

Collins, Y.E. and Stotzky, G. 1992. Heavy metals alter the electrokinetic properties of bacteria, yeasts, and clay minerals. *Applied and Environmental Microbiology*. **58**(5), pp.1592-1600.

Cornell, R. and Schwertmann, U. 1996. *The Iron Oxides - Structure, Properties, Reactions, Occurrences and Uses*. [Online]. Weinham: VCH.

Cornell, R.M. and Schwertmann, U. 2003. *The iron oxides: Structure, properties, reactions, occurrences and uses*. [Online]. 2nd ed. WILEY-VCH Verlag GmbH & Co.

Cornell, R.M.a.S., U. 1996. *The Iron Oxides - Structure, Properties, Reactions, Occurrences and Uses*. [Online]. Weinham: VCH.

Craig, H. 1957. Isotopic standards for carbon and oxygen and correction factors for mass spectrometric analysis of carbon dioxide. *Geochim. Cosmochim. Acta*. **12**, pp.133-149.

Crowder, M.J. and Hand, D.J. 1990. *Analysis of Repeated Measures*. Taylor & Francis.

Day, M., Aravena, R., Hunkerler, D. and Gulliver, T. 2002. Application of carbon isotopes to document biodegradation of tert-butyl alcohol under field conditions. . *Contam. Soil Sediment Water*. pp.88-92.

De Burca, R., Morgan, H., Jefferies, J. and Earl, N. 2009. *Soil Guideline Values for Toluene in Soil*. Bristol: Environment Agency.

Demeestere, K., Dewulf, J., De Witte, B. and Van Langenhove, H. 2007. Sample preparation for the analysis of volatile organic compounds in air and water matrices. *Journal of Chromatography A*. **1153**(1–2), pp.130-144.

Dempster, H.S., Lollar, B.S. and Feenstr, S. 1997. Tracing organic contaminants in groundwater: A new methodology using compound-specific isotopic analysis. *Environmental Science and Technology*. **31**, no. **11**, pp.3193-3197.

Diggle, P. 2002. *Analysis of Longitudinal Data*. OUP Oxford.

Dollhopf, M.E., Neelson, K.H., Simon, D.M. and G.W., L.I. 2000. Kinetics of Fe (III) and Mn (IV) reduction by the Black Sea strain of *Shewanella putrefaciens* using in situ solid state voltametric Au / Hg electrodes. *Mar. Chem.* **70**, pp.171-180.

Doncaster, C.P. and Davey, A.J.H. 2007. *Analysis of Variance and Covariance: How to Choose and Construct Models for the Life Sciences*. Cambridge University Press.

Dragun, J. 1998. *The Soil Chemistry of Hazardous Materials*. 2nd Edition ed. Amherst, MA.: Amherst Scientific Publisher.

Driese, S.G., Ludvigson, G.A., Roberts, J.A., Fowler, D.A., González, L.A., Jon Jay, S., M., V., Vulava, M. and McKay, L.D. 2010. Micromorphology and Stable-Isotope Geochemistry of Historical Pedogenic Siderite Formed in PAH-Contaminated Alluvial Clay Soils, Tennessee, U.S.A. *Journal of Sedimentary Research*. **80**, pp.943-954.

Dromgoogle, E.L. and Walter, L.M. 1990. Inhibition of Calcite Growth Rates by Mn²⁺ in CaCl₂ Solutions at 10, 25, and 50°C. *Geochimica Et Cosmochimica Acta* **54**, pp.2991-3000.

Edwards, E.A. and Grbic-Galic, D. 1992. Complete mineralisation of benzene by aquifer microorganisms under strictly anaerobic conditions. *Appl Environ Microbiol.* **58**, pp.2663-2666.

Ehrlich, H.L. 1998. Geomicrobiology: its significance for geology. *Earth-Science Reviews*. **45**, pp.45-60.

Ellis, L.B.M. 1998. The University of Minnesota Biocatalysis/Biodegradation Database: Specialised Metabolism for Functional Geomics. *Nucl. Acids Res.* **27**, pp.373-376.

Elshahed, M., Gieg, L., McInerney, M. and Suflita, J. 2001. Signature Metabolites attesting to the insitu attenuation of alkylbenzenes in anaerobic environments. *Environ Sci Technol.* **35**, pp.682-689.

Enander, R.T. 1995. *Hazardous Waste Tracking and Cost Accounting Practice*. Taylor & Francis.

Determination of major and trace elements in eight Argonne premium coal samples (ash and whole coal) by x-ray fluorescence spectrometry. 2003. [Online database]. U.S. Geological Survey.

Evans, P.J., Mang, D.T., Kim, K.S. and Young, L.Y. 1991. Anaerobic degradation of toluene by a denitrifying bacterium. *Appl Environ Microbiol.* **57**, pp.1139-1145.

Farhadian, M., Vachelard, C., Duchez, D. and Larroche, C. 2008. In situ bioremediation of monoaromatic pollutants in groundwater: A review. *Bioresource Technology.* **99**(13), pp.5296-5308.

Ferris, F., Phoenix, V., Fujita, Y. and R., S. 2003. Kinetics of calcite precipitation induced by ureolytic bacteria at 10 to 20°C in artificial groundwater. *Geochim. Cosmochim. Acta.* **67**(8), pp.1701–1710.

Field, J.A. 2002. Limits of anaerobic biodegradation. *Water Science Technology.* **45**(10), pp.9-18.

Foght, J. 2008. Anaerobic Biodegradation of Aromatic Hydrocarbons: Pathways and Prospects. *Journal of Molecular Microbiology and Biotechnology.* **15**, pp.93-120.

Förstner, U. 1993. Metal Speciation - General Concepts and Applications. *International Journal of Environmental Analytical Chemistry*. **51**(1-4), pp.5-23.

Fortin, D. and Langley, S. 2005. Formation and occurrence of biogenic iron-rich minerals. *Earth-Science Reviews*. **72**(1-2), pp.1-19.

Fries, M., Zhou, J., Chee-Sanford, J. and J, T. 1994. Isolation, characterisation and distribution of denitrifying toluene degraders from a variety of habitats. *Appl Environ Microbiol*. **60**, pp.2802-2810.

Fritz, P., Reardon, E., Barker, J., Brown, R., Cherry, J., Killey, R. and McNaughton, D. 1978. The carbon isotope geochemistry of a small groundwater system in northeast Ontario *Water Resour. Res.* . **14**, pp.1059-1067.

Fry, B., and Sherr, E.B. 1984. Change in ^{13}C measurements as indicators of carbon flow in marine and freshwater ecosystems. *Contrib. Mar. Sci.* . **27**, pp.13-47.

Gavrilescu, M. 2010. Environmental Biotechnology: Achievements, Opportunities and Challenges. *Dynamic Biochemistry, Process Biotechnology and Molecular Biology*. **4**(1), pp.1-36.

George, I., Stenuit, B., Agathos, S. 2010. Application of Metagenomics to Bioremediation. In: Marco, D. ed. *Metagenomics: Theory, Methods and Applications*. [Online]. Horizon Scientific.

Gieg, L.M., Davidova, I.A., Duncan, K.E. and Suflita, J.M. 2010. Methanogenesis, sulfate reduction and crude oil biodegradation in hot Alaskan oilfields. *Environmental Microbiology*. **12**(11), pp.3074-3086.

Gliner, J.A., Morgan, G.A. and Leech, N.L. 2009. *Research Methods in Applied Settings: An Integrated Approach to Design and Analysis, Second Edition*. Taylor & Francis.

Gogoi, B.K., Dutta, N.N. and Krishnamohn, T.R. 2003. A case study of bioremediation of petroleum hydrocarbon contaminated soil at a crude oil spill site. *Advances in Environmental Research*. **7**, pp.767-782.

Goldsmith, J.R. 1990. Phase relations of rhombohedral carbonates. In: Reeder, R.J. ed. *Carbonates: Mineralogy and Chemistry*. [Online]. 2nd printing ed. Reviews in Mineralogical Society of America, pp.49-76.

Goudie, A.S. 1996. Organic agency in calcrete development', *Journal of Arid Environments*. **32**. pp. 103-110.

Gough, M.A. and Rowland, S.J. 1990. Characterisation of unresolved complex mixtures of hydrocarbons in petroleum. . *Nature*. **344**, pp.648-650

Grbic-Galic, D. and Vogel, T.M. 1987. Transformation of toluene and benzene mixed methanogenic cultures. *Appl Environ Microbiol*. **53**, pp.254-260.

Gueorguieva, R. and Krystal, J.H. 2004. Move over ANOVA: progress in analyzing repeated-measures data and its reflection in papers published in the Archives of General Psychiatry. *Arch Gen Psychiatry*. **61**(3), pp.310-317.

Guimarães, B.C.M., Arends, J.B.A., van der Ha, D., Van de Wiele, T., Boon, N. and Verstraete, W. 2010. Microbial services and their management: Recent progresses in soil bioremediation technology. *Applied Soil Ecology*. **46**(2), pp.157-167.

Hammel, J., Papendick, R. and Campbell, G. 1981. Fallow tillage effects on evaporation and seedzone water content in a dry summer climate. *Soil Science Society of America Journal*. **45**(6), pp.1016-1022.

Hammes, F. and Verstraete, W. 2002. Key roles of Ph and calcium metabolism in microbial carbonate precipitation. *Rev. Environ. Sci. Biotechnol*. **1**, pp.3-7.

Haner, A., P, H. and Zeyer, J. 1995. Degradation of p-xylene by a denitrifying enrichment culture. *Appl Environ Microbiol*. **61**, pp.3185-3188.

Hansel, C.M., Benner, S.G., Neiss, J., Dohnalkova, A., Kukkadapur, R.K. and Fendorf, S. 2003. Secondary mineralisation pathways induced by dissimilatory iron reduction of ferrihydrite under advective flow. *Geochim. Cosmochim. Acta.* **67**, pp.2977-2992.

Harrington, R.R., Poulson, J.I., Drever, P.J.S. and E.F., C.a. 1999. Carbon isotope systematics of monoaromatic hydrocarbons: Vaporization and adsorption experiments. *Organic Geochemistry.* **30, no. 8A** pp.765-775.

Harwood, C.S., Burchhardt, G., Herrmann, H. and Fuchs, G. 1999. Anaerobic metabolism of aromatic compounds via the benzoyl-CoA pathway. *FEMS Microbiol Ecol.* **22**, pp.439-458.

Hatzinger, P.B. and Alexander, M. 1995. Effect of aging of chemicals in soil on their biodegradability and extractability. *Environ Sci. Technol.* **29**, pp.537-545

Heath, J.S., Koblis, K. and Sager, S.L. 1993. Review of chemical, physical, and toxicologic properties of components of total petroleum hydrocarbons. *Journal of Soil Contamination.* **2(1)**, pp.1-25.

Helgeson, H.C., Murphy, W.M. and Aagaard, P. 1984. Thermodynamic and kinetic constraints on reaction rates among minerals and aqueous solutions. II. Rate constants, effective surface area, and the hydrolysis of feldspar. *Geochim. Cosmochim. Acta.* **48**, pp.2405-2432.

Henning, M. 2004. In situ measurement of soil pH. *Journal of Archaeological Science.* **31**, pp.1373-1381.

Hering, J.G.a.S., W. 1990. Oxidative and reductive dissolution of minerals. [Online]. Mineralogical Society of America, pp.427-465.

Hershberger, S.L. and Moskowitz, D.S. 2013. *Modeling Intraindividual Variability With Repeated Measures Data: Methods and Applications.* Taylor & Francis.

Hess, A., Zards, B., Hahn, D., Haner, A., Stax, D., Hohener, P. and Zeyer, J. 1997. In situ analysis of denitrifying toluene- and m-xylene-degrading bacteria in a diesel fuel-contaminated laboratory aquifer column. *Appl Environ Microbiol.* **63**(2136-2141).

Hewitt, A.D. 1998. Comparison of Sample Preparation Methods for the Analysis of Volatile Organic Compounds in Soil Samples: Solvent Extraction vs Vapor Partitioning. *Environmental Science & Technology.* **32**(1), pp.143-149.

Design and Analysis of Experiments: Introduction to Experimental Design. 2008. [Database]. John Wiley and Sons.

Ho, Y., Jackson, M., Yang, Y., Mueller, J.G. and H., P.P. 2000. Characterization of fluoranthene- and pyrene-degrading bacteria isolated from PAH-contaminated soils and sediments and comparison of several *Sphingomonas* spp. *Journal of Industrial Microbiology and Biotechnology.* **24**, pp. 100-112.

Hochella, M.F., Jr. and Banfield, J.F. 1995. Chemical weathering of silicates in nature: A microscopic perspective with theoretical considerations In: White, A.F. and Brantley, S.L. eds. *Chemical Weathering Rates of Silicate Minerals, Reviews in Mineralogy.* [Online]. Mineralogical Society of America, pp.353-406.

Houghton, S.L. and Hall, S. 2005. Simultaneous High Throughput and Quantitative Analysis of MTBE and BTEX by P&T-GCMS Using a Precept Autosampler *Mineralogical Magazine.* **69**(5), pp.677-686.

Howitt, D. and Cramer, D. 2003. *First Steps In Research and Statistics: A Practical Workbook for Psychology Students.* Taylor & Francis.

Huesemann, M., Hausmann, T. and Fortman, T. 2004. Does bioavailability limit biodegradation? a comparison of hydrocarbon biodegradation and desorption rates in aged soils. *Biodegradation* **15**, pp.261-274.

- Huesemann, M.H. 1995. Predictive model for estimating the extent of petroleum hydrocarbon biodegradation in contaminated soils. *Environ. Sci. Technol.* **29**, pp.7-18
- Huijgen, W.J.J. 2007. *Carbon dioxide sequestration by mineral carbonation*. thesis, Energy research Centre of the Netherlands.
- Huitema, B. 2011. *The Analysis of Covariance and Alternatives: Statistical Methods for Experiments, Quasi-Experiments, and Single-Case Studies*. Wiley.
- Hunkeler, D., Andersen, N., Aravena, R., Bernasconi, M. and Butler, B.J. 2001. Hydrogen and carbon isotope fractionation during aerobic biodegradation of benzene. *Environ Sci Technol* **35**, pp.3462-3467.
- Hunkeler, D. and Aravena, R. 2000. Determination of Compound-Specific Carbon Isotope Ratios of Chlorinated Methanes, Ethanes, and Ethenes in Aqueous Samples. *Environmental Science & Technology*. **34**(13), pp.2839-2844.
- Islam, M.A. and Chowdhury, R.I. 2017. *Analysis of Repeated Measures Data*. Springer Singapore.
- ISO. 1993. *Determination of dry matter and water content on a mass basis: Gravimetric method*.
- Jahn, M., Haderlein, S. and Meckenstock, R.U. 2005. Anaerobic degradation of benzene, toluene, ethylbenzene, and o-xylene in sediment-free iron-reducing enrichment cultures. *Appl Environ Microbiol.* **71**, pp.3355-3358.
- Jin, Y., Streck, T. and Jury, W.A. 1994. Transport and biodegradation of toluene in unsaturated soil. *Journal of Contaminant Hydrology.* **17**(2), pp.111-127.
- Jochman, M.A., Yuan, X. and Schmidt, T.C. 2007. Determination of volatile organic hydrocarbons in water samples by solid-phase dynamic extraction. *Anal. Bioanal. Chem.* **387**(6), pp.2163-2174.

Johnsen, A.R., Winding, A., Karlson, U. and Roslev, P. 2002. Linking of microorganisms to phenanthrene metabolism in soil by analysis of ¹³C-labelled cell-lipids. *Applied Environmental Microbiology*. **68**, pp.6106-6113.

Johnson, S.J., Woolhouse, K.J., Prommer, H., Barry, D.A. and Christofi, N. 2003. Contribution of anaerobic microbial activity to natural attenuation of benzene in groundwater. *Engineering Geology*. **70**, pp.343-349.

Judd, C.M., McClelland, G.H. and Ryan, C.S. 2011. *Data Analysis: A Model Comparison Approach, Second Edition*. Taylor & Francis.

Kabata-Pendias, A., and Pendias, H. 1992. *Trace elements in soils and plants*. 2nd ed. Boca Raton, FL: CRC Press.

Kao, C.M., Chien, H.Y., Surampalli, R.Y., Chien, C.C. and Chen, C.Y. 2010. Assessing of Natural Attenuation and Intrinsic Bioremediation Rates at a Petroleum-Hydrocarbon Spill Site: Laboratory and Field Studies. *Journal of Environmental Engineering*.

Kappler, A., Newman, D.K. 2004. Formation of Fe (III)-minerals by Fe (II)-oxidising photoautotrophic bacteria. *Geochim. Cosmochim. Acta*. **68**, pp.1217-1226.

Kasai, Y., Kodama, Y., Takahata, Y., Hoaki, T. and Watanabe, K. 2007. Degradative capacities and bioaugmentation potential of an anaerobic benzene-degrading bacterium strain DN11. *Environ Sci Technol*. **41**, pp.6222-6227.

Kasai, Y., Takahata, Y., Manefield, M. and Watanabe, K. 2006. RNA -based stable isotope probing and isolation of anaerobic benzene-degrading bacteria from gasoline-contaminated groundwater *Appl Environ Microbiol*. **72**, pp.3586-3592.

Kazumi, J., Caldwell, M.E., M, S.J., Lovley, D.R. and Young, L.Y. 1997. Anaerobic degradation of benzene in diverse anoxic environments. *Environ Sci Technol*. **31**, pp.813-818.

Kermanshahi pour, A., Karamanev, D. and Margaritis, A. 2005. Biodegradation of petroleum hydrocarbons in an immobilised cell airlift bioreactor. *Water Research*. **39**(15), pp.3704-3714.

Kielhorn, J., Melber, C., Wahnschaffe, U., Aitio, A., Mangelsdorf, I. 2000. Vinyl chloride: still a cause for concern. *Environmental health perspectives*. **108**, pp.579-588.

Kleinstauber, S., Schleinitz, K., Breitfeld, J., Harms, H., Richnow, H. and Vogt, C. 2008. Molecular characterisation of bacterial communities mineralizing benzene under sulphate-reducing conditions. *FEMS Microbiol Ecol.* (66), pp.143-157.

Kolb, B. and Ettre, L.S. 2006. *Static Headspace-Gas Chromatography: Theory and Practice*. Wiley.

Konhauser, K. 2007. *Introduction to Geomicrobiology*. [Online]. Oxford: Blackwell Science Ltd.

Konhauser, K.O. 1998. Diversity of bacterial iron mineralisation. *Earth Science Reviews* **43**(), pp.91-121.

Kostka, J.E., et al. 2002. Growth of Fe (III)-Reducing Bacteria on Clay Minerals as the Sole Electron Acceptor and Comparison of Growth Yields on a Variety of Oxidised Forms. *Appl. Envir. Microbiol.* **68**(12), pp.6256-6262.

Kostka, J.E. and Nealson, K.H. 1995. Dissolution and reduction of magnetite by Bacteria. *Environ. Sci. Technol.* **29**, pp.2535-2540.

Kot, A. and Namiesnik, J. 2000. The role of speciation in analytical chemistry. *Trends in analytical chemistry*. **19**.

Kraemer, S.M. 2004. Iron oxide dissolution and solubility in the presence of siderophores. *Aquatic Sciences*. **66**(1), pp.3-18.

Krauth, J. 2000. *Experimental Design: A Handbook and Dictionary for Medical and Behavioral Research*. Elsevier.

Kube, M., Heider, J., Amann, J., Hufnagel, P., Kuhner, S. and Beck, A. 2004. Genes involved in the anaerobic degradation of toluene in a denitrifying bacterium, strain EbN1. *Arch Microbiol.* **181**, pp.182-194.

Kuhn, E.P., Coldberg, P.J., Schnoor, J., Wanner, O., Zehnder, A.J.B. and Schwarzenbach, R.P. 1985. Microbial transformations of substituted benzenes during infiltration of river water to groundwater: laboratory column studies. *Environ Sci Technol* **19**, pp.961-968.

Kuhn, E.P., Coldberg, P J, Schnoor, J L, Wanner, O, Zehnder, A J B & Schwarzenbach, R P. 1985. Microbial transformations of substituted benzenes during infiltration of river water to groundwater: laboratory column studies. *Environ Sci Technol* **19**, pp.961-968.

Kuhn, E.P., Zeyer, J., Eicher, P. and P, S.R. 1988. Anaerobic degradation of alkylbenzenes in denitrifying laboratory aquifer columns. *Appl Environ Microbiol.* **54**, pp.490-496.

Kunapuli, U., Leuders, T. and Meckenstock, R.U. 2007. The use of stable isotope probing to identify key iron-reducing microorganisms involved in anaerobic benzene degradation. *ISME.* **1**(643-653).

Lackner, K.S. 2002. Carbonate chemistry for sequestering fossil carbon. *Annual Reviews, Energy and the Environment.* **27**, pp.193-232.

Lackner, K.S., Wendt, C.H., Butt, D.P., Joyce, E.L., Jr. and Sharp, D.H. 1995. Carbon dioxide disposal in carbonate minerals. *Energy.* **20**, pp.1153-1170.

Lagenoff, A., Zehnder, A. and Schraa, G. 1996. Behaviour of toluene, benzene, naphthalene under anaerobic conditions in sediment columns. *Biodegradation.* **7**, pp.267-274.

Langmuir, D. 1997. *Aqueous Environmental Geochemistry.* Prentice Hall.

Langwaldt, J.H. and Puhakka, J.A. 2000. On-site biological remediation of contaminated groundwater: a review *Environmental Pollution*. **107**(2), pp.187-197.

Larsen, O. and Postma, D. 2001. Kinetics of reductive bulk dissolution of lepidocrocite, ferrihydrite and goethite. *Geochim. Cosmochim. Acta* **65**, pp.1367-1379.

Lasat, M.M. 2002. Phytoextraction of toxic metals – a review of biological mechanisms

J. Environ. Qual. **31**, pp.109-120.

Lawrence, S.J. 2006. *Description, Properties, and Degradation of Selected Volatile Organic Compounds Detected in Ground Water - A Review of Selected Literature*. US Department of the Interior.

Leahy, J.G. and Colwell, R.R. 1990. Microbial degradation of hydrocarbons in the environment. *Microbiol. Rev.* **54**, pp.305-315

Lee, E.Y., Youn, S.J., Kyung, S.C. and R., H.W. 2002. Degradation Characteristics of Toluene, Benzene, Ethyl benzene, and Xylene by *Stenotrophomonas maltophilia* T3-c. *J. Air & Waste Manage. Assoc.* **52**, pp.400-406.

Leik, R.K. 1997. *Experimental Design and the Analysis of Variance*. SAGE Publications.

Leutwein, C. and J. Heider, J. 2001. Succinyl-CoA:(R)-Benzylsuccinate CoA-Transferase: an Enzyme of the Anaerobic Toluene Catabolic Pathway in Denitrifying Bacteria. *J.Bacteriol.* **183**, pp.4288-4295.

Liu, C., Zachara, J.M., Gorby, Y.A., Szecsody, J.E. and Brown, C.F. 2001. Microbial reduction of Fe(III) and sorption/precipitation of Fe(II) on *Shewanella putrefaciens* strain CN32. *Environ Sci Technol.* **35**(7), pp.1385-1393.

Liu, H. 1995. *Model Selection in Repeated Measures Random Effects Models*. University of California, Los Angeles.

Lloyd, J.R., Sole, V.A., Van Praagh, C.V.G. and Lovley, D.R. 2000. Direct and Fe(II)-mediated reduction of technetium by Fe(III)-reducing bacteria. *Applied and Environmental Microbiology*. **66**(9), pp.3743–3749.

Loffler, F.E., Edwards, E.A. 2006. Harnessing microbial activities for environmental clean up. *Current Opinion in Biotechnology*. **17**, pp.274-284.

Lomax, R.G. and Hahs-Vaughn, D.L. 2013. *Statistical Concepts: A Second Course*. Taylor & Francis.

Lonergan, D.J., Jenter, H.L., Coates, J.D., Phillips, E.J., Schmidt, T.M. and Lovley, D.R. 1996. Phylogenetic analysis of dissimilatory Fe(III)-reducing bacteria. *Journal of Bacteriology*. **178**(8), pp.2402-2408.

Lovley, D.R. 1991. Dissimilatory Fe(III) and Mn(IV) reduction. *Microbiological Reviews*. **55**(2), pp.259-287.

Lovley, D.R. 1997a. Microbial Fe (III) reduction in subsurface environments. *FEMS Microbiol Ecol*. **20**, pp.305-313.

Lovley, D.R. 1997b. Potential for anaerobic bioremediation of BTEX in petroleum-contaminated aquiferes. *Journal of Industrial Microbiology and Biotechnology*. **18**, pp.75-81.

Lovley, D.R. 2000. Reduction of iron and humics in subsurface environments. *Subsurface microbiology and biogeochemistry*. [Online]. John Wiley and Sons, pp.193-217.

Lovley, D.R., Baedecker, M J, Lonergan, D J, Cozzarelli, M, Phillips E J P & Siegel, D. 1989. Oxidation of aromatic contaminants coupled to microbial iron reduction. *Nature*. **339**, pp.297-299.

Lovley, D.R., D, C.J., Woodward, J.C. and J, P.E. 1995. Benzene oxidation coupled to sulphate reduction. *Appl Environ Microbiol*. **61**, pp.953-958.

Lovley, D.R. and Lonergan, D.J. 1990. Anaerobic Oxidation of Toluene, Phenol, and p-Cresol by the Dissimilatory Iron-Reducing Organism, GS-15. *Appl. Environ. Microbiol.* **56**(6), pp.1858-1864.

Lu, J.C., Li, Z.T., Hussain, K. and Yang, G.K. 2011. Bioremediation: The New Directions of Oil Spill Cleanup. *Middle-East Journal of Scientific Research.* **7**(5), pp.738-740.

Lueders, T. 2017. The ecology of anaerobic degraders of BTEX hydrocarbons in aquifers. *FEMS Microbiology Ecology.* **93**(1), pfiw220.

Luu, Y.S. and Ramsay, J.A. 2003. Review: Microbial mechanisms of accessing insoluble Fe (III) as an energy source. *World J. Microbiol. Biotechnol.* **19**, pp.215-225.

Madden, A.S. and Hochella, M.F. 2005. A test of geochemical reactivity as a function of mineral size: manganese oxidation promoted by hematite nanoparticles. *Geochim. Cosmochim. Acta.* **69**, pp.389-398.

Madden, A.S., Hochella, M.F. and Luxton, T.P. 2006. Insights for size-dependent reactivity of hematite nanomineral surfaces through Cu²⁺ sorption. *Geochim. Cosmochim. Acta.* **70**(4095-4104).

Mancini, S., Ulrich, A., Lacrampe-Coulome, G., Sleep, B., Edwards, E. and Lollar, B. 2003. Carbon and hydrogen isotopic fractionation during anaerobic biodegradation of benzene. *Appl Environ Microbiol.* **159**, pp.336-344.

Manning, D.A.C. 2008. Biological enhancement of soil carbonate precipitation: passive removal of atmospheric CO₂. *Mineralogical Magazine.* **72**, pp.639-649.

Mannweiler, U. 1966. Vergleich dreier methoden zur bestimmung spezifischer oberflächen von poulvern *Chimia.* **20**, pp.363-364.

Margesin, R., Walder, G. and Schinner, F. 2003. Bioremediation Assessment of a BTEX-Contaminated Soil. *Acta Biotechnologica.* **23**(1), pp.29-36.

Marsh, C. and Elliott, J. 2008. *Exploring Data: An Introduction to Data Analysis for Social Scientists*. Wiley.

Mathura, A.K. and Majumder, C.B. 2010. Kinetics modelling of the biodegradation of benzene, toluene and phenol as single substrate and mixed substrate by using *Pseudomonas putida*. *Chem. Biochem. Eng. Q.* **24** (1), pp.101–109.

McCarty, P.L., Semprini, L. 1994. *Handbook of bioremediation*. FL: Lewis Publishers Boca Raton.

McCrea, J.M. 1950. On the Isotopic Chemistry of Carbonates and a Paleotemperature Scale. *The Journal of Chemical Physics*. **18**(6), pp.849-857.

Meckenstock, R.U. 1999. Fermentative toluene degradation in anaerobic defined syntrophic cocultures. *FEMS Microbiol Lett.* **177**, pp.67-73.

Meckenstock, R.U., Morasch, B., Kästner, M., Vieth, A. and Richnow, H.H. 2002. Assessment of Bacterial Degradation of Aromatic Hydrocarbons in the Environment by Analysis of Stable Carbon Isotope Fractionation. *Water, Air and Soil Pollution: Focus*. **2**(3), pp.141-152.

Meckenstock, R.U., Warthmann, R.J. and W, S. 2004. Inhibition of anaerobic microbial o-xylene degradation by toluene in sulfidogenic sediment columns and pure cultures. *FEMS Microbiol Ecol.* **47**, pp.381-386.

Megharaj, M., Ramakrishnan, B., Venkateswarlu, K., Sethunathan, N. and Naidu, R. 2011. Bioremediation approaches for organic pollutants: A critical perspective. *Environment International*. **37**(8), pp.1362-1375.

Mermut, A.R., Amundson, R. and Cerling, T.E. 2000. The use of stable isotopes in studying carbonate dynamics in soils. In: Lal, R., et al. eds. *Global Climate Change and Pedogenic Carbonates*. Washington, DC: Lewis Publishers, pp.65–85.

Mitchell, A.C. and Ferris, F.G. 2006. The influence of *Bacillus pasteurii* on the nucleation and growth of calcium carbonate. *Geomicrobiol. J.* **23**(3–4), pp.213–226.

Montgomery, D.C. 2006. *Design and Analysis of Experiments*. John Wiley & Sons.

Morasch, B., Schink, B., Tebbe, C.C. and R.U., M. 2004. Degradation of o-xylene and m-xylene by a novel sulphate-reducer belonging to the genus *Desulfotomaculum*. *Arch Microbiol.* **181**, pp.407-417.

Morgan, H., Jeffries, J., Waterfall, E. and Earl, N. 2009. *Soil Guideline Values for Benzene in Soil*. (Science Report SC050021/toluene SGV). Almondsbury, Bristol, United Kingdom: Environmental Agency, Bristol.

Mortimer, R.J., Galsworthy, M.J., Bottrell, S.H., Wilmot, L.E. and Newton, R.J. 2011. Experimental evidence for rapid biotic and abiotic reduction of Fe (III) at low temperatures in salt marsh sediments: a possible mechanism for formation of modern sedimentary siderite concretions. *Sedimentology.* **58**, pp.1514-1529.

Mortimer, R.J.G., Harris, S.J., Krom, M.D., Freitag, T.E., Prosser, J.I., Barnes, J., Anshutz, P., Hayes, P.J. and Davies, I.M. 2004. Anoxic Nitrification in Marine Sediments. *Marine Ecology - Progress Series.* **276**, pp.37-51.

Mos, Y. 2010. *Bioremediation of a Light NAPL (Toluene) Contaminated Soil under Different Environmental Conditions*. MSc Hydrology thesis, Universiteit Utrecht, The Netherlands.

Murphy, W.M. 1989. Dislocations and feldspar dissolution *Eur. J. Mineral.* **1**, pp.315-326.

Musat, F. and Widdel, F. 2008. Anaerobic degradation of benzene by a marine sulphate-reducing enrichment culture, and cell hybridization of the dominant phylotype. *Environ Microbiol.* **10**, pp.10-19.

Myers, J.L., Well, A.D. and Lorch, R.F. 2013. *Research Design and Statistical Analysis: Third Edition*. Taylor & Francis.

Navarro, G., Acevedo, R., Soto, A., Herane, M. 2008. Synthesis and characterisation of lepidocrocite and its potential applications in the adsorption of pollutant species. *Journal of Physics*. (Conference Series 134).

Nemec, A.F.L. and Branch, B.C.M.o.F.R. 1996. *Analysis of Repeated Measures and Time Series: An Introduction with Forestry Examples*. Province of British Columbia, Ministry of Forests Research Program.

Newton, R. and Bottrell, S. 2007. Stable isotopes of carbon and sulphur as indicators of environmental change: past and present. *Journal of the Geological Society*. **164**, pp.691-708.

Nordt, L.C., Wilding, L.P., Halmark, C.T. and Jacop, J.S. 1996. Stable carbon isotope composition of pedogenic carbonates and their use in studying pedogenesis. In: Boutton, T.W. and Yamasaki, S. eds. *Mass Spectrometry of Soils*. New York: Marcel Dekker, Inc., pp.133-154.

Nyer, E.K. and Duffin, M.E. 1997. The State of the Art of Bioremediation. *Ground Water Monitoring & Remediation*. **17**(2), pp.64-69.

Oana, S. and Deevey, E.S. 1960. Carbon 13 in lake waters, and its possible bearing on paleolimnology. *Am. J. Sci.* . **258A**, pp.253-272.

Oelkers, E.H. 2002. The surface areas of rocks and minerals. In: *Proceedings of the Arezzo Seminar on Fluid Geochemistry, Arezzo, August 29th-September 1st, 2000*, Pisa. Pacini editore, pp.18-30.

Oka, A.R., Phelps, C.D., McGuinness, L.M., Mumford, A., Young, L.Y. and Kerkhof, L.J. 2008. Identification of critical members in a sulfidogenic benzene-degrading consortium by DNA stable isotope probing. *Appl Environ Microbiol.* (74), pp.6476-6480.

Page, A.L., Miller, R.F. and Keeney, D.R. 1982. Methods of soil analysis. Part 2: Chemical and Microbiological Properties. *American Society of Agronomy, Soil Science Society of America (ASA — SSSA), Wisconsin*. pp.937-970.

Parkman, R.H., Charnock, J.M., Bryan, N.D., Livens, F.R. and Vaughan, D.J. 1999. Reactions of copper and cadmium ions in aqueous solution with goethite, lepidocrocite, mackinawaite and pyrite. *American Mineralogist*. **84**(1), pp.407-419.

Parkman, R.H., Charnock, J.M., Bryan, N.D., Livens, F.R., and Vaughan, D.J. 1999. Reactions of copper and cadmium ions in aqueous solution with goethite, lepidocrocite, mackinawite and pyrite. *American Mineralogist*. **84**(1), pp.407-419.

Parr, J.L., Claff, R.E., Kocurek, D.S. and Lowry, J.C. 1996. *Inter-laboratory study of analytical methods for petroleum hydrocarbons*. Arvada, Colorado Technical report, Quanterra Environmental Services.

Paul, E.A. 2007. *Soil Microbiology and Geochemistry*. [Online]. Elsevier Inc.

Pawellek F, V., J 1994. Carbon cycle in the upper Danube and its tributaries: $\delta^{13}\text{C}_{\text{DIC}}$ constraints. *Israel J Earth Sci* **43**, pp.187-194.

Pawliszyn, J. 1995. New directions in sample preparation for analysis of organic compounds. *TrAC Trends in Analytical Chemistry*. **14**(3), pp.113-122.

Pazos, F. 2004. MetaRouter: Bioinformatics for Bioremediation. *Nucl. Acids Res.* **33**, pp.588-592.

Perez-Guzman, L., Bogner, K.R. and Lower, B.H. 2012. Earth's Ferrous Wheel. *Nature Education Knowledge*. **3**(10), p32.

Phelps, C.D. and Young, L.Y. 1999. Anaerobic biodegradation of BTEX and gasoline in various aquatic sediments. *Biodegradation*. **10**, pp.15-25.

Pohl, H.R., Roney, N., Wilbur, S., Hansen, H. and DeRosa, C.T. 2003. Six interaction profiles for simple mixtures *Chemosphere*. **53**(2), pp.183-197.

Pokrovsky, O.S. and Golubev, S.V. 2009. Calcite, Dolomite and Magnesite Dissolution Kinetics in Aqueous Solutions at Acid to Circumneutral pH, 25 to 150°C and 1 to 55 Atm pCO₂: New Constraints on CO₂ Sequestration in Sedimentary Basins. *Chemical Geology* **265**, pp.20-32.

Pollard, S.J.T. and Herbert, S.M. 1998. Contaminated land regulation in the UK: The role of the Environment Agency (EA) and Scottish Environment Protection Agency. In: *Proceedings of Contaminated Soil Conference ConSoil'98, 7-21 May 1998, Edinburgh*. pp.33-42.

Pollock, J., Weber, K.A., Lack, J., Achenbach, L.A., Mormile, M.R. and Coates, J.D. 2007. Alkaline iron(III) reduction by a novel alkaliphilic, halotolerant, *Bacillus* sp. isolated from salt flat sediments of Soap Lake. *Appl. Microbiol. Biotechnol.* **7**, pp.927–934.

Poulton, S.W. and Canfield, D.E. 2005. Development of a sequential extraction procedure for iron: implications for iron partitioning in continentally derived particulates. *Chemical Geology*. **214**, pp.209-221.

Poulton, S.W., Krom, M.D. and Raiswell, R. 2004. A revised scheme for the reactivity of iron (oxyhydr)oxide minerals towards dissolved sulphide. *Geochimica et Cosmochimica Acta*. **68**, pp.3703-3715.

Quade, J., Cerling, T.E. and Bowman, J. 1989. Systematic variations in the carbon and oxygen isotopic composition of pedogenic carbonate along elevation transects in the southern Great Basin, United States. *Geol. Soc. Am. Bull.* **101**, pp.464-475.

Quinn, G.P. and Keough, M.J. 2002. *Experimental Design and Data Analysis for Biologists*. Cambridge University Press.

Rabus, R. and Widdel, F. 1995. Anaerobic degradation of ethylbenzene and other aromatic hydrocarbons by new denitrifying bacteria. *Arch Microbiol.* **163**, pp.96-103.

Railsback, L.B. 1999. Patterns in the compositions, properties, and geochemistry of carbonate minerals. *Carbonates and Evaporites*. **14**(1), p1.

Ramos, J.-L., Marqués, S., van Dillewijn, P., Espinosa-Urgel, M., Segura, A., Duque, E., Krell, T., Ramos-González, M.-I., Bursakov, S., Roca, A., Solano, J., Fernández, M., Niqui, J.L., Pizarro-Tobias, P. and Wittich, R.-M. 2011. Laboratory

research aimed at closing the gaps in microbial bioremediation. *Trends in Biotechnology*. **29**(12), pp.641-647.

Rao, C.R.M., Sahuquillo, A. and Sanchez, J.F.L. 2008. A review of the different methods applied in environmental geochemistry for single and sequential extraction of trace elements in soils and related materials. *Water Air Soil Poll.* **189**, pp.291-333.

Rauret, G. 1998. Extraction procedures for the determination of heavy metals in contaminated soil and sediment. *Talanta*. **46**, pp.449-455.

Raykov, T. and Marcoulides, G.A. 2012. *Basic Statistics: An Introduction with R*. Rowman & Littlefield Publishers.

Reeburgh, W.S. 1983. Rates of biogeochemical processes in anoxic sediments. *Annu. Rev. Earth Planet. Sci.* (11), pp.269-298.

Reeder, R.J. 1990. Crystal chemistry of the rhombohedral carbonates. Reviews in Mineralogy. In: Reeder, R.J. ed. *Carbonates: Mineralogy and Chemistry*. [Online]. 2nd printing ed. Mineralogical Society of America pp.1-47.

Reimens, C. and de Caritat, P. 1998. *Chemical elements in the environment: Factsheets for the Geochemist and Environmental Scientist*.

Reineke, V., Rullkotter, J., Smith, E.L. and Rowland, S.J. 2006. Toxicity and compositional analysis of aromatic hydrocarbon fractions of two pairs of undegraded and biodegraded crude oils from the Santa Maria (California) and Vienna basins. *Organic Geochemistry*. **37**(12), pp.1885-1899.

Reinhard, M., Shang, S., Kitanidis, P.K., Orwin, E., Hopkins, G. and LeBron, C. 1997. In situ BTEX biotransformation under enhanced nitrate- and sulphate-reducing conditions. *Environ Sci Technol*. **31**, pp.28-36.

Renard, F., Putnis, C.V., Montes-Hernandez, G. and King, H.E. 2017. Siderite dissolution coupled to iron oxyhydroxide precipitation in the presence of arsenic revealed by nanoscale imaging. *Chemical Geology*. **449**, pp.123-134.

Reporter. 1999. *An Appraisal of the Oil Spill that occurred at Bodington Hall on the 29th March 1999*. [Accessed December 2012]. Available from: <http://reporter.leeds.ac.uk/438/diesel.htm>

Riser-Roberts, E. 1998. *Remediation of Petroleum Contaminated Soils: Biological, Physical, and Chemical Processes*. CRC Press.

Ritchie, G., Still, K., Rossi, J., 3rd, Bekkedal, M., Bobb, A. and Arfsten, D. 2003. Biological and health effects of exposure to kerosene-based jet fuels and performance additives. *J Toxicol Environ Health B Crit Rev*. **6**(4), pp.357-451.

Roden, E.E. 2003. Fe (III) oxide reactivity toward biological versus chemical reduction. *Environ Sci Technol*. **37**, pp.1319-1324.

Romanov, V., Soong, Y., Carney, C., Rush, G.E., Nielsen, B. and O'Connor, W. 2015. Mineralization of Carbon Dioxide: A Literature Review. *ChemBioEng Reviews*. **2**(4), pp.231-256.

Romheld, V., and Marschner, H. 1986. Mobilisation of iron in the rhizosphere of different plant species. In: Tinker, B., Lauchli, A. ed. *Advances in Plant Nutrition, Volume 2*. [Online]. New York: Praeger Scientific, pp.155-204.

Rooney-Varga, J., Anderson, R., Fraga, J., Ringelberg, D. and Lovley, D.R. 1999. Microbial communities associated with anaerobic benzene degradation in a petroleum-contaminated aquifer. *Appl Environ Microbiol*. **65**, pp.3056-3063.

Ryan, T.P. 2006. *Modern Experimental Design*. Wiley.

Sahuquillo, A., Lopez-Sanchez, J.F., Rubio, R., Rauret, G., Thomas, R.P., Davidson, C.M. and Ure, A.M. 1999. Use of a certified reference material for extractable trace

metals to assess sources of uncertainty in the BCR threestage sequential extraction procedure. *Anal. Chim. Acta.* **382**(3), pp.317–327.

Sawyer, C.C., Parking, G.F. and McCarty, P L. 1994. *Chemistry for environmental engineering*. 4th Edition ed. New York: McGraw-Hill.

Scherr, K., Aichberger, H., Braun, R. and Loibner, A.P. 2007. Influence of soil fractions on microbial degradation behaviour of mineral hydrocarbon. *European Journal of Soil Biology.* **43**, pp.341-350.

Schlesinger, W.H. 1982. Carbon storage in the caliche of arid soils: A case study from Arizona. *Soil Sci.* **133**, pp.247-255.

Schmidt, T.C., Zwank, L., Elsner, M., Berg, M., Meckenstock, R.U. and Hardelein, S.B. 2004. Compound-specific stable isotope analysis of organic contaminants in natural environments: a critical review of the state of the art, prospects, and future challenges. *Anal. Bioanal. Chem.* **378**, pp.283-300.

Schultze-Lam, S., Fortin, D., Davis, B.S. and Beveridge, T.J. 1996. Mineralization of bacterial surfaces. *Chemical Geology.* **132**(1), pp.171-181.

Schwarzenbach, R.P. and Westall, J. 1981. Transport of nonpolar organic compounds from surface water to groundwater. Laboratory sorption studies. *Environmental Science & Technology.* **15**(11), pp.1360-1367.

Schwertmann, U. 1991. Solubility and dissolution of iron oxides. *Plant Soil.* **130**, pp.1-25.

Schwertmann, U., and Fitzpatrick, R.W. 1992. Iron Minerals in Surface Environments. In: Skinner, H.C.W.a.F., R.W. ed. *Biomineralisation Processes of Iron and Manganese*. [Online]. Catena, Cremlingen, pp.7-31.

Schwertmann, U., and Taylor, R.M. 1973. The in vitro transformation of soil lepidocrocite to goethite. *Pseudogley and gley Trans Comm V & VI Int Sci Soc.* **1971**, pp.45-54.

Schwertmann, U. and Cornell, U. 2000. *Iron oxides in the laboratory: Preparation and characterisation*. [Online]. Weinheim, Germany: Wiley-VCH.

Schwertmann, U. and Fitzpatrick, R.W. 1992. *Iron Minerals in Surface Environments*. Skinner, H.C.W. and Fitzpatrick, R.W. Biomineralisation Processes of Iron and Manganese. Catena, Cremlingen. pp.7-31.

Schwertmann, U. and Taylor, R.M. 1979. Natural and synthetic poorly crystallized lepidocrocite. *Clay Miner.* **14**, pp.285-293.

Schwertmann, U. and Taylor, R.M. 1989. *Iron oxides*. [Online]. Madison, Wisconsin: Soil Sci. Soc.

Schwertmann, U., Taylor, R.M. 1989. Iron oxides. Minerals in Soil Environments. [Online].

Semple, K.T., Doick, K.J., Jones, K.C., Burauel, P., Craven, A. and Harms, H. 2004. Defining bioavailability and bioaccessibility of contaminated soil and sediment is complicated. *Environ Sci Technol.* **38**(12), pp.228A-231A.

Semple, K.T., Morriss, W.J. and Paton, G.I. 2003. Bioavailability of hydrophobic organic contaminants in soils; fundamental concepts and techniques for analysis. *European Journal of Soil Biology.* **54**, pp.809-818.

Shesky, S. 1997. Vol. 2004 Niton Corporation. In: *International Symposium of Field Screening Methods for Hazardous Wastes and Toxic Chemicals*.

Shukla, P.K., Singh, N.K. and Sharma, S. 2010. Bioremediation: Developments, Current Practices and Perspectives. *Genetic Engineering and Biotechnology Journal.* **GEBJ-3**.

Sikkema, J., De Bont, J.A.M. and Poolman, B. 1995. Mechanisms of membrane toxicity of hydrocarbons. *Microbiological Reviews.* **59**(2), pp.201-222.

Sims, R.C. 1990. Soil remediation techniques at uncontrolled hazardous waste sites: a critical review. *Journal of the air and waste management association*. **40**, pp.704-732

Singer, J.D. and Willett, J.B. 2003. *Applied longitudinal data analysis: modeling change and event occurrence*. New York: Wiley.

Singh, R.L. 2016. *Principles and Applications of Environmental Biotechnology for a Sustainable Future*. Springer Singapore.

Song, X.K. and Song, P.X.K. 2007. *Correlated Data Analysis: Modeling, Analytics, and Applications*. Springer.

Sorensen, J. and Thorling, L. 1991. Stimulation by lepidocrocite (γ -FeOOH) of Fe (II)-dependent nitrite reduction. *Geochim. Cosmochim. Acta*. **67**, pp.4223-4230.

Søvik, A.K., Alfnes, E., Breedveld, G.D., French, H.K., Pedersen, T.S. and Aagaard, P. 2002. Transport and Degradation of Toluene and o-Xylene in an Unsaturated Soil with Dipping Sedimentary Layers A.K. Søvik, present address: Jordforsk (Norwegian Centre for Soil and Environmental Research), Frederik A. Dahls vei 20, 1432 Ås, Norway. *Journal of Environmental Quality*. **31**, pp.1809-1823.

Spence, K.H. 2005. *The Biodegradation of MTBE and Fuel Hydrocarbons in the Chalk Aquifer*. PhD thesis, University of Leeds.

Spence, M.J., Bottrell, S.H., Thornton, S.F., Richnow, H.H. and Spence, K.H. 2005. Hydrochemical and Isotopic Effects associated with Petroleum Fuel Biodegradation Pathways in a Chalk Aquifer. *Journal of Contaminant Hydrology*. **79**, pp.67-88.

Stocks-Fischer, S., Galinat, J.K. and Bang, S.S. 1999. Microbiological precipitation of CaCO. *Soil Biol. Biochem*. **31**, pp.1563-1571.

Stucki, J.W., Lee, K., Goodman, B.A. and Kostka, J.E. 2007. Effects of in situ biostimulation on iron mineral speciation in a sub-surface soil. *Geochim. Cosmochim. Acta*. **71**, pp.835-843.

Sulzberger, B., Suter, D., Siffert, C., Banwart, S., and Stumm, W. 1989. Dissolution of Fe (III)(hydr)oxides in natural waters; laboratory assessment on the kinetics controlled by surface coordination. *Marine Chemistry*. **28**, pp.127-144.

Sun, F. and Zhou, Q. 2007. Metal accumulation in the polychaete *Hediste japonica* with emphasis on interaction between heavy metals and petroleum hydrocarbons. *Environ Pollut* **149**, pp.92–98.

Sweeton, F.H. and Baes, C.F. 1970. The solubility of magnetite and hydrolysis of ferrous ion in aqueous solutions at elevated temperatures. *J.Chem.Thermodyn.* **2**, pp.479-500.

Tango, T. 2017. *Repeated Measures Design with Generalized Linear Mixed Models for Randomized Controlled Trials*. Taylor & Francis Incorporated.

Taris, T. 2000. *A primer in longitudinal data analysis*. London: Sage Publications.

Tessier, A., Campbell, P.G.C. and Bisson, M. 1979. Sequential extraction procedure for the speciation of particulate trace metals. *Analytical Chemistry*. **51**(7), pp.844-851.

Tessier, A., Carignan, R. and Belzile, N. 1994. Processes occurring at the sediment-water interface: emphasis on trace elements. In: Buffle, J. and De Vitre, R.R. eds. *Chemical and Biological Regulation of Aquatic Processes*. Chelsea: Lewis Publishers, pp. 137–175.

Tessier, A., Fortin, D., Belzile, N., DeVitre, R.R. and Leppard, G.G. 1996. Metal sorption to diagenetic iron and manganese oxyhydroxides and associated organic matter: Narrowing the gap between field and laboratory measurements. *Geochimica et Cosmochimica Acta*. **60**(3), pp.387-404.

Thamdrup, B. 2000. Bacterial manganese and iron reduction in aquatic sediments. *Adv Microb Ecol*. **16**, pp.41-84.

Tobler, N.B., Hofstetter, T.B., Straub, K.L., Fontana, D. and Scharzenbach, R.P. 2007. Iron-Mediated Microbial Oxidation and Abiotic Reduction of Organic Contaminants under Anoxic Conditions. *Environ. Sci. Technol.* (41), pp.7765-7772.

Tokalioglu, S., Kartal, S. and Birol, G. 2003. Application of a three-stage sequential extraction procedure for the determination of extractable metal contents in highway soils. *Chemistry*. **27**, pp.333-346.

Turner, A. and Olsen, Y.S. 2000. Chemical versus Enzymatic Digestion of Contaminated Estuarine Sediment: Relative Importance of Iron and Manganese Oxides in Controlling Trace Metal Bioavailability. *Estuarine, Coastal and Shelf Science*. **51**, pp.717-728.

Ulrich, A.C. 2004. *Characterisation of anaerobic benzene-degrading culture*. thesis, University of Toronto.

Ure, A.M. and Davidson, C.M. 2008. *Chemical Speciation in the Environment*. Wiley.

USEIA. 2014. *Annual energy outlook 2014 with projections to 2040*. Washington, DC: U.S. Energy Information Administration. Office of Integrated and International Energy Analysis.

USEPA. 1998. *Carcinogenic Effects of Benzene: An Update*. US Environmental Protection Agency, National Centre for Environmental Assessment. Washington Office, Washington DC.

Edition of the Drinking Water Standards and Health Advisories 2006. Washington, D.C.:

Van Hamme, J., Singh, A. and Ward, O. 2003. Recent Advances in petroleum microbiology *Microbiol Mol Biol Rev.* (67), pp.503-549.

van Oosterhout, G.W. 1967. The transformation of γ -FeO(OH) to α -FeO(OH). *Journal of Inorganic and Nuclear Chemistry*. **29**, pp.1235-1238.

Verbeke, G. 1997. Linear Mixed Models for Longitudinal Data. *Linear Mixed Models in Practice: A SAS-Oriented Approach*. New York, NY: Springer New York, pp.63-153.

Verma, J.P. 2015. *Repeated Measures Design for Empirical Researchers*. Wiley.

Verrecchia, E.P., Dumont, J.L. and Rolko, K.E. 1990. Do fungi building limestones exist in semi-arid regions? *Naturwissenschaften*. **77**, pp.584-586.

Vieira, P.A., Vieira, R.B., de Franca, F.P., Cardoso, V.L. 2007. Biodegradation of effluent contaminated with diesel fuel and gasoline. *Journal of Hazardous Materials*. **140**(1-2), pp.52-59.

Vieth, A. and Wilkes, H. 2010. Stable Isotopes in Understanding Origin and Degradation Processes of Petroleum. In: Timmis, K.N. ed. *Handbook of Hydrocarbon and Lipid Microbiology*. Berlin, Heidelberg: Springer Berlin Heidelberg, pp.97-111.

Vodyanitskii, Y.N. 2008. Iron hydroxides in soils: A review of publications. *Soil Chemistry*. **11**, pp.1341-1352.

Vodyanitskii, Y.N. and Shoba, S.A. 2016. Ferrihydrite in soils. *Eurasian Soil Science*. **49**(7), pp.796-806.

Vogel, T.M. and Grbic-Galic. 1986. Incorporation of oxygen from water into toluene and benzene during anaerobic fermentative transformation. *Appl Environ Microbiol*. **52**, pp.200-202.

Vrionis, H.A., Anderson, R.T., Ortiz-Bernad, I., O'Neill, K., Resch, C.T., Peacock, A.D., Dayvault, R., White, D.C., Long, P.E. and Lovley, D.R. 2005. Microbiological and geochemical heterogeneity in an in situ uranium bioremediation field site. *Appl Environ Microbiol*. **71**, pp.6308–6318.

Wang, L.A. and Goonewardene, Z. 2004. The use of MIXED models in the analysis of animal experiments with repeated measures data. *Canadian Journal of Animal Science*. **84**(1), pp.1-11.

Wang, Z., Fingas, M., Blenkinsopp, S., Sergy, G., Landriault, M., Sigouin, L., Foght, J., Semple, K. and Westlake, D.W.S. 1998. Comparison of oil composition changes due to biodegradation and physical weathering in different soils. *Journal of Chromatography*. pp.89-107.

Warren, L.A., Maurice, P.A., Parmar, N. and Ferris, F.G. 2001. Microbially mediated calcium carbonate precipitation: Implications for Interpreting calcite precipitation and for solid-phase capture of inorganic contaminants. *Geomicrobiology Journal*. **18**(1), pp.93-115.

Washer, C.E. 2004. *Molecular Characterization of a Methanogenic Toluene-Degrading Consortium*. thesis, University of Toronto.

Watson, J.S., Jones, D.M. and Swannell, R.P.J. 1999. Formation of carboxylic acids during biodegradation of crude oil. In: Alleman, B.C. and Leeson, A. eds. *In situ Bioremediation of Petroleum hydrocarbon and Other Organic Compounds*. [Online]. Columbus. Battelle., pp.251-255.

Weber, K.A., Achenbach, L.A. and Coates, J.D. 2006. Microorganisms pumping iron: anaerobic microbial iron oxidation and reduction. *Nat Rev Microbiol*. **4**(10), pp.752-764.

Weelink, S.A.B., Eekert, M.H.A. and Stams, A.J.M. 2010. Degradation of BTEX by anaerobic bacteria: physiology and application. *Rev Environ Sci Biotechnol* **9**, pp.359-385.

Weiner, J.M., Lauck, T.S. and Lovley, D.R. 1998. Enhanced Anaerobic Benzene Degradation with the Addition of Sulfate. *Bioremediation Journal*. **2**, pp.159-173.

Weiner, J.M. and Lovley, D.R. 1998. Rapid benzene degradation in methanogenic sediments from a petroleum-contaminated aquifer. *Appl Environ Microbiol.* **18**, pp.62-66.

Wenk, H.R., Barber, D.J. and Reeder, R.J. 1990. Microstructures in carbonates. In: Reeder, R.J. ed. *Carbonates: Mineralogy and Chemistry, Reviews in Mineralogy*. [Online]. 2nd printing ed. Mineralogical Society of America, pp.301-367.

West, B.T., Welch, K.B. and Galecki, A.T. 2014. *Linear Mixed Models: A Practical Guide Using Statistical Software, Second Edition*. CRC Press.

Whittaker, M., Pollard, S.J.T. and Fallick, T.E. 1995. Characterisation of refractory wastes at heavy oil-contaminated sites: review of analytical methods. *Environmental Technology*. . **16**, pp.1009-1033.

Woltman, H., Feldstain, A., MacKay, J.C. and Rocchi, M. 2012. An introduction to hierarchical linear modeling. *Tutorials in Quantitative Methods for Psychology*. **8**(1), pp.52-69.

Wu, L. 2009. *Mixed Effects Models for Complex Data*. CRC Press.

Yan, B., Wren, B.A., Basak, S., Biwas, P., and Giammarm D.E. 2008. Microbial reduction of Fe (III) in hematite nanoparticles by *Geobacter sulfurreducens*. *Environ Sci Technol.* **42**, pp.6526-6531.

Yu, J.-Y., Park, Misun, Kim, Jinhwan. 2002. Solubilities of synthetic schwertmannite and ferrihydrite. *Geochemical Journal.* **36**, pp.119-132.

Yu, J.Y., Park, M. and Kim, J. 2002. Solubilities of synthetic schwertmannite and ferrihydrite. *GEOCHEMICAL JOURNAL.* **36**(2), pp.119-132.

Zachara, J.M., Cowan, C.E., and Resch, C.T. 1991. Sorption of divalent metals on calcite. *Geochim. Cosmochim. Acta.* **55**, pp.1549-1562.

Zachara, J.M., Fredrickson, J.K., Smith, S.C. and Gassman, P.L. 2001. Solubilization of Fe(III) oxide-bound trace metals by a dissimilatory Fe(III) reducing bacterium. . *Geochim Cosmochim Acta*. **65**, pp.75–63.

Zachara, J.M., Kukkadapu, R.K., Peretyazhko, T., Bowden, M., Wang, C., Kennedy, D.W., Moore, D. and Arey, B. 2011. The mineralogic transformation of ferrihydrite induced by heterogeneous reaction with bio-reduced anthraquinone disulfonate (AQDS) and the role of phosphate. *Geochimica et Cosmochimica Acta*. **75**(21), pp.6330-6349.

Zeger, S.L., Liang, K.-Y. and Albert, P.S. 1988. Models for Longitudinal Data: A Generalized Estimating Equation Approach. *Biometrics*. **44**(4), pp.1049-1060.

Zhilina, T.N., Zavarzina, D.G., Kolganova, T.V., Lysenko, A.M. and Tourova, T.P. 2009. *Alkaliphilus peptidoferrum* sp. nov., a new alkaliphilic bacterial soda lake isolate capable of peptide fermentation and Fe(III) reduction. *Microbiology*. **78**, pp.445–454.

Zytner, R.G. 1994. Sorption of benzene, toluene, ethylbenzene and xylenes to various media. *Journal of Hazardous Materials*. **38**(113-126).

Glossary

Bioavailability

The capacity of a particular compound or group of compounds to participate in biological reactions.

Biodegradation

The conversion of an organic compound, ultimately to carbon dioxide and water, by microbiological catalysis.

Bioremediation

A managed process for removing soil contaminants through the enhancement of natural microbiological processes.

Characterisation

The process through which the physical, chemical and/or biological properties of a particular compound or product are distinguished.

Confidence interval

A 95% confidence interval is the range of values which would not be rejected by a test of the null hypothesis at the 5% level

Covariate

A variable that may influence our DV but which we cannot control experimentally is called a covariate. Usually, especially in the context of ANCOVA, it is a continuous variable.

Degrees of freedom

Degrees of freedom are usually used as the denominator in calculating an average where there is some constraint on the values in the numerator.

Dependent variable

A dependent variable is a variable that measures the outcome of the experiments i.e. it is a phenomenon we want to study

Effect

The difference made to the DV by a change in the IV. Estimating the statistical significance and the size of an effect are usually tasks of ANOVA.

Factor

In ANOVA the IVs are usually referred to as factors.

Factorial design

In a factorial design, each level of each independent variable is paired with each level of each other independent variable, a 2 x 3 factorial design consists of the 6 possible combinations of the levels of the independent variables.

Factor levels

The values taken by the factors (IVs).

General Linear Model

A class of models including ANOVA, ANCOVA, MANOVA and regression (simple and multiple).

Generalised Linear Model

An extension of the General Linear Model that includes (among others) logistic regression and log-linear models.

Goodness of fit

Various statistics, known collectively as measures of goodness of fit or goodness-of-fit statistics, are used to determine how well a model fits the data.

Heteroscedasticity

Refers to the circumstance in which the variability of a variable (variance) is unequal across the range of values of a second variable that predicts i.e. residuals. Called heterogeneity of variance in ANOVA context, heteroscedasticity in regression analysis.

Homoscedasticity

Refers to the circumstance in which the variability of a variable (variance) is the same across the range of values of a second variable that predicts i.e. residuals. Called homogeneity of variance in ANOVA context, homoscedasticity in regression analysis.

Hydrocarbons

Compounds consisting solely of hydrogen and carbon.

Independent variable

An independent variable is a variable that is manipulated by the experimenter i.e. it is a phenomenon that when it changes makes another phenomenon change

Intrinsic bioremediation

The management of natural microbial processes to reduce the amount of contaminant in soil or groundwater.

Ion chromatogram

In GC-El MS, the set of peaks produced by ions possessing one particular mass-to-charge ratio.

Isotope ratio

A representation of the ratio of C-13 to C-12 within a particular compound or mixture of compounds (in the context of this study).

Isotopic composition

In this study, the relative amounts of C-13 and C-12, as shown by the Isotope Ratio.

Independence

Observations or variables are independent if the value on one of them does not affect the probabilities for values on the other.

Interaction

Two factors in an ANOVA interact if the effect of one differs at different levels of the other (plots will show non-parallel lines).

Intercept

The values at which a straight line graph intersects the vertical (DV) axis, so it is the constant a in the equation $y = a + bx$. With more than one IV it is the constant in the linear equation that predicts the DV.

Independent variable

An independent variable is a variable that is manipulated by the experimenter i.e. it is a phenomenon that when it changes makes another phenomenon change

Level (of a factor i.e. variable)

When a factor consists of various treatment conditions, each treatment condition is considered a level of that factor. For example, if the factor were drug dosage, and three doses were tested, then each dosage would be one level of the factor and the factor would have three levels.

Likelihood

The likelihood of a hypothesis or parameter value, given our data, is proportional to the probability of our data with that hypothesis or parameter values.

Main effect

If we have more than one factor in an ANOVA, the main effect of a factor is the effect of that factor averaged over all the other factors.

Mediating effects

An indirect effect of an IV on a DV via its effect on a variable intermediate between the IV and DV in a hypothesised causal chain.

Microcosm/Mesocosm

Pertains in this study to the experimental apparatus through which microbial activity was studied in the laboratory

Missing observations

If observations that are required by an experimental design are not obtained, perhaps because a participant is ill or drops out, then we have missing observations. Analysis may be considerably more difficult if there are missing observations.

Mineralisation

The complete microbially-induced conversion of an organic compound to carbon dioxide and water.

Model

The model is an equation that predicts or accounts for the observed values of the DV in terms of the values of the IV(s) and some random variation. A linear model predicts the DV as a sum of multiples of the IVs plus a constant and some random variation.

Multiple correlation coefficient

The correlation between the observed and predicted values of the DV in a regression analysis.

Natural Attenuation

Synonymous in this case with Intrinsic Bioremediation

Null hypothesis

In hypothesis testing, the null hypothesis is the one we test.

Paired comparisons

In an ANOVA, if the difference in the DV is tested for every pair of values taken for an IV, we call these pair comparisons.

Parameter

A numerical value that has to be estimated for a model.

Parametric assumptions

The assumptions that the DV is (at least approximately) normally distributed and has a variance that is the same for all values of the IV(s) in the study.

Petroleum products

Individual fossil fuel products obtained from the atmospheric and vacuum distillation of crude oil.

Planned comparisons

Comparisons or contrasts that are planned when the experiment is designed.

Post hoc tests

Tests that are done after viewing the data, or multiple tests that are not based on specific planned comparisons.

Probability plot

A method for checking whether data are likely to be from a normal distribution.

Remediation

The process through which contaminants in soil are removed or transformed to a less harmful form.

Residuals

The difference between an observed value of the DV and the value predicted by a model.

Replicates

In statistical terms, observations with the same combination of factor levels.

Saturated zone

The area of the soil subsurface below the permanent water table mark (i.e. below the groundwater level).

Sediment

Sediments may be described as a material deposited in either air or water or near the surface of the earth. Sediments may be compacted, cemented or altered to form sedimentary rocks.

Soil

Soils may be regarded as a heterogeneous mixture of air, water, inorganic and organic solids and microorganisms.

Type I error

Rejecting a null hypothesis that is true.

Type II error

Failing to reject a null hypothesis that is false.

Unsaturated zone

The area of the soil subsurface above the highest permanent water table mark (i.e., above the level of soil groundwater).

Appendix A
Presentations, Publications and List of Courses Attended

A.1 Publications currently submitted for publication and in press

A.2 Conference and poster presentations

Orlu, R.N., Stewart, D.I., and Bottrell, S.H. Geochemical controls during the biodegradation of petroleum hydrocarbons in soils. School of Civil Engineering Post Graduate Researchers (PGR) Conference. University of Leeds. September 2013

Orlu, R.N., Stewart, D.I., and Bottrell, S.H. Harnessing iron mineralogy and bioavailability in contaminated aquifers. 13th International UFZ-Deltares Conference on Sustainable Use and Management of Soil, Sediment and Water Resources 9–12 June 2015, Copenhagen, Denmark.

A.3 Conference platform presentations

Orlu, R.N., Stewart, D.I., and Bottrell, S.H. Anaerobic toluene degradation in contaminated aquifers. School of Civil Engineering Post Graduate Researchers (PGR) Conference. University of Leeds. September 2014

A.4 Courses attended

(University of Leeds 2012-2015)

An Introduction to Effective Research Writing	22/07/2015
5th Postgraduate Researcher Conference	04/12/2014
Matlab and Simulink	24/06/2014
Excel for Research 'Absolute Beginner'	07/05/2014
How Vital Are Your Statistics: Part 2	11/04/2014
How Vital Are Your Statistics: Part 1	07-08/04/2014
SPSS Beginners	04/04/2014
A-Z of Publication	27/03/2014
Labview Introductory Hands-on Workshop	19/03/2014
LaTeX Beginners	19/03/2014
Preparing for Your Transfer	19/11/2012
Effective Learning, Teaching and Assessment for Tutors and Demonstrators	23/10/2012

Project Managing Your Research Degree	31/05/2012
Writing for Research Students in the Sciences	30/05/2012
Digital Images Theory	16/05/2012
Digital Images Theory	10/05/2012
Introduction to C++	02-04/04/2012
Introduction to Programming	28/03-12/04/2012
CIEH Level 2 Health and Safety	28/03/2012
Starting Your Research Degree - Engineer	26/03/2012
Researcher @ Leeds	20/03/2012
Welcome Induction: Faculty of Engineering	13/03/2012
A Balancing Act	09/03/2012
Talking about your Research to Non-Specialists	27/02/2012
Working with Literature	16/02/2012
Endnote - Online webinar	15/02/2012
Search and Save	14/02/2012
Finding PhD dissertations and theses	13/02/2012
RSS and publication alerts: online web	08/02/2012
Word for Thesis Part 1	06/02/2012

Appendix B
Laboratory Apparatus

B.1 Degradation experiments

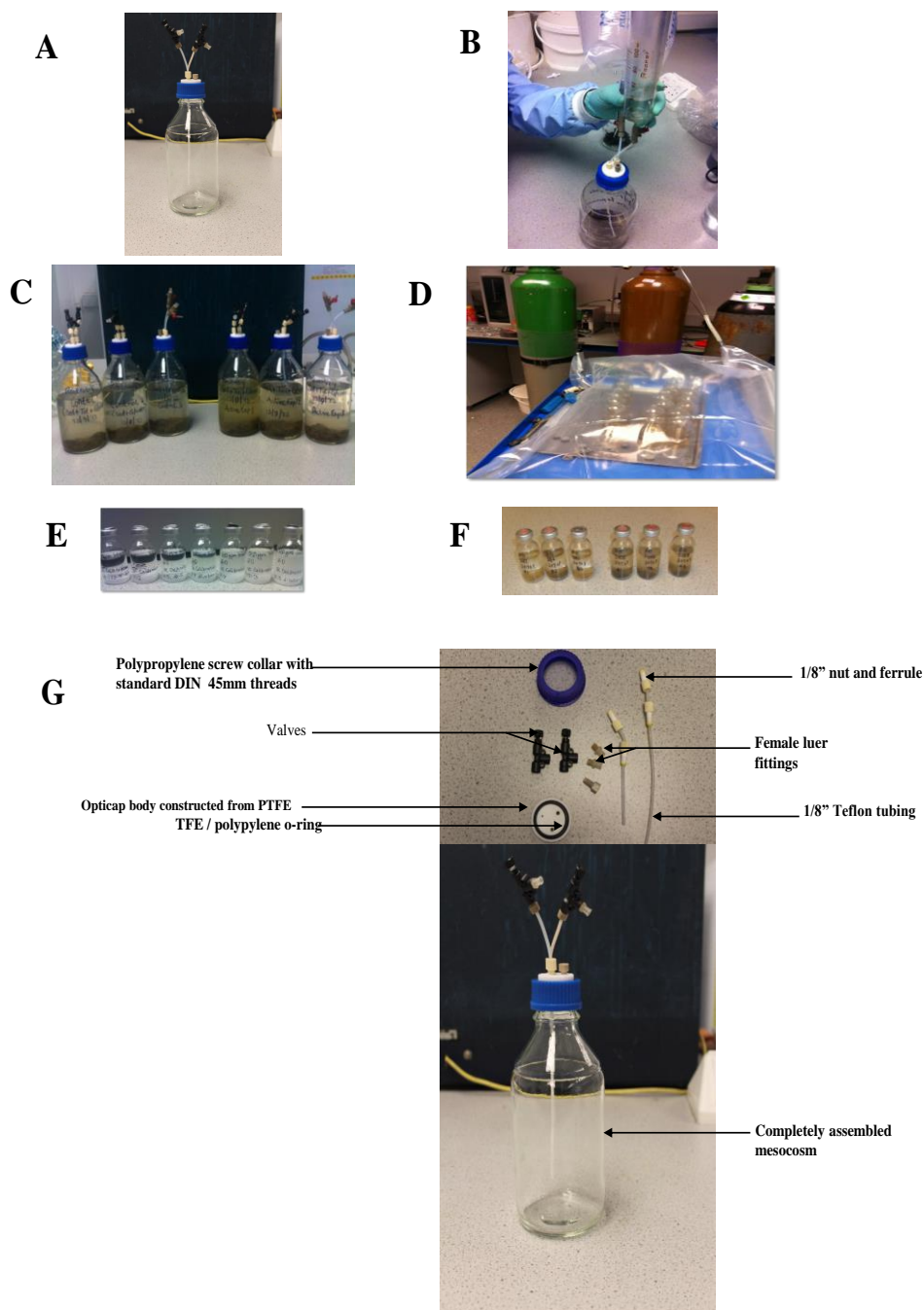
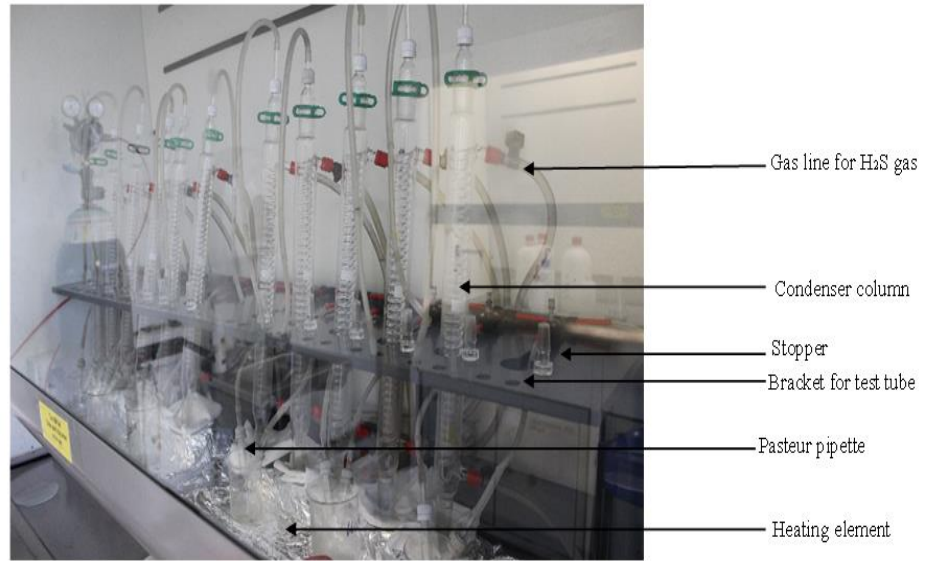


Figure B.1 Laboratory apparatus showing A - VICI cap assembly and PEEK fittings attached to a Schott bottle, B - Nitrogen-filled ballast volume and syringe used during spiking and sampling procedures, C - Mesocosms with soil-water mixture under anoxic conditions, D - Self fabricated anaerobic glove box, E - Sealed salted vials containing toluene stock solutions for GC calibration, F - Sealed salted vials containing liquid samples from sealed mesocosms and G - Components of VIC-CAP assembly

B.2 Sequential chemical extractions

A



B

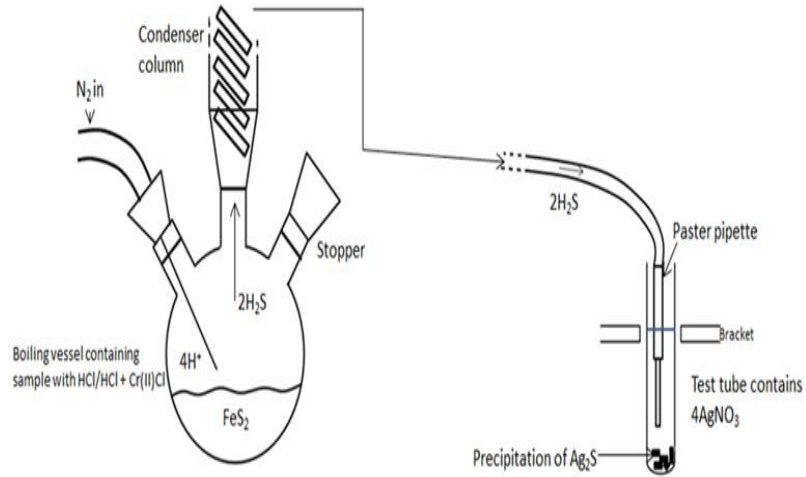
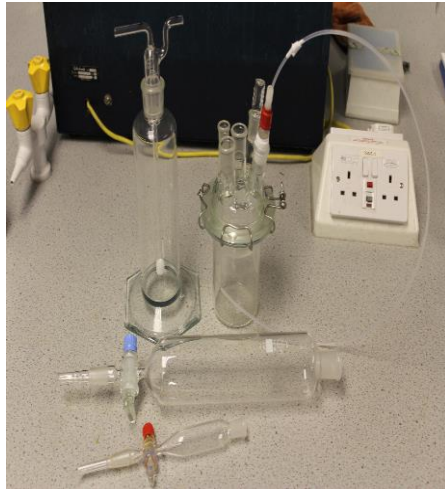


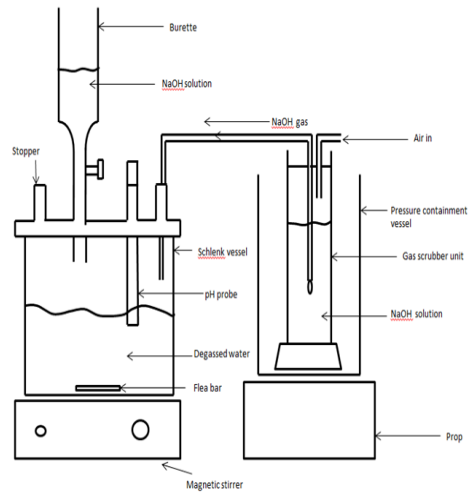
Figure B.2 Laboratory apparatus for pyrite and AVS extraction showing A – Condenser columns for extraction by chromous chloride distillation and B – Illustration of initial stage of the extraction process showing reaction vessel attached to the condenser column in which the extractant and sample are reacted to release $\text{H}_2\text{S}_{(g)}$ precipitated as Ag_2S

B.3 Mineral synthesis

A



B



C



D

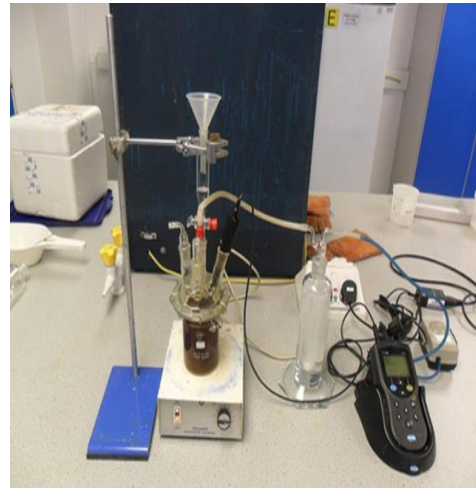


Figure B.3 Apparatus for mineral synthesis showing A – Glassware, B – Illustration of experimental set up and apparatus for mineral synthesis, C – Freeze-dried lepidocrocite mineral sample from the synthesis experiments and D- Experimental set up and apparatus for synthesis experiments

B.4 Analysis of total Fe and $\delta^{13}\text{C}$

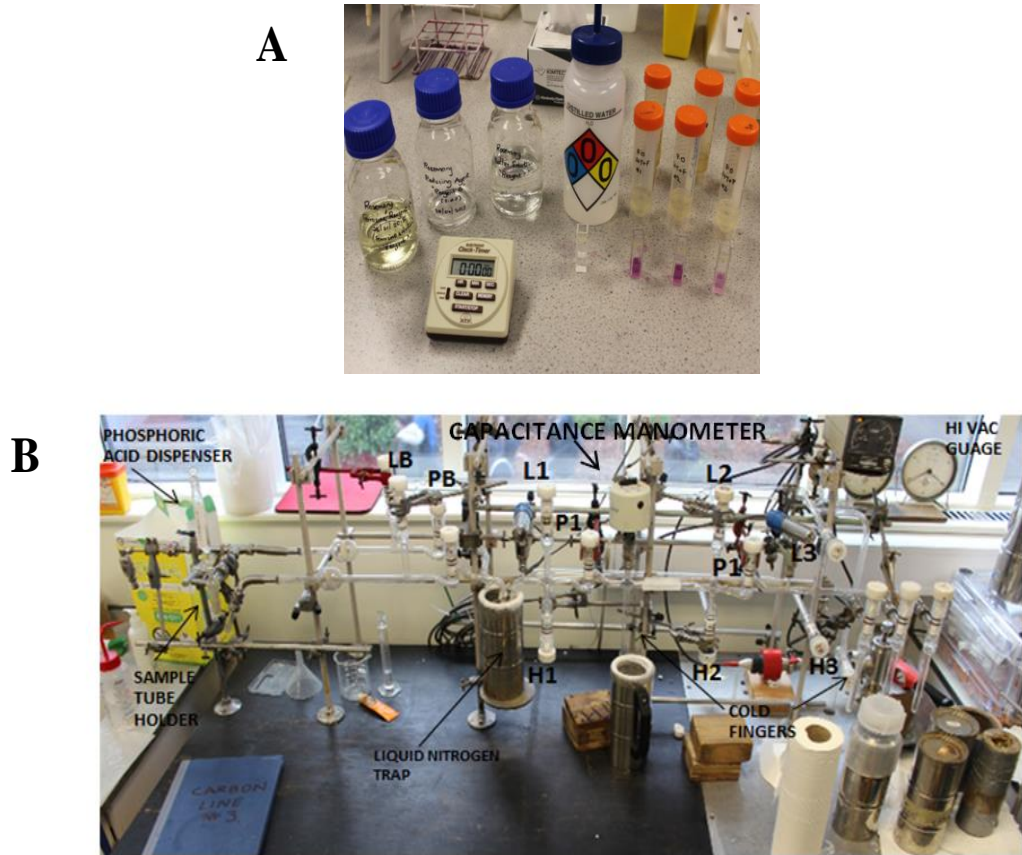


Figure B.4 Apparatus for total Fe test (ferrozine assay) and stable carbon isotope analysis showing A – Samples for ferrozine assay and B - Sealed vacuum line for sample preparation for ^{12}C and ^{13}C isotope analysis

Appendix C
Supporting Information

C.1 Experiment matrix of mesocosm experiments and variables measured

Table C.1 Experimental matrices and variables measured

Meso	Content	Variables measured
S _O	Soil, Water	pH, toluene, total dissolved aqueous Fe, ¹⁵ C/ ¹² C ratios, operationally-defined Fe mineral
S _T	Soil, water,	pH, toluene, total dissolved aqueous Fe, ¹⁵ C/ ¹² C ratios, operationally-defined Fe mineral
H _M	Soil, water,	pH, toluene, total dissolved aqueous Fe, ¹⁵ C/ ¹² C ratios
G _E	Soil, water,	pH, toluene, total dissolved aqueous Fe, ¹⁵ C/ ¹² C ratios
M _T	Soil, water,	pH, toluene, total dissolved aqueous Fe, ¹⁵ C/ ¹² C ratios
F _C	Soil, water, ate	pH, toluene, total dissolved aqueous Fe, ¹⁵ C/ ¹² C ratios
F _H	Soil, water, ite	pH, toluene, total dissolved aqueous Fe, ¹⁵ C/ ¹² C ratios
L _P	Soil, water, crite	pH, toluene, total dissolved aqueous Fe, ¹⁵ C/ ¹² C ratios
S _I	Original ent amendment	pH, toluene, total dissolved aqueous Fe, ¹⁵ C/ ¹² C ratios

Meso	Content	Variables measured
S ₂	Original at amendment, ,	pH, toluene, total dissolved aqueous Fe, ¹⁵ C/ ¹² C ratios
S ₃	Original at amendment, ,	pH, toluene, total dissolved aqueous Fe, ¹⁵ C/ ¹² C ratios

C.2 Soil sampling locations

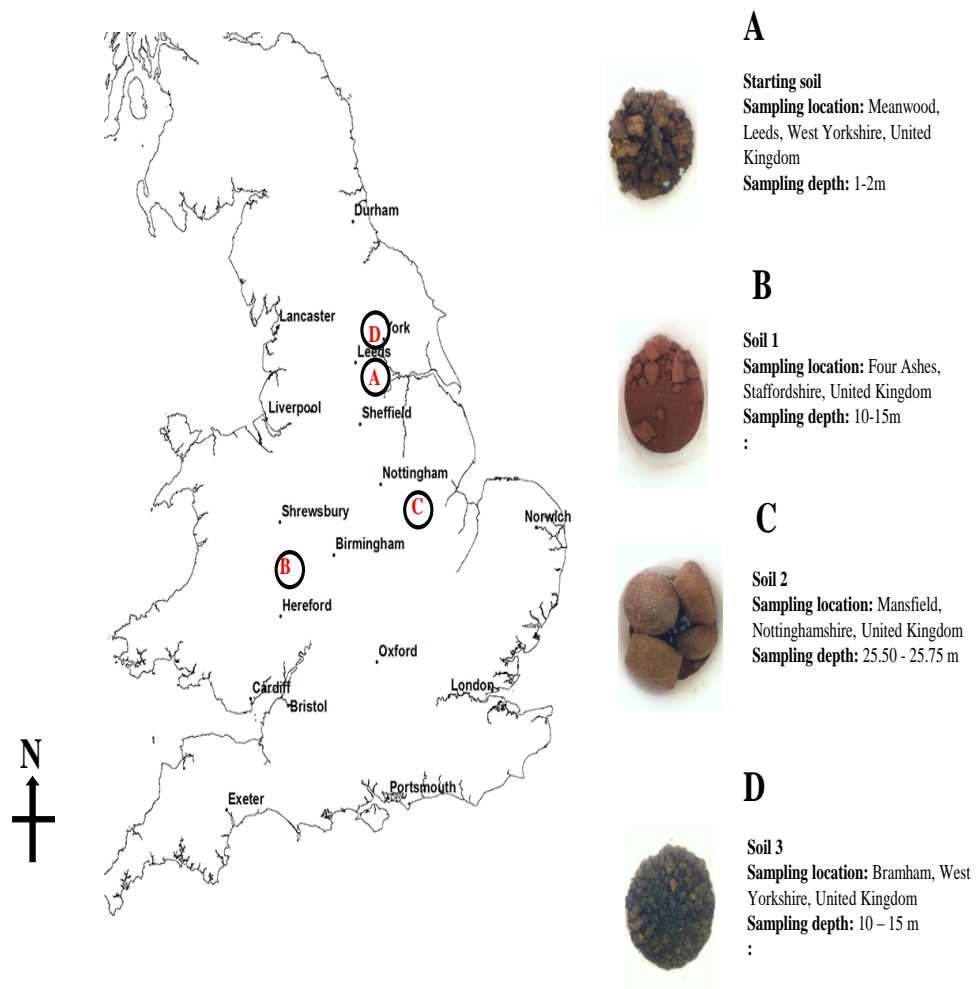


Figure C.2 Sampling locations of starting soil (SS) and soil amendments (Soil 1, Soil 2, Soil 3) (Image Source: GoogleImages)

C.3 Instrument calibration curves

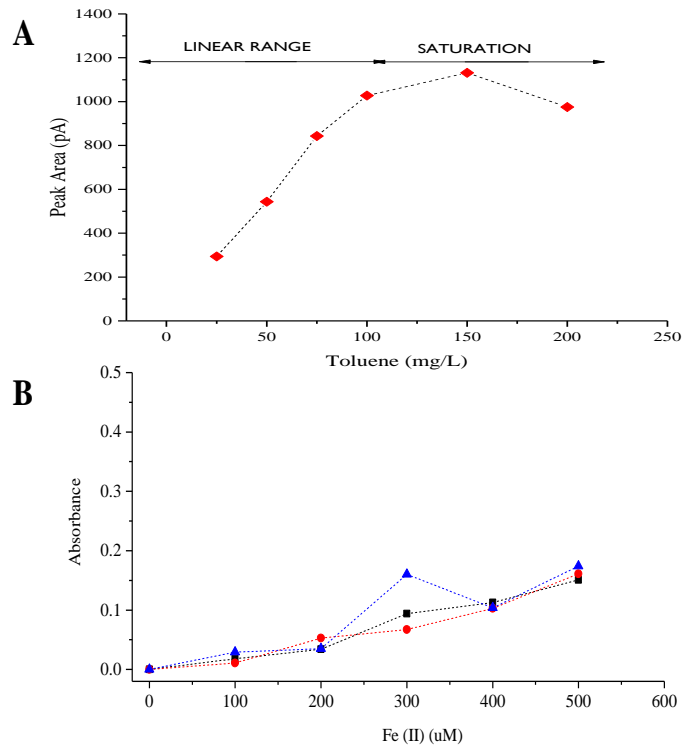


Figure C.3 Initial calibration curves for A - toluene analysis on GC instrument and B - ferrozine tests (calibration performed in triplicate) on UV-VIS

C.4 Calculations and estimates

C.4.1 Toluene removal (in mg)

Toluene removed = mass of toluene x $\frac{C_0 - C_t}{C_0}$ **Equation C.4-1**

where

‘mass of toluene’ is the amount of toluene in stock solution (in mg)

C_0 is the total concentration of dissolved / aqueous phase toluene (in mg/L) at the time of spiking †

C_t is the total concentration of dissolved / aqueous phase toluene (in mg/L) at the end of a given spike period †

$\frac{C_0 - C_t}{C_0}$ represents the fraction of toluene removed during the spiking period

† C_0 and C_t concentrations represent the theoretical concentrations expected under the assumption that all of the added toluene went into solution

C.4.2 Relative sorption

The amount of sorption that may have occurred is given by the relationship below:

$$\text{Relative sorption} = \frac{\text{Starting concentration in amended mesocosms (mM)}}{\text{Starting concentration in un - amended mesocosms (mM)}}$$

Equation C.4-2

$S_1: \quad \frac{0.2}{0.6} = \quad 0.333$

$$S_2: \quad \frac{0.3}{0.6} = 0.500$$

$$S_3: \quad \frac{0.8}{0.6} = 1.333$$

where S_1 , S_2 and S_3 represent mesocosms amended with Soil 1, Soil 2 and Soil 3 respectively

C.5 Experimental procedures

C.5.1 Laboratory synthesis of lepidocrocite and 2-line ferrihydrite

by Simon Bottrell and Rosemary Orlu

The procedure for synthesis of ferrihydrite and lepidocrocite adopted from (Navarro, 2008) (Yu, J.-Y., Park, Misun, Kim, Jinhwan, 2002) (Parkman, R.H., Chamock, J.M., Bryan, N.D., Livens, F.R., and Vaughan, D.J., 1999) is described below.

Materials

Schlenk vessel

Gas scrubber

pH metre

Magnetic stirrer

Burette attachment for schlenk vessel

Connector tubes (2)

Reagents

1M NaOH (sodium hydroxide or caustic soda)

0.1M $\text{FeCl}_2 \cdot 4\text{H}_2\text{O}$ (iron (ii) chloride tetrahydrate)

0.2M $\text{Fe}(\text{NO}_3)_3 \cdot 9\text{H}_2\text{O}$ (iron (iii) nitrate nonahydrate)

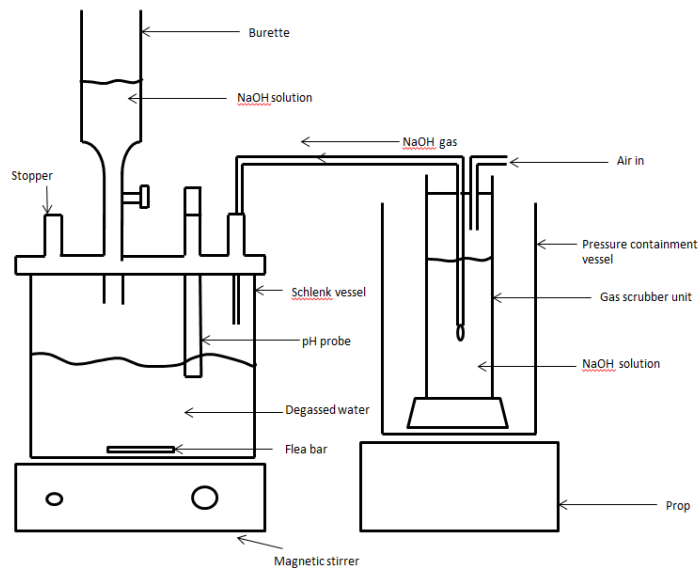


Figure C.5.1 Experimental set up for ferrihydrite and lepidocrocite synthesis

Procedure for lepidocrocite

Fill schlenk vessel with deionised water

Connect the nitrogen line to schlenk vessel and leave over night

Put flea bar in schlenk vessel, set on magnetic stirrer and switch on instrument

Add solid 19.9g $\text{FeCl}_2 \cdot 4\text{H}_2\text{O}$ to 300mL of degassed water, stir and dissolve

Fill the second vessel with NaOH and connect tubes, one to the inlet (air), the other to the outlet (NaOH)

Pour NaOH solution in burette

Place pH probe in schlenk vessel

Release NaOH into schlenk vessel until pH goes between 6.7-6.9

Start air flow through gas scrubber

Switch on N₂ flow from clean air flow (outlet from gas scrubber)

Monitor pH change – should start to fall

Add more NaOH solution to burette to keep pH ~ 6.8

Reaction is finished when pH stops changing (pH = 9)

Centrifuge, wash severally with DIW and freeze-dry

Confirm mineral with XRD analysis

Procedure for 2-line ferrihydrite

Repeat procedure using 0.2M $\text{Fe}(\text{NO}_3)_3 \cdot 9\text{H}_2\text{O}$ (40.4g in 500mL degassed water)

Precautions

Care must be taken when handling sodium hydroxide, the reagent is corrosive and also may permanently adhere glass components

The gas scrubber unit will be under pressure due to the in-filling of air, care must be taken by releasing air at a slow rate and by the use of a containing vessel such as a plastic bucket.

C.5.2 Analysis of aqueous phase toluene (salting-out method)

Procedure

1. Weigh out 7.5g of NaCl into a 15ml Whatman vial
2. Anaerobically seal this vial by crimping the vial
3. With the aid of a syringe insert 10ml of liquid sample for analysis
4. Store at room temperature in an upturned position to minimise losses by volatilisation

C.5.3 Analysis of total iron (Fe²⁺ and Fe³⁺) in solution (ferrozine method)

Theory

The determination of iron is based on the reaction of Fe(II) with Ferrozine agent in solution, forming a stable magenta coloured complex between pH 4 and 9. At 562nm the complex yields the maximum absorbance.

Analysis of Total Fe Fe(II)+Fe(III) is only achieved after reduction of Fe(III) to Fe(II) under strong acidic conditions.

The method applies for concentrations between ~0.010 mg/L and ~ 3mg/L.

Reagents (Use volumetric flasks for preparation)

- Ferrozine (0.01M ferrozine prepared in an 0.1M ammonium-acetate (CH₃COONH₄) solution)

Make 100ml of ferrozine solution by diluting 0.5077g of ferrozine and 0.7708g of ammonium-acetate in DI water. Keep only for a month as this solution oxidises over the time.

- Reducing Agent (1.4M hydroxylamine hydrochloride (H₂NOH.HCl) in an 2M hydrochloric acid solution)

Make 100ml dissolving 9.728g of hydroxylamine hydrochloride in 50mL of DI water and 17ml of concentrated HCl (aristar), complete the solution with DI water. Hygroscopic reagent, weight rapidly and keep container closed.

- Buffer (5M ammonium acetate adjusted to pH 9.5 with a 28-30% ammonium hydroxide (NH₄OH)

Make 100ml dissolving 38.54g of ammonium acetate in DI water and adjusted to pH 9.5.

Standards

1000 ppb Stock Solution

Take 1mL of 100ppm Fe standard solution and make up to 100mL.

Standards 10ppb-250ppb

Take the aliquots (below) of 1000ppb Fe stock solution and make up to 25 mL of DI water. Please bear in mind that you need to adjust the matrix of your samples (e.g. acid concentration, ionic strength, etc).

Table B.5.2 Standards for ferrozine assay

Std Fe (ppb)	µL of 1000 ppb Fe Std
10	250
50	1250
100	2500
150	3750
200	5000
250	6250

To make different sets of standards, please follow the equation:

$$\text{Concentration std.} \times 25 \text{ mL} = \text{Concentration stock std. solution} \times \text{Vol. needed}$$

Procedure

Total Fe [Fe(II)+Fe(III)] determination

Switch on the instrument 15 minutes before the measurements and set up to 562nm.

Add the following volumes of reagents to the samples, standards and the blank (DI water instead of sample) in the spectrophotometric cells.

1000 µL of sample (standard or water for the blank)

100 µL of reagent A

200 µL of reagent B

Wait 10 minutes for complete reduction of Fe(III) to Fe(II)

Add 50 µL of reagent C to each sample, standard and blank

Put the spectrophotometric cell with the blank solution into the spectrophotometer and push the zero key.

Measure the standards and samples and write down the absorbance.

Note: Measure ASAP to avoid Fe oxidation

C.5.4 Sequential chemical extractions for operationally-defined iron pools

by Simon Poulton

Step 1: Iron Carbonates, Fe_{carb}

The extractant sodium acetate (C₂H₃NaO₂) targets iron carbonate phases (including siderite and ankerite), evolving CO₂ in the process. To prevent excess build-up of pressure in centrifuge tubes, samples were degassed as a precaution by unscrewing the tube caps and re-tightening after 1 hour and subsequently after 8hours.

Sodium acetate solution was prepared from 82.03g of sodium acetate added per litre of solution using 400-500mL DI H₂O. This solution was adjusted to the desired pH while adding deionised water (DI H₂O) to reach the correct volume of solution without altering the pH of the solution. 10mL of the solution was added to each sample, and placed on the shaking table for 48hours at 50°C. After centrifuging, the liquid was then analysed for Fe content by automatic absorption spectrophotometry (AAS) while the semi-solid was stored for the next extraction step.

Step 2: Easily reducible iron oxides, Fe_{ox1}

Sodium dithionite targets reducible iron oxide phases (including ferrihydrite and lepidocrocite). This solution was prepared from 50.0g of sodium dithionite, 58.82g of tri-sodium citrate and 20mL of glacial acetic acid in DI H₂O. 10mL of the solution was added to the semi-solid samples from the previous extraction step, and placed on the shaking table for 2hours at room temperature. After shaking, the samples were centrifuged, the liquid analysed for iron content by AAS and solid used in the next step.

Step 3: Reducible iron oxides Fe_{ox2}

The extraction for the reducible iron oxide was performed in two steps. The first was performed for Fe (II) / Fe (III) mineral phases using a solution of hydroxylamine HCl. 10 mL of the solution was added to each sample from the previous extraction and placed on the shaking table for 2 hours at room temperature and centrifuged. A portion of this was stored for analysis by AAS. The second step was the analysis of a 1 mL aliquot for Fe (II) by UV-VIS following the ferrozine-HEPES method. The difference between the concentrations of iron in both fractions (expressed as percentage weights) was taken to be representative of the reducible oxide fraction in the sample.

Step 4: Magnetite, Fe_{mag}

As stated in Table 3.5, the extractant ammonium oxalate targets the magnetite iron phase. An ammonium oxalate solution was prepared from 28.42g of ammonium oxalate dissolved in DI H_2O . 10mL of the final solution was added to each sample from the previous step and placed on the shaking table for 6 hours at room temperature. After centrifuging, the liquid was then analysed for Fe content by AAS.

Sulphate extractions

The two-step sulphate extraction sequence and one-step total iron extraction sequence began with an extraction of the acid-volatile sulphates (AVS) followed by a second step targeting iron sulphates in the form of pyrites.

Step 1: Acid-volatile sulphates (Fe_{AVS})

The extraction for AVS was performed on 6g of sample weighed out in reaction vessels. The pyrite line with traps was prepared by adding 0.5mL silver nitrate (prepared by dissolving 17g in 100 mL water).

After all parts of the set up were checked and heating elements switched on, the reaction was commenced by adding 8mL of 50% HCl to the reaction vessel drop-wise until bubbling ceased. The stopper was then placed on the vessel and the heat source switched on for 10 minutes. Significant precipitation of Ag_2S (see Figure 3.3) was an indication of the presence of acid-volatile sulphur (AVS). To ensure complete reaction the samples were left to react for 45 minutes after which new traps were prepared for the subsequent extraction of pyrites.

Step 2: Iron pyrites Fe_{PY}

The extraction for pyrites was performed using a volume of chromous chloride added to the samples and left for 1hour to complete reaction. The formation of a dark or opaque precipitate in the test tubes containing silver nitrate within the first 10minutes indicated excess pyrite content.

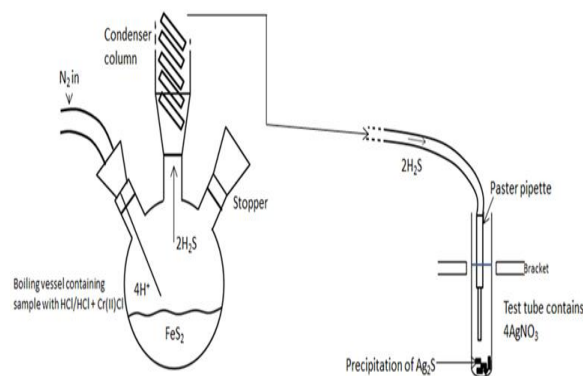


Figure C.5.4.1 Illustration of apparatus for pyrite extraction step showing reaction vessel for chromous chloride distillation

In the absence of this precipitate, the solution was to be mixed with silver nitrate until a transparent liquid was formed, which occurs because silver nitrate traps pyrite in solution. The precipitates from the AVS and pyrite extractions were filtered and dried using the suction-based filtering system. The mass of iron present as both fractions (pyrite and AVS) was obtained by a simple stoichiometric mass balance.

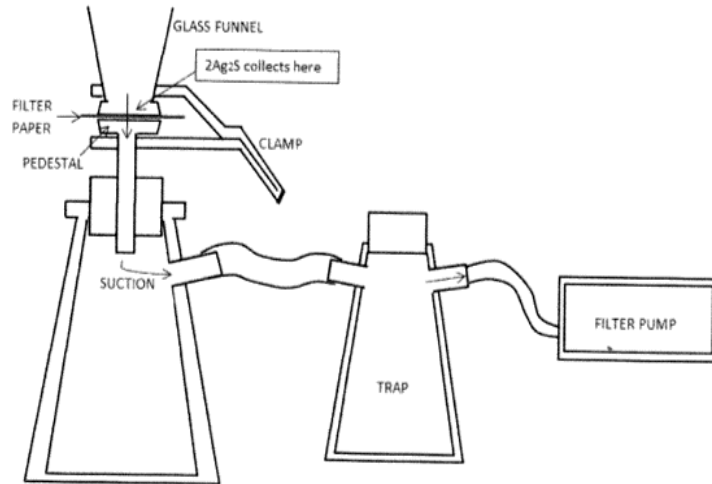


Figure C.5.4.2 Illustration of filtration apparatus for AVS and pyrite precipitate

Total Fe, Fe_T

This analysis was performed in the School of Earth and Environment by Romain Guildbald. 100 mg of the freeze-dried samples were prepared for the total Fe extraction by first “ashing” in a muffle-oven at 550°C overnight. The procedure was continued by adding HF acid and perchloric acid to each sample, and finally 2 mL boric acid for 2 hours at 130°C, followed by cooling in a fumehood. 5 mL of 50% HCl was added and heated on hot plate to dissolve the sample without boiling. The solution was made up to 100 mL in a volumetric flask and diluted by adding 1 mL of the 100 mL solution to 4 mL DI H₂O (prepared in test tubes). This solution was analysed by automated absorption spectrophotometry.

C.5.5 Stable carbon isotope analysis (cryogenic distillation)

Safe system of work: CO₂ vacuum line preparation

by Simon Bottrell

Procedure:

- 1) Fill the dropper with appropriate amount of phosphoric acid

Place dry ice/solvent trap onto spiral glass trap as per training.

- 2) Weigh out sample (observing all assessed risk minimization procedures) onto foil.

Record in logbook and label a reaction tube.

Use a funnel to place sample into a reaction tube.

Ensure there are no drips of acid on the dropper and place tube onto the cone.

3) When sample tube is attached, OPEN LB (do this carefully if sample is > ~1 g) – observe low vac vacuum gauge.

IF gauge falls as expected, CLOSE LB then OPEN PB.

If not, either determine cause of leak and rectify or seek advice.

4) Observe fall in pressure on high-vac gauge – when threshold mark is passed CLOSE H1.

Check that P2 is closed!

Then use tap to add acid to sample (volume will depend on type of sample). Note time in logbook.

Reaction times are:

SrCO₃ standard – 10 minutes;

SrCO₃ sample – 25 minutes;

Rock powders – variable dependant on mineralogy, but usually at least 45 min.

5) When reaction is complete TOP UP DRY ICE, place liquid nitrogen dewar on “measuring finger”.

CLOSE H2 then OPEN P1.

Allow gas to transfer for three minutes - MOVE LABEL.

CLOSE PB then top-up or raise liquid nitrogen dewar and wait a few seconds, then OPEN H1.

Watch Hi Vac gauge and wait for it to stop falling quickly, then CLOSE P1 and remove liquid nitrogen dewar.

6) Allow cold finger to warm to room temperature and take YEILD READING.

[NB: once proficient, the next sample can be attached at this stage – See 10 below].

7) Place liquid nitrogen dewar on an empty sample finger with its valve open. CLOSE H3 then OPEN P2.

Allow gas to transfer for two minutes MOVE LABEL, then top-up or raise liquid nitrogen dewar and wait a few seconds, then OPEN H2.

Watch Hi Vac gauge and wait for it to stop falling quickly, then CLOSE SAMPLE FINGER VALVE (be sure to support sample finger!) and remove liquid nitrogen dewar.

8) If all sample fingers are full:

- IF you have already attached another sample, CLOSE LB and OPEN PB (= 3) above)

– CLOSE P2, change sample fingers, OPEN L3, continue with next sample (4) above), wait for Low Vac gauge to fall, CLOSE L3, OPEN H3.

9) If empty fingers remain – CLOSE P2, OPEN H3. Continue with next sample

10) To continue with next sample use air inlet valve to fill used sample reaction tube with air and shut immediately.

Remove used reaction tube, check for acid drips, place new reaction tube on cone and begin procedure again from 3) above.

In some cases rock powder samples need to be recovered by filtration – in which case dilute acid with distilled water and move to that procedure

NB - this will need to be assessed for each group of samples.

ELSE dispose/collect sample and acid as appropriate for samples being run.

Clean reaction tubes, rinse 3 times in tap water, once with distilled water and place in glassware drying oven.

C.5.6 Predictive modelling with the mixed effects models approach

Using mixed effects model, there are two approaches to model within- and between-subjects variability. The first approach is the correlation (covariate type) model in which variation among subjects is estimated through residual correlations. The second approach estimates the subjects' variation as a random effect. In order to fit a mixed model on SPSS using this approach, the random and fixed effects must be specified. These are determined by the outcome and explanatory variables to be used. In the context of the mesocosm experiments, the quantitative outcome is 'toluene' (representing toluene concentration at a measured time point) and the explanatory variables 'group' (mesocosm group of the subject under study i.e. the soil-water mixture) and 'time' (which represents the times at which toluene concentrations in the mesocosms were observed). The corresponding parameters estimated from the explanatory variable or interaction represents the mean relations if there is a corresponding random effect. When specifying a random effect for a variable, the fixed effect must also be included because the fixed effects represent the average value around which the random effect varies. On SPSS more than one random effect may be specified, for example a random intercept and a random slope may be specified as random effects. Where more than one random effect is being considered in the model, the covariance structure type must be changed from the default 'identity' type structure in the Covariance type drop box. Options for covariance structure for multiple random effects include unstructured, which assumes correlation among random effects, or diagonal, which assumes no correlation between the random effects.

Parameter estimates are needed for interpretation of the results. There are two methods available in SPSS for estimating parameter values, namely the maximum likelihood and restricted maximum likelihood (REML); the default method in SPSS is the restricted maximum likelihood. In this analysis reported in this chapter, attention is given to the following output data:

Model dimension: The model dimensions show the number of parameters used in the analysis including the subject variables.

Estimates of fixed effects: The estimates of fixed effects compare the fixed effects of the reference category / group to the other groups in the data.

Estimates of covariance parameters: The model dimensions shows the model in terms of which variables (and their number levels) are fixed and / or random effects and the number of parameters being estimated.

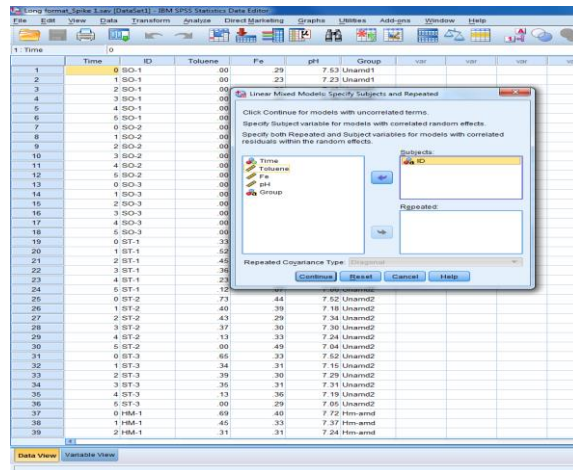
On SPSS the data was entered in long format with five variables specified namely 'ID', 'Toluene', 'Fe', 'pH' and 'Group'. The variable 'ID' represents each replicate and the grouping variables ('Group') are used to identify each variable as belonging to a particular level of the data hierarchy. The time-related variable ('Time') was coded '0' for Day 0, '1' for Day 3, '2' for Day 6, '3' for Day 9... '17' for Day 51. This pattern identifies the intercept in the model as initial (Time 0) toluene concentrations. Group, time and ID are entered as categorical variables while the dependent variables toluene, Fe and pH are continuous variables.

In SPSS the fixed effects dialog box specifies the structural model for the typical subject. By this command, the explanatory variable (or interaction) specified has a parameter estimated. The estimate demonstrates the relationship between the explanatory variable and the outcome (if there is no corresponding random effect) or the mean relationship (if there is a corresponding random effect). The random effects dialog box specifies model parameters which demonstrate the fixed effects are means around which individual subjects (replicate mesocosms) vary randomly. The intercept for a given subject is equal to the fixed effect plus a random deviation from that fixed effect (which is zero on average) and as a magnitude controlled by the size of the random effect. It should be noted that this random effect is a variance while the fixed effects are essentially means. On SPSS a separate intercept for each subject random effect is specified.

Procedure for modelling toluene removal without level 1 and 2 predictors

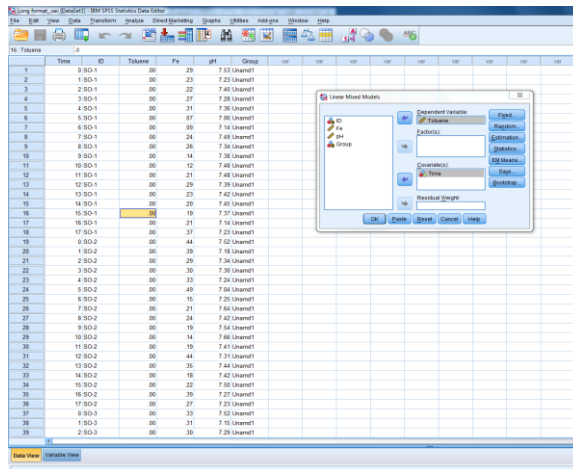
Step 1

Specify the upper level of the hierarchy by moving the identifier for that level into the 'subjects' box. The subject is ID (our individual replicates)



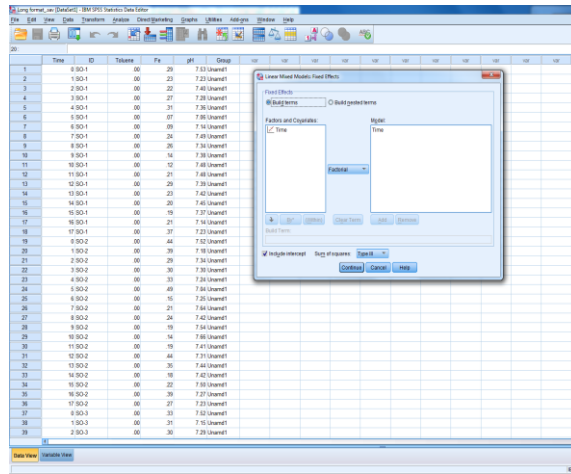
Step 2

Enter 'Toluene' in the dependent variable box (it is the quantitative outcome variable). Enter 'Time' in the covariate box.



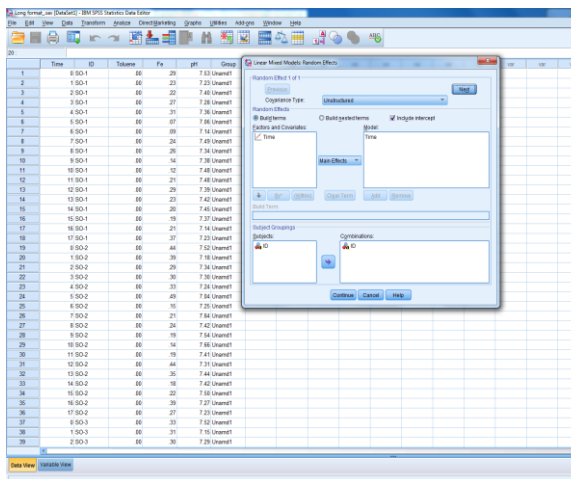
Step 3

Enter 'Time' as the fixed effect to be modeled, choose the Factorial option.



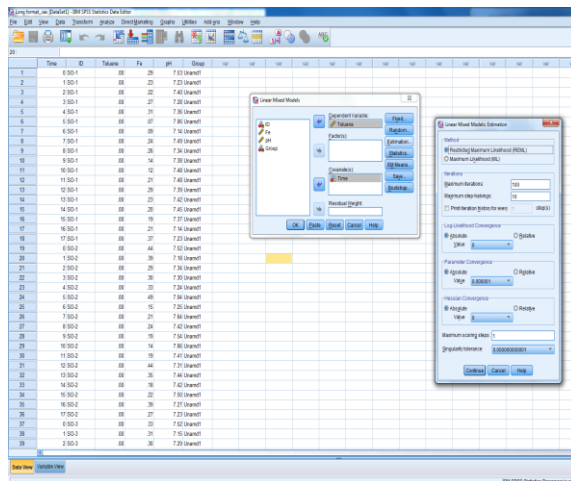
Step 4

Enter 'Time' as the random effect to be modeled, choose 'Main Effects'.



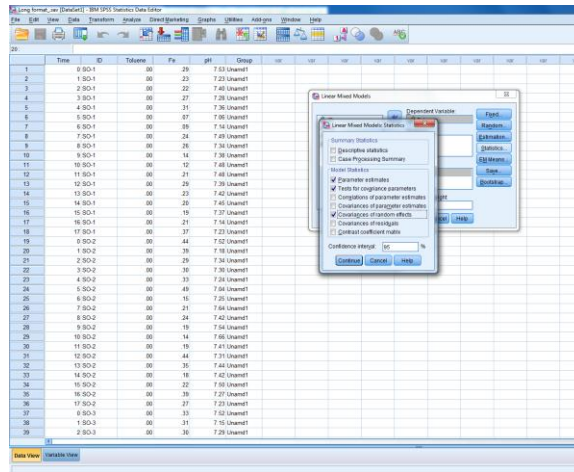
Step 5

Choose the restricted maximum likelihood method under Estimation tab.



Step 6

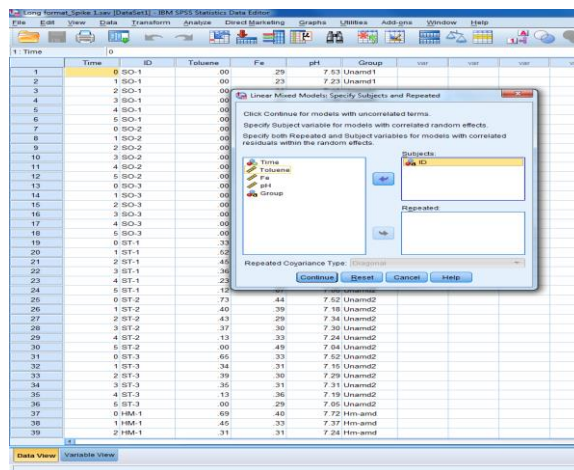
Tick 'Parameter estimates', 'Tests for covariance estimates' and 'Covariances of random effects' in the Statistics option.



Procedure for modelling toluene removal with Fe and pH as level 1 and 2 predictors

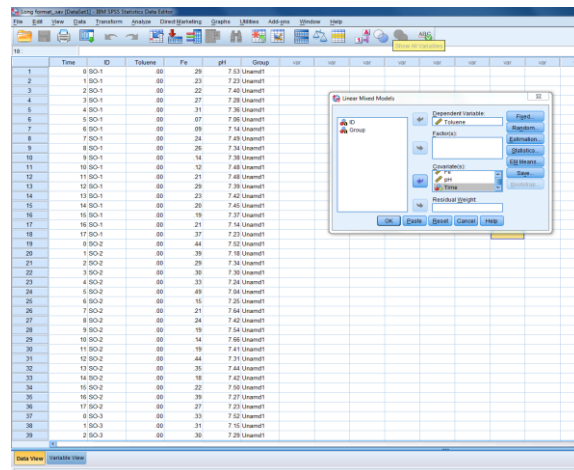
Step 1

The upper level hierarchy is specified as in the previous model.



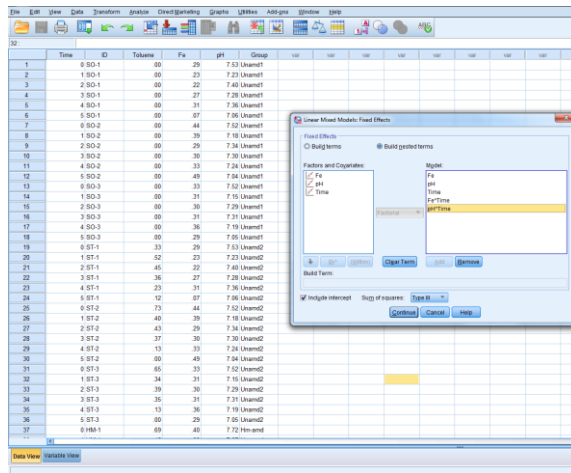
Step 2

Predictor variables are specified. In this model, Fe, pH and Time.

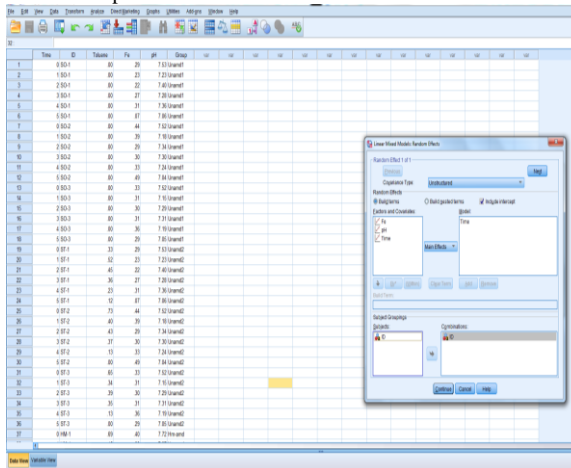


Step 3

The predictor variables are entered as fixed effects. Two interactions - Fe*Time and pH*Time are also included as fixed effects.



Step 4
Time is entered as random effect as in the previous model.



C.6 Analytical and experimental data

C.6.1 Characterisation tests: soil amendments

Table C.6.1a Physico-chemical properties of the soil amendments. Soil 1, Soil 2, and Soil 3 represent the individual soil amendments used

Physico-chemical property	Results per sample		
	Soil 1	Soil 2	Soil 3
Particle size distribution	0.6% <u>sand</u> 48.0% <u>silt</u> 51.4% <u>clay</u>	2.5% <u>sand</u> 77.8% <u>silt</u> 19.7% <u>clay</u>	0.6% <u>sand</u> 16.3% <u>silt</u> 83.1% <u>clay</u>
Surface area (m ² /g)	8	4	21
pH	7.6	7.7	7.7

C.6.2 Characterisation tests: mineral amendments

Table C.6.1b BET surface area of iron mineral amendments

Mineral	Hematite	Goethite	Magnetite	Ferrihydrite	Lepidocrocite
Surface area (m ² /g)	3	10	9	37	0.1

C.6.3 Characterisation tests: moisture content analysis

The moisture content of the starting soil was calculated as shown below and summarised in Table B-4:

$$M_{soil\ water} + M_{soil\ solid} * \%_{water\ content}$$

$$= 30 \times 0.3171$$

$$= 9.513\text{ g}$$

$$M_{soil} + M_{soil\ solid} + M_{water}$$

$$= 22.86 + 9.513$$

$$= 32.373\text{ g}$$

Table C.6.1c Gravimetric moisture content analysis for the starting soil material

Sample no. and Ref.	Label (g)	Value obtained
Mass of empty container	M ₁	29.84
Mass of wet soil + container	M ₂	59.95
Mass of dry soil + container	M ₃	52.7
Mass of moisture loss in soil	M ₂ - M ₃	7.25
Mass of dry soil	M ₃ - M ₁	22.86
Moisture content	W (%)	31.71%

C.6.4 Characterisation tests: particle size distribution analysis

Table C.6.1d Particle size distribution (PSD) of starting soil material and soil amendments

Textural group	Starting Soil (%)	Soil 1 (%)	Soil 2 Soil (%)	Soil 3 Soil (%)
Clay	0.5	51.4	19.7	83.1

Textural group	Starting Soil (%)	Soil 1 (%)	Soil 2 Soil (%)	Soil 3 Soil (%)
(less than 0.002 microns)				
<u>Total clay fraction</u>	<u>0.5 %</u>	<u>51.4 %</u>	<u>19.7 %</u>	<u>0.6 %</u>
Very Fine Silt (0.002-0.004 microns)	2.8	29.2	29.4	2.5
Fine Silt (0.004 – 0.008 microns)	5.0	9.6	28.3	4.0
Medium Silt (0.008 – 0.016 microns)	7.3	5.0	11.6	4.8
Coarse Silt (0.016 – 0.031 microns)	12.6	3.0	4.8	3.2
Very Coarse Silt (0.031 – 0.063 microns)	22.7	1.2	3.7	1.7
<u>Total silt fraction</u>	<u>50.4 %</u>	<u>48.0 %</u>	<u>77.8 %</u>	<u>16.3 %</u>
Very Fine Sand (0.063 – 0.0135 microns)	26.4	0.6	2.1	0.6
Fine Sand (0.0135 – 0.250 microns)	15.4	0.0	0.4	0.0
Medium Sand (0.250 – 0.500 microns)	5.2	0.0	0.0	0.0
Coarse Sand (0.500 microns – 1.000 mm)	2.2	0.0	0.0	0.0
Very Coarse Sand (1.000– 2.000 mm)	0.0	0.0	0.0	0.0
<u>Total sand fraction</u>	<u>49.2 %</u>	<u>0.6 %</u>	<u>2.5 %</u>	<u>0.6 %</u>

† Interpretation of data from particle size distribution analysis was performed using the GRADISTAT® software

C.6.5 Degradation experiments

Table C.6.3 Mean \pm standard error for pH and total iron concentrations in mesocosms with soil and water only (un-amended live controls)

Time (days)	Total Fe (mM)	Toluene (mM)	pH
0	-	1.5 \pm 0.19	7.3 \pm 0.00
3	-	0.2 \pm 0.07	7.6 \pm 0.03
6	-	0.1 \pm 0.03	7.0 \pm 0.00
9	-	0.2 \pm 0.03	7.5 \pm 0.05
12	-	0.4 \pm 0.05	7.5 \pm 0.05
15	-	0.8 \pm 0.21	7.6 \pm 0.03
18	-	0.5 \pm 0.06	7.5 \pm 0.03
21	-	0.8 \pm 0.11	7.4 \pm 0.05
24	-	1.0 \pm 0.24	7.4 \pm 0.08
27	-	1.0 \pm 0.24	7.4 \pm 0.08
30	-	1.4 \pm 0.24	7.4 \pm 0.03
33	-	1.4 \pm 0.31	7.3 \pm 0.00
36	-	1.9 \pm 0.36	7.6 \pm 0.03
39	-	2.2 \pm 0.21	7.6 \pm 0.07
42	-	3.0 \pm 0.13	7.6 \pm 0.05
45	-	3.2 \pm 0.25	7.4 \pm 0.05
48	-	1.9 \pm 0.20	7.4 \pm 0.05
51	-	2.9 \pm 0.46	7.4 \pm 0.05

Table C.6.4 Mean \pm standard error for pH, total iron, and toluene concentrations in mesocosms with no amendment (un-amended active controls)

Time (days)	Total Fe (mM)	Toluene (mM)	pH
0	0.4 \pm 0.04	0.6 \pm 0.10	7.5 \pm 0.00
3	0.3 \pm 0.04	0.4 \pm 0.04	7.2 \pm 0.02
6	0.3 \pm 0.02	0.4 \pm 0.02	7.3 \pm 0.03
9	0.3 \pm 0.01	0.4 \pm 0.00	7.3 \pm 0.01
12	0.3 \pm 0.01	0.2 \pm 0.03	7.3 \pm 0.04
15	0.3 \pm 0.10	0.0 \pm 0.03	7.1 \pm 0.00

Time (days)	Total Fe (mM)	Toluene (mM)	pH
18	0.1 ± 0.02	0.6 ± 0.12	7.2 ± 0.03
21	0.2 ± 0.03	0.4 ± 0.20	7.6 ± 0.04
24	0.2 ± 0.02	0.4 ± 0.10	7.4 ± 0.03
27	0.2 ± 0.01	0.5 ± 0.08	7.5 ± 0.05
30	0.1 ± 0.01	0.4 ± 0.03	7.6 ± 0.05
33	0.2 ± 0.02	0.2 ± 0.08	7.5 ± 0.05
36	0.3 ± 0.36	0.9 ± 0.10	7.4 ± 0.03
39	0.3 ± 0.21	0.8 ± 0.12	7.5 ± 0.03
42	0.2 ± 0.13	0.6 ± 0.09	7.4 ± 0.01
45	0.2 ± 0.25	0.4 ± 0.03	7.5 ± 0.04
48	0.3 ± 0.20	0.4 ± 0.04	7.2 ± 0.05
51	0.3 ± 0.46	0.4 ± 0.04	7.3 ± 0.04

Table C.6.5 Mean ± standard error for pH, total iron, and toluene concentrations in mesocosms with hematite amendment

Time (days)	Total Fe (mM)	Toluene (mM)	pH
0	0.4 ± 0.03	0.7 ± 0.02	7.6 ± 0.04
3	0.3 ± 0.03	0.4 ± 0.01	7.3 ± 0.03
6	0.3 ± 0.026	0.3 ± 0.02	7.3 ± 0.03
9	0.3 ± 0.04	0.2 ± 0.01	7.3 ± 0.06
12	0.3 ± 0.05	0.1 ± 0.04	7.2 ± 0.06
15	0.3 ± 0.05	0.0 ± 0.03	7.2 ± 0.02
18	0.1 ± 0.06	0.6 ± 0.10	7.4 ± 0.03
21	0.2 ± 0.02	0.5 ± 0.03	7.7 ± 0.03
24	0.2 ± 0.02	0.5 ± 0.05	7.6 ± 0.03
27	0.2 ± 0.02	0.2 ± 0.06	7.6 ± 0.03
30	0.1 ± 0.01	0.1 ± 0.05	7.6 ± 0.02
33	0.2 ± 0.00	0.0 ± 0.03	7.7 ± 0.03
36	0.3 ± 0.03	0.8 ± 0.11	7.5 ± 0.03
39	0.3 ± 0.02	0.6 ± 0.10	7.5 ± 0.02
42	0.2 ± 0.01	0.6 ± 0.09	7.7 ± 0.01
45	0.2 ± 0.03	0.2 ± 0.08	7.5 ± 0.02

Time (days)	Total Fe (mM)	Toluene (mM)	pH
48	0.3 ± 0.01	0.2 ± 0.03	7.3 ± 0.03
51	0.3 ± 0.01	0.2 ± 0.05	7.4 ± 0.01

Table C.6.6 Mean ± standard error for pH, total iron, and toluene concentrations in mesocosms with goethite amendment

Time (days)	Total Fe (mM)	Toluene (mM)	pH
0	0.1 ± 0.02	0.5 ± 0.01	7.7 ± 0.04
3	0.3 ± 0.02	0.4 ± 0.01	7.6 ± 0.01
6	0.3 ± 0.01	0.2 ± 0.07	7.3 ± 0.03
9	0.3 ± 0.01	0.4 ± 0.03	7.5 ± 0.02
12	0.3 ± 0.04	0.2 ± 0.02	7.3 ± 0.02
15	0.4 ± 0.02	0.0 ± 0.03	7.6 ± 0.00
18	0.3 ± 0.03	0.7 ± 0.06	7.3 ± 0.02
21	0.2 ± 0.04	0.5 ± 0.07	7.4 ± 0.01
24	0.3 ± 0.03	0.4 ± 0.05	7.4 ± 0.01
27	0.3 ± 0.04	0.1 ± 0.08	7.5 ± 0.02
30	0.3 ± 0.03	0.1 ± 0.06	7.5 ± 0.01
33	0.3 ± 0.01	0.0 ± 0.00	7.4 ± 0.03
36	0.3 ± 0.05	0.5 ± 0.02	7.3 ± 0.06
39	0.3 ± 0.01	0.4 ± 0.03	7.3 ± 0.07
42	0.5 ± 0.04	0.3 ± 0.01	7.2 ± 0.02
45	0.3 ± 0.05	0.3 ± 0.05	7.3 ± 0.01
48	0.4 ± 0.01	0.2 ± 0.01	7.6 ± 0.00
51	0.3 ± 0.07	0.2 ± 0.00	7.5 ± 0.01

Table C.6.7 Mean ± standard error for pH, total iron, and toluene concentrations in mesocosms with magnetite amendment

Time (days)	Total Fe (mM)	Toluene (mM)	pH
0	0.2 ± 0.06	0.6 ± 0.05	7.7 ± 0.02
3	0.3 ± 0.05	0.3 ± 0.10	7.7 ± 0.01
6	0.2 ± 0.01	0.1 ± 0.07	7.5 ± 0.00
9	0.2 ± 0.03	0.1 ± 0.04	7.5 ± 0.00

Time (days)	Total Fe (mM)	Toluene (mM)	pH
12	0.3 ± 0.01	0.0 ± 0.10	7.4 ± 0.01
15	0.3 ± 0.01	0.0 ± 0.00	7.6 ± 0.03
18	0.4 ± 0.00	0.5 ± 0.05	7.4 ± 0.01
21	0.4 ± 0.00	0.2 ± 0.17	7.6 ± 0.08
24	0.3 ± 0.01	0.2 ± 0.07	7.5 ± 0.02
27	0.3 ± 0.03	0.2 ± 0.03	7.4 ± 0.01
30	0.2 ± 0.01	0.0 ± 0.03	7.4 ± 0.02
33	0.3 ± 0.05	0.0 ± 0.00	7.5 ± 0.01
36	0.3 ± 0.01	0.7 ± 0.02	7.4 ± 0.02
39	0.3 ± 0.05	0.5 ± 0.05	7.3 ± 0.03
42	0.6 ± 0.02	0.4 ± 0.08	7.3 ± 0.01
45	0.2 ± 0.0	0.4 ± 0.09	7.4 ± 0.01
48	0.3 ± 0.01	0.3 ± 0.07	7.4 ± 0.01
51	0.3 ± 0.01	0.3 ± 0.04	7.4 ± 0.04

Table C.6.8 Mean ± standard error for pH, total iron, and toluene concentrations in mesocosms with ferrihydrite amendment

Time (days)	Total Fe (mM)	Toluene (mM)	pH
0	0.4 ± 0.10	0.2 ± 0.01	6.5 ± 0.07
3	0.5 ± 0.10	0.1 ± 0.13	6.3 ± 0.09
6	0.4 ± 0.13	0.0 ± 0.00	6.2 ± 0.08
9	0.4 ± 0.14	0.0 ± 0.00	6.1 ± 0.17
12	0.5 ± 0.13	0.0 ± 0.00	5.6 ± 0.32
15	0.5 ± 0.12	0.0 ± 0.00	5.5 ± 0.15
18	0.4 ± 0.10	0.3 ± 0.06	6.4 ± 0.09
21	0.6 ± 0.13	0.5 ± 0.02	6.2 ± 0.07
24	0.5 ± 0.13	0.5 ± 0.03	6.3 ± 0.05
27	0.5 ± 0.14	0.5 ± 0.03	6.0 ± 0.05
30	0.5 ± 0.16	0.5 ± 0.04	6.6 ± 0.08
33	0.5 ± 0.12	0.4 ± 0.05	5.9 ± 0.08

Table C.6.9 Mean \pm standard error for pH, total iron, and toluene concentrations in mesocosms with lepidocrocite amendment

Time (days)	Total Fe (mM)	Toluene (mM)	pH
0	0.3 \pm 0.06	0.3 \pm 0.01	8.4 \pm 0.04
3	0.4 \pm 0.05	0.4 \pm 0.02	8.3 \pm 0.03
6	0.3 \pm 0.01	0.4 \pm 0.02	8.2 \pm 0.05
9	0.3 \pm 0.03	0.4 \pm 0.02	8.5 \pm 0.07
12	0.3 \pm 0.01	0.4 \pm 0.04	8.4 \pm 0.05
15	0.0 \pm 0.00	0.4 \pm 0.03	8.3 \pm 0.04

Table C.6.10 Mean \pm standard error for pH, total iron, and toluene concentrations in mesocosms with Soil 1 amendment

Time (days)	Total Fe (mM)	Toluene (mM)	pH
0	0.2 \pm 0.02	0.2 \pm 0.03	7.6 \pm 0.03
3	0.3 \pm 0.01	0.1 \pm 0.04	7.1 \pm 0.03
6	0.4 \pm 0.01	0.1 \pm 0.04	7.5 \pm 0.02
9	0.5 \pm 0.02	0.1 \pm 0.04	7.1 \pm 0.02
12	0.2 \pm 0.02	0.1 \pm 0.07	7.5 \pm 0.06
15	0.3 \pm 0.01	0.0 \pm 0.00	7.6 \pm 0.03
18	0.4 \pm 0.03	0.7 \pm 0.04	7.1 \pm 0.09
21	0.4 \pm 0.02	0.4 \pm 0.05	7.0 \pm 0.03
24	0.4 \pm 0.01	0.4 \pm 0.09	7.0 \pm 0.03
27	0.3 \pm 0.03	0.2 \pm 0.03	7.0 \pm 0.03
30	0.3 \pm 0.01	0.3 \pm 0.03	6.8 \pm 0.05
33	0.3 \pm 0.01	0.3 \pm 0.04	6.7 \pm 0.06

Table C.6.11 Mean \pm standard error for pH, total iron, and toluene concentrations in mesocosms with Soil 2 amendment

Time (days)	Total Fe (mM)	Toluene (mM)	pH
0	0.2 \pm 0.01	0.3 \pm 0.09	7.7 \pm 0.01
3	0.2 \pm 0.03	0.2 \pm 0.10	7.4 \pm 0.12
6	0.3 \pm 0.01	0.1 \pm 0.05	7.5 \pm 0.02
9	0.4 \pm 0.01	0.1 \pm 0.06	7.3 \pm 0.00

Time (days)	Total Fe (mM)	Toluene (mM)	pH
12	0.2 ± 0.05	0.1 ± 0.03	7.5 ± 0.05
15	0.2 ± 0.02	0.1 ± 0.03	7.4 ± 0.04
18	0.4 ± 0.04	0.6 ± 0.08	7.2 ± 0.06
21	0.4 ± 0.02	0.4 ± 0.07	7.3 ± 0.04
24	0.3 ± 0.00	0.1 ± 0.06	7.0 ± 0.01
27	0.3 ± 0.04	0.2 ± 0.07	7.0 ± 0.03
30	0.3 ± 0.01	0.2 ± 0.07	6.9 ± 0.04
33	0.3 ± 0.02	0.1 ± 0.06	6.8 ± 0.05

Table C.6.12 Mean ± standard error for pH, total iron, and toluene concentrations in mesocosms with Soil 3 amendment

Time (days)	Total Fe (mM)	Toluene (mM)	pH
0	0.3 ± 0.03	0.8 ± 0.02	7.7 ± 0.02
3	0.2 ± 0.00	0.5 ± 0.02	7.6 ± 0.02
6	0.2 ± 0.01	0.4 ± 0.02	7.7 ± 0.06
9	0.2 ± 0.01	0.1 ± 0.01	7.8 ± 0.09
12	0.2 ± 0.02	0.0 ± 0.00	7.9 ± 0.07
15	0.2 ± 0.01	0.0 ± 0.00	8.0 ± 0.12
18	0.2 ± 0.03	0.6 ± 0.03	7.3 ± 0.01
21	0.2 ± 0.01	0.4 ± 0.06	7.4 ± 0.02
24	0.2 ± 0.01	0.2 ± 0.06	7.5 ± 0.02
27	0.2 ± 0.01	0.2 ± 0.01	7.5 ± 0.03
30	0.2 ± 0.02	0.1 ± 0.07	7.6 ± 0.00
33	0.1 ± 0.02	0.2 ± 0.02	7.6 ± 0.01

C.6.6 Sequential chemical extractions

Table C.6.13 Mean \pm standard error of operationally-defined iron pools in the starting and incubated material in the un-amended live and active control mesocosms

Mesocosms	Operationally-defined iron pool				
	Fe _{total} (mg/kg)	Fe _{er} (mg/kg)	Fe _{carb} (mg/kg)	Fe _{red} (mg/kg)	Fe _{mag} (mg/kg)
Starting soil	10,181.7 \pm 370.5	6,736.3 \pm 270.7	196.1 \pm 11.4	2,504.4 \pm 1,445.9	277.7 \pm 24.4
Un-amended soil (live control)	9,023.3 \pm 1,454.2	4,711.6 \pm 579.7	196.1 \pm 11.4	2,308.1 \pm 343.3	238.9 \pm 45.0
Un-amended (active control)	10,702.8 \pm 918.0	4,387.7 \pm 557.5	5,252.1 \pm 291.8	375.6 \pm 20.8	253.2 \pm 32.3

C.6.7 Stable carbon isotope analysis

Table C.6.14 Mean \pm standard error of $\delta^{13}\text{C}$ and carbonate carbon (mg per g of sample) of the starting and incubated soil material (starting soil material was not analysed in triplicate)

Mesocosms	Fast-reacting soil carbonate pool		Slow-reacting soil carbonate pool	
	Carbonate carbon (mg/g)	$\delta^{13}\text{C}$ (‰)	Carbonate carbon (mg/g)	$\delta^{13}\text{C}$ (‰)
Starting soil	0.04	-9.06	0.005	-19.49
Un-amended soil (live control)	0.04 \pm 0.009	-15.20 \pm 0.990	0.03 \pm 0.002	-16.10 \pm 0.759
Un-amended (active control)	0.02 \pm 0.004	-17.71 \pm 0.375	0.03 \pm 0.002	-21.53 \pm 3.590
Hematite-amended soil	0.04 \pm 0.018	-22.70 \pm 2.829	0.03 \pm 0.010	-14.13 \pm 4.250
Hematite mineral	0.00 \pm 0.000	0.00 \pm 0.000	0.00 \pm 0.000	0.00 \pm 0.000
Goethite-amended soil	0.04 \pm 0.002	-14.30 \pm 0.173	0.02 \pm 0.006	-16.85 \pm 0.087
Goethite mineral	0.005 \pm 0.001	-17.50 \pm 0.000	0.004 \pm 0.001	
Magnetite-amended soil	0.06 \pm 0.002	-10.90 \pm 0.072	0.03 \pm 0.003	-13.40 \pm 3.434
Magnetite mineral	0.98 \pm 0.161	-4.60 \pm 0.144	0.05 \pm 0.016	-11.15 \pm 3.666
Ferrihydrite-amended soil	0.13 \pm 0.086	-9.40 \pm 1.830	0.09 \pm 0.027	-11.33 \pm 1.544
Lepidocrocite-amended soil	0.04 \pm 0.001	-13.10 \pm 3.360	0.03 \pm 0.000	-15.50 \pm 1.328

Mesocosms	Fast-reacting soil carbonate pool		Slow-reacting soil carbonate pool	
S₁ soil-amended material	0.01 ± 0.000	-11.60 ± 0.346	0.01 ± 0.000	-13.65 ± 0.144
S₂ soil-amended material	0.59 ± 0.108	-5.70 ± 0.098	0.44 ± 0.019	-1.43 ± 0.054

C.6.8 Reaction kinetics - zeroth and first order rate fittings

Table C.6.15 Zeroth and first order rate fittings for mesocosms with no amendment (S_T)

Mesocosm	Zeroth order rate constant, k ₁ (mg ⁻¹ l ¹ day ⁻¹)	First order rate constant, k ₂ (day ⁻¹)
S_T -1	1.76	0.04
S_T -2	3.95	0.12
S_T -3	3.43	0.11
MEAN	3.05 ± 0.54	0.09 ± 0.02
Second Spike Period		
S_T -1	3.45	0.05
S_T -2	2.17	0.01
S_T -3	0.24	0.11
MEAN	1.95 ± 0.76	0.06 ± 0.02
Third Spike Period		
S_T -1	4.29	0.08
S_T -2	2.19	0.06
S_T -3	4.31	0.08
MEAN	3.60 ± 0.57	0.06 ± 0.01

Table C.6.16 Zeroth and first order rate fittings for mesocosms with hematite amendment

Mesocosms	Zeroth order rate constant, k ₁ (mg ⁻¹ l ¹ day ⁻¹)			First order rate constant, k ₂ (day ⁻¹)			
	First Spike Period			First Spike Period			
S_T -1	1.76	H_M -1	4.05	S_T -1	0.04	H_M -1	0.16
S_T -2	3.95	H_M -2	3.54	S_T -2	0.12	H_M -2	0.13
S_T -3	3.43	H_M -3	4.35	S_T -3	0.11	H_M -3	0.31
MEAN	3.05 ± 0.54		3.98 ± 0.19		0.09 ± 0.02		0.20 ± 0.05

Mesocosms	Zeroth order rate constant, k_1 ($\text{mg}^{-1} \text{l}^{-1} \text{day}^{-1}$)				First order rate constant, k_2 (day^{-1})			
	Second Spike Period				Second Spike Period			
S_T -1	3.45	H_M -1	5.06	S_T -1	0.05	H_M-1	0.32	
S_T -2	2.17	H_M -2	3.81	S_T -2	0.01	H_M-2	0.09	
S_T -3	0.24	H_M -3	2.96	S_T -3	0.11	H_M-3	0.13	
MEAN	1.95 ± 0.76		3.94 ± 0.50		0.06 ± 0.02		0.18 ± 0.06	
	Third Spike Period				Third Spike Period			
S_T -1	4.29	H_M -1	4.85	S_T -1	0.08	H_M-1	0.13	
S_T -2	2.19	H_M -2	4.50	S_T -2	0.06	H_M-2	0.14	
S_T -3	4.31	H_M -3	3.05	S_T -3	0.08	H_M-3	0.23	
MEAN	3.60 ± 0.57		4.13 ± 0.45		0.07 ± 0.01		0.17 ± 0.03	

Table C.6.17 Zeroth and first order rate fittings for mesocosms with goethite amendment

Mesocosms	Zeroth order rate constant, k_1 ($\text{mg}^{-1} \text{l}^{-1} \text{day}^{-1}$)				First order rate constant, k_2 (day^{-1})			
	First Spike Period				First Spike Period			
S_T -1	1.76	G_E -1	2.33	S_T -1	0.04	G_E-1	0.07	
S_T -2	3.95	G_E -2	2.32	S_T -2	0.12	G_E -2	0.06	
S_T -3	3.43			S_T -3	0.11			
MEAN	3.05 ± 0.54		2.33 ± 0.003		0.09 ± 0.02		0.07 ± 0.003	
	Second Spike Period				Second Spike Period			
S_T -1	3.45	G_E -1	4.85	S_T -1	0.05	G_E -1	0.12	
S_T -2	2.17	G_E -2	3.88	S_T -2	0.01	G_E -2	0.38	
S_T -3	0.24			S_T -3	0.11			
MEAN	1.95 ± 0.76		4.37 ± 0.280		0.06 ± 0.02		0.25 ± 0.0075	
	Third Spike Period				Third Spike Period			
S_T -1	4.29	G_E -1	1.99	S_T -1	0.08	G_E -1	0.07	
S_T -2	2.19	G_E -2	1.68	S_T -2	0.06	G_E -2	0.08	
S_T -3	4.31			S_T -3	0.08			
MEAN	3.60 ± 0.57		1.84 ± 0.089		0.07 ± 0.01		0.08 ± 0.003	

Table C.6.18 Zeroth and first order rate fittings for mesocosms with magnetite amendment

Mesocosms	Zeroth order rate constant, k_1 ($\text{mg}^{-1} \text{l}^{-1} \text{day}^{-1}$)				First order rate constant, k_2 (day^{-1})			
	First Spike Period				First Spike Period			
S_T -1	1.76	M_T-1	4.66	S_T -1	0.04	M_T.1	0.15	
S_T -2	3.95	M_T-2	2.88	S_T -2	0.12	M_T -2	0.13	
S_T -3	3.43	M_T-3	2.89	S_T -3	0.11	M_T -3	0.15	

Mesocosms	Zeroth order rate constant, k_1 ($\text{mg}^{-1} \text{l}^{-1} \text{day}^{-1}$)				First order rate constant, k_2 (day^{-1})			
MEAN	3.05 ± 0.54		3.48 ± 0.48		0.09 ± 0.02		0.14 ± 0.01	
	Second Spike Period				Second Spike Period			
S_T -1	3.45	M_T -1	4.00	S_T -1	0.05	M_T -1	0.15	
S_T -2	2.17	M_T -2	1.85	S_T -2	0.01	M_T -2	0.13	
S_T -3	0.24	M_T -3	2.03	S_T -3	0.11	M_T -3	0.15	
MEAN	1.95 ± 0.76		2.63 ± 0.56		0.06 ± 0.02		0.14 ± 0.01	
	Third Spike Period				Third Spike Period			
S_T -1	4.29	M_T -1	2.37	S_T -1	0.08	M_T -1	0.04	
S_T -2	2.19	M_T -2	2.28	S_T -2	0.06	M_T -2	0.07	
S_T -3	4.31	M_T -3	3.02	S_T -3	0.08	M_T -3	0.12	
MEAN	3.60 ± 0.57		2.56 ± 0.19		0.07 ± 0.01		0.08 ± 0.02	

Table C.6.19 Zeroth and first order rate fittings for mesocosms with ferrihydrite amendment

Mesocosms	Zeroth order rate constant, k_1 ($\text{mg}^{-1} \text{l}^{-1} \text{day}^{-1}$)				First order rate constant, k_2 (day^{-1})			
	First Spike Period				First Spike Period			
S_T -1	1.76	F_H -1	0.81	S_T -1	0.04	F_H -1	0.19	
S_T -2	3.95	F_H -2	1.19	S_T -2	0.12	F_H -2	0.27	
S_T -3	3.43	F_H -3	1.29	S_T -3	0.11	F_H -3	0.28	
MEAN	3.05 ± 0.54		1.1 ± 0.12		0.09 ± 0.02		0.25 ± 0.02	
	Second Spike Period				Second Spike Period			
S_T -1	3.45	F_H -1	0.11	S_T -1	0.05	F_H -1	0.01	
S_T -2	2.17	F_H -2	1.60	S_T -2	0.01	F_H -2	0.09	
S_T -3	0.24	F_H -3	0.39	S_T -3	0.11	F_H -3	0.02	
MEAN	0.95 ± 1.76		0.70 ± 0.37		0.06 ± 0.02		0.04 ± 0.02	

Table C.6.20 Zeroth and first order rate fittings for mesocosms with lepidocrocite amendment

Mesocosms	Zeroth order rate constant, k_1 ($\text{mg}^{-1} \text{l}^{-1} \text{day}^{-1}$)				First order rate constant, k_2 (day^{-1})			
	First Spike Period				First Spike Period			
S_T -1	1.76	L_P -1	0.07	S_T -1	0.04	L_P -1	-	
S_T -2	3.95	L_P -2	1.02	S_T -2	0.12	L_P -2	-	
S_T -3	3.43	L_P -3	0.56	S_T -3	0.11	L_P -3	-	
MEAN	3.05 ± 0.54		0.55 ± 0.22		0.09 ± 0.02			

Table C.6.21 Zeroth and first order rate fittings for mesocosms amended with Soil 1

Mesocosms	Zeroth order rate constant, k_1 ($\text{mg}^{-1} \text{ l}^{-1} \text{ day}^{-1}$)				First order rate constant, k_2 (day^{-1})			
	First Spike Period				First Spike Period			
S_T -1	1.76	S_I-1	0.98	S_T -1	0.04	S_I-1	0.20	
S_T -2	3.95	S_I-2	0.44	S_T -2	0.12	S_I-2	0.01	
S_T -3	3.43	S_I-3	0.75	S_T -3	0.11	S_I-3	0.07	
MEAN	3.05 ± 0.54		0.72 ± 0.13		0.09 ± 0.02		0.09 ± 0.05	
	Second Spike Period				Second Spike Period			
S_T -1	3.45	S_I-1	3.54	S_T -1	0.05	S_I-1	0.12	
S_T -2	2.17	S_I-2	2.62	S_T -2	0.01	S_I-2	0.07	
S_T -3	0.24	S_I-3	0.22	S_T -3	0.11	S_I-3	0.08	
MEAN	1.95 ± 0.76		2.13 ± 0.81		0.06 ± 0.02		0.09 ± 0.01	

Table C.6.22 Zeroth and first order rate fittings for mesocosms amended with Soil 2

Mesocosms	Zeroth order rate constant, k_1 ($\text{mg}^{-1} \text{ l}^{-1} \text{ day}^{-1}$)				First order rate constant, k_2 (day^{-1})			
	First Spike Period				First Spike Period			
S_T -1	1.76	S₂-1	1.73	S_T -1	0.04	S₂-1	0.1	
S_T -2	3.95	S₂-2	0.51	S_T -2	0.12	S₂-2	0.02	
S_T -3	3.43	S₂-3	1.58	S_T -3	0.11	S₂-3	0.28	
MEAN	3.05 ± 0.54		1.27 ± 0.31		0.09 ± 0.02		0.13 ± 0.06	
	Second Spike Period				Second Spike Period			
S_T -1	3.45	S₂-1	2.78	S_T -1	0.05	S₂-1	0.1	
S_T -2	2.17	S₂-2	1.71	S_T -2	0.01	S₂-2	0.06	
S_T -3	0.24	S₂-3	2.25	S_T -3	0.11	S₂-3	0.34	
MEAN	1.95 ± 0.76		2.25 ± 0.25		0.06 ± 0.02		0.17 ± 0.07	

Table C.6.23 Zeroth and first order rate fittings for mesocosms amended with Soil 3

Mesocosms	Zeroth order rate constant, k_1 ($\text{mg}^{-1} \text{ l}^{-1} \text{ day}^{-1}$)				First order rate constant, k_2 (day^{-1})			
	First Spike Period				First Spike Period			
S_T -1	1.76	S₃-1	4.7	S_T -1	0.04	S₃-1	0.32	
S_T -2	3.95	S₃-2	4.84	S_T -2	0.12	S₃-2	0.34	
S_T -3	3.43			S_T -3	0.11			
MEAN	3.05 ± 0.54		1.27 ± 0.31		0.09 ± 0.02		0.33 ± 0.01	
	Second Spike Period				Second Spike Period			
S_T -1	3.45	S₃-1	2.93	S_T -1	0.05	S₃-1	0.94	
S_T -2	2.17	S₃-2	0.62	S_T -2	0.01	S₃-2	0.72	

Mesocosms	Zeroth order rate constant, k_1 ($\text{mg}^{-1} \text{l}^{-1} \text{day}^{-1}$)		First order rate constant, k_2 (day^{-1})	
S _T -3	0.24		S _T -3	
MEAN	1.95 ± 0.76	1.78 ± 1.16	0.11	0.06 ± 0.02
				0.83 ± 0.06

Table C.6.24 Mean ± standard error of zeroth and first order rate fittings

Meso cosm	Zeroth order rate constant, k_1 ($\text{mg}^{-1} \text{l}^{-1} \text{day}^{-1}$)	First order rate constant, k_2 (day^{-1})	Zeroth order rate constant, k_1 ($\text{mg}^{-1} \text{l}^{-1} \text{day}^{-1}$)	First order rate constant, k_2 (day^{-1})	Zeroth order rate constant, k_1 ($\text{mg}^{-1} \text{l}^{-1} \text{day}^{-1}$)	First order rate constant, k_2 (day^{-1})
	First Spike		Second Spike		Third Spike	
S _T	3.05 ± 0.54	0.09 ± 0.02	1.95 ± 0.76	0.06 ± 0.02	3.60 ± 0.57	0.06 ± 0.01
H _M	3.98 ± 0.19	0.20 ± 0.05	3.94 ± 0.50	0.18 ± 0.06	4.13 ± 0.45	0.17 ± 0.03
G _E	2.33 ± 0.003	0.07 ± 0.003	4.37 ± 0.280	0.25 ± 0.0075	1.84 ± 0.089	0.08 ± 0.003
M _T	3.48 ± 0.48	0.14 ± 0.01	2.63 ± 0.56	0.14 ± 0.01	2.56 ± 0.19	0.08 ± 0.02
F _H	1.1 ± 0.12	0.25 ± 0.02	0.70 ± 0.37	0.04 ± 0.02	-	-
L _P	0.55 ± 0.22	-	-	-	-	-
S ₁	0.72 ± 0.13	0.09 ± 0.05	2.13 ± 0.81	0.09 ± 0.01	-	-
S ₂	1.27 ± 0.31	0.13 ± 0.06	2.25 ± 0.25	0.17 ± 0.07	-	-
S ₃	1.27 ± 0.31	0.33 ± 0.01	1.78 ± 1.16	0.83 ± 0.06	-	-

† This is with the exception of the GO and SD 3 mesocosms which only had two replicates due to blockage of tubings during sampling

Table C.6.25 Toluene removal rates in the mesocosms (expressed per square metre of mesocosm soil and obtained as the average of three replicates)

Mesocosms	First Spike Period ($\text{m}^2 \text{day}^{-1}$)	Second Spike Period ($\text{m}^2 \text{day}^{-1}$)	Third Spike Period ($\text{m}^2 \text{day}^{-1}$)
H _M	2.4 x 10 ⁻⁴	2.4 x 10 ⁻⁴	2.2 x 10 ⁻⁴
G _E	4.2 x 10 ⁻⁴	4.2 x 10 ⁻⁴	1.3 x 10 ⁻⁴
M _T	2.8 x 10 ⁻⁴	2.8 x 10 ⁻⁴	1.6 x 10 ⁻⁴
F _H	5.7 x 10 ⁻⁵	5.7 x 10 ⁻⁴	-
L _P	-	-	-
S _I	1.6 x 10 ⁻⁴	1.6 x 10 ⁻⁴	-

Mesocosms	First Spike Period (m ² day ⁻¹)	Second Spike Period (m ² day ⁻¹)	Third Spike Period (m ² day ⁻¹)
S ₂	6.8 x 10 ⁻⁴	8.9 x 10 ⁻⁴	-
S ₃	2.0 x 10 ⁻⁴	4.9 x 10 ⁻⁴	-

C.6.9 BET surface areas of the starting and incubated soils

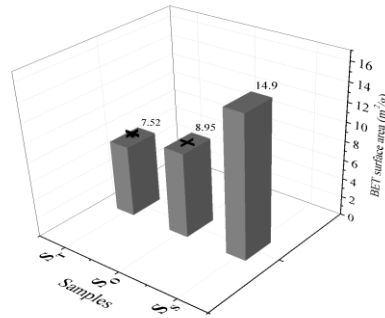


Figure C.6.1 Results of BET analysis for i) the starting soil material (S_S) ii) incubated material from the mesocosms with soil and water (S_O) and iii) incubated material from the mesocosms with no amendment (S_T)

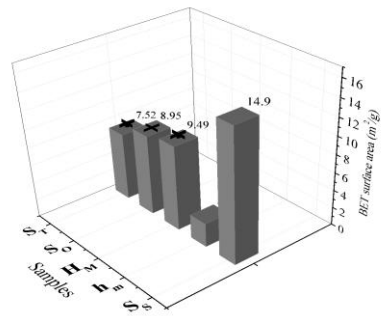


Figure C.6.2 Results of BET analysis for i) the starting soil material (S_S) ii) incubated material from the mesocosms with soil and water (S_O) iii) incubated material from the mesocosms with no amendment (S_T) iv) incubated material from the mesocosms with hematite mineral amendment (H_M) v) hematite mineral amendment (h_m)

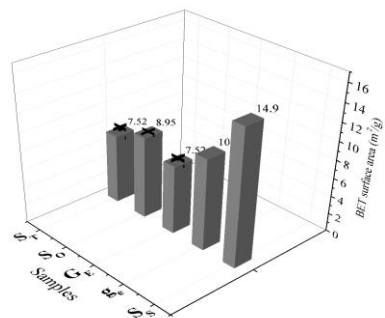


Figure C.6.3 Results of BET analysis for i) the starting soil material (S_S) ii) incubated material from the mesocosms with soil and water (S_O) iii) incubated material from the mesocosms with no amendment (S_T) iv) incubated material from the mesocosms with goethite mineral amendment (G_E) v) goethite mineral amendment (g_e)

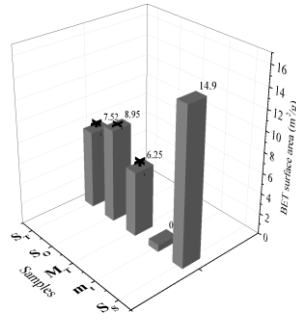


Figure C.6.4 Results of BET analysis for i) the starting soil material (S_s) ii) incubated material from the mesocosms with soil and water (S_o) iii) incubated material from the mesocosms with no amendment (S_T) iv) incubated material from the mesocosms with magnetite mineral amendment (M_T) v) magnetite mineral amendment (g_e)

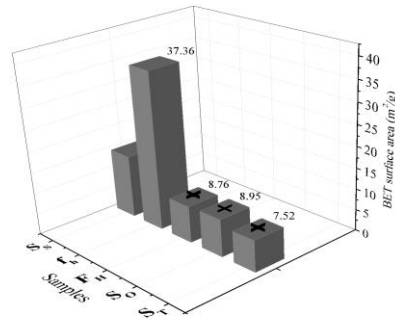


Figure C.6.6 Results of BET analysis for i) the starting soil material (S_s) ii) incubated material from the mesocosms with soil and water (S_o) iii) incubated material from the mesocosms with no amendment (S_T) iv) incubated material from the mesocosms with ferrihydrite mineral amendment (F_H) v) ferrihydrite amendment (f_h)

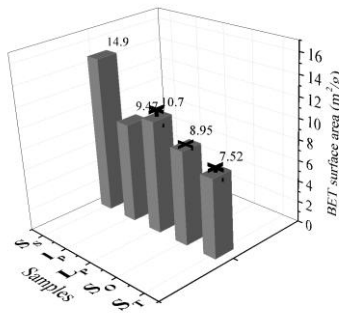


Figure C.6.7 Results of BET analysis for i) the starting soil material (S_s) ii) incubated material from the mesocosms with soil and water (S_o) iii) incubated material from the mesocosms with no amendment (S_T) iv) incubated material from the mesocosms with lepidocrocite mineral amendment (L_P) v) lepidocrocite amendment (l_p)

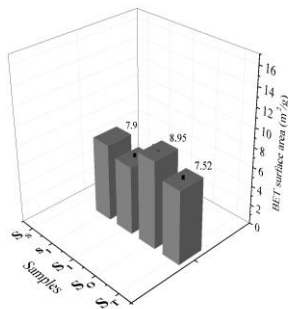


Figure C.6.8 Results of BET analysis for i) the starting soil material (S_s) ii) incubated material from the mesocosms with soil and water (S_o) iii) incubated material from the mesocosms with no amendment (S_T) iv) incubated material from the mesocosms amended with Soil 1 (S₁) v) soil 1 sample (s₁)

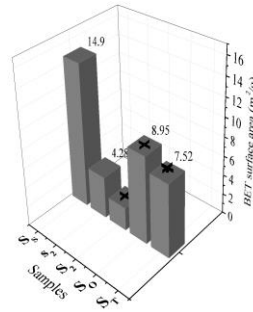


Figure C.6.9 Results of BET analysis for i) the starting soil material (S_s) ii) incubated material from the mesocosms with soil and water (S_o) iii) incubated material from the mesocosms with no amendment (S_t) iv) incubated material from the mesocosms amended with Soil 2 (S₂) v) soil 2 sample (s₂)

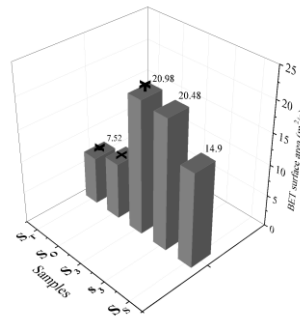


Figure C.6.10 Results of BET analysis for i) the starting soil material (S_s) ii) incubated material from the mesocosms with soil and water (S_o) iii) incubated material from the mesocosms with no amendment (S_t) iv) incubated material from the mesocosms amended with Soil 3(S₃) v) Soil 3 sample (s₃)

C.7 Summary of observations and findings

Table C.7.1 Summary of findings - un-amended active mesocosms

Parameters observed	Findings
Rates of toluene degradation	Fastest during the third spike period and slowest during the second spike period
Amounts of toluene degraded	Highest during the first spike period. The second and third spike periods showed similar amounts of toluene removal
Time at which mesocosms were completely saturated with toluene	Occurred after the third toluene spike
Total dissolved iron concentrations	Progressively higher in control mesocosms; unchanged in the toluene-spiked mesocosms
Solid-phase iron	<p>Similar total iron content found in the starting material as well as material from the control mesocosms and active/toluene-spiked mesocosm</p> <p>The easily reducible, magnetite, pyrite and acid volatile sulphur fractions unaffected by incubation period in both control and active/toluene-spiked mesocosms</p> <p>A decrease in reducible oxide content was observed in the active/toluene-spiked material in comparison to the material from control mesocosms and starting soil material</p>

Parameters observed	Findings
	Similarly an increase in the carbonate-bound iron fraction was observed in the active/toluene-spiked material in comparison to the material from control mesocosms and starting soil material
pH after addition of first toluene spike	A 0.5-unit increase and 0.5-unit decrease in the pH of the control and active/toluene-spiked mesocosms respectively was observed. The pH however remained largely unchanged during the incubation period
Surface area at the end of incubation period	The toluene-spiked material was slightly lower in comparison to the material from the blank mesocosms however both mesocosm material had lower surface areas than the starting soil material

Table C.7.2 Summary of findings - un-amended vs. hematite-amended mesocosms

Parameters observed	Findings
Rates of toluene degradation	Faster rates were observed in hematite-amended mesocosms compared to un-amended mesocosms
Amounts of toluene degraded	A higher amount of toluene was degraded in the hematite-amended mesocosms
Time at which mesocosms were completely saturated with toluene	Both the un-amended and hematite-amended mesocosms were completely saturated after the addition of the third toluene spike
Total dissolved iron concentrations after addition of first toluene spike	Progressively lower total dissolved iron concentrations were observed during the first spike period, and were likely to be due to the presence of the hematite amendment
pH after addition of first toluene spike	The hematite-amended mesocosms showed slightly higher pH levels (+0.1 units)
Surface area at the end of incubation period	The surface area of the hematite-amended soil material was significantly lower than the starting soil material but slightly higher in hematite-amended soil material compared to soil material from un-amended mesocosms

Table C.7.3 Summary of findings - un-amended vs. goethite-amended mesocosms

Parameters observed	Findings
Rates of toluene degradation	There were no significant differences in rates of toluene degradation in both mesocosms
Amounts of toluene degraded	A higher amount of toluene was degraded in the goethite-amended mesocosms
Time at which mesocosms were completely saturated with toluene	Both the un-amended and goethite-amended mesocosms were completely saturated after the addition of the third toluene spike

Parameters observed	Findings
Total dissolved iron concentrations after addition of first toluene spike	Higher dissolved iron concentrations in goethite-amended mesocosms compared to the un-amended mesocosms
pH after addition of first toluene spike	Goethite-amended mesocosms showed slightly higher pH levels (+0.5 units)
Surface area at the end of incubation period	The surface area of the goethite-amended soil material was significantly lower than starting soil material but similar in comparison to soil material from un-amended mesocosms

Table C.7.4 Summary of findings - un-amended vs. magnetite-amended mesocosms

Parameters observed	Findings
Rates of toluene degradation	There were no significant differences observed in the rates of toluene degradation in both mesocosms
Amounts of toluene degraded	A higher amount of toluene was degraded in the magnetite-amended mesocosms
Time at which mesocosms were completely saturated with toluene	Both the un-amended and magnetite-amended mesocosms were completely saturated after the addition of the third toluene spike
Total dissolved iron concentrations after addition of first toluene spike	Similar iron concentrations were observed in the un-amended and magnetite-amended mesocosms
pH after addition of first toluene spike	The magnetite-amended mesocosms showed slightly higher pH levels (+0.2 units)
Surface area at the end of incubation period	The surface area of the magnetite-amended soil material was significantly lower than starting material and also lower in comparison to soil material from un-amended mesocosms

Table C.7.5 Summary of findings - un-amended vs. mesocosms with ferric citrate amendment

Parameters observed	Findings
Rates of toluene degradation	There were no significant differences observed in the rates of degradation in both mesocosms
Amounts of toluene degraded	A higher amount of toluene was degraded in the mesocosms with the ferric citrate amendment after the addition of the first toluene spike however a lower amount was degraded in these mesocosms after the addition of the second spike
Time at which mesocosms were completely saturated with toluene	The mesocosms with the ferric citrate amendment were saturated with toluene in less time (after the addition of the second toluene spike) in comparison with the un-amended mesocosms

Parameters observed	Findings
Total dissolved iron concentrations after addition of first toluene spike	Higher total dissolved iron concentrations were observed in the mesocosms amended with ferric citrate (+1.0 units), reflective of additional dissolved iron from the added ferric citrate solution
pH after addition of first toluene spike	Higher pH levels were observed in the mesocosms amended with ferric citrate (+1.0 units)
Surface area at the end of incubation period	The surface area of the ferric citrate-amended soil material was significantly lower than starting material but similar in comparison to soil material from un-amended mesocosms

Table C.7.6 Summary of findings - un-amended vs. ferrihydrite-amended mesocosms

Parameters observed	Findings
Rates of toluene degradation	Significantly lower rates were observed in mesocosms with the ferrihydrite amendment
Amounts of toluene degraded	A significantly higher amount of toluene was degraded in the mesocosms with the ferrihydrite amendment after the addition of the first toluene spike however a lower amount was degraded, in comparison, after the addition of the second spike
Time at which mesocosms were completely saturated with toluene	The mesocosms with the ferrihydrite amendment were saturated with toluene in less time (after the addition of the second toluene spike) in comparison with the un-amended mesocosms
Total dissolved iron concentrations after addition of first toluene spike	Similar iron concentrations were observed in both mesocosms
pH after addition of first toluene spike	Higher pH levels were observed in the mesocosms with the ferrihydrite amendment (+0.5 units) however a progressive decline in pH was observed as toluene was degraded
Surface area at the end of incubation period	The surface area of the ferrihydrite-amended soil material was significantly lower than starting material but higher in comparison to soil material from un-amended mesocosms

Table C.7.7 Summary of findings - un-amended vs. lepidocrocite-amended mesocosms

Parameters observed	Findings
Rates of toluene degradation	Significantly lower rates were observed in the mesocosms with the lepidocrocite amendment
Amounts of toluene degraded	The mesocosms with the lepidocrocite amendment did not support toluene degradation
Time at which mesocosms were completely saturated with toluene	N/A

Parameters observed	Findings
Total dissolved iron concentrations after addition of first toluene spike	Similar iron concentrations were observed in both mesocosm sets
pH after addition of first toluene spike	Higher pH levels were observed in the mesocosms with the ferrihydrite amendment (+1.0 unit)
Surface area at the end of incubation period	The surface area of the lepidocrocite-amended soil material was significantly lower than starting material but similar to the material from un-amended mesocosms

Table C.7.8 Summary of findings -un-amended vs. mesocosms amended with Soil 1

Parameters observed	Findings
Rates of toluene degradation	Significantly lower rates were observed in mesocosms with the contaminated soil amendment
Amounts of toluene degraded	A significantly higher amount of toluene was degraded in the mesocosms with the contaminated soil amendment after the addition of toluene
Time at which mesocosms were completely saturated with toluene	The mesocosms with the contaminated soil amendment were saturated with toluene in less time (after the addition of the second toluene spike) in comparison with the un-amended mesocosms
Total dissolved iron concentrations after addition of first toluene spike	Slightly lower total dissolved iron concentrations were observed in the mesocosms with the contaminated soil amendment, these concentrations were seen to increase progressively over the course of the experiments
pH after addition of first toluene spike	Similar pH levels were observed in both mesocosm sets
Surface area at the end of incubation period	The surface area of the soil-amended material was significantly lower than starting material but similar to soil material from un-amended mesocosms

Table C.7.9 Summary of findings - un-amended vs. mesocosms with Soil 2

Parameters observed	Findings
Rates of toluene degradation	The two mesocosm sets were observed to have degraded toluene at similar rates during the period of incubation
Amounts of toluene degraded	Both mesocosm sets degraded similar amounts of toluene during individual spike periods
Time at which mesocosms were completely saturated with toluene	The mesocosms with the soil amendment were saturated with toluene in less time (after the addition of the second toluene spike) in comparison with the un-amended mesocosms
Total dissolved iron concentrations after addition of first toluene spike	Slightly lower total dissolved iron concentrations were observed in the mesocosms with the soil amendment, these concentrations were seen to increase progressively over the course of the experiments

Parameters observed	Findings
pH after addition of first toluene spike	Similar pH levels were observed in both mesocosm sets at the start of the experiments however the pH in the soil-amended mesocosms declined steadily over the course of the experiments
Surface area at the end of incubation period	The surface area of the soil-amended material was significantly lower than both the starting soil material and soil material from un-amended mesocosms

Table C.7.10 Summary of findings - un-amended vs. mesocosms with Soil 3

Parameters observed	Findings
Rates of toluene degradation	The two mesocosm sets were observed to have degraded toluene at similar rates after the first toluene spike however the soil-amended mesocosms degraded toluene at higher rates after the addition of the second toluene spike
Amounts of toluene degraded	Both mesocosm sets degraded similar amounts of toluene after the addition of the first toluene spike however a slightly higher amount of toluene was degraded in the soil-amended mesocosms after the addition of the second spike
Time at which mesocosms were completely saturated with toluene	The mesocosms with the soil amendment were saturated with toluene in less time (after the addition of the second toluene spike) in comparison with the un-amended mesocosms
Total dissolved iron concentrations after addition of first toluene spike	Similar total dissolved iron concentrations were observed in both mesocosm sets
pH after addition of first toluene spike	Similar pH levels were observed in both mesocosm sets at the start of the experiments however the pH in the soil-amended mesocosms increased steadily over the course of the experiments
Surface area at the end of incubation period	The surface area of the soil-amended material was significantly lower than both the starting soil material and soil material from un-amended mesocosms

C.8 Combined concentration-time profiles

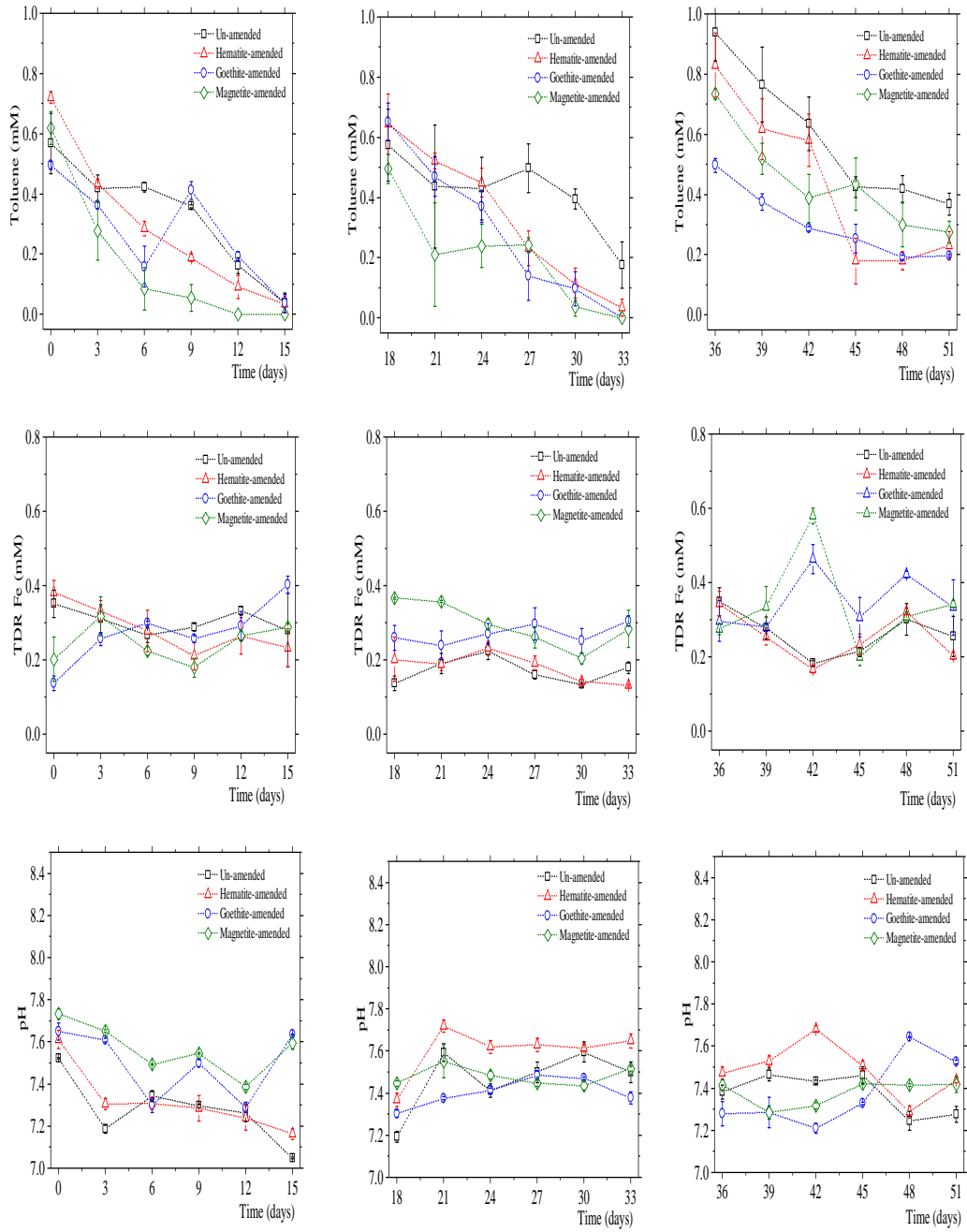


Figure C.8.1 Concentration-time profiles comparing toluene, total iron and pH in the un-amended mesocosms and mesocosms amended with the mesocosms amended with natural iron minerals

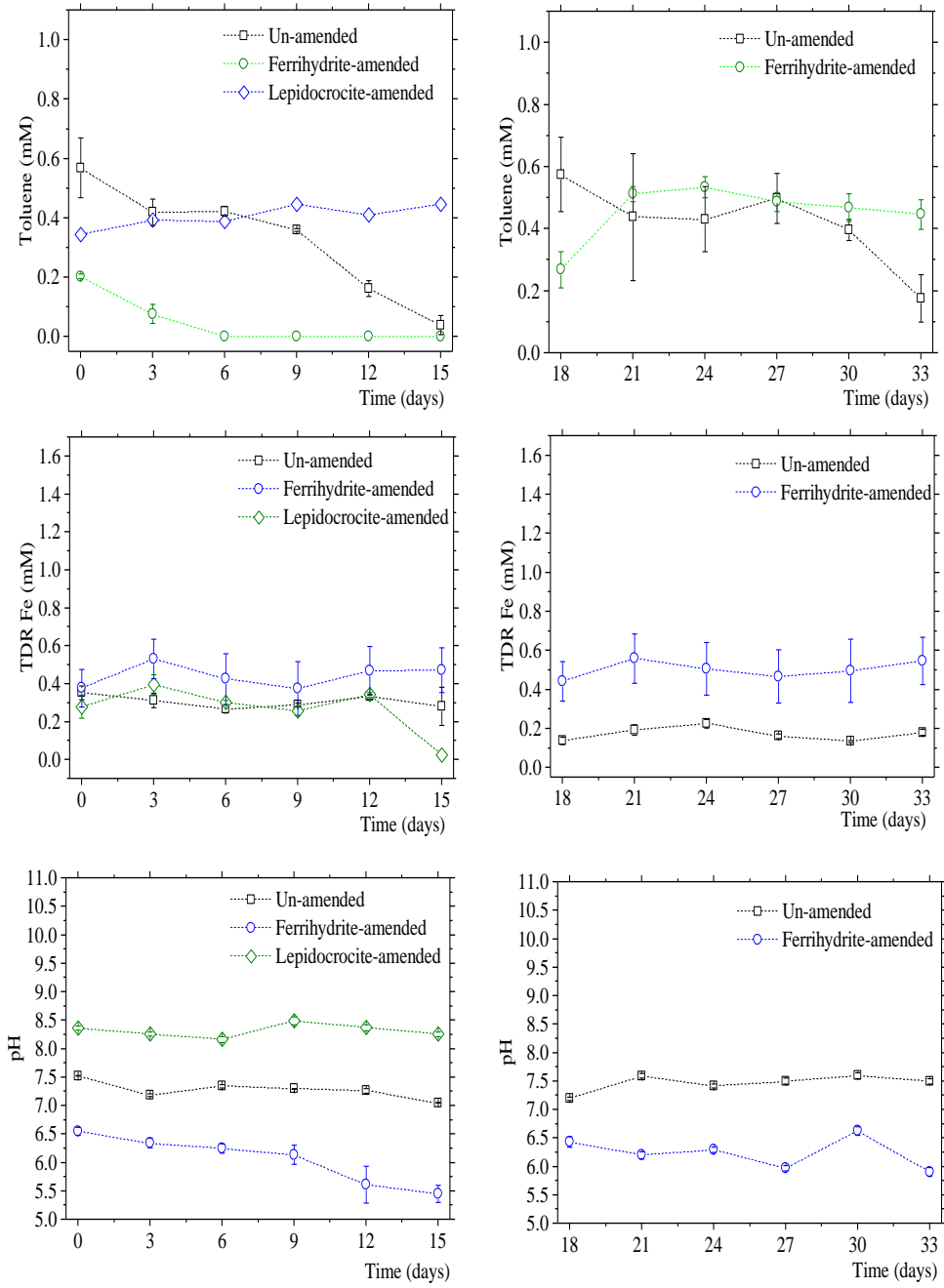


Figure C.8.2 Concentration-time profiles comparing toluene, total iron and pH in the un-amended mesocosms and mesocosms amended with the synthesised iron minerals

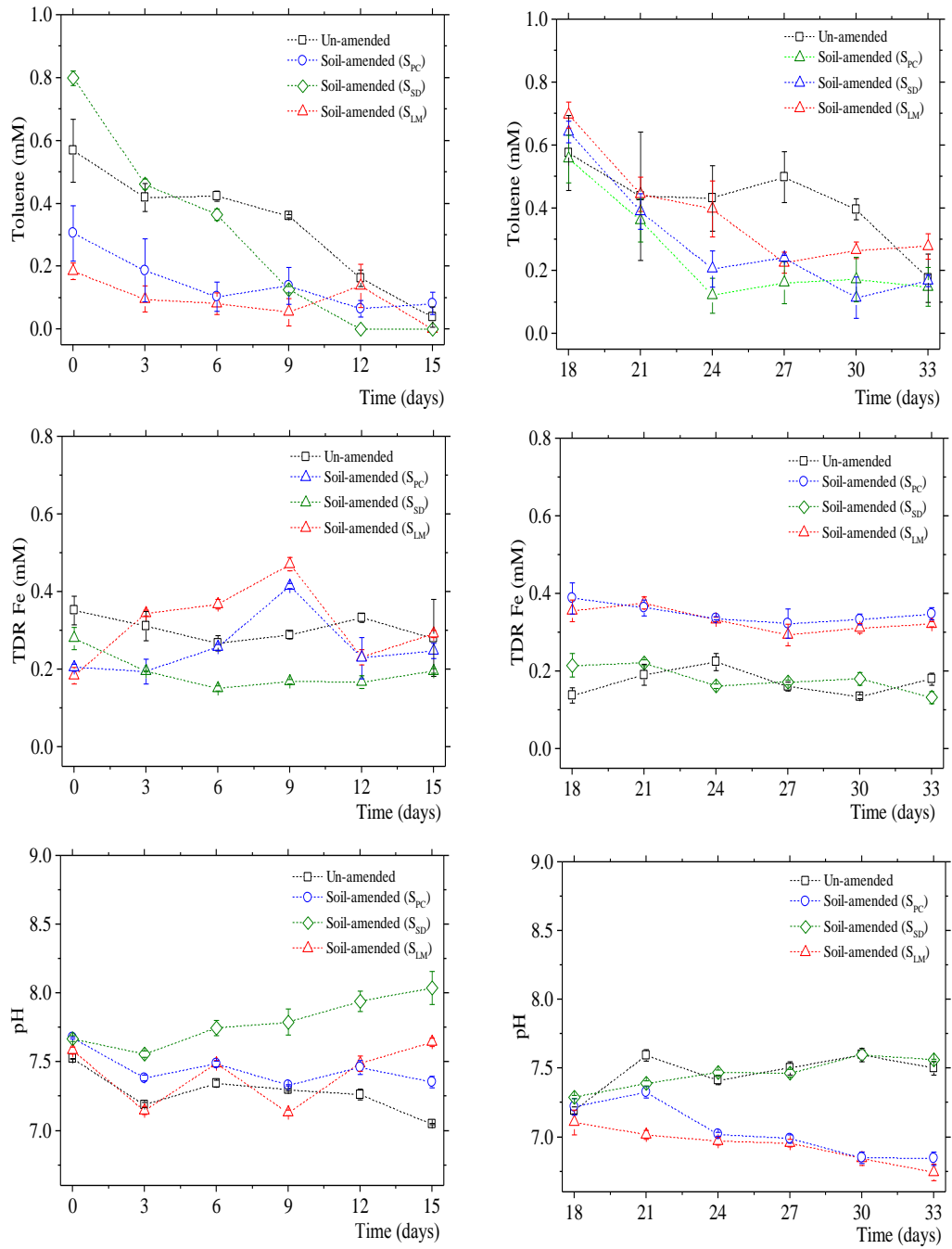


Figure C.8.3 Concentration-time profiles comparing toluene, total iron and pH in the un-amended mesocosms and mesocosms amended with the soil-amended mesocosms

C.9 Statistical analysis

C.9.1 Descriptive statistics

Table C.9.1 Descriptive statistics

(Period A)

		Group	Statistic	Std. Error	
Toluene	Fh-amd	Mean	.0467	.01918	
		95% Confidence Interval for Mean	Lower Bound	.0062	
			Upper Bound	.0871	
		Variance	.007		
		Std. Deviation	.08139		
		Skewness	1.393	.536	
		Kurtosis	.301	1.038	
		Ge-amd	Mean	.2767	.04112
			95% Confidence Interval for Mean	Lower Bound	.1899
			Upper Bound	.3634	
	Variance		.030		
	Std. Deviation		.17446		
	Skewness		-.313	.536	
	Hm-amd	Kurtosis	-1.052	1.038	
		Mean	.2933	.05737	
		95% Confidence Interval for Mean	Lower Bound	.1723	
			Upper Bound	.4144	
		Median	.2200		
		Variance	.059		
		Std. Deviation	.24341		
		Skewness	.722	.536	
Kurtosis		-.424	1.038		

Group		Statistic	Std. Error
Lp-amd	Mean	.4039	.01336
	95% Confidence Interval for Mean	Lower Bound	.3757
		Upper Bound	.4321
	Variance	.003	
	Std. Deviation	.05669	
	Skewness	.340	.536
	Kurtosis	-.852	1.038
	Mt-amd	Mean	.1728
95% Confidence Interval for Mean		Lower Bound	.0497
		Upper Bound	.2958
Variance		.061	
Std. Deviation		.24748	
Skewness		1.235	.536
Kurtosis		.192	1.038
S1-amd		Mean	.0928
	95% Confidence Interval for Mean	Lower Bound	.0454
		Upper Bound	.1402
	Variance	.009	
	Std. Deviation	.09529	
	Skewness	.459	.536
	Kurtosis	-.942	1.038
	S2-amd	Mean	.1472
95% Confidence Interval for Mean		Lower Bound	.0760
		Upper Bound	.2185
Variance		.021	

Group		Statistic	Std. Error
	Std. Deviation	.14327	
	Skewness	1.077	.536
	Kurtosis	.638	1.038
S3-amd	Mean	.1517	.04558
	95% Confidence Interval for Mean	Lower Bound	.0555
		Upper Bound	.2478
	Variance	.037	
	Std. Deviation	.19340	
	Skewness	2.471	.536
	Kurtosis	6.034	1.038
Unamd2	Mean	.3294	.04736
	95% Confidence Interval for Mean	Lower Bound	.2295
		Upper Bound	.4294
	Variance	.040	
	Std. Deviation	.20092	
	Skewness	.082	.536
	Kurtosis	-.181	1.038
Fe	Fh-amd	Mean	.4389
	95% Confidence Interval for Mean	Lower Bound	.3243
		Upper Bound	.5535
	Variance	.053	
	Std. Deviation	.23044	
	Skewness	.533	.536
	Kurtosis	-1.148	1.038
	Ge-amd	Mean	.2750
	95% Confidence Interval for Mean	Lower Bound	.2302

Group	Statistic	Std. Error
	Mean	
	Upper Bound	.3198
	Variance	.008
	Std. Deviation	.09005
	Skewness	.030
	Kurtosis	.372
Hm-amd	Mean	.2850
	95% Confidence Interval for Mean	.2366
	Lower Bound	
	Upper Bound	.3334
	Variance	.009
	Std. Deviation	.09739
	Skewness	-.472
	Kurtosis	-.653
Lp-amd	Mean	.2611
	95% Confidence Interval for Mean	.1905
	Lower Bound	
	Upper Bound	.3317
	Variance	.020
	Std. Deviation	.14200
	Skewness	-.738
	Kurtosis	.177
Mt-amd	Mean	.2472
	95% Confidence Interval for Mean	.2075
	Lower Bound	
	Upper Bound	.2870
	Variance	.006
	Std. Deviation	.07991
	Skewness	.386

Group		Statistic	Std. Error
	Kurtosis	.978	1.038
S1-amd	Mean	.3111	.02542
	95% Confidence Interval for Mean	Lower Bound	.2575
		Upper Bound	.3647
	Variance	.012	
	Std. Deviation	.10786	
	Skewness	.073	.536
	Kurtosis	-.273	1.038
S2-amd	Mean	.2611	.02160
	95% Confidence Interval for Mean	Lower Bound	.2155
		Upper Bound	.3067
	Variance	.008	
	Std. Deviation	.09164	
	Skewness	.405	.536
	Kurtosis	-.883	1.038
S3-amd	Mean	.2000	.01143
	95% Confidence Interval for Mean	Lower Bound	.1759
		Upper Bound	.2241
	Variance	.002	
	Std. Deviation	.04851	
	Skewness	.000	.536
	Kurtosis	2.444	1.038
Unamd1	Mean	.3072	.02092
	95% Confidence Interval for Mean	Lower Bound	.2631
		Upper Bound	.3514

Group		Statistic	Std. Error				
pH	Unamd2	Variance	.008				
		Std. Deviation	.08877				
		Skewness	-.507	.536			
		Kurtosis	2.792	1.038			
		Mean	.3072	.02092			
		95% Confidence Interval for Mean	Lower Bound		.2631		
			Upper Bound		.3514		
		Variance	.008				
		Std. Deviation	.08877				
		Skewness	-.507	.536			
		Kurtosis	2.792	1.038			
		pH	Fh-amd	Mean	6.0567	.11918	
				95% Confidence Interval for Mean	Lower Bound		5.8052
					Upper Bound		6.3081
Variance	.256						
Std. Deviation	.50564						
Skewness	-.789			.536			
Kurtosis	-.668			1.038			
pH	Ge-amd			Mean	7.4978	.03817	
				95% Confidence Interval for Mean	Lower Bound		7.4172
					Upper Bound		7.5783
				Variance	.026		
				Std. Deviation	.16196		
				Skewness	-.478	.536	
				Kurtosis	-1.206	1.038	
		pH	Hm-amd	Mean	7.3200	.03849	

Group		Statistic	Std. Error	
	95% Confidence Interval for Mean	Lower Bound	7.2388	
		Upper Bound	7.4012	
	Variance	.027		
	Std. Deviation	.16331		
	Skewness	.993	.536	
	Kurtosis	.739	1.038	
	Lp-amd	Mean	8.3172	.03271
	95% Confidence Interval for Mean	Lower Bound	8.2482	
		Upper Bound	8.3862	
		Variance	.019	
	Std. Deviation	.13877		
	Skewness	.526	.536	
	Kurtosis	.860	1.038	
Mt-amd	Mean	7.5683	.02789	
95% Confidence Interval for Mean	Lower Bound	7.5095		
	Upper Bound	7.6272		
	Skewness	-.053	.536	
	Kurtosis	-.628	1.038	
S1-amd	Mean	7.4483	.03077	
95% Confidence Interval for Mean	Lower Bound	7.3834		
	Upper Bound	7.5132		
	Variance	.017		
	Std. Deviation	.13053		
	Skewness	.690	.536	
	Kurtosis	-.453	1.038	

Group		Statistic	Std. Error
S2-amd	Mean	7.4483	.03077
	95% Confidence Interval for Mean	Lower Bound	7.3834
		Upper Bound	7.5132
	Variance	.017	
	Std. Deviation	.13053	
	Skewness	.690	.536
	Kurtosis	-.453	1.038
	S3-amd	Mean	7.7900
95% Confidence Interval for Mean		Lower Bound	7.6849
		Upper Bound	7.8951
Variance		.045	
Std. Deviation		.21130	
Skewness		.644	.536
Kurtosis		-.429	1.038
Unamd1		Mean	7.2772
	95% Confidence Interval for Mean	Lower Bound	7.2008
		Upper Bound	7.3536
	Variance	.024	
	Std. Deviation	.15365	
	Skewness	.152	.536
	Kurtosis	-.635	1.038
	Unamd2	Mean	7.2772
95% Confidence Interval for Mean		Lower Bound	7.2008
		Upper Bound	7.3536
Variance		.024	

Group		Statistic	Std. Error
	Std. Deviation	.15365	
	Skewness	.152	.536
	Kurtosis	-.635	1.038

(Period B)

Group		Statistic	Std. Error		
Toluene	Fh-amd	Mean	.4528	.02765	
		95% Confidence Interval for Mean	Lower Bound		.3944
			Upper Bound		.5111
		Variance	.014		
		Std. Deviation	.11731		
		Skewness	-1.387	.536	
		Kurtosis	1.978	1.038	
		Ge-amd	Mean	.3313	.06649
			95% Confidence Interval for Mean	Lower Bound	
	Upper Bound				.4739
	Variance		.066		
	Std. Deviation		.25751		
	Skewness		.078	.580	
	Kurtosis		-.946	1.121	
	Hm-amd		Mean	.3333	.05876
			95% Confidence Interval for Mean	Lower Bound	
		Upper Bound			.4573
		Variance	.062		
Std. Deviation		.24928			
Skewness		.224	.536		

Group		Statistic	Std. Error
	Kurtosis	-.982	1.038
M1-amd	Mean	.2044	.05174
	95% Confidence Interval for Mean	Lower Bound	.0953
		Upper Bound	.3136
	Variance	.048	
	Std. Deviation	.21950	
	Skewness	.755	.536
	Kurtosis	-.677	1.038
S1-amd	Mean	.3861	.04407
	95% Confidence Interval for Mean	Lower Bound	.2931
		Upper Bound	.4791
	Variance	.035	
	Std. Deviation	.18696	
	Skewness	.777	.536
	Kurtosis	-.564	1.038
S2-amd	Mean	.2533	.04704
	95% Confidence Interval for Mean	Lower Bound	.1541
		Upper Bound	.3526
	Variance	.040	
	Std. Deviation	.19956	
	Skewness	.623	.536
	Kurtosis	.245	1.038
S3-amd	Mean	.0400	.01206
	95% Confidence Interval for Mean	Lower Bound	.0135
		Upper Bound	.0665

Group		Statistic	Std. Error
	Variance	.002	
	Std. Deviation	.04178	
	Skewness	.000	.637
	Kurtosis	-2.444	1.232
Unamd2	Mean	.4189	.05699
	95% Confidence Interval for Mean	Lower Bound	.2986
		Upper Bound	.5391
	Variance	.058	
	Std. Deviation	.24180	
	Skewness	.165	.536
	Kurtosis	-.061	1.038
Fe	Fh-amd	Mean	.5111
	95% Confidence Interval for Mean	Lower Bound	.3931
		Upper Bound	.6291
	Variance	.056	
	Std. Deviation	.23736	
	Skewness	.535	.536
	Kurtosis	-1.191	1.038
	Ge-amd	Mean	.2687
	95% Confidence Interval for Mean	Lower Bound	.2333
		Upper Bound	.3041
	Variance	.004	
	Std. Deviation	.06390	
	Skewness	-.184	.580
	Kurtosis	-.852	1.121
	Hm-amd	Mean	.1828

Group		Statistic	Std. Error
	95% Confidence Interval for Mean	Lower Bound	.1522
		Upper Bound	.2134
	Variance	.004	
	Std. Deviation	.06153	
	Skewness	1.392	.536
	Kurtosis	1.936	1.038
Mt-amd	Mean	.2967	.01669
	95% Confidence Interval for Mean	Lower Bound	.2615
		Upper Bound	.3319
	Variance	.005	
	Std. Deviation	.07079	
	Skewness	-.582	.536
	Kurtosis	-1.190	1.038
S1-amd	Mean	.3167	.01213
	95% Confidence Interval for Mean	Lower Bound	.2911
		Upper Bound	.3423
	Variance	.003	
	Std. Deviation	.05145	
	Skewness	.324	.536
	Kurtosis	.923	1.038
S2-amd	Mean	.3389	.01432
	95% Confidence Interval for Mean	Lower Bound	.3087
		Upper Bound	.3691
	Variance	.004	
	Std. Deviation	.06077	

Group		Statistic	Std. Error			
S3-amd	Skewness	1.362	.536			
	Kurtosis	1.126	1.038			
	Mean	.2000	.01231			
	95% Confidence Interval for Mean	Lower Bound		.1729		
		Upper Bound		.2271		
	Variance	.002				
	Std. Deviation	.04264				
	Skewness	.000	.637			
	Kurtosis	5.500	1.232			
	Unamd1	Mean	.1717	.01091		
95% Confidence Interval for Mean		Lower Bound		.1486		
		Upper Bound		.1947		
Variance		.002				
Std. Deviation		.04630				
Skewness		.372	.536			
Kurtosis		-.551	1.038			
Unamd2		Mean	.1717	.01091		
		95% Confidence Interval for Mean	Lower Bound		.1486	
			Upper Bound		.1947	
	Variance	.002				
	Std. Deviation	.04630				
	Skewness	.372	.536			
	Kurtosis	-.551	1.038			
	pH	Fh-amd	Mean	6.2367	.06764	
			95% Confidence Interval for Mean	Lower Bound		6.0939
				Upper Bound		

Group		Statistic	Std. Error
		Upper Bound	6.3794
	Variance	.082	
	Std. Deviation	.28699	
	Skewness	.185	.536
	Kurtosis	-.741	1.038
Ge-amd	Mean	7.3967	.01791
	95% Confidence Interval for Mean	Lower Bound	7.3583
		Upper Bound	7.4351
	Variance	.005	
	Std. Deviation	.06935	
	Skewness	-.165	.580
	Kurtosis	-.285	1.121
Hm-amd	Mean	7.6011	.02928
	95% Confidence Interval for Mean	Lower Bound	7.5393
		Upper Bound	7.6629
	Variance	.015	
	Std. Deviation	.12423	
	Skewness	-1.152	.536
	Kurtosis	1.041	1.038
Mt-amd	Mean	7.4811	.01817
	95% Confidence Interval for Mean	Lower Bound	7.4428
		Upper Bound	7.5194
	Variance	.006	
	Std. Deviation	.07707	
	Skewness	2.305	.536
	Kurtosis	7.409	1.038

Group		Statistic	Std. Error
S1-amd	Mean	7.0411	.04671
	95% Confidence Interval for Mean	Lower Bound	6.9426
		Upper Bound	7.1397
	Variance	.039	
	Std. Deviation	.19819	
	Skewness	.411	.536
	Kurtosis	-.769	1.038
	S2-amd	Mean	7.0411
95% Confidence Interval for Mean		Lower Bound	6.9426
		Upper Bound	7.1397
Variance		.039	
Std. Deviation		.19819	
Skewness		.411	.536
Kurtosis		-.769	1.038
S3-amd		Mean	7.4625
	95% Confidence Interval for Mean	Lower Bound	7.3919
		Upper Bound	7.5331
	Variance	.012	
	Std. Deviation	.11104	
	Skewness	-.371	.637
	Kurtosis	-.980	1.232
	Unamd1	Mean	7.4661
95% Confidence Interval for Mean		Lower Bound	7.3867
		Upper Bound	7.5455
Variance		.026	

Group		Statistic	Std. Error	
Unamd2	Std. Deviation	.15971		
	Skewness	-.632	.536	
	Kurtosis	-.409	1.038	
	Mean	7.4661	.03764	
	95% Confidence Interval for Mean	Lower Bound		7.3867
		Upper Bound		7.5455
	Variance	.026		
	Std. Deviation	.15971		
	Skewness	-.632	.536	
	Kurtosis	-.409	1.038	

(Period C)

Group		Statistic	Std. Error		
Toluene	Ge-amd	Mean	.3017	.03503	
		95% Confidence Interval for Mean	Lower Bound		.2246
	Upper Bound			.3788	
	Variance	.015			
	Std. Deviation	.12134			
	Skewness	.729	.637		
	Kurtosis	-.467	1.232		
	Hm-amd	Mean	.4372	.06978	
		95% Confidence Interval for Mean	Lower Bound		.2900
			Upper Bound		.5844
		Variance	.088		
		Std. Deviation	.29605		

Group		Statistic	Std. Error	
	Skewness	.513	.536	
	Kurtosis	-.827	1.038	
Mt-amd	Mean	.4276	.04585	
	95% Confidence Interval for Mean	Lower Bound	.3305	
		Upper Bound	.5248	
	Variance	.036		
	Std. Deviation	.18903		
	Skewness	.441	.550	
	Kurtosis	-.883	1.063	
Unamd2	Mean	.5922	.06017	
	95% Confidence Interval for Mean	Lower Bound	.4653	
		Upper Bound	.7192	
	Variance	.065		
	Std. Deviation	.25526		
	Skewness	.751	.536	
	Kurtosis	-.787	1.038	
Fe	Ge-amd	Mean	.3525	.03146
		95% Confidence Interval for Mean	Lower Bound	.2833
			Upper Bound	.4217
		Variance	.012	
		Std. Deviation	.10897	
		Skewness	-.127	.637
	Kurtosis	-1.214	1.232	
Hm-amd	Mean	.2561	.01768	
	95% Confidence Interval for Mean	Lower Bound	.2188	

Group		Statistic	Std. Error
		Upper Bound	.2934
	Variance	.006	
	Std. Deviation	.07500	
	Skewness	.529	.536
	Kurtosis	-.104	1.038
Mt-amd	Mean	.3465	.03189
	95% Confidence Interval for Mean	Lower Bound	.2789
		Upper Bound	.4141
	Variance	.017	
	Std. Deviation	.13148	
	Skewness	.935	.550
	Kurtosis	.171	1.063
Unamd1	Mean	.2650	.01964
	95% Confidence Interval for Mean	Lower Bound	.2236
		Upper Bound	.3064
	Variance	.007	
	Std. Deviation	.08333	
	Skewness	.557	.536
	Kurtosis	-.467	1.038
Unamd2	Mean	.2650	.01964
	95% Confidence Interval for Mean	Lower Bound	.2236
		Upper Bound	.3064
	Variance	.007	
	Std. Deviation	.08333	
	Skewness	.557	.536
	Kurtosis	-.467	1.038

	Group		Statistic	Std. Error
pH	Ge-amd	Mean	7.3792	.05064
		95% Confidence Interval for Mean	Lower Bound	7.2677
			Upper Bound	7.4906
		Variance	.031	
		Std. Deviation	.17542	
		Skewness	.284	.637
		Kurtosis	-1.194	1.232
	Hm-amd	Mean	7.4878	.02989
		95% Confidence Interval for Mean	Lower Bound	7.4247
			Upper Bound	7.5508
		Variance	.016	
		Std. Deviation	.12680	
		Skewness	-.142	.536
		Kurtosis	.075	1.038
	Mt-amd	Mean	7.3835	.01770
		95% Confidence Interval for Mean	Lower Bound	7.3460
			Upper Bound	7.4210
		Variance	.005	
		Std. Deviation	.07297	
		Skewness	-.721	.550
		Kurtosis	.675	1.063
Unamd1	Mean	7.3783	.02563	
	95% Confidence Interval for Mean	Lower Bound	7.3243	
		Upper Bound	7.4324	
	Variance	.012		

Group		Statistic	Std. Error	
Unamd2	Std. Deviation	.10875		
	Skewness	-.599	.536	
	Kurtosis	-.169	1.038	
	Mean	7.3783	.02563	
	95% Confidence Interval for Mean	Lower Bound		7.3243
		Upper Bound		7.4324
	Variance	.012		
	Std. Deviation	.10875		
	Skewness	-.599	.536	
	Kurtosis	-.169	1.038	

C.9.2 Difference in means tests

Table C.9.2 Difference in means tests for mean toluene across mesocosm groups ^a

(I) Group	Mean Difference	p-value
Fh-amd	.197*	.000
Ge-amd	.145*	.001
Hm-amd	.092*	.021
Lp-amd	.043	.445
Mt-amd	.174*	.000
S1-amd	.207*	.000
S2-amd	.247*	.000
S3-amd	.340*	.000
Unamd1	.447*	.000

a. The un-amended (S_T) mesocosm groups served as the baseline

C.9.3 Model parameters (Model 1)

Table C.9.5 Model dimension ^a (Model 1)

(Period A)

		Number of Levels	Covariance Structure	Number of Parameters	Subject Variables
Fixed Effects	Intercept	1		1	
	Time	1		1	
Random Effects	Intercept + Time ^b	2	Unstructured	3	ID
Residual			1		
Total	4		6		

(Period B)

		Number of Levels	Covariance Structure	Number of Parameters	Subject Variables
Fixed Effects	Intercept	1		1	
	Time	1		1	
Random Effects	Intercept + Time ^b	2	Unstructured	3	ID
Residual				1	
Total	4	4		6	

(Period C)

		Number of Levels	Covariance Structure	Number of Parameters	Subject Variables
Fixed Effects	Intercept	1		1	
	Time	1		1	
Random Effects	Intercept + Time ^b	2	Unstructured	3	ID
Residual				1	
Total	4	4		6	

a. Dependent Variable: Toluene.

Table C.9.6 Estimates of fixed effects ^a (Model 1)

(Period A)

Parameter	Estimate	t	p-value
Intercept	.329206	8.096	.000
Time	-.055105	-5.467	.000

(Period B)

Parameter	Estimate	t	p-value
Intercept	.795826	6.875	.000
Time	-.061377	-5.186	.000

(Period C)

Parameter	Estimate	t	p-value
Intercept	1.481808	5.515	.000
Time	-.077669	-5.326	.000

a. Dependent Variable: Toluene.

Table C.9.7 Estimates of covariance parameters ^a (Model 1)
(Period A)

	Parameter	Estimate	Wald Z	p-value
Residual		.008750	7.746	.000
Intercept + Time [subject = ID]	UN (1,1)	.045022	3.452	.001
Intercept + Time [subject = ID]	UN (2,1)	-.008893	-3.000	.003
	UN (2,2)	.002548	3.173	.002

(Period B)

	Parameter	Estimate	Wald Z	p-value
Residual		.011523	7.122	.000
Intercept + Time [subject = ID]	UN (1,1)	.296399	3.013	.003
Intercept + Time [subject = ID]	UN (2,1)	-.028287	-2.868	.004
	UN (2,2)	.002931	2.849	.004

(Period C)

	Parameter	Estimate	Wald Z	p-value
Residual		.007838	5.263	.000
Intercept + Time [subject = ID]	UN (1,1)	.007838	5.263	.000
Intercept + Time [subject = ID]	UN (2,1)	-.047751	-2.233	.026
	UN (2,2)	.002510	2.156	.031

^a. Dependent Variable: Toluene.

C.9.4 Model parameters (Model 2)

Table C.9.8 Model dimension ^a (Model 2)

(Period A)

		Number of Levels	Covariance Structure	Number of Parameters	Subject Variables	Number of Subjects
Fixed Effects	Intercept	1		1		
	Fe	1		1		
	pH	1		1		
	Time	1		1		
	Fe * Time	1		1		
	pH * Time	1		1		
Random Effects	Intercept + Time ^b	2	Unstructured	3	ID	
Residual	Time ^b					
Total	8			10		

(Period B)

		Number of Levels	Covariance Structure	Number of Parameters	Subject Variables	Number of Subjects
Fixed Effects	Intercept	1		1		
	Fe	1		1		
	pH	1		1		
	Time	1		1		
	Fe * Time	1		1		
	pH * Time	1		1		
Random Effects	Intercept + Time ^b	2	Unstructured	3		
Residual				1		
Total	7			9		

(Period C)^b

		Number of Levels	Covariance Structure	Number of Parameters	Subject Variables	Number of Subjects
Fixed Effects	Intercept	1		1		
	Fe	1		1		
	pH	1		1		
	Time	1		1		
	Fe * Time	1		1		
	pH * Time	1		1		
Random Effects	Intercept + Time ^b	2	Unstructured	3	ID	
Total		8		10		

a. Dependent Variable: Toluene.

b. Parameter estimates obtained using maximum likelihood

Table C.9.9 Estimates of fixed effects^a (Model 2)

(Period A)

Parameter	Estimate	t statistic	p-value
Intercept	1.610196	-3.305	.001
Fe	.59492	-.365	.715
pH	.260823	4.132	.000
Time	.259396	2.140	.035
Fe * Time	.010197	-.218	.828
pH * Time	.040981	-2.615	-.010

(Period B)

Parameter	Estimate	t statistic	p-value
Intercept	1.773124	-1.078	.283
Fe	1.201205	1.889	.062

Parameter	Estimate	t statistic	p-value
pH	.308800	1.415	.160
Time	.331798	1.865	.065
Fe * Time	.114236	-1.607	.112
pH * Time	.049993	-2.141	.035

(Period C)

Parameter	Estimate	t statistic	p-value
Intercept	15.207728	-1.696	.096
Fe	.763769	.655	.515
pH	2.225823	1.854	.069
Time	.984682	1.691	.097
Fe * Time	.057688	-.733	.467
pH * Time	.141366	-1.810	.076

a. Dependent Variable: Toluene.

b. Parameter estimates obtained using maximum likelihood

Table C.9.10 Estimates of covariance parameters ^a (Model 2)

(Period A)

Parameter		Estimate	z statistic	p-value
Residual		.007872	7.612	.000
Intercept + Time [subject = ID]	UN (1,1)	.046779	3.368	.001
	UN (2,1)	-.010751	-3.079	.002
	UN (2,2)	.003038	3.115	.002

(Period B)

Parameter		Estimate	z statistic	p-value
Residual		.011534	7.000	.000
Intercept + Time [subject = ID]	UN (1,1)	.294104	2.904	.004
	UN (2,1)	-.026989	-2.747	.006
	UN (2,2)	.002578	2.640	.008

(Period C)

Parameter		Estimate	z statistic	p-value
Residual		.007675	5.049	.000
Intercept + Time [subject = ID]	UN (1,1)	.853430	2.269	.023
	UN (2,1)	-.044404	-2.184	.029
	UN (2,2)	.002319	2.093	.036

a. Dependent Variable: Toluene.

b. Parameter estimates obtained using maximum likelihood

Dedication

I would like to dedicate this thesis in memory of the recent passing of my aunts Dr Juliet Orlu and Josephine Orlu, and grandparents Chief London Ihunwo, Selina Ihunwo, Mary Orlu and Chief (Sir) Isaac Orlu, Paramount Ruler of Okporowo-Ogbakiri Kingdom. Also to, the one whom I was privileged to call sister over the brief 14-year period of her life. Your memory lives on.

Rest... in peace.